Pyridinium-based cationic lipids: correlations of molecular structure with nucleic acid transfection efficiency

by

Paria Parvizi
MSc, Amirkabir University of Technology, 2007
BSc, Amirkabir University of Technology, 2005

A Dissertation Submitted in Partial Fulfillment
of the Requirements for the Degree of

Doctor of Philosophy

in the Department of Chemistry

Supervisory Committee

Pyridinium-based cationic lipids: correlations of molecular structure with nucleic acid transfection efficiency

by

Paria Parvizi
MSc, Amirkabir University of Technology, 2007
BSc, Amirkabir University of Technology, 2005

Supervisory Committee

Dr. Thomas Fyles, Department of Chemistry
Supervisor

Dr. Fraser Hof, Department of Chemistry
Departmental Member

Dr. Jeremy Wulff, Department of Chemistry
Departmental Member

Dr. Terry Pearson, Department of Biochemistry
Outside Member

Abstract

Supervisory Committee
Dr. Tom Fyles, Department of Chemistry
Supervisor
Dr. Fraser Hof, Department of Chemistry
Departmental Member
Dr. Jeremy Wulff, Department of Chemistry
Departmental Member
Dr. Terry Pearson, Department of Biochemistry
Outside Member

A series of pyridinium cationic lipids was designed, synthesized and characterized. These lipids varied in the lipophilic part, bearing C9 to C20 saturated, unsaturated, straight and branched hydrocarbon chains.

The lipid shape parameter was calculated from the molecular structure of these lipids based on the partial molar volumes of the atoms, and standard bond lengths and bond angles, using fragment additive methods. The shape parameter controls the lamellar/hexagonal phase balance in lipoplexes of the lipid with deoxyribonucleic acid (DNA). The lipid phase behaviour of the lipoplexes was derived from small-angle X-ray scattering experiments and was successfully correlated with the calculated lipid shape parameter.

The synthesized pyridinium lipids were co-formulated (1:1) with 1,2-dimyristoyl-sn-glycero-3-ethylphosphocholine (EPC) as the co-cationic lipid in 1:1 ratio, and the mixed cationic lipids were co-formulated (3:2) with the neutral lipids 1,2-dioleoyl-sn-glycero-3-phosphatidylethanolamine (DOPE) or cholesterol. The effect of variation in cationic lipid structure and lipoplex formulation on the transfection of nucleic acid (β-galactosidase and green fluorescent protein (GFP)) into CHO-K1 cells and the cytotoxicity of these formulations was assessed.

Initial studies on the synthesized lipids bearing saturated and terminally unsaturated C16 chains showed that a Transfection Index (TI_{PSV}) which encompasses the variation in the lipid shape parameter, the phase packing in a hexagonal lipoplex and the partition of these lipids into the lipoplex successfully correlated with transfection efficiency.

To further investigate the effect of the variation of the partition of these lipids to the lipoplex, transfection studies were performed on a series of pyridinium lipids with straight saturated and unsaturated chains of varied lengths, with similar shape parameters but varied partition coefficients (clogP). The correlation of these experimental transfection data with the initial TI_{PSV} was unsuccessful, but the data suggested that chain length as it relates to chain mixing and chain melting behaviours of pure lipids played a role in transfection. A refined transfection index (TI_{PSVM}) was proposed which contained terms for the lipid shape parameter, the phase packing into a hexagonal lipoplex, the partition of these lipids into the lipoplex and a chain melting term. TI_{PSVM} gave an acceptable correlation with the experimental transfection efficiency for the range of compounds. Additional experimental transfection data were obtained for compounds with widely variable lipid shape parameters, either as pure compounds, blends of two pure compounds, or statistically produced mixtures of mixed-chain compounds. Although very short-chain compounds (C9) and very lipophilic compounds (C20) performed poorly, the results from the blends allow the assessment of the role of the shape parameter in the TI. Since the shape parameter and the volume filling term are both calculated with the same molecular parameter, the experimental work demonstrated that only one of these terms is required. Thus a three parameter transfection index (TI_{PVM}) was proposed and found to correlate with the entire set of comparable data.

A Quantitative structure–activity relationship (QSAR) study was done on the cytotoxicity of the transfection formulations utilized. The toxicity of the synthesized pyridinium lipids was shown to correlate with the shape parameter, the lipid mixture partition co-efficient (clogP) and the charge ratio of the lipoplex formulation.

Taken together, the developed transfection index TI_{PVM} and the cytotoxicity correlation uncovered can be used in the design of low-toxicity, high activity pyridinium lipids for transfection of DNA.

Table of Contents

List of Tables

List of Figures

List of Schemes

List of abbreviations

β-gal	β-galactosidase
Å	angstroms
a_0	lipid headgroup area
AI	amphipathic index
br	broad
CHO-K1	chinese hamster ovarian
Chol	cholesterol
CR	charge ratio of cationic lipid N to anionic DNA P
DCM	dichloromethane
dd	doublet of doublets
DHP	3,4-dihydro-2H-pyran
DIC	*N*,*N*-diisopropyl carbodiimide
DiPEA	diisopropyl ethylamine
DLPC	1,2-Dilauroyl-sn-glycero-3-phosphocholine
DLS	dynamic light scattering
DMF	dimethylformamide
DMPC	1,2-Dimyristoyl-sn-glycero-3-phosphocholine
DOGS	dioctadecylamidoglycylspermine
DOPC	1,2-Dioleoyl-sn-glycero-3-phosphocholine
DOPE	1,2-dioleoyl-*sn*-glycero-3-phosphatidylethanolamine
DOSPA	2,3-Dioleyloxy-N-[2-(sperminecarboxamido)ethyl]-N,N-dimethyl-1-propylammonium chloride
DOTAP	2,3-Dioleyloxypropyltrimethylammonium chloride
DOTMA	1,2-di-O-octadecenyl-3-trimethylammonium propane
DPPC	1,2-Dipalmitoyl-sn-glycero-3-phosphocholine
DSPC	1,2-Distearoyl-sn-glycero-3-phosphocholin
EPC (EDMPC)	1,2-dimyristoyl-sn-glycero-3-ethylphosphocholine
f_{lat}, f_{cyl}	filling factors of the lattice and cylinder unit cell
GFP	green fluorescent protein
h	hours
HGS	head group size
HOBt:	hydroxybenzotriazole
Hz	Hertz, s^{-1}
J	coupling constant
l_c, l_{lip}	critical chain length of the hydrocarbon portion of a lipid; overall length of the lipid including the headgroup
LDS	lipid domain size
LI	lipofection Index
clogP	calculated octanol-water partition coefficient
M	molar
m	multiplet
m/*z*	mass to charge ratio

mg	milligrams
mmol	millimoles
MVL	N1-[2-((1S)-1-[(3-Aminopropyl)amino]-4-[di(3-aminopropyl)amino]butylcarboxamido)ethyl]-3,4-di[oleyloxy]-benzamide
n_{exp}	molar amount of lipid in the experiment with respect to the unit cell
n_{lat}, n_{cyl}	optimum molar amount of a lipid to fill the unit cell of a hexagonal lattice or a cylinder outside of the volume occupied by DNA
NMR	nuclear magnetic resonance
°C	degrees Celcius
PC	phosphatidylcholine
*p*DNA	plasmid DNA
PE	phosphatidylethanolamine
PG	phosphatidylglycerol
PS	phosphatidylserine
pTsOH	*para*-toluenesulfonic acid
QSAR	quantative structure activity relationship
R	ratio of cationic lipid to neutral lipid
r. t.	room temperature
S	shape parameter
S_+, S_{mix}	mole weighted average value of S for cationic lipids or mixed lipids
SAXS	small angle x-ray scattering
SAXD	Small angle x-ray diffraction
t	triplet
TE	transfection efficiency
THF	tetrahydrofuran
THP	tetrahydropyran
TI_{PSV}	transfection index with partition, shape and volume fill terms
TI_{PSVM}	transfection index with partition, shape, volume fill terms and melting parameters
TI_{PSVMM}	transfection index with partition, shape, volume fill terms, melting and mixing parameters
TI_{PVM}	transfection index with partition, volume fill terms and melting parameters
TLC	thin-layer chromatography
T_m	melting temperature
V_C, V_{lip}, V_{mix}	partial molar volume of the hydrocarbon portion of a lipid, the overall lipid molecule including a counterion if required, mole weighted average value of a mixture
α	alpha
β	beta
δ	delta
σ_M	membrane charge density

List of numbered compounds

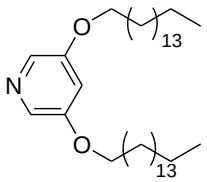

1-1

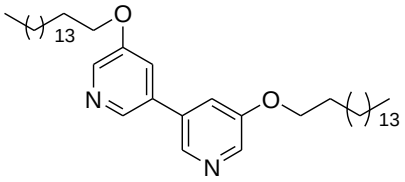

1-2

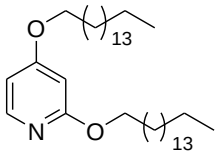

1-3

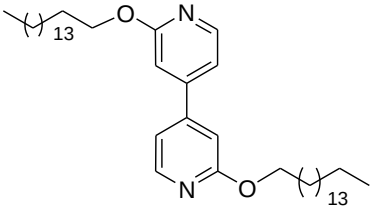

1-4

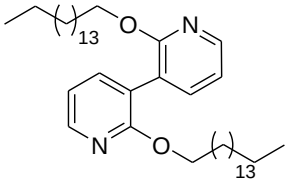

1-5

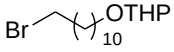

2-1

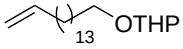

2-2

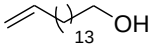

2-3

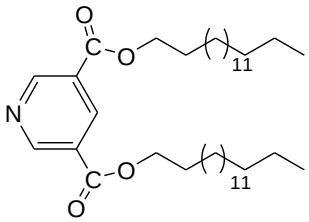

2-4

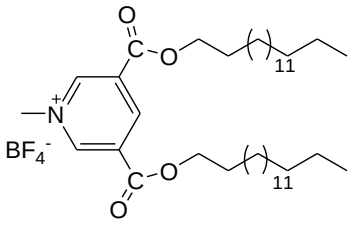

2-5
diC16:0

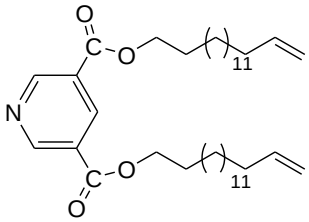

2-6

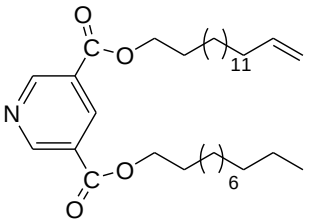

2-7

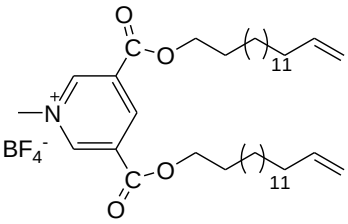

2-8
diC16:1

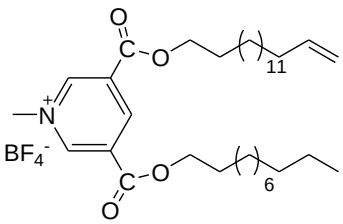

2-9
(C16:1)(C11:0)

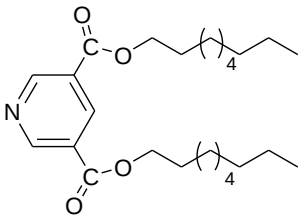

2-10

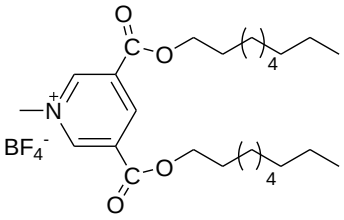

2-11

diC9:0

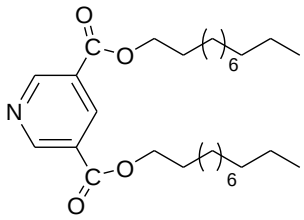

2-12

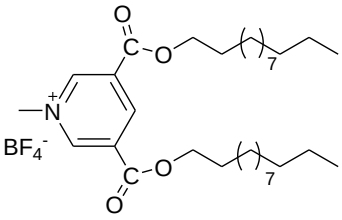

2-15

diC12:0

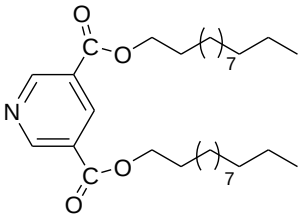

2-14

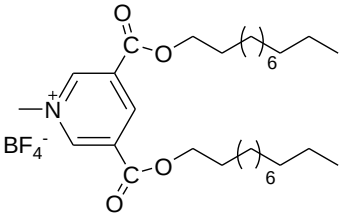

2-13

diC11:0

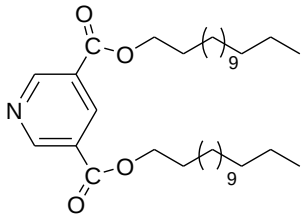

2-16

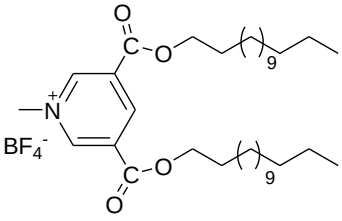

2-17

diC14:0

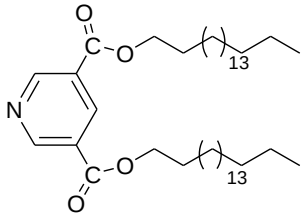

2-18

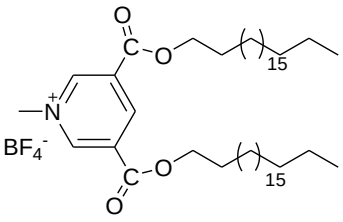

2-21

diC20:0

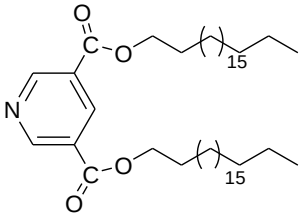

2-20

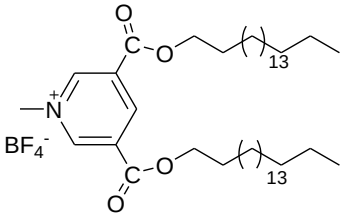

2-19

diC18:0

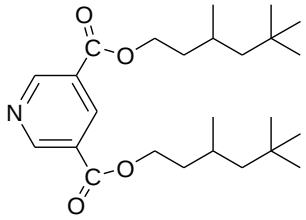

2-22

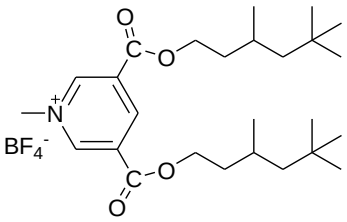

2-23

diisoC9:0

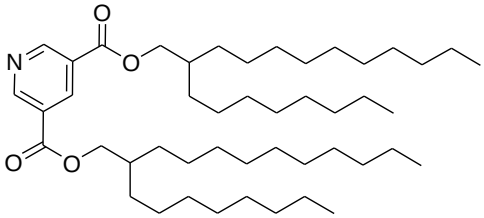

2-24

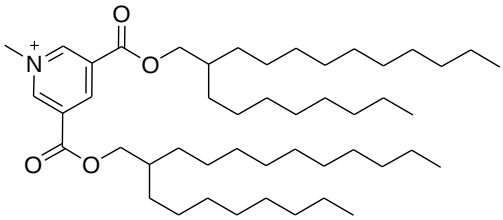

2-25

dibrC20:0

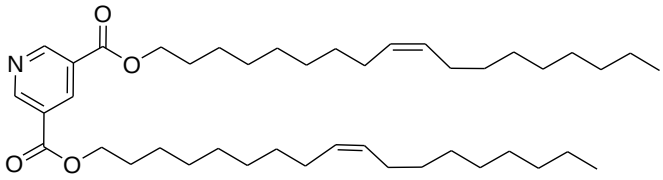

2-26

2-27

diC18:1

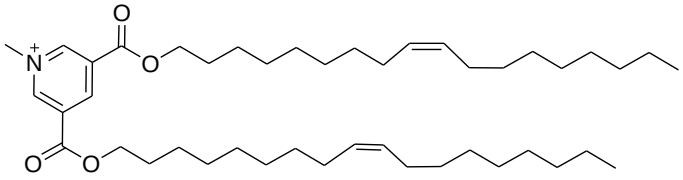

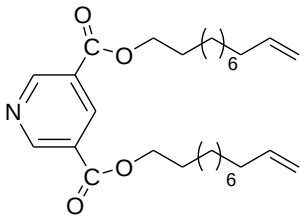

2-28

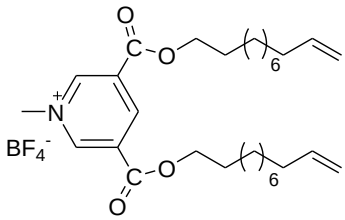

2-29

diC11:1

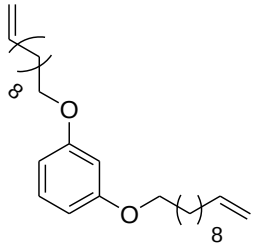

3-1

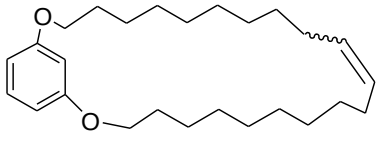

3-2

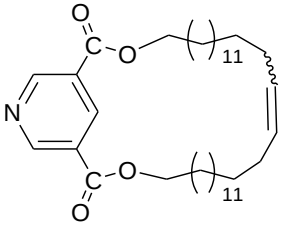

3-3

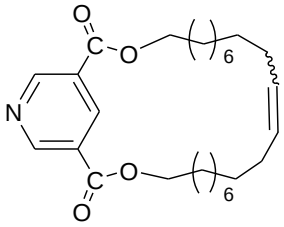

3-4

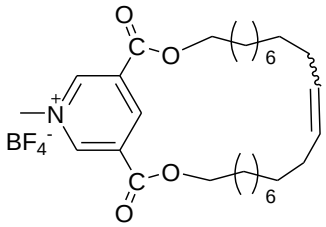

3-5
cycloC20

4-1

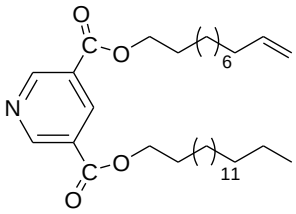

4-2

(C16:0)(C11:1)

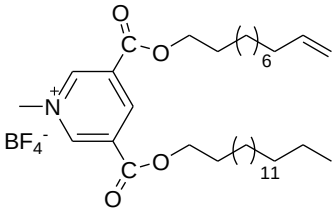

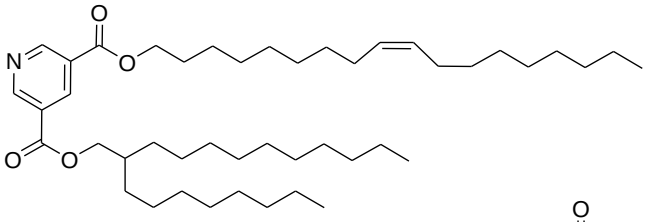

4-3

4-4

(C18:1)(brC20:0)

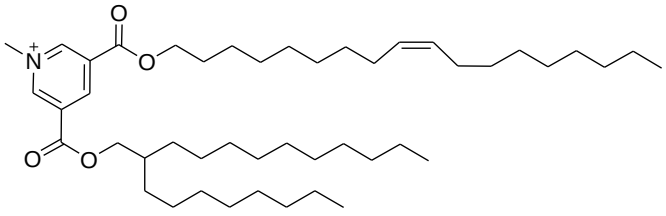

Acknowledgments

I would like to acknowledge and thank my supervisor, Dr. Tom Fyles for his guidance and help during this project. He's the most intelligent, kind and wise person that I have met and I am forever grateful to him for his mentorship and support.

I would also like to thank my collaborator, Dr. Michael Pungente for his suggestions and encouragement during this project. In addition, I like to acknowledge the Pungente research group, Dr. David Nicholson and Dr. Helge Larsen for their great work and collaboration.

I like to thank the past and present members of Fyles group, especially Dr. Joanne Moszynski, Dr. Andrew Dambenieks and Dr. Jonathan Chui for all their assistance and inspiration. I also like to thank my group mates, Gavin Mitchell, Mengxiu Zheng, Mike Meanwell, Ye Zong, Paul Vu and Burford group for their suggestions and companionship. I would like to thank my committee members for their time and valuable inputs. I am grateful to the faculty and staff of department of chemistry at University of Victoria and NSERC for funding. I also like to thank Dr. Cornelia Bohne and her group for their assistance and suggestions with my other projects during my PhD. I like to thank my parents, my brother and sister in law, Ehsan and Samin and all my friends in department of Chemistry, for their encouragement and support. I am deeply grateful to my partner, Omid for his love and motivation during the past year.

And finally I like to thank my closest friend, Sadaf for our thirteen years of friendship, specially the last five years, when her constant support and infinite encouragement made it possible for me to make this accomplishment.

Dedication

I would like to dedicate this work to my parents, Sousan & Ali Parvizi. Without their unconditional love and support, I wouldn't have accomplished any of my goals. I am grateful for all their sacrifices and always believing in me. They encouraged me to reach for the highest goals and helped me to achieve them. I am forever thankful to them and I am the most fortunate to have such wonderful parents.

Chapter 1: Introduction

1.1-Nucleic acid delivery

Gene therapy is a potential method for curing genetic disorders such as cystic fibrosis, immunodeficiency diseases and even as an alternative method for cancer therapy which currently shows a promising future[2]. The first clinical trial was performed in 1989, followed by numerous others. However, in 1999 a clinical trial patient died, and this caused a great setback to gene therapy research. In 2012, when the EMA (European Medicines Agency) approved the treatment Glybera as a gene therapy product for treatment of lipoprotein lipase deficiency, there was a general restart of efforts for development of gene therapy. In 2013 there were 1800 clinical trials using gene therapy being conducted worldwide for treatment of different diseases, 65% for cancer[3].

To fulfill the promise of gene therapy, it is important to study and find efficient ways to deliver nucleic acid into cells. Nucleic acid can be delivered to the targeted cells via electroporation and by direct injection[2]. The use of these methods is limited as it is very difficult to deliver the naked nucleic acid because of enzymatic degradation by enzymes in the patient's plasma and the negative charge of the DNA which prevents uptake through the cell membrane[4,5]. So a delivery vehicle (a vector), is required to pack and protect the nucleic acid (DNA or Small interfering RNA (siRNA)), to deliver it to the cell and to facilitate its uptake inside the cell. Once inside the cell, the nucleic acid should be released and delivered across the nucleosome membrane to be later on expressed in to the nucleus. A measure of the success of this process is what is known as the transfection efficiency (TE).

Viral vectors such as adenoviruses and retroviruses have been the main vectors used in the 68% of clinical trials[2, 6], which while being able to protect and deliver the DNA to many types of cells with high efficiency, can also cause viral inflammation and these have high toxicity and immunogenicity. Apart from their toxicity, viral vectors have limited capacity in carrying the nucleic acid cargo and are difficult to scale up for large scale pharmaceutical production[2, 4, 7].

The shortcomings of viral vectors have necessitated an ongoing effort to design, synthesize and apply a series of non-viral vectors such as cationic lipids, dendrimers, polymers and peptides. Though these non-viral vectors have been found to be more biocompatible and less toxic, they are not as efficient in gene delivery as viral vectors and they are hindered by extra- and intra-cellular obstacles.

Considering the advantages of non-viral vectors such as biocompatibility and ease of potential large scale production, many studies have been done to design and synthesize such vectors with increased transfection efficiency[2, 4, 8]. As useful as these studies are in understanding the required characteristics for these vectors, they are largely empirical and therefore not helpful in designing very highly active non-viral vectors. Although an ideal solution is unlikely, such high-activity vectors would pack and protect the nucleic acid cargo until its approach to the cell membrane, would aid in the cellular uptake and eventually in the release of the nucleic acid inside the cell to deliver it to the nucleosome for the intended interaction, all the while being biocompatible with the cellular system. A high-activity vector should combine high transfection efficiency with low toxicity.

To achieve this goal, it is of utmost importance to study and understand the mechanism of delivery of the nucleic acid in vitro, as a biomedical tool. Understanding the effect of

the structural properties of the vectors on the delivery process will allow the design and synthesis of a high-activity vector based on the ability to predict the efficiency and toxicity in transfection of the nucleic acid.

1.2-Nucleic acid delivery mechanism

Cationic lipids have been used as non-viral delivery vehicles for nucleic acids. The positively charged lipids form liposomes with neutral lipids and then form aggregates with nucleic acid which results in the formation of lipoplexes. These lipoplexes are incubated with the growing cells inside a culture medium. As the cells grow, the lipoplexes are harvested from the medium via normal cellular uptake pathways, but once inside the cell the lipoplex dissociates to release the nucleic acid within the cell. Each of the stages in the process involves the lipids in one role or another as discussed in the next sections[2, 9].

1.2.1-Lipoplex formation and morphology

Cationic lipids form complexes with poly anionic nucleic acids via electrostatic interaction that results in counterion and water displacement as the amphiphile coats the nucleic acid.

Studies have shown that lipid structural parameters play a major role in determining the phase of the lipoplexes to be lamellar or hexagonal[10]; this issue will be discussed in detail in section 1.4. The morphology of the lipoplex affects transfection efficiency and toxicity[11]. Lipids in an aqueous solution typically form a lamellar phase. Upon mixing with DNA, the following steps are assumed to occur:

-Adhesion of the DNA to the surface of the liposome by charge-neutralization. This produces a high local concentration of DNA during titration of the lipid headgroup charge;

-Rearrangement of the lamellae of the liposomes to expose more vacant surface to the DNA;

-Growth and coalescence of these layers of lipid/DNA to form the lipoplex particles[2, 8a].

Depending on the lipids used, the lipoplex can adopt different morphologies. Figure 1.1 shows possible structures of lipoplexes. The adopted phases of lipoplexes have been studied using cryo-electron microscopy and small angle X-ray scattering (SAXS)[8a, 10c].

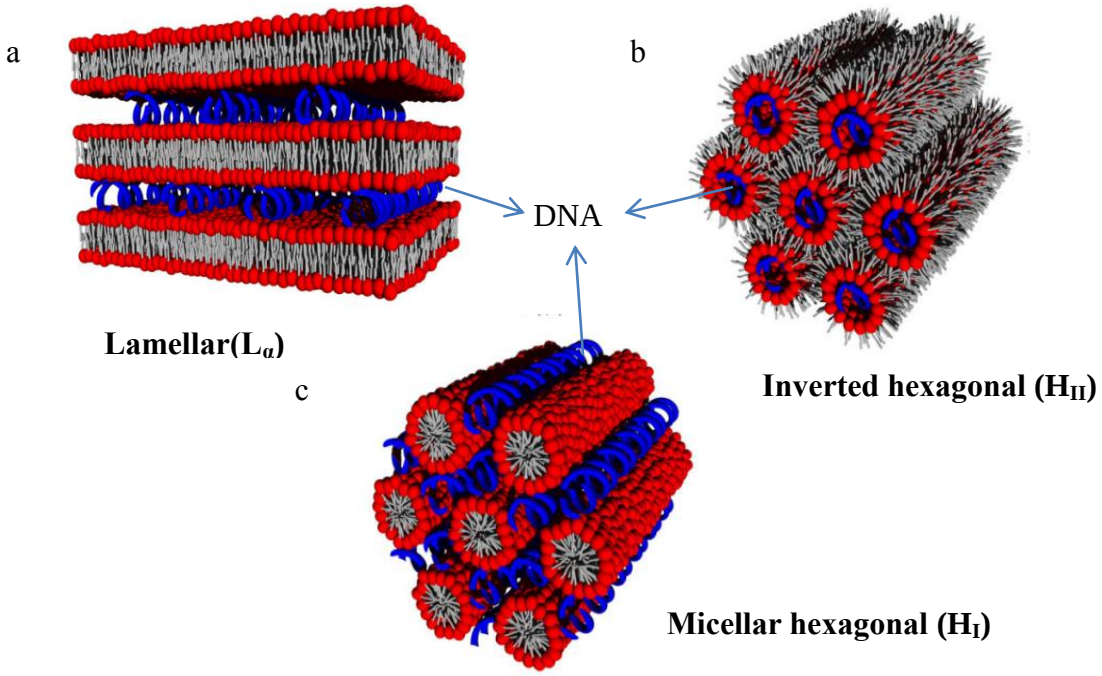

Figure 1.1-Lipoplex phase upon complexing of DNA with cationic lipids, (a) lamellar phase (L_α), (b) hexagonal phase (H_{II}), (c) micellar hexagonal phase (H_I). (Figure reproduced with permission from reference 1[1].)

Structure “a” in Figure 1.1, shows a lamellar packing, forming a bilayer with the nucleic acid between layers of headgroups. In structure “b” the lipoplex is in a hexagonal phase, where lipid-coated DNA strands are arranged on a hexagonal lattice. In structure “c”, a micellar hexagonal phase is formed where the DNA is arranged between rod-like micelles of lipids. The lipid parameters that control the morphology of the lipoplex and the effect that lipoplex morphology has in controlling transfection are discussed in later sections of this chapter. At this stage it is convenient to treat the lipoplex as a multi-lamellar liposome containing DNA as in Figure 1.1, structure “a”.

In addition to the particle morphology, the lipoplex effective surface charge (zeta potential) affects the interaction with the normal net negative surface charge of cell membranes; transfection efficiency is higher for lipoplexes with higher positive surface charge in comparison with lipoplexes with net negative surface charge[8a]. Depending on the charge of the cationic lipid and its efficiency in condensing the DNA, the size of the lipoplex can range between 70 nm to 500 nm or larger.

1.2.2-Cellular uptake of lipoplex

Once the DNA has made a complex with the cationic lipids and formed the lipoplex, it has to be internalized into the cell. The most common pathway is through the endocytosis process as it occurs in a normal cell. The endocytosis process can occur via various pathways, however studies have shown that endocytosis for lipoplexes usually happens via either clathrin-mediated endocytosis or via coated pits (Figure 1.2, b). Other endocytosis pathways such as phagocytosis, macropinocytosis and caveolae-mediated endocytosis have also been discussed[12]. The phase of the lipoplex does not have a significant effect on the endocytosis step. Rather it is dependent on the size of the

lipoplexes and the type of the cell. For lipoplex size up to 250 nm diameter it has been shown that endocytosis is almost exclusively via clathrin coated pits, whereas for lipoplexes larger than 500 nm diameter uptake may be through a caveolae mechanism[2, 10c, 12].

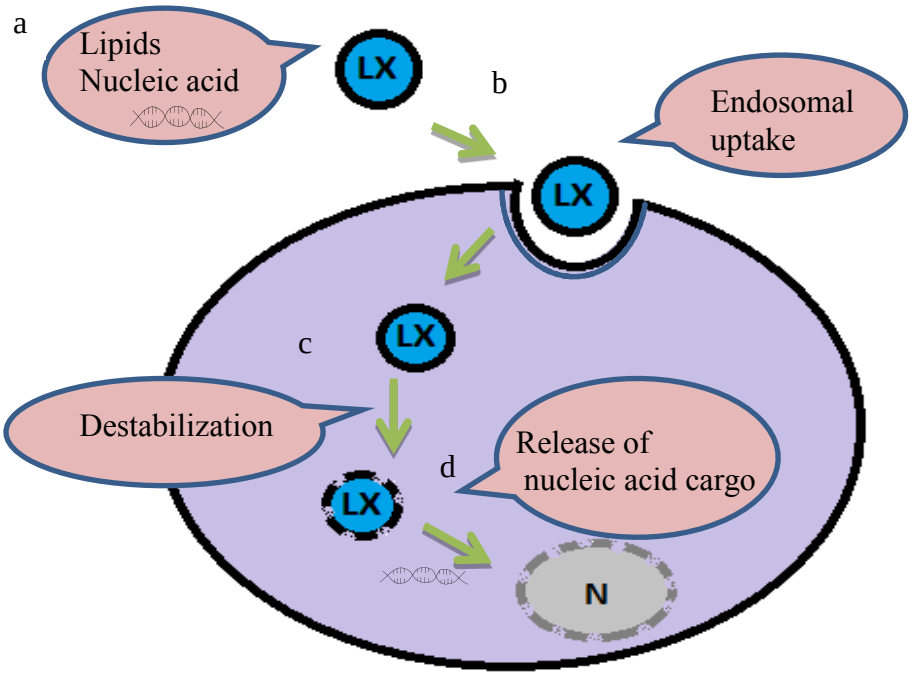

Figure 1.2-Mechanism of nucleic acid delivery with lipids, (a) lipoplex formation, (b) clathrin mediated endocytosis, (c) destabilization of the endosome, (d) release of nucleic acid cargo.

1.2.3-Mechanism of Nucleic Acid Release from Lipoplexes

For successful delivery of DNA to the nucleus, the lipids should disassociate from the complex and then destabilize the endosomal membrane to allow DNA release to the cytosol. One initial driving force for release of DNA from the lipoplex is the neutralization of the cationic lipid charge of the lipoplex with the anionic lipid charge of the endosomal membrane. However, studies with anionic lipids in lipoplexes have shown

that this could not be the only factor, and the shape of the anionic lipid affects the release process as well[4, 8a, 13]. The morphology and lipid phase of the lipoplex plays a key role here. For efficient release of DNA from a lamellar lipoplex, it has been demonstrated that there is a required phase transition sequence from lamellar to disordered lamellar, then to one of several possible "inverted" phases as the different lipids in the lipoplex migrate from the lipoplex to the endosomal membrane[9, 11b, 14]. Not only is conversion to an inverted phase necessary for the destabilization of the endosomal membrane, phase change also initiates the DNA release from the endosome. Considering the effect of these essential phase changes in efficient gene delivery, it is expected that lipids that form the lipoplexes in the hexagonal phase will have higher efficiency as these lipids are already in an inverted phase. Lipids that inherently form lamellar lipoplexes can be mixed with other neutral helper lipids that promote the hexagonal phase, hence facilitating the delivery.

1.2.4-The effect and necessity of co-lipid in the formation of lipoplex

While cationic lipids are necessary for condensing and protecting the DNA, they cannot deliver the DNA on their own, especially in vivo, as they cannot form stable lipoplexes. Cationic lipids are usually mixed with neutral or zwitterionic lipids such as cholesterol, diolelyphosphatidyl ethanolamine (DOPE) and diolelyl phosphatidyl-choline (DOPC), or other phosphatidylcholine (PC) lipids. The key role of helper neutral lipids is to assist in the required phase change in the release of nucleic acid cargo from the destabilized endosomal membrane[8a, 10a, 10c, 12].

Binary cationic lipid systems typically show better transfection efficiency than individual lipids and mixed lipids are recommended as mixing two cationic lipids will

increase the disorder at phase transitions involving solid-liquid crystalline phases which will facilitate the endocytosis process into the membrane[8a, 11a, 15]. The phase behaviour of the lipids and their transition temperature from solid gel phase to liquid phase has an important role in the phase changes required for an efficient delivery of nucleic acid. For mixtures where the phase transition temperature is the same as the temperature of the transfection experiment, the transfection efficiency increases notably[15b].

Considering the role of lipids in the transfection process, it becomes evident that the molecular parameters of the lipids have a considerable effect here and can be optimized to enhance the transfection of the nucleic acid.

1.3-Cationic lipids

Before discussing synthetic lipids, a short overview of natural lipids is provided in Figure 1.3. This figure shows that natural lipids have a range of headgroups (phosphatidyl choline (PC), phosphatidylethanolamine (PE), phosphatidylglycerol (PG)) on a glycerol backbone esterified with fatty acids having different hydrocarbon chain lengths either saturated (e.g. stearoryl, 18:0) or unsaturated (e.g. oleyl, 18:1). Other lipids include cholesterol, sphingomyelins, and other very non-polar materials produced in nature. Lipids are comprised of three structurally important domains: a polar headgroup, a hydrophobic portion and a linker between the two domains.

Cationic lipids are amphipathic structures that show overall physico-chemical properties and structures that are closely related to natural lipids (Figure 1.4).

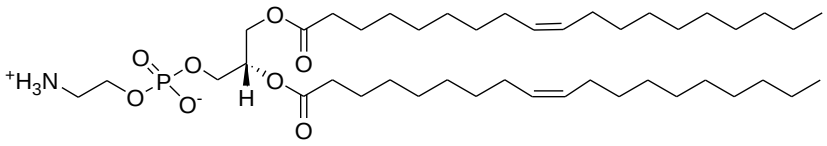

1,2-dioleoyl-sn-glycero-3-phosphoethanolamine (DOPE)

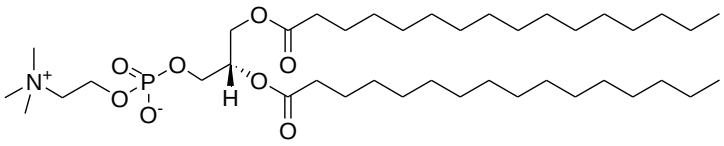

1,2-dipalmitoyl-sn-glycero-3-phosphocholine (DPPC)

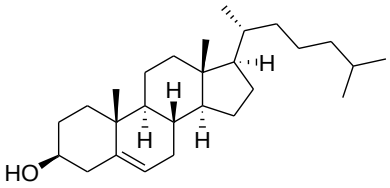

Cholesterol

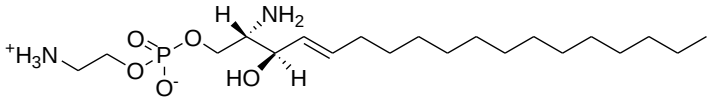

Sphingosyl PE (d18:1)

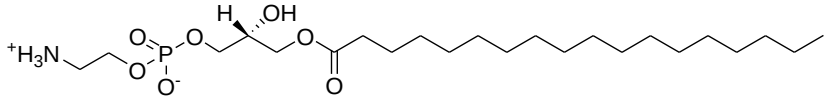

L-a-lysophosphatidylethanolamine

Figure 1.3-Natural lipids with varied headgroups and lipophilic parts.

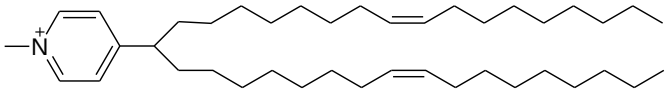

SAINT-2

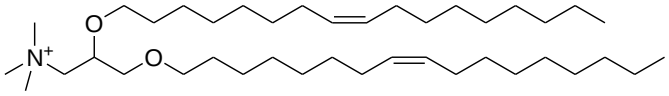

DOTMA (Lipofectin)

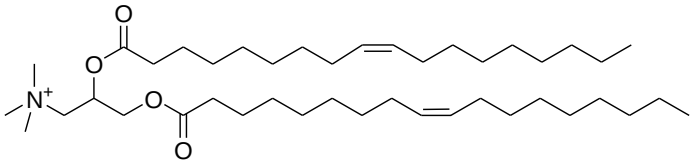

DOTAP

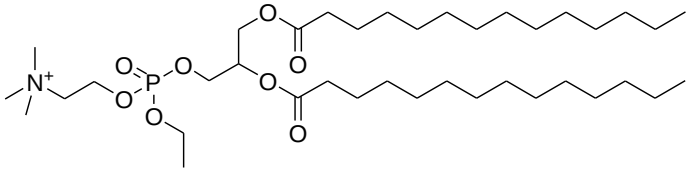

EDMPC (EPC-di14:0)

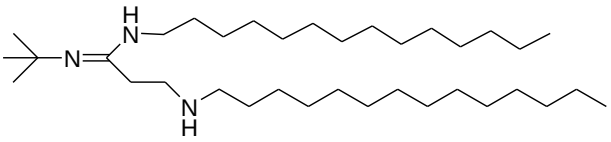

diC14-amidine

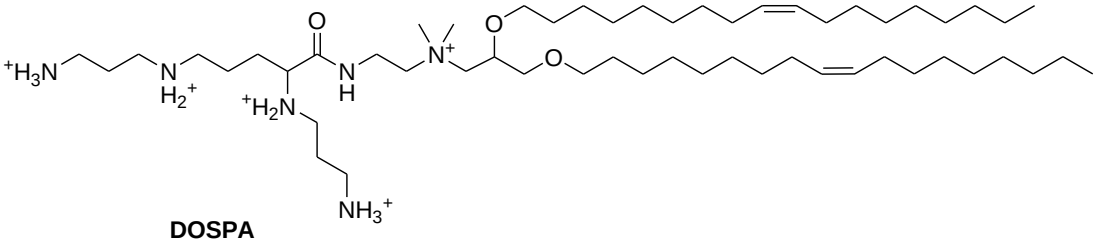

DOSPA

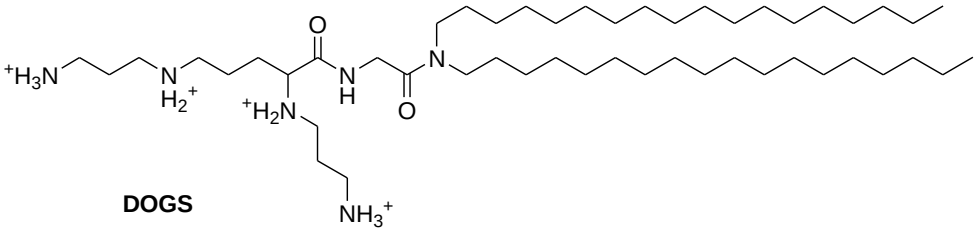

DOGS

Figure 1.4-Some commonly used cationic lipids.

The headgroups of cationic lipids are positively charged at physiological pH so amine derivatives such as primary, secondary, tertiary and quaternary ammonium have been used. Other commonly used headgroups are pyridinium, guanidinium, amidinium, etc. The cationic lipid can bear single or multiple charges. DNA is better condensed and protected when the headgroup is multi charged, however this will lead to a more difficult DNA release later in the cytoplasm, which may affect the transfection efficiency[9]. Also multi-charged cationic lipids are prone to form micelles which can increase their toxicity[16].

Cationic lipids where the nitrogen in an ammonium group has been replaced with phosphorous (phosphonium) or arsenic (arsonium) showed decrease in toxicity attributed to increase in the radius of P and As compared to N which leads to a lower charge density[17].

Another favoured headgroup is pyridinium. Pyridinium lipids are relatively non-toxic, because of the delocalized positive charge compared to commercial lipofectin[18]. In addition to the headgroup charge, because of the size of the pyridinium, these lipids will form lipoplexes with the morphology of an inverted hexagonal which enhances the transfection[12, 18c, 19].

Ethers, esters and carbamates are the common linkers to link the hydrophilic part to the cationic headgroup[2, 9, 20].

Ethers have the highest chemical stability when used as the linking group[21], while esters can potentially be cleaved inside the cell[22].

Carbamates are both cleavable and stable. Cleavable lipids are interesting, as they can perhaps facilitate DNA release into the cytoplasm. Cleavable lipids can be photo or pH sensitive, or cleave via redox or other biodegrading enzymes[23].

The length and type of the aliphatic chains also affects the transfection efficiency and toxicity. In addition to aliphatic chains, other hydrophobic moieties have been studied to investigate the effect of rigidity (cholesterol shape), biodegradability and fusogenic capability. Bile acid based cationic facial lipids, diacetylene based, and tetra alkyl chain (cone shaped) cationic lipids have been used in delivery of nucleic acid[2, 21b, 24].

Considering the importance of the electrostatic interaction role in transfection efficiency, most of the modification attempts have been performed on the polar headgroup and the hydrophobic part has been less studied. However, the length, structure and saturation of the chains play a key role in the transfection process, affecting the phase transition and lipoplex morphology[11b, 14a, 15b].

It has been shown that there is an inverse relationship between alkyl chain length and activity. Shorter hydrocarbon chains are better at fusion and penetration through the cell membrane which correlates with their higher transfection efficiency[25].

Cationic phosphatidyl cholines in which the phosphate group occurs as a triester are a favoured class because of their biodegradability and relatively good transfection efficiency. One of the examples of this class with straight saturated chains was shown in Figure 1.4 (EPC) where the third ester is connected to an ethyl group. Other derivatives with varied ester chain length and saturation have been synthesized and their transfection efficiency studied[8a].

Within this class of cationic PC derivatives, lipids with a total hydrocarbon chain length of 30 carbons and with 2 alkene bonds, one in each chain, have demonstrated the highest transfection efficiency[14a]. Studies on a larger library of this class, with different linkers and headgroups, showed that transfection depends on the number of carbons and on the saturation degree (0-2 double bond) in the hydrocarbon chains; cationic lipids with two saturated chains that average 14 carbons each are the most efficient[20, 26].

Studies on pyridinium lipids showed that while increasing the chain length from 16 to 18 carbon decreases the transfection, adding a double bond reverses the effect[18d].

1.4-Lipid structural parameters

Previous sections have indicated that lipid structure plays a variety of roles in the transfection process, but the process is multi-stage and the roles for the lipids vary considerably. At the same time, many of the roles involve the influence of lipids on phase behaviours of complex lipid mixtures and membranes. “Phase behaviour” is a composite term that includes the overall morphology or structure of the phase (micelle, liposome), the molecular organization of the phase (lamellar, hexagonal, cubic), and the fluidity of the hydrocarbons and headgroups at a given temperature (chain frozen, chain melted, headgroup melted) or over a range of temperatures in which phase changes occur. Complex lipid mixtures can phase separate into coexisting phases[11a, 14b, 15b, 27]. As it has been shown that the phase and the structure of the lipoplex is a dominant factor to optimize the transfection, better understanding of these parameters is necessary in any study that seeks to relate transfection efficiency to specific cationic lipid structures.

1.4.1-Lipid packing or shape parameter

The lipid packing parameter provides some indication of the overall morphology of a lipid phase and its internal molecular organization. The shape parameter (S) is defined as follows[28]:

$$S = \frac{V_C}{(l_c \times a_0)} \qquad \textit{Equation 1.1}$$

where V_C is the volume of the lipophilic tail of the amphiphile, a_0 is the cross-sectional area occupied by the headgroup of the amphiphile at local equilibrium in the phase, and l_c is the critical chain length of the hydrocarbon chains (Figure 1.5). These terms previously have been obtained experimentally. However as the variety of synthetic lipids increases, there is a need to be able to calculate these terms based solely on the molecular structures of the lipids, as shape parameter indicates the phase behaviour of lipids and is important to be able to predict this behaviour.

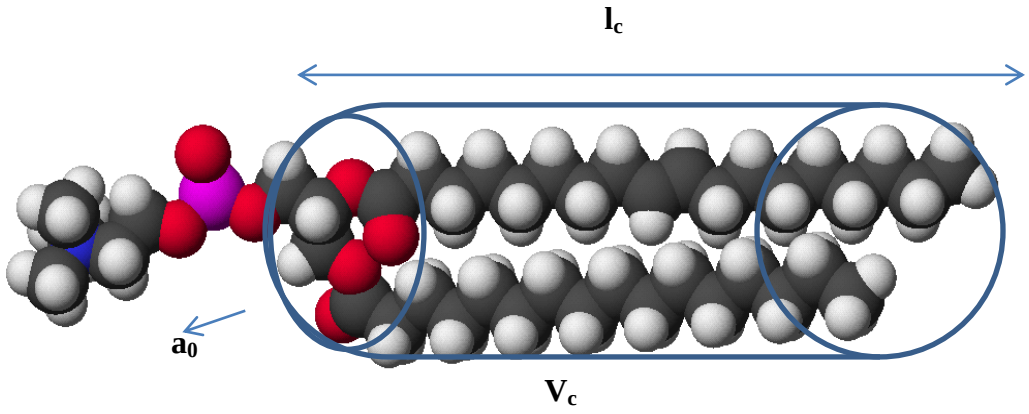

Figure 1.5-Geometrical properties of lipids.

The lipid shape parameter was designed to rationalize the different morphologies observed for dispersions of lipids in aqueous solutions. Conical lipids (large a_0 relative to chain length and volume) with S ~ 0.5 form micellar phases, cylindrical lipids with $0.7 < S < 1$ have a propensity to form lamellar phases, and inverted cone lipids with $S > 1$

(small headgroup relative to chain length and volume) have a tendency to form inverted phases of either the hexagonal or cubic organization (Figure 1.6)[29]. As discussed above, inverted phase structures play a key role in packing and condensing the DNA and later on in delivering it to the cytosol. Relatively few natural lipids have S > 1 with the exception of PE (e.g. DOPE, experimental S = 1.38[30]) and cholesterol (estimated S = 1.20[28b]), and these lipids are frequently used as co-lipids in lipoplexes.

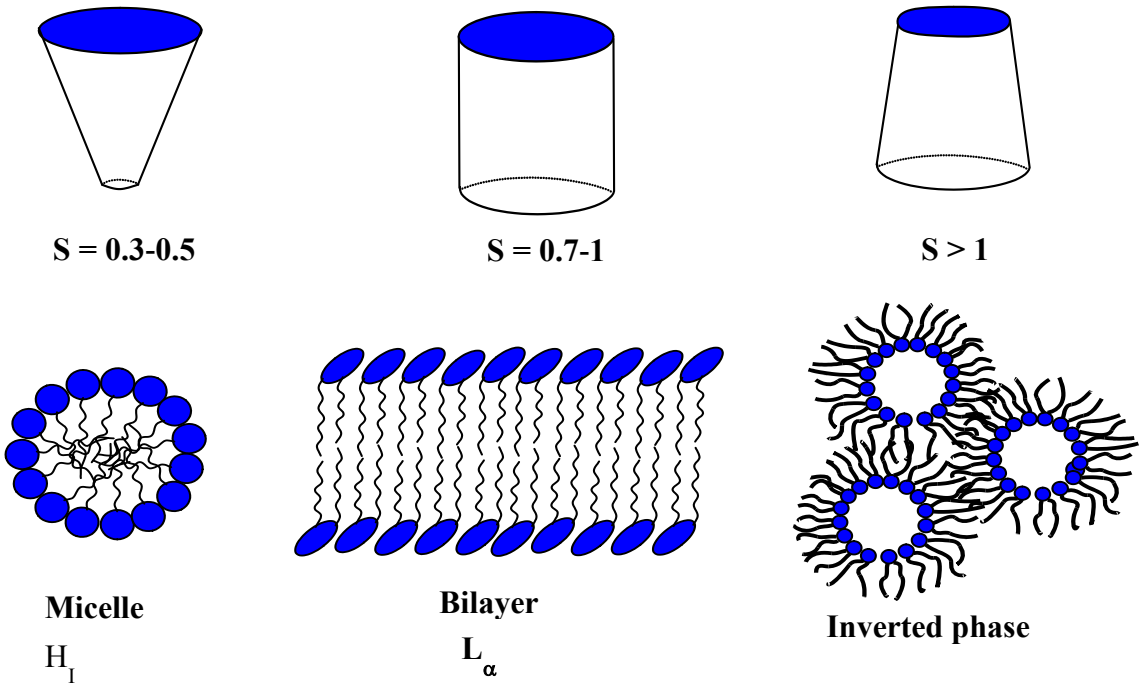

Figure 1.6-Phase structure of lipid aggregates in aqueous solution.

1.4.2-Lipophilicity index and chain length related parameters

The length of the chains of the lipophilic parts of the lipids is one of their key structural parameters. It directly affects the phase behaviour, which in turn affects the transfection efficiency. It is impossible to predict the phase behaviour of any real lipid mixture[31], however from studies on melting behaviour of pure lipids, a direct correlation between chain length and melting temperature can be observed[31-32]. At lower temperatures, a pure lipid is in a crystalline or gel phase, where both the chains and the headgroups are solid-

ordered. As the temperature increases, the chains start to melt to form a ripple phase in which the chains have fluid-like character but the headgroups maintain a solid order. Further heating eventually reaches a sharp transition at a melting temperature (T_m), where both the headgroups and chains are melted and the lipids are in a liquid-ordered fluid phase. Comparison of melting temperature of phosphatidyl choline lipids with chain length shows an increase in T_m with the addition of methylene groups to the chain. Though the presence of varied headgroups can offset the melting temperatures they do not change the slope of the dependency of T_m on the number of carbons in the chains[31-32]. The data correlating the chain length to melting temperature all extrapolate to an intercept around lipids with chains of nine carbons; lipids with alkyl chains shorter than nine are believed to be incapable of forming lipid-like phases. In addition to chain length, the saturation of the chains affects the melting temperature. The presence of a cis-alkene bond, depending on the position of the double bond on the chain, lowers the T_m. For example in the case of 18:1PC, T_m decreases from 40°C to -20°C, when the cis alkene bond moves from the second carbon on the chain to the ninth[32].

In a study of a series of phosphotriester lipids, it was shown that for binary mixtures of these cationic lipids, the phase structures can be predicted based on the T_m of the mixture which can be related to the number of the carbons in the chains[15b].

Chain length affects other structural parameters of the lipids, such as the critical micelle concentration which was one of the key experimental parameters used to define values for the calculation of partition coefficients. Partition coefficient (clogP), is the partition of a molecule in octanol-saturated water, which has been used to determine membrane permeability of solutes in biological applications. ClogP can be calculated

directly from structure using the Hansch and Leo method[33] based on addition of structural increments of different groups within a molecule. Since addition of a methylene contributes a fixed structural increment, clogP of lipids correlates its value directly to chain length and indirectly to melting temperature. Table 1.1, shows calculated values of clogP using the software in ACDlab ChemSketch and the experimental T_m of series of PC lipids with varied chain length. While there is a good agreement between calculated and experimental T_m, it can be seen that as more CH_2 are added to the chain, there's an increase in these values and clogP is reliable for demonstration of this correlation[31].

Table 1.1-Calculated clogP and calculated and experimental T_m of PC lipids with chain length of 12 to 18 carbons.

PC lipid	Number of carbons	Calc. T_m (°C)	Exp. T_m (°C)	clogP
DLPC	12	-11.2	-3.8	6.6
DMPC	14	28.8	23.6	8.7
DPPC	16	44.5	41.3	10.9
DSPC	18	52.9	54.7	13.0

1.5- Previous "QSAR" studies on transfection

Quantitative structure–activity relationship (QSAR) is a model, used in biological and chemical sciences, using structural parameters to predict a chemical, physical or biological property of the molecule[34]. Considering the growing necessity for establishing an efficient non-toxic, non-viral nucleic acid delivery system and the effect of structural parameters of lipids on the mechanism and efficiency of transfection, there is a need to develop a method to be able to predict the transfection efficiency of the lipid mixtures used in lipoplexes based on the molecular parameters of the pure components and the

stoichiometric composition of the lipoplex mixtures. Currently, such a model cannot be applied to transfection efficiency because there is insufficient information about what is important from a molecular perspective to allow a focussed QSAR effort. The current state of knowledge that can be applied to transfection and used for its prediction can be called “pre-QSAR” studies.

Previous studies typically looked at one or two headgroups with variable chains. Such studies uncover the effect of headgroup and chain length as noted above. However most of these studies were empirically inspired and though valuable in highlighting the important structural requirements for optimizing the efficiency of cationic lipids, they cannot be used as a general predictive tool for the activity of the same lipids in transfection[8, 35].

A detailed review was carried out on the qualitative relationship between molecular parameters of cationic lipids and their transfection efficiency[8a]. The effect of headgroup, chain length and structure of the hydrophobic moiety, linker and counterion has been studied here. Within a series of lipids, it is evident that cationic phospholipids are a favoured group of cationic lipids, because of their good transfection efficiency and their relatively low toxicity. One of the best studied lipids of this class, EDOPC, has been shown to have a similar transfection efficiency as a commercial mixture Lipofectamine®[36]. The transfection efficiency of cationic PC lipids is dependent on the length and unsaturation of the alkyl groups. It has been shown that transfection increases with increasing the unsaturation from 0 to 2 alkene bonds. It is concluded that optimum transfection occurs in cationic PCs with total carbon numbers between 30-50, as the

number of carbons in the chains affects the melting temperature and phase behaviour which is related to transfection efficiency.

In an earlier study, Horobin and Weissig[35] have explored a QSAR for the effect of molecular parameters on transfection efficiency by the cationic lipids published prior to 2004. Among the lipids chosen for this study, were phospho-and sphingo-lipids with small and large headgroups with saturated and mono unsaturated chains of 16-18 carbons. The dataset was dominated by compounds related to DOTAP, DOSMA, DOTMA and DOGS (Figure 1.4).

To quantitatively describe the structures of these lipids, these authors define the following parameters: amphipathic index (AI), clogP (logarithm of the octanol-water partition coefficient), headgroup charge (Z), critical chain length (l_c), lipid domain size and headgroup size (HGS, LDS, see below). All these parameters are directly available from the structure by simple additive calculation. The clogP was calculated using the Hansch and Leo method[37]. The amphipathic index, which is used to predict the surfactant character of the amphiphile, uses the clogP of only the hydrophobic moiety of the cationic lipid. To measure the geometric parameters of the lipid, the critical chain length (l_c) was calculated using the Israelachvili method[29]. This method ascribes a distance increment to each methylene in the chain so is directly related to the chain length. LDS (lipid domain size) has been defined using the sum of the atomic masses of the lipophilic part. HGS (headgroup size) was calculated as the sum of atomic masses of atoms in the headgroup.

HGS, LDS and l_c could in principle be used to determine a parameter like the shape parameter but this was not explicitly done. Using the parameters for the set of cationic

lipid experimental transfection data, this study correlated only two parameters at a time, mainly AI-clogP and AI-HGS. Though lipids with different shapes were included in this study, the effect of shape was not considered and was not correlated to transfection efficiency.

Diamond and Gruneich[8b] conducted another QSAR study on five sterol-based cationic lipids bearing a common spermine headgroup. They formed the lipoplex with DOPE as the co-lipid (Figure 1.7). A related cholesterol based lipid had previously shown good transfection efficiency, so it was chosen as the parent compound for this study and was included in the QSAR study.

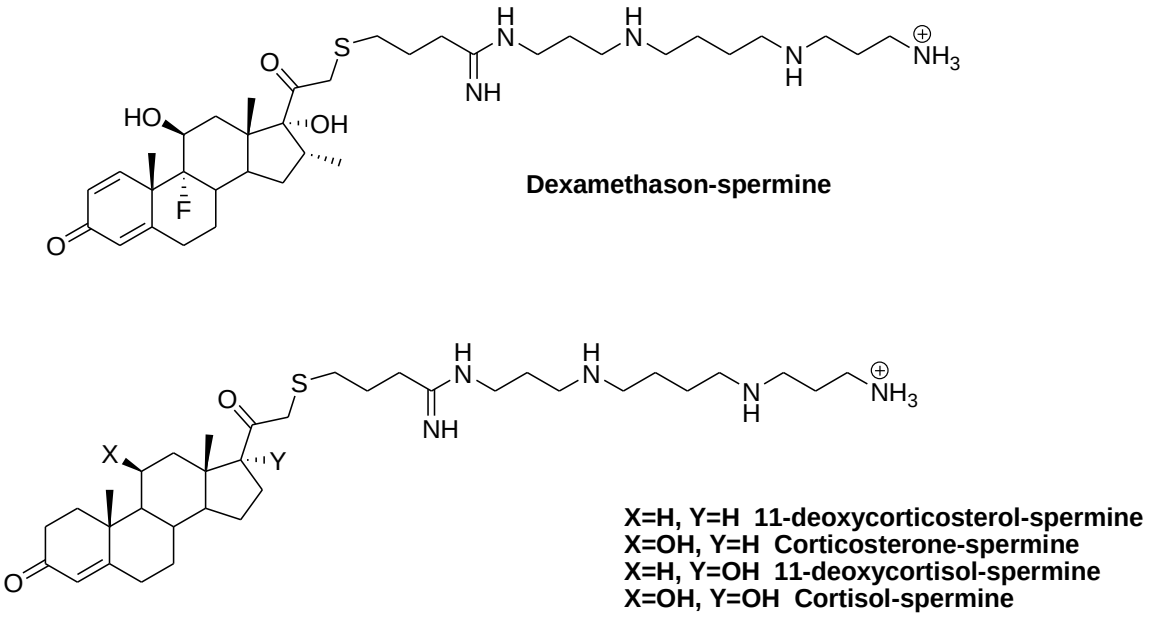

Figure 1.7-Structures of spermine linked sterol based cationic lipids[8b].

These authors noted that the main stoichiometric parameters affecting transfection are the ratio of cationic charge of the lipid to the anionic charge of DNA (charge-ratio, CR), the total lipid to DNA weight ratio, and the ratio of cationic lipid to neutral lipid mole

ratio. The lipoplexes were made with cationic lipid: DOPE ratios of 2:1, 2:2, and 2:4, and CR ranging from 2 to 24. The transgene expression (Enhanced Green Fluorescent Protein

(EGFP) fluorescence per well) was measured at 24 h and 48 h. The results showed that the transfection efficiency was dependent on the hydrophobic moiety of the cationic lipid which is represented by logP(which is the calculated value); as logP increased, so did the transfection efficiency. The data are dominated by the relationship between the transfection and CR which rises to a maximum at some critical value in the raw data of each compound.

The relationships observed in the combined dataset lead to development of a lipofection index (LI) defined as

$$LI = CR\left[\frac{R}{R+1}\right]\left(logP_{\ liposome}\right)\left(\frac{logP_{ster}}{|logP|}\right) \qquad \textbf{\textit{Equation 1.2}}$$

Where logP = $logP_{DOPE}$ -$logP_{ster}$ and $logP_{liposome}$ is the mole weighted average of the DOPE/cationic lipid obtained as:

$logP_{liposome} = (n_{ster}\, logP_{ster} + n_{DOPE}\, logP_{DOPE})/(n_{ster} + n_{DOPE})$ ***Equation 1.3***

where n_{Ster} and n_{DOPE} are the number of steroid molecules and DOPE molecules per phosphate in the DNA, respectively.

The lipofection index (LI) encompasses several of the known variables which affect transfection. The first two terms of Equation 1.2 directly relate to the lipoplex size and indirectly influence the internal morphology (lamellar/hexagonal lipid phase), the third term relates to the overall lipophilicity of the formulation, and the final term was viewed by these authors as proportional to the ability of the components to migrate from the

lipoplex to the endosomal wall as the lipoplex unravels in the endosome. A plot of the transfection results against the CR and LI is shown in Figure 1.8.

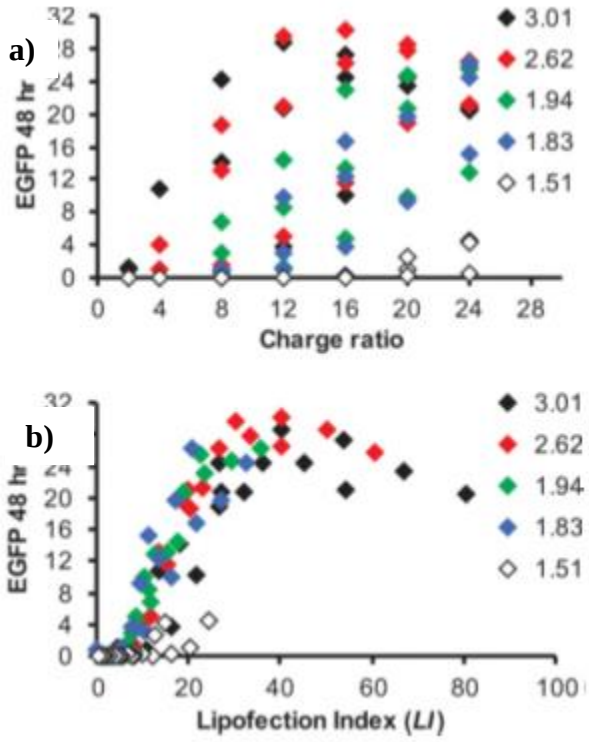

Figure 1.8-EGFP expression in BAEC 48 h (a) post-transfection for cationic steroid-spermine conjugates. Expression data (a) can be remapped to a master curve (b) using the dimensionless parameter, lipofection index (LI). (Figure adopted from[8b] with permission of John Wiley and sons.)

The obtained data suggest that CR is a key parameter in transfection and the best lipoplexes are formed at intermediate CR which also are less cytotoxic than higher CR formulations. The effect of CR and the effect of clogP can be also observed in the bell shaped master curves of EGFP transfection against LI. The shape parameter implicit in the work of Horobin[35] was not considered here. It would be relatively constant for these sterol based lipids.

In another approach, Safinya et al[8c] studied a series of multivalent lipids (MVL) with varied valence (charge) headgroups with co lipids DOPE and DOPC, using a DOTAP and DOPC mixture as the control (Figure 1.4). Some of the mixtures produce lamellar lipoplexes while others produce lipoplexes with hexagonal morphologies. They had shown previously that transfection efficiency in lipoplexes with a lamellar phase is dependent on the membrane charge density (σ_M), whereas lipoplexes with a hexagonal phase are independent of σ_M[38]. These authors conclude that in lamellar systems, the transfection efficiency is determined by efficiency of endosomal uptake of the lipoplex into the cell which is dependant of the membrane charge density. Investigating the transfection efficiency of these lipids, it was shown that there is a Gaussian relationship between transfection efficiency and σ_M (Figure 1.9).

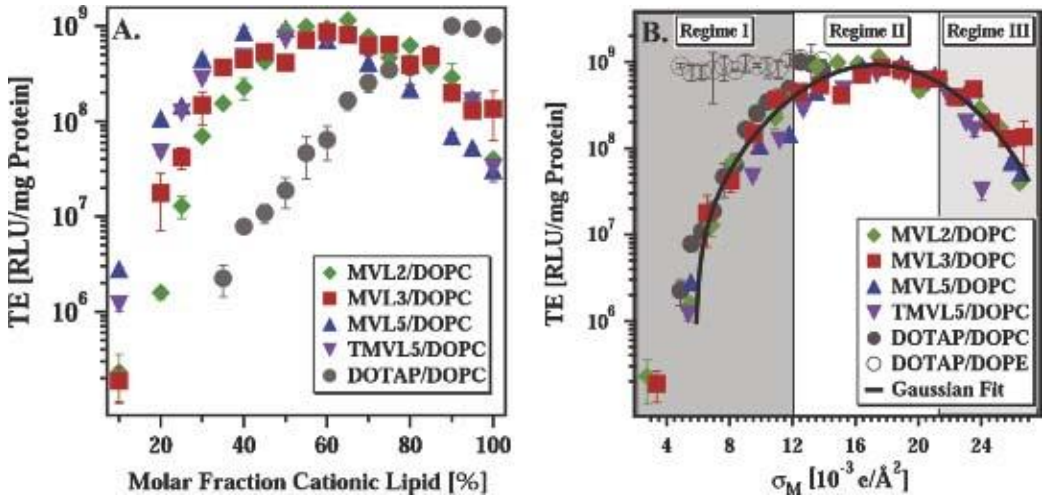

Figure 1.9-(A.) Transfection efficiency (TE) as a function of mol% DOPC for DNA complexes prepared with MVL2 (diamonds), MVL3 (squares), MVL5 (triangles), TMVL5 (inverted-triangles), and DOTAP (open circles). All data was taken at CR 2.8. (B.) The same TE data plot. (Figure adopted from[8c] with permission of Springer.)

Though there was good correlation between transfection efficiency and σ_M, applying it to lipids forming a hexagonal phase gave a poor fit (DOTAP/DOPE; data on the upper left of panel B).

1.6-Cytotoxicity of cationic lipids in transfection

Cationic lipids can cause toxic effects to cells and lipoplexes can cause cells to shrink, reduce mitosis and induce vacuolization of the cytoplasm. Studies have shown that toxicity depends on the cell type, as well as structural parameters of the cationic lipids[8c, 10a, 17, 19, 26, 39]. Cationic lipids can interact with protein kinase C (PKC) enzymes[19].

One of the main causes of toxicity is the cationic nature of the lipids so the hydrophilic part and its positive charge are key points. To reduce the toxicity, heterocyclic headgroups with delocalized positive charge, such pyridinium and imidazolium, have been used to replace the more localized charges of ammonium headgroups. In some cases the transfection efficiency remains high[18c, 39a].

The stability and biodegradability of linkers is also effective in determining the toxicity of cationic lipids. While ether linkers are more stable and can have high transfection efficiency (Lipofectin), they cannot undergo biodegradation at a later stage, either to release the nucleic acid cargo or simply to degrade to non-cytotoxic components[19]. Because of their biodegradability, esters and amides are advantageous; however they are susceptible to hydrolysis in circulatory systems which could limit their application *in vivo*. Carbamates have been found to be stable in circulation systems, and to undergo acid hydrolysis once inside the cell (where the pH of cytoplasm is lower compared to the circulatory system)[26].

For lipids with aliphatic chains, single chain lipids have been shown to be more toxic than double chains[40].

Another critical factor is the CR of the lipoplexes; lipoplexes with higher CR are more toxic to cells. As the CR increases there is a larger dose of cationic lipids in the system. It is desired to have the lipoplex with optimal transfection efficiency at the lowest possible CR to achieve low toxicity.

1.7-Project goals

Looking at the previous QSAR studies, it was evident that the σ_M approach is not directly predictive because the optimum value is a fitted parameter of the data and is not defined by the molecular structure of the lipids at any point in the analysis. Also most of this data is applicable in lamellar systems. We do not know if the steroidal system discussed above was lamellar or hexagonal but it does employ a useful approach for a QSAR which does not rely on the dataset to produce the linearization parameter. An empirical approach of observing correlations and optima as done previously does suggest that it should be possible to shift from the observational to the predictive.

The main goal of this project is to develop a "pre-QSAR" tool based on molecular parameters of cationic lipids to predict transfection efficiency. Were such a tool to be developed, it would permit function-oriented design of cationic lipids with high likelihood of high activity. Considering that an efficient vector should also have low toxicity as well as high transfection efficiency, the development should also study, and eventually predict, the toxicity of the cationic lipids, again based on molecular parameters and lipoplex parameters.

To this purpose, a class of pyridinium lipids was selected for study. Pyridinium headgroups are favoured because of their delocalized positive charge which gives favourable electrostatic interactions. This diffused charge was expected to provide the necessary balance between binding of DNA and its later release from the lipoplex. It was also expected to reduce cytotoxicity. Also, pyridinium lipids were expected to form lipoplexes with an internal hexagonal phase which was expected to be an advantage in the transfection efficiency.

The lead compound **diC16:0** (Figure 1.10) has been synthesized previously[18a] and is known to have reasonable transfection efficiency with relatively low cytotoxicity, depending on the cell line. The initial targets selected for study were ether linked-lipids; as developed in the synthesis chapter we later shifted to ester linkers for synthetic access to a larger library of structures. Hydrocarbon chains with varied length, unsaturation and structure were selected in line with the development of the structure-activity relationships uncovered (Figure 1.10).

The complete set of structures comprises a series of cationic lipids with a range of shape parameter, clogP, and chain length which will allow exploration of potential quantitative correlation of the structures to their activity.

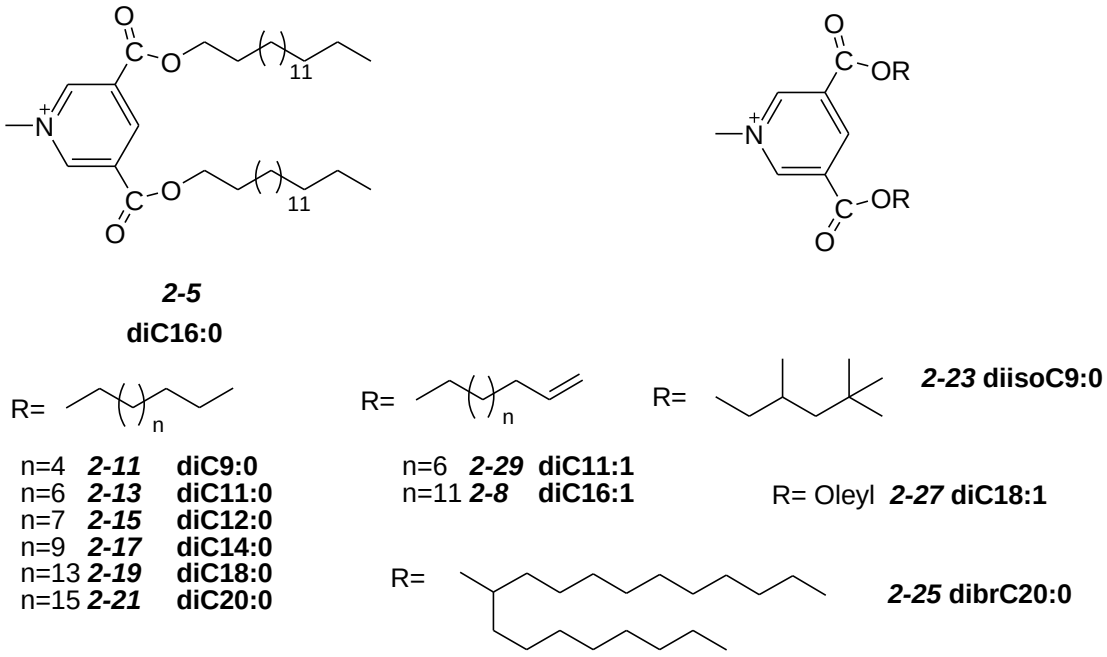

Figure 1.3-Some of the synthesized pyridinium lipids.

Considering the advantages of binary mixtures of cationic lipids, the lipoplexes were formed using the synthesized pyridinium lipid and a commercial cationic lipid 1,2-dimyristoyl-sn-glycero-3-ethylphosphocholine (EPC). As for neutral co-lipids, DOPE and cholesterol were used to facilitate the fusogenistic process, the release of nucleic acid, and to increase the stability of the lipoplex. The formed lipoplexes were studied using small angle x-ray scattering (SAXS) and their transfection activity and cytotoxicity in Chinese hamster ovarian-K1 (CHO-K1) cells was studied and measured. These results were used to correlate the computed lipid structural parameters and other lipoplex properties to transfection efficiency. The analysed data were used to develop a Transfection Index (TI) to predict the transfection efficiency of these lipids. In parallel the cytotoxicity of these lipids was correlated to structural parameters and lipoplex formulation variables.

1.8-Thesis overview

The second chapter of this thesis will provide an overview of the materials and methods used for obtaining the data. Chapter three will discuss the synthesis and characterization of the synthesized compounds. The results of lead compounds (**diC16:0** and **diC16:1**) and initial TI development will be presented in chapter four. Further development of TI and application to the full dataset on synthesized cationic lipids leads to a more detailed look into lipid properties and a refined TI as discussed in chapter five. Chapter six will present a summary of the work done and will suggest future work.

The key data on which these studies are based are presented in three appendices. Appendix A includes the detailed synthesis information and the characterization of synthesized compounds including the ^{1}HNMR, ^{13}CNMR, and mass spectroscopy data while Appendix B gives the archival spectra. These data are from my own work. All the data from the project collaborators are presented in Appendix C. These data are unpublished and remain the property of my collaborators.

Chapter 2: Materials and methods

2.1-Synthesis

The general procedures of the main reactions are described here. Full details and compound characterization are presented in Appendix A.

2.1.1-Ether coupling:

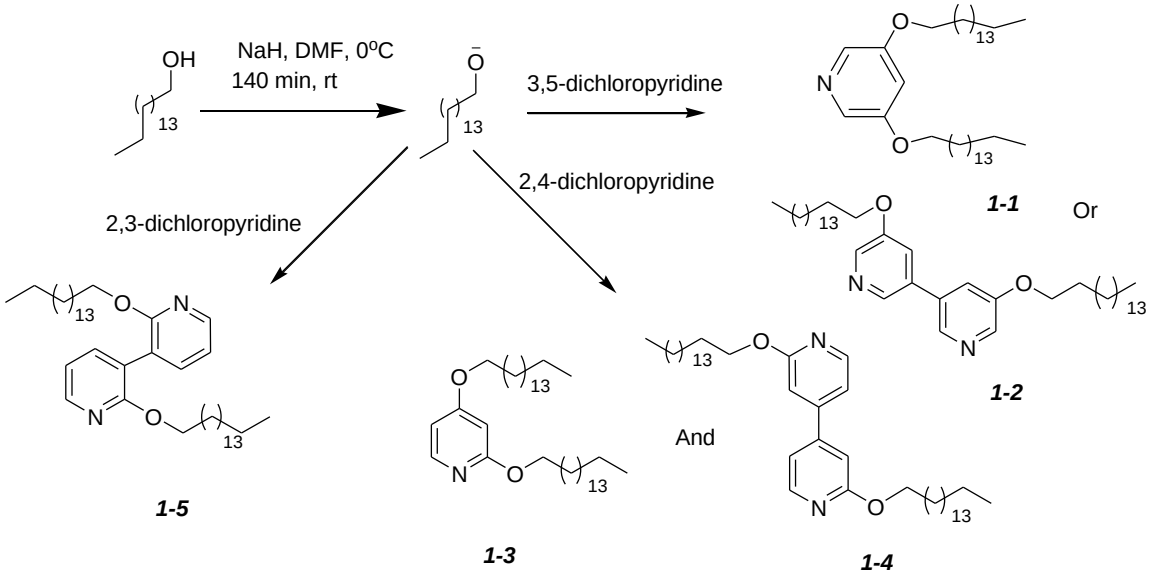

Scheme 2.1-Ether coupling for synthesis of compounds *1-1* to *1-5*.

To an anhydrous suspension[41] (Scheme 2.1) of 1 equivalent (relative to the alcohol) of NaH (60% in oil) in distilled DMF in a round bottom flask, alcohol was added at 0°C and the solution was stirred for 140 min at room temperature. Dichloropyridine was added and the mixture was stirred for 60 h at 120°C. The reaction was quenched by adding water, and the product was extracted with DCM (4 times), and then washed with water (twice) and saturated $NaHCO_3$ (3 times) and dried over sodium sulphate. The crude product was purified by column chromatography on silica gel, using ether/hexanes as eluent.

2.1.2-Ester coupling (Scheme 2.2)[42]:

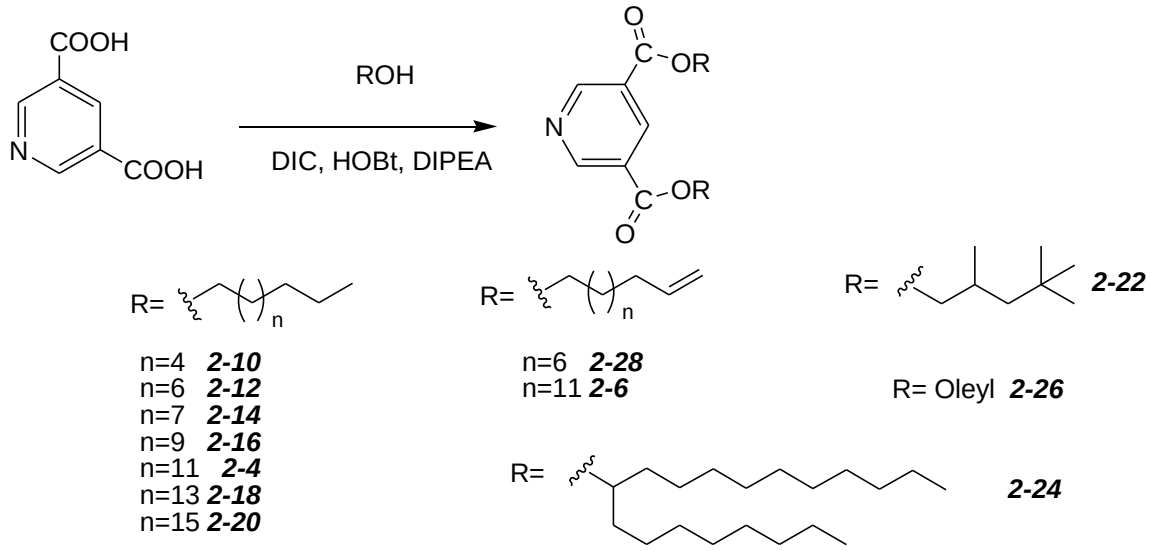

Scheme 2.2-Ester coupling for synthesis of 3,5-dialkyloate pyridine.

To a solution of 1 equivalent of 3,5-pyridinedicarboxylic acid (Scheme 2.2) in THF 2.4 equivalent of DIC, HOBt, alcohol and N,N-diisopropylethyl amine were added. The reaction was sealed under an atmosphere of N_2, and stirred for 24 h at room temperatures. Once complete, the reaction was filtered to remove DIU, and diluted with DCM. The organic phase was extracted with phosphate buffer (pH= 3) (twice), water (twice) 10% NaCl (twice) and rinsed with sat. NaCl (once), dried with anhydrous sodium sulfate, and concentrated under vacuum. The crude product was purified by column chromatography on silica gel, using ether/hexanes as eluent.

2.1.3-Methylation reaction (Scheme 2.3):

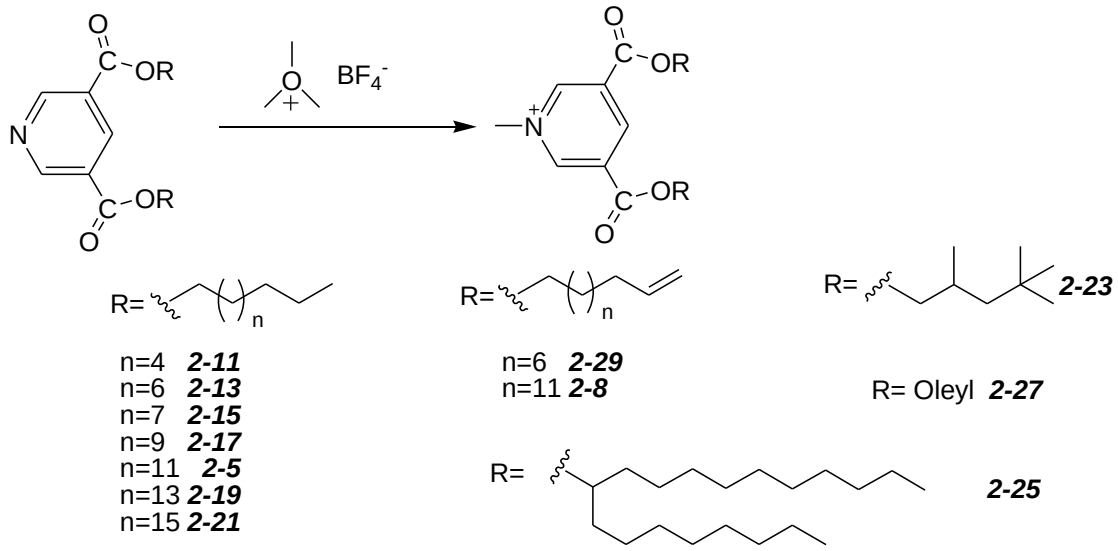

Scheme 2.3-Methylation reaction for synthesis of 3,5-dialkyloate methyl pyridinium.

To a solution of 1 equivalent of the synthesized diester pyridine in DCM (Scheme 2.3), 1 equivalent of trimethyloxoniumtetrafluoroborate was added and stirred at room temperature overnight. The mixture was concentrated in vacuu to give the tetrafluoroborate salt of the target compound in quantitative yield.

2.2-Analysis of mixture of products

The products of ternary mixture of compounds were analyzed using ^{1}HNMR and ESI-MS. Using the ratio of integration of relevant peaks of ^{1}H shifts, the composition of the mixture could be determined in some cases.

For a more precise analysis, solutions of the compounds were prepared in three different concentrations of 0.1, 0.2 and 0.5 mM and the ionization efficiency of the compounds present in the ternary mixture were shown to be the same using ESI-MS. The ratio of ion intensity of each compound was then measured to determine the composition of the mixture.

2.3-Biological methods

These procedures were done in the collaborators' lab, the group of Dr. Michael Pungente, Dr. Emile Jubeli, Nada Abdul Khalique, Liji Raju, Ahmed Almeer, Hebatalla Allam, Maryem Al Manaa and Zara Awais, and are given here for completeness. The procedures are published in "Aspects of non-viral gene therapy: Correlation of molecular parameters with lipoplex structure and transfection efficacy in pyridinium-based cationic lipids", Parvizi, Paria; Jubeli, Emile; Raju, Liji; Khalique, Nada Abdul; Almeer, Ahmed; Allam, Hebatalla; Al Manaa, Maryem; Larsen, Helge; Nicholson, David; Pungente, Michael D.; Fyles, Thomas M., *International Journal of Pharmaceutics*, 461, 145-156, **2014**. The assembled biological data on which the thesis is based are given in Appendix C.

2.3.1-General

Cationic lipids included the synthetic pyridinium lipids and commercial lipid 1,2-dimyristoyl-sn-glycero-3-ethylphophocholine (EPC). The co-lipids used for the formulation of liposomes and lipoplexes were 1,2-dioleoyl-sn-glycero-3-phosphoethanolamine (DOPE) and cholesterol. As neutral lipids, the concentrations of DOPE and cholesterol were not included in the final calculation of charge ratios when forming lipoplexes between cationic lipids and DNA (Figure 2.1).

2.3.2-Preparation of lipid ethanolic stock solutions

Stock solutions of synthesized pyridinium lipids, commercial cationic lipid EPC and co-lipids DOPE and cholesterol were made by dissolving a known amount of each lipid in dichloromethane in a round-bottom flask at rt. The solutions were placed on a rotary evaporator for 1 h to obtain a film. The film was dissolved in a known amount of anhydrous EtOH in order to achieve a 1 mM stock, and subsequently stored at −80°C .

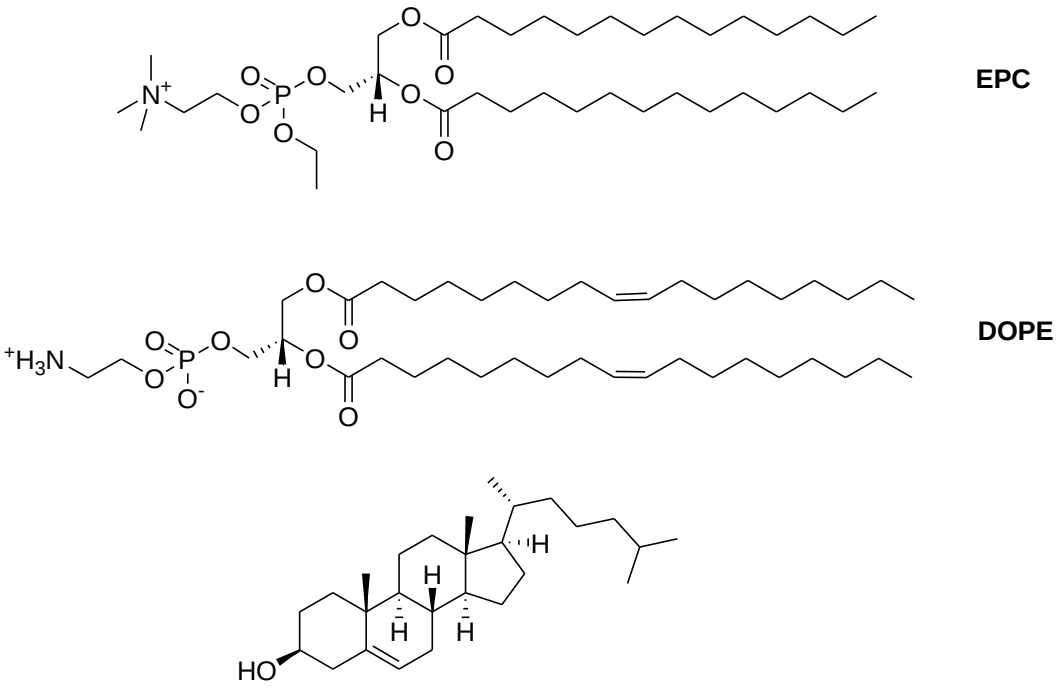

Figure 2.1-Cationic and neutral co-lipids in the liposome formulation.

2.4- Liposome formulations

An overall 3:2 molar ratio of total cationic lipid (synthetic lipid combined 1:1 with EPC, or control lipid EPC alone) to co-lipid, DOPE or cholesterol, in ethanolic solutions were prepared separately at rt and evaporated under reduced pressure to generate thin films. The lipid films were hydrated with a known amount of sterile water to give 2 mM final hydrated stock solutions, which were stored overnight at 4°C. Before use, the hydrated stocks were warmed to 37°C and sonicated for 30 min.

2.4.1-Preparation of lipoplexes (lipid/pDNA complexes)

Lipoplexes of concentrations 0.081 mM, 0.243 mM, 0.486 mM, 0.81 mM and 1.62 mM, corresponding to the N/P (+/−) molar charge ratios of 0.5:1, 1.5:1, 3:1, 5:1 and 10:1, respectively, were prepared from the 2 mM liposome stocks. OPTI-MEM buffer (57.6 µL) and pDNA (14.4 µL; 250 ng/ µL) in Elution solution, were first combined, followed by the addition of an equal volume of corresponding liposome (72 µL) to this and mixed.

These lipoplex formulations were incubated at rt for 30 min. 48 µL of lipoplex formulation was used for the gel assays and to each of the remaining lipoplex formulations, 204 µL of OPTI-MEM was added prior to use for transfection experiments. The Lipofectamine 2000^{TM}/DNA control was prepared according to the manufacturer's protocol.

2.4.2-Liposome and lipoplex sizing

The hydrodynamic diameter, d_H, of liposomes and lipoplexes was measured by dynamic light scattering (DLS) with a Zetasizer APS(Malvern Instruments, Worcestershire, UK) at 25°C with a detection angle of 90º. All data are the mean ± standard deviation (SD) of three measurements.

2.4.3-Gel retardation assays of lipoplexes

To 20 µL of the lipoplexes, 2 µL of the gel loading dye (6X) was added and mixed by pipetting. Eighteen microliters of each sample were then loaded onto a 1% agarose gel impregnated with ethidium bromide and run at 105 V for 1 h in 1× TBE buffer. The migration of pDNA complexed with the cationic lipids was impeded in the electric field. The pDNA bands were observed using a Geliance transilluminator.

2.4.4-DNase I degradation assays of lipoplexes

Twenty microliters of the lipoplexes was incubated with DNase I (1 µL) at 37°C for 1h. After incubation, 5% sodium dodecyl sulfate (SDS) (4 µL) were added and incubated for an additional 30 min, followed by 2 µL of gel loading dye (6x). Eighteen microliters of each sample was then loaded onto a 1% agarose gel impregnated with ethidium bromide and run at 105 V for 1h in 1× TBE buffer. The pDNA bands were observed using a Geliance transilluminator.

2.5-Cell culture

CHO-K1 cells were grown in RPMI medium supplemented with10% fetal bovine serum and 100 U/mL of penicillin/streptomycin and 0.25 µg/mL amphotericin B. Cells were seeded 48 h before transfection in to both opaque and transparent 96-well plates at a density of 104 cells/well and incubated at 37°C in presence of 5% CO_2 atmosphere. Cells were grown to 80% confluence before being washed with 1× PBS and incubated with 45 µL of each lipid-pDNA complex in triplicate for 4 h at 37°C in the presence of 5% CO_2 atmosphere. Complexes were then removed and the cells washed with 1× PBS before adding 100 µL of complete RPMI medium. Cells were left to incubate for an additional 44 h. Following the incubation, transfection and cytotoxicity assays were performed according to the protocols described below.

2.6-β-Galactosidase assay

Forty-eight hours after the application of lipoplexes, β-galactosidase activity was determined using a Beta-Glo®AssaySystem (Promega). Treated cells in the opaque 96-well plate were washed with 1x PBS, then 50 µL of DMEM (phenol red-free medium) was added to each well. This was followed by the addition of 50 µL of Beta-GloTM working solution, prepared according to the manufacturer's directions (Promega), to each well and thorough mixing by pipetting. After 1 h incubation at rt, luminescence was then read on a Victor Envision high throughput plate reader. β-Galactosidase activity was expressed as relative light units produced by the luminescence of luciferin, which was normalized for protein content.

2.6.1-Total protein (BCA) assay

Total protein content was measured using Pierce®BCA Protein Assay (Pierce Biotechnology, Rockford, IL). Forty-eight hours after the application of lipoplexes, treated cells in the transparent 96-well plate were washed with 1× PBS, and 10 µL of passive lysis buffer (Promega) were added to each well. Plates were incubated at rt for 30 min. BCA working reagent (200 µL), prepared according to the manufacturer's directions, was then added to each well, gently mixed by pipetting, and incubated at rt for 1 h prior to reading at 562 nm on a Victor Envision plate reader. A calibration curve obtained from a bovine serum albumin standard solution was used to determine cellular protein content per well.

2.7-Cytotoxicity assay

The cytotoxicity associated with the lipoplex formulations at N/P (+/−) molar charge ratios ranging from 0.5:1 to 10:1was evaluated using an MTS (3-(4,5-dimethylthiazol-2-yl)-5-(3-carboxymethoxyphenyl)-2-(4-sulfophenyl)-2H-tetrazolium) assay. Forty-eight hours after the application of lipoplexes, CHO-K1 cells in the transparent 96-well plates were washed with 1× PBS, 50 µL of DMEM (phenol red-free media) followed by 10 µL of CellTiter96®Aqueous One Solution Cell Proliferation Assay (Promega) was added to each well and mixed by gentle rocking. The plates were incubated further for 1 h at 37°C. The absorbance of converted dye, which correlates with the number of viable cells, was measured at 492 nm using a Victor Envision high throughput plate reader. The percentage of viable cells was calculated as the absorbance ratio of treated to untreated cells.

2.8-Fluorescence imaging

For fluorescence experiments, lipoplexes were prepared using N/P (+/−) charge ratio of 3 (in a 3:2 molar ratio of cationic to co-lipid, respectively) as previously described. Plasmid DNA containing the β-galactosidase gene was replaced in these formulations with plasmid encoding green fluorescent protein (pCMVTnT-GFP) that was used at a concentration of 2.4 µg/ well. Cells were plated in Corning 35-mm tissue culture dishes modified by punching a 7-mm diameter hole in the bottom and reseating with 22-mm × 22-mm #1 glass coverslip (Clay Adams Gold Seal,VWR, Inc.) using a melted solution of paraffin and Vaseline® (3:1) (Baird et al., 1994). After coating the exposed glass surface with poly-d-lysine (0.1 mg/ml, 1 h), coverslip dishes were seeded with 2.5×10^4cells and maintained at 37°C with 5% CO_2 for 24 h, after which 100 µL of GFP-lipoplexes (prepared as described previously) were added and incubated with cells for 4 h before the medium was replaced with complete RPMI medium, followed by incubation for an additional 44 h. Images of the GFP expression within cells were obtained using an Olympus IX51 inverted light microscope with epifluorescence optics and a 40× dry objective (Olympus, Japan). The excitation light was provided by an X-cite® exacte mercury arc lamp (Lumen Dynamics, Canada), excitation wavelength was 460-490 nm (blue), barrier emission filter was 520 nm (Olympus filter sets UMWB2 and UMWG2). The images were acquired using a DP72 camera (Olympus).

2.9-Structural characterization of the CL/pDNA lipoplexes using synchrotron SAXS

Structural information, such as the nature of the lipoplex packing morphologies and bilayer-bilayer distance, was obtained by SAXS (Small-angle X-ray scattering) techniques. Owing to the ordered packing a diffraction pattern is superimposed on the

SAXS curve. The SAXS experiments were performed at the European Synchrotron Radiation Facility (ESRF), Grenoble, France, on the bending magnet, BM29 BioSAXS beam line. BM29 is equipped with a double multilayer monochromator (energy band pass ~ 10^{-2}) and 4 mrad torodial mirror 1.1 m long. The experimental hutch is equipped with a marble table housing the modular-length flight tube, 2D detector (Pilatus 1 M) and sample handling equipment (automated sample changer). The sample-to-detector distance was 2.8 m. Samples were prepared in 1 mL Eppendorf tubes, and loaded into the 1.8 mm diameter quartz capillary sample cell by the automated sample changer. Data collection was performed in 16-bunch mode at an energy of 12.5 keV with an exposure time of 2 s per frame using the dedicated beam line software BsxCuBE. The SAXS-curves were obtained by integration and averaging of 20 2D images. Subsequent processing (such as background subtraction and scaling) and analysis were performed using the ATSAS-software package[43] and MATHEMATICA (Mathematica, 2010)[44].

Chapter 3: Synthesis

3.1-Initially designed compounds

The lead cationic lipid (Figure 3.1) structure was inspired by the Engbert pyridinium lipids with a lipophilic part containing a 16 carbon saturated chain with an ester group as the linker between the headgroup and chain[18a]. An ether linker was introduced instead of an ester linker as it has been shown that ether groups increase transfection efficiency and are more stable because of their higher resistance to hydrolysis.

Two additional analogues were designed, one with the same headgroup and linker, but with terminal alkene bonds which would act as the metathesis precursor for the cyclic analogue with a 35 membered ring (Figure 3.1). This compound was of interest because of the potential of a cyclic compound to alter transfection efficiency. This target is similar to cholesterol in overall size and might have improved miscibility with a cell membrane.

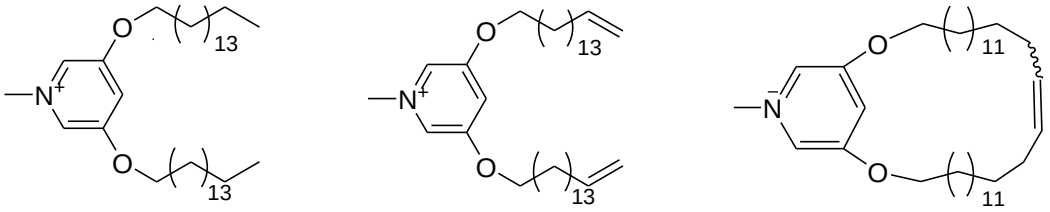

Figure 3.1-Initial designed structures.

The synthesis was based on previous examples from the literature as shown in Scheme 3.1. One published route used the alkoxide of hexadecanol produced by reaction with sodium hydride in a nucleophilic displacement of chloride from 3,5-dichloropyridine[41]. A reported alternative used Pd-catalysed coupling of the same partners[45].

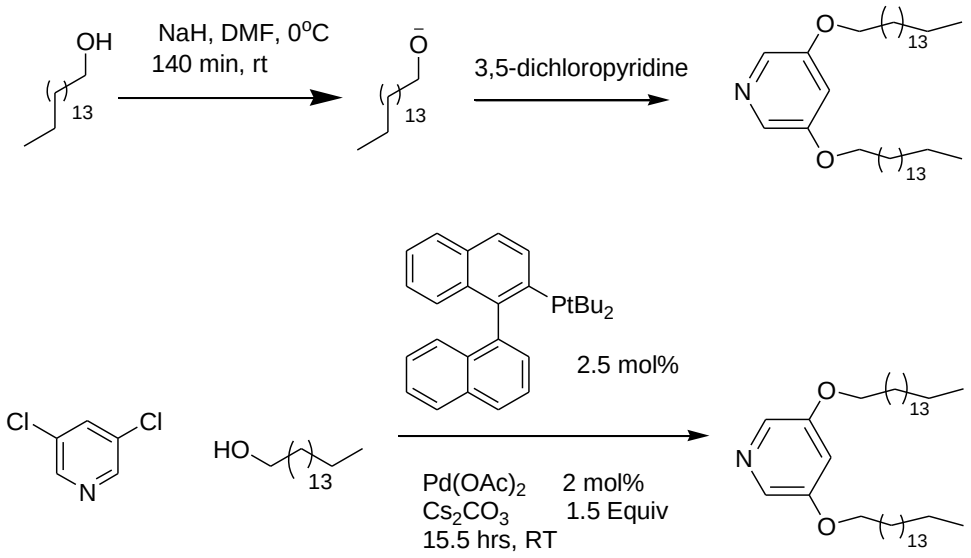

Scheme 3.1-Reported synthesis routes of ether pyridines.

An initial reaction using the sodium hydride method produced a sample of the required product ***1-1*** isolated by recrystallization in 33% yield. The product showed the expected ^{1}HNMR spectrum for a 3,5-substituted pyridine bearing two alkoxy chains. However, this proved to be an isolated result which was not reproducible and did not yield the desired product.

To improve the yield the temperature of the nucleophilic displacement was increased to 120ºC from 85ºC. However this yielded an alternative product and failed to produce any of the expected pyridine diether. Numerous attempts to reproduce compound ***1-1*** were not successful and the alternative product ***1-2*** appeared in low to moderate yield in most attempts.

To explore the synthesis of diether products further, other derivatives were investigated: 2,3-and 2,4-dichloro pyridine (done by Alyssa Neal), and 2,4-dibromo and 3,5-dibromo pyridine. Synthesis with 2,4-dichloro pyridine yielded a mixture of both product mono-and bi-pyridines whereas in the cases of 2,3 and 3,5-dichloro pyridine only

bipyridine products were formed (Scheme 3.2). To analyse these products, their ^{1}HNMR spectra were studied thoroughly. The ratio between the integration between the protons of the terminal methyl group (H_d) to the protons of the methylene groups next to oxygen (H_c) to protons on the pyridine can determine the product. The observed ratio for each compound in Scheme 3.2, confirms the structures. The ^{13}CNMR establishes the number of carbons in the pyridine and the symmetry. For example, in the products of 2,4-dichloro pyridine, in compound ***1-3***, five shifts are seen for each of 5 carbons in the pyridine group, whereas compound ***1-4*** showed five shifts, different from ***1-3***, each shift for a pair of equivalent carbons. The value of ^{1}HNMR and ^{13}CNMR shifts in the structures were also confirmed the structure of these products. The ESI-MS results were obtained for these compounds, but were not conclusive to be reported.

As the reaction of 2,4-dichloro pyridine resulted in both products, the isolated and purified products were analysed with elemental analysis which confirmed the structures as well. For compound ***1-3***, the ratio between the sums of atomic masses of the carbon atoms to nitrogen atoms (C/N) was calculated to be 31.7, and from the result of elemental analysis it was obtained to be 27.9. For compound ***1-4***, this ratio was calculated to be 18.0 and from the elemental analysis was determined to be 18.0 as well.

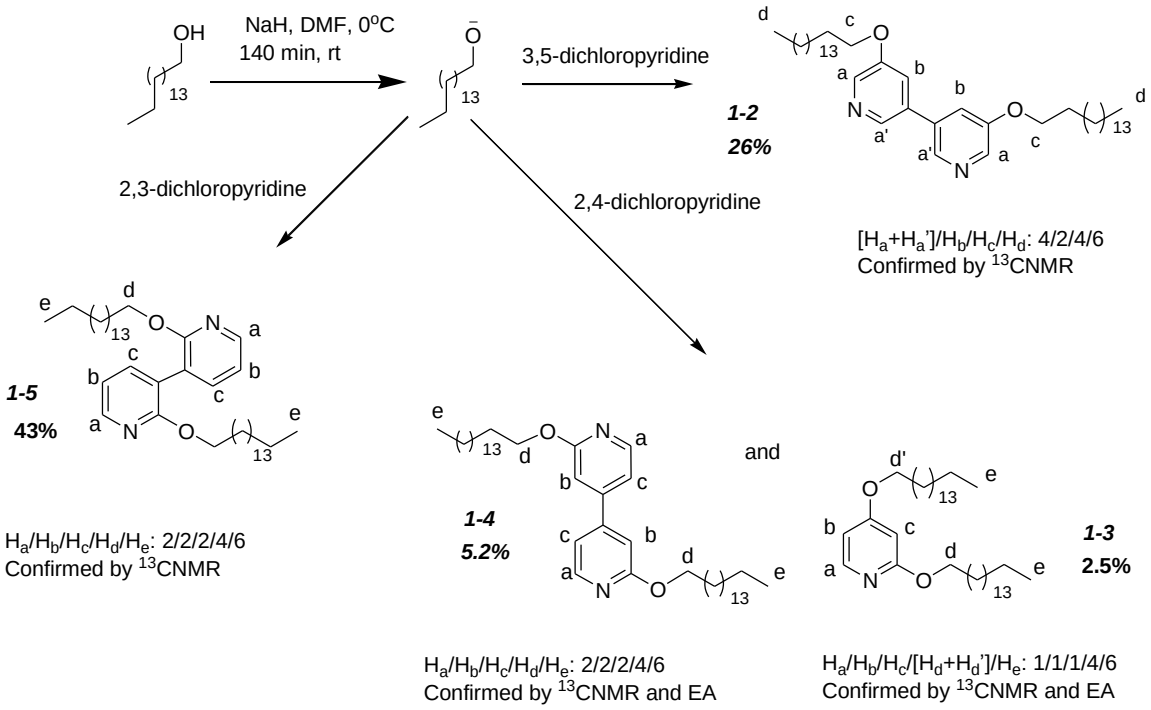

Scheme 3.2-Summary of reaction products in attempted synthesis of diether pyridines by nucleophilic displacement.

To find the reason for formation of bipyridines products, the mechanism for this reaction was considered. The main reaction mechanism leading to ether pyridine products follows a S_NAr mechanism with alkoxide as the nucleophile[46]. However there is a possibility of another mechanism of $S_{RN}1$, caused by thermal electron transfer (ET) from the alkoxide to form an anion radical substrate followed by loss of the chloride leaving group, to form the radical species which could react with other radicals and take part in other reactions. In the review of Rossi et al[47], it was shown that the substrates with two leaving groups can form an intermediate with one leaving group and one substitution which, depending on the final step, can yield side products. The proposed mechanism for reaction of 2,4-dichloro pyridine is given in Scheme 3.3.

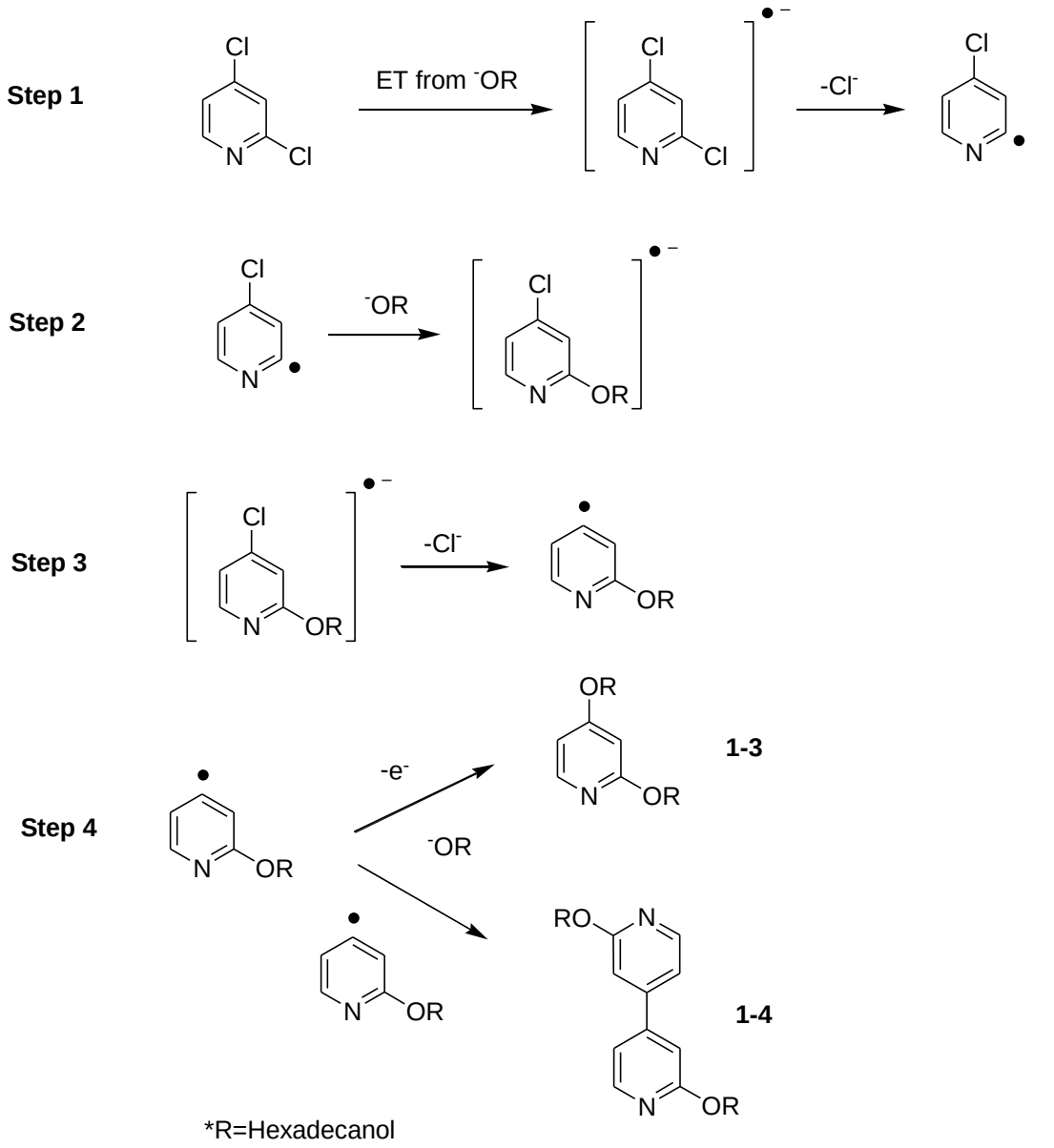

Scheme 3.3-Proposed mechanism for side products in synthesis of 2,4-diether pyridines.

Another method from the literature, shown in Scheme 3.1, was applied using Pd-catalyzed intermolecular coupling of primary alcohols and aryl halides which also has worked for electron deficient substrates[45]. Using 3,5-dichloro and 3,5-dibromo pyridines as substrate and reacting them with hexadecanol in the presence of palladium acetate, caesium carbonate and di-tert butyl phosphine ligand in toluene at room temperature

resulted in no conversion. Increasing the catalyst amount from 2 mol% to 4 and 10%, changing the substrate from dichloro to dibromo and increasing the temperature of reaction also yielded no or very low conversion of the desired ether product. At this point it was concluded that the synthesis of products with ether linkers is not an efficient pathway to synthesize a library of products. Nucleophilic substitution with pyridine halides is apparently prone to side reactions and low reactivity, making a general synthesis a difficult target.

As an alternative, ester linkers were introduced; these may be less efficient in transfection but because of their biodegradability, may be less toxic[39a]. These resulted in the design of a new class of compounds which ultimately grew to a library comprising over a dozen pure compounds and several mixed chain compositions.

3.2-Synthesis of pyridinium diester cationic lipid lead compounds

The preliminary targets were redesigned based on similar structures, only replacing the ether linker with the ester linker. This type of compound has been previously synthesized and studied to show moderate to good transfection efficiency and less toxicity to cells because of presence of the ester linkers[39a]. From this structure, additional compounds were designed, one with terminal alkene bonds which would act as the metathesis precursor for the cyclic analogue with a 35 membered ring (Figure 3.2).

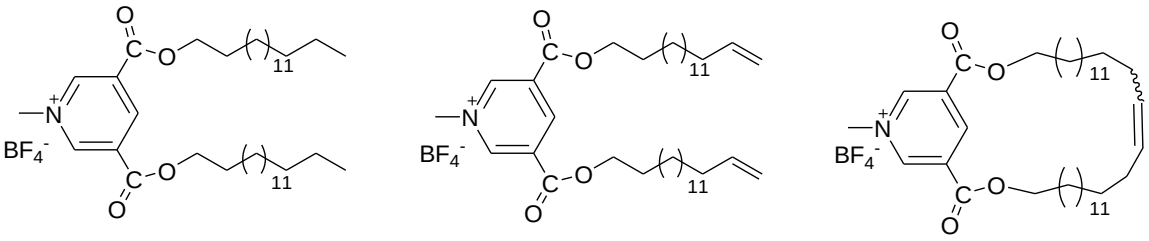

2-5 ***2-8*** **methylated *3-3***

Figure 3.2-Preliminary pyridinium lipids.

3.2.1-Synthesis of hexadec-15-en-1-ol (*2-3*)

Before detailing the general synthesis of the pyridinium diesters, the synthesis of the hexadeca-15-en-1-ol (***2-3***), required for the synthesis of ***2-8***, will be discussed. This synthesis is derived from a literature precedent[48]. At the outset, 11-bromo-1-undecanol was protected as the THP-ether (***2-1***) (compound 2-(11-bromo-undecyloxy)-tetrahydropyran (**13**)) which had the reported spectroscopic properties[49]) (Scheme 3.4).

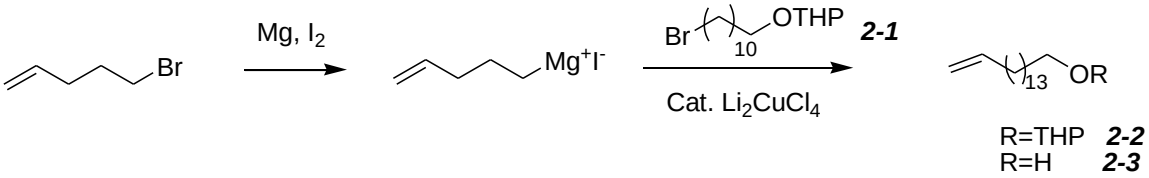

Scheme 3.4-Synthesis of hexadec-15-en-1-ol *(2-3)*.

For the chain extension, 5-bromo-1-pentene was reacted with magnesium and iodine in ether under reflux to form the Grignard reagent, followed by reaction with ***2-1*** in the presence of lithium tetrachlorocuprate as the catalyst. A product obtained appeared to be ***2-2***, however integration of peaks in the ^{1}HNMR were incorrect and there were additional peaks showing the presence of methylene next to Br which suggested the conversion was incomplete. To optimize the yield and conversion of ***2-2*** and have fewer purification steps, the following parameters were investigated; solvent, reflux time, the time of coupling reaction, temperature of the addition of the bromide and the catalyst amount.

Studying THF, ether and dioxane proved that the most suitable solvent is THF for forming the Grignard reagent. Increasing the time of reflux from 0.5 h to 2 h, and the time of the coupling reaction to overnight increased the product yield, however still there were significant amounts of 5-bromo-1-pentene in the product mixture. To avoid the decomposition of the Grignard reagent the temperature of adding the bromide was decreased to -78ºC and the amount of lithium tetrachlorocuprate was increased from the suggested 10mol% to 30mol%. Under optimized conditions 100% conversion of the THP-protected bromide ***2-1*** was achieved. The product was deprotected with pTsOH in a methanol/DCM mixture and alcohol ***2-3*** was purified by chromatography in 70% overall yield based on the starting bromo alcohol. Upon full analysis of the product, a small inseparable impurity was detected. Based on close inspection of NMR data and ESI-mass spectra of subsequent products, the impurity was determined to be 1-undecanol apparently caused by reduction of an intermediate radical by hydrogen abstraction during the Grignard coupling reaction. From integration of the ^{1}HNMR, this impurity comprised about 10% of the sample of the ***2-3*** used in subsequent reactions; the composition of the derived products from this mixed starting material is discussed below.

3.2.2-Esterification

The esterification reaction was carried out based on an established procedure used in the Fyles group. The 3,5-pyridinedicarboxylic acid was reacted with 1-hexadecanol to yield the required diester using N,N-diisopropyl carbodiimide (DIC), hydroxyl-benzotriazole (HOBT) and N,N-diisopropylethyl amine (DIPEA) (Scheme 3.5). The product was purified using column chromatography to give an isolated yield of 59% of ***2-4***.

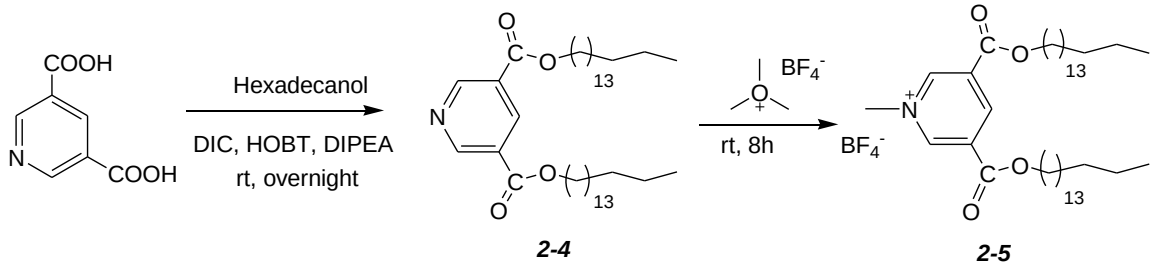

Scheme 3.5-Synthesis of diester product *(2-4)* and diC16:0 *(2-5)*.

The purified product was characterized with ^{1}HNMR and ^{13}CNMR, specifically observing the pyridine peaks, a doublet at 9.35 and a triplet at 8.85 ppm, and the methylene peaks next to ester group, a triplet at 4.38 ppm. In the ^{13}CNMR, the shifts of the carbons on the ring and on the ester group indicated the presence of the expected product. These shifts are common between all of the 3,5-pyridine bis-alkyl esters prepared. ESI-MS was used for further characterization of the purified product, using a sample in methanol with 0.1% TFA acid to improve the ionization; the expected molecular ion (M+H) was observed at 615.7 amu.

Using the same esterification conditions, 3,5-pyridinedicarboxylic acid was reacted with synthesized hexadec-15-en-1-ol ***(2-3)*** to give the desired diester pyridine (***2-6***) (Scheme 3.6). Here the presence of 1-undecanol impurity in the hexadec-15-en-1-ol (***2-3***) resulted in a mixture consisting of predominantly the symmetrical diester ***2-6*** with a small amount of a mixed chain ester with a single unsaturated C16 chain and a saturated C11 chain (***2-7***). A product with two C11 chains is also present but is at a low concentration due to the small amount of undecanol in the starting alcohol. The composition of the mixture was determined by careful integration of ^{1}HNMR signal of methylene next to ester at 4.47 ppm and the terminal methyl protons at 0.88 ppm, to be 10% of ***2-7*** and 90% ***2-6***. The ESI-MS for the sample showed two signals, 612.8 amu for

2-6 and 544.8 for ***2-7***, confirming the identities of the main components in the mixed sample.

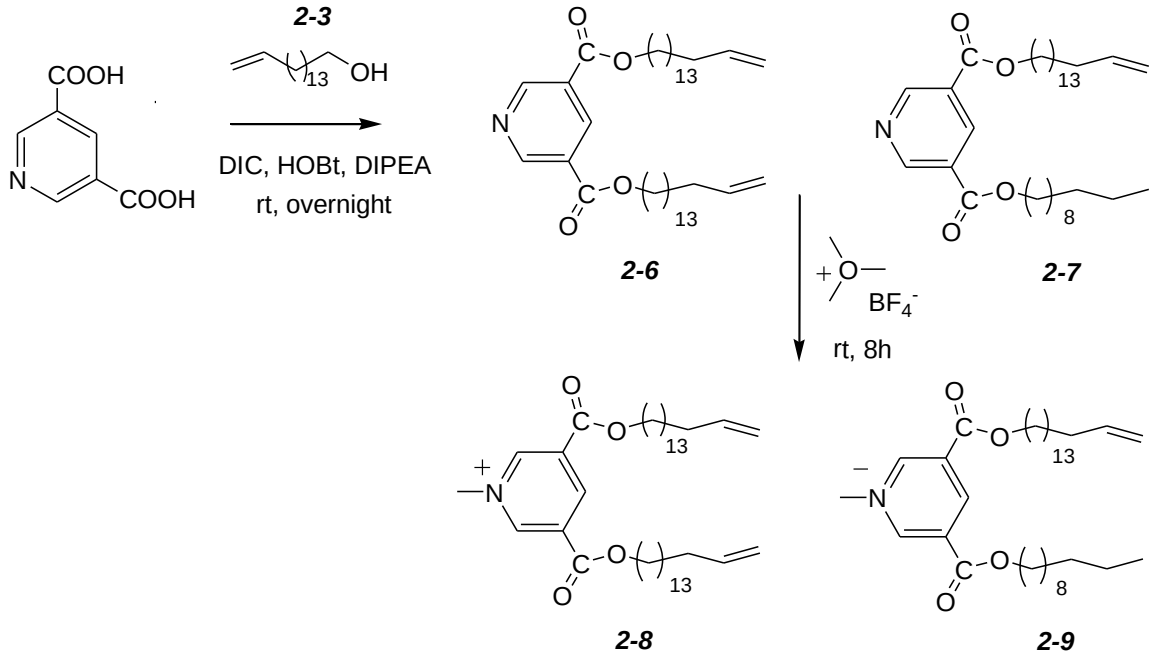

Scheme 3.6-Synthesis route for compound *2-8* with a small percentage of *2-9*.

3.2.3-Methylation of the pyridine esters

In literature reports, the methylation of pyridine lipids to form methyl pyridinium salts was done using methyl iodide and followed by ion exchange to yield chloride salts[18a]. However, the previous reports provided very limited spectroscopic characterization of the product pyridinium lipids. Following this protocol, the synthesized diester pyridines were methylated with methyl iodide, followed by an ion exchange to yield the chloride salt of the methylated product. The ^{1}HNMR spectra always showed that the methylated product was accompanied with small amounts of a contaminant σ-adduct in which the chloride counterion added to the pyridine to produce neutral chlorodihydropyridines (Figure 3.3), resulting in associated doublet peaks at 7.41, 8.02 and 8.85 ppm.

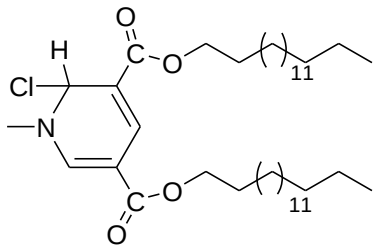

Figure 3.3-Chlorodihydropyridines, σ-adduct product

To avoid this contaminant, the non-nucleophilic tetrafluoroborate salt was prepared by methylation with trimethyl oxonium tetrafluoroborate in DCM to yield the pure methylated products in 100% yield (Scheme 3.5). Considering the charged pyridinium compounds, ESI-MS was a useful tool for their further characterization to give the parent ion at 626.7 amu for ***2-8*** and at 558.6 amu for ***2-9***.

3.2.4-Ring closing metathesis (RCM) reaction

To synthesize the 36 membered ring diester Grubbs 2nd generation catalyst was used under conditions reported in the literature[50] (Scheme 3.7).

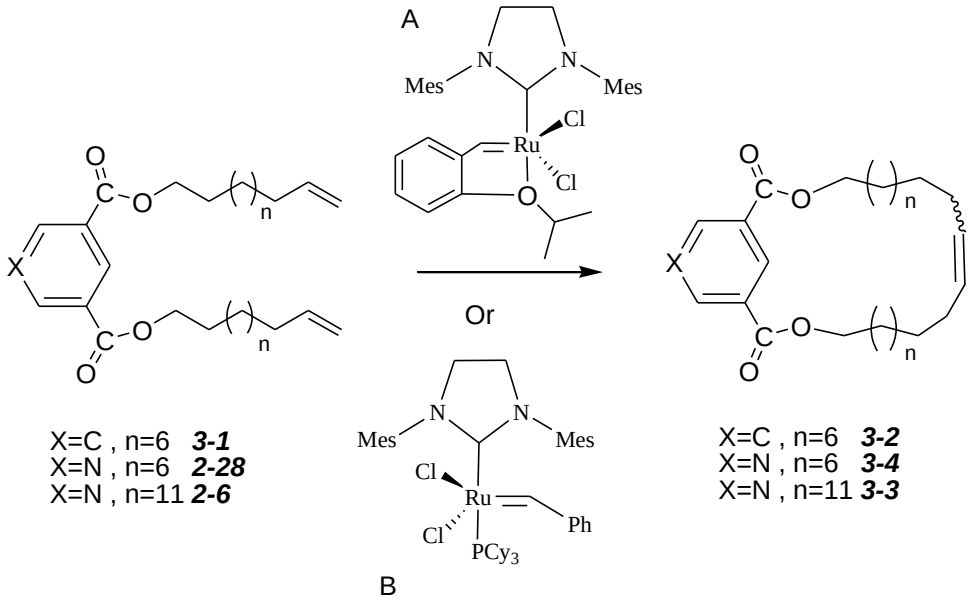

Scheme 3.7-Ring closing metathesis reaction, (A) Hoveyda-Grubbs 2nd generation catalyst, (B) Grubbs 2nd generation catalyst.

A model compound was synthesized and used to determine the catalyst load and temperature of the reaction in initial studies (Scheme 3.7). Compound 1,3-bis(undec-10-enyloxy)benzene ***(3-1)*** was synthesized[51] and underwent the RCM reaction using Grubbs 2nd generation catalyst at 10 mol% loading in toluene at 70ºC, leading to a macrocyclic product ***3-2*** which was purified by column chromatography.

After the successful synthesis of the model compound, unmethylated **diC16:1** (90% pure as discussed above) was used with 10 mol % Grubbs 2nd generation catalyst at 70ºC. However even after 72 h of reaction, the reaction didn't reach full conversion as assessed by NMR integration of the residual terminal alkene signals relative to the product internal alkene signals.

To optimize the conversion, the temperature was increased to 110ºC, and the reaction was monitored for 48 h. Even under these conditions it reached only 75% conversion. The full conversion was achieved by using 20% of catalyst loading for 24 h. Unfortunately the catalyst could not be removed fully using chromatography techniques which had worked previously with the model compound. All "purified" samples showed residual catalyst associated with all fractions containing the presumed macrocyclic product. The impurities could be seen as extra signals in the ^{1}HNMR spectra that roughly correspond to the Ru ligands of the catalyst. It is possible that the pyridine displaced a ligand in the catalyst complex resulting in a Ru-bound product species being isolated along with the desired compound.

To decrease the catalyst loading, 5 mol% of the Hoveyda-Grubbs 2nd generation catalyst was used at 110ºC; this increased the conversion to 85% after 48 h. Increasing the catalyst to 10 mol% yielded the macrocyclic product in 24 h. However all purification attempts were unsuccessful in this case as well. To facilitate removal of catalyst, the loading was decreased to 3 mol% and the reaction time was increased to 72 h which yielded the macrocyclic product in acceptable conversion. Other purification techniques such as activated charcoal powder in alcohol or thio urea scavenger resin for extracting Ru to a solid phase, did not completely remove the catalyst.

To avoid the presumed issue of Ru-pyridine coordination, methylated **diC16:1** (***2-8***) was used for the metathesis synthesis. This product did not fully convert to macrocyclic product and the purification proved to be complicated because of charged headgroup.

As part of the investigation of the effect of the length of the hydrocarbon chains on transfection, and another precursor for RCM reaction, **diC11:1** ***(2-29)*** was synthesized

and characterized by José Mendez. Unmethylated **diC11:1** ***(2-28)*** was used as precursor to synthesize a 26 member ring, believing that purification and removing of catalyst would be facilitated because of smaller hydrophobic region and altered migration on silica chromatography (Scheme 3.7).

The reaction was carried out with 5 mol % of Hoveyda-Grubbs 2nd generation catalyst at 110°C in toluene for 72 h with 100% conversion. This crude product was purified with column chromatography to yield a sample of unmethylated **cycloC20** which was free of the Ru-ligand impurities together with fractions contaminated with Ru as had been noted in the previous attempts using ***2-6***. The ^{1}HNMR of ***3-4*** gave a multiplet at 5.37 ppm for the internal olefin that showed that the macrocyclic product is present in a mixed composition of cis and trans. All other resonances correspond to the proposed structure with chemical shifts closely similar to other pyridine diesters. The ESI-Ms gave the expected M+H ion at 444.2 amu. The yield of the purified product was only 28% due to extensive losses during purification. This product was methylated as in other cases, to yield compound **cycloC20** (***3-5***).

3.3-Library of prepared of compounds

A full library of these lipids was synthesized with various alcohols, differing in length, saturation and branching. This led to compounds with a range of calculated clogP which relates to length of hydrocarbon chain, different shape parameters depending on the branching of chains, and varied miscibility and melting behaviour due to unsaturation in hydrocarbon chains which will be further discussed in chapter 5.

From the synthesis perspective, the esterification reaction was done as discussed before (Scheme 3.8). The diester pyridine lipids were synthesized with esterification conditions

discussed in 3.2.2 with yields between 16-84%. The main loss of products is believed to occur during the column chromatography.

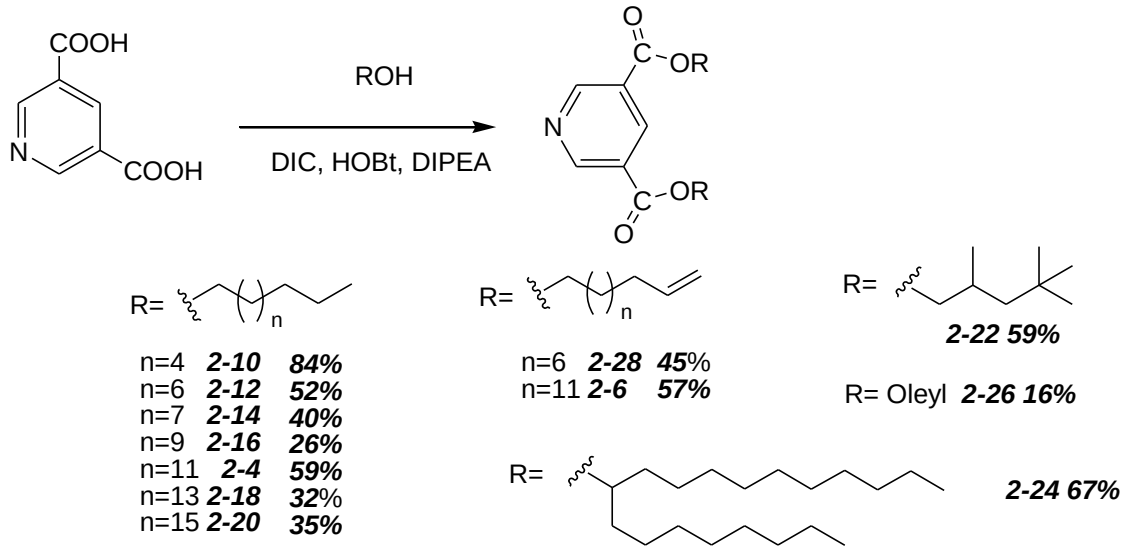

Scheme 3.8-Esterification reaction for prepared library.

These products were methylated with trimethyloxoniumtetrafluoroborate (Scheme 3.9), yielding the desired pyridinium lipids in quantative yields to prepare 100-200 mg of compounds for further studies. (Compounds **diC11:0**, **diC12:0** and **diC14:0** were synthesized by Ryan Woloschuk).

To name the pyridinium compounds, the length and structure of chains were used, as they all had the similar methyl pyridinium headgroup and ester linkers. Compounds with saturated straight chains, were named diCn:0 and diCn:1 for a mono unsaturated chain, with n showing the number of carbons in the chain. For the branched chain compound ***2-23***, isoC9:0 was used, as the number of carbons was the same with compound **diC9:0** (***2-11***) and for compound ***2-25***, brC20:0 was used to show the relation with compound **diC20:0** (***2-21***).

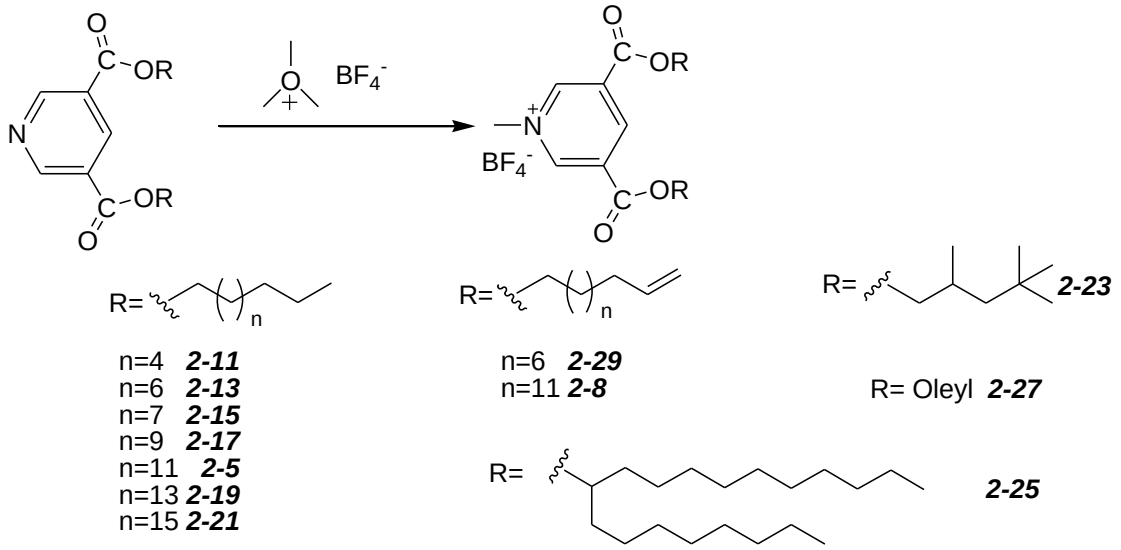

Scheme 3.9-Methylation step to synthesis the final library of compounds in quantative yield.

3.4-Mixed chain compounds

To study the potential effect of an asymmetric hydrophobic part in **diC16:1** (***2-8*** & ***2-9***), an intentional mixture of pyridinium lipid with mixed chains from hexadecanol and 10-undecen-1-ol was synthesized by Ryan Woloschuk (Scheme 3.10). The esterification and methylation was carried out under standard conditions and the product was purified to yield a mixture of compounds ***4-2***, ***2-29*** and ***2-5***. The ^{1}HNMR integration of the alkene protons and terminal methyl protons showed the ratio between compounds was as expected from the initial mixture of alcohols which would give a statistical distribution of 25% of ***2-5***, 50% of ***4-2*** and 25% of ***2-29***.

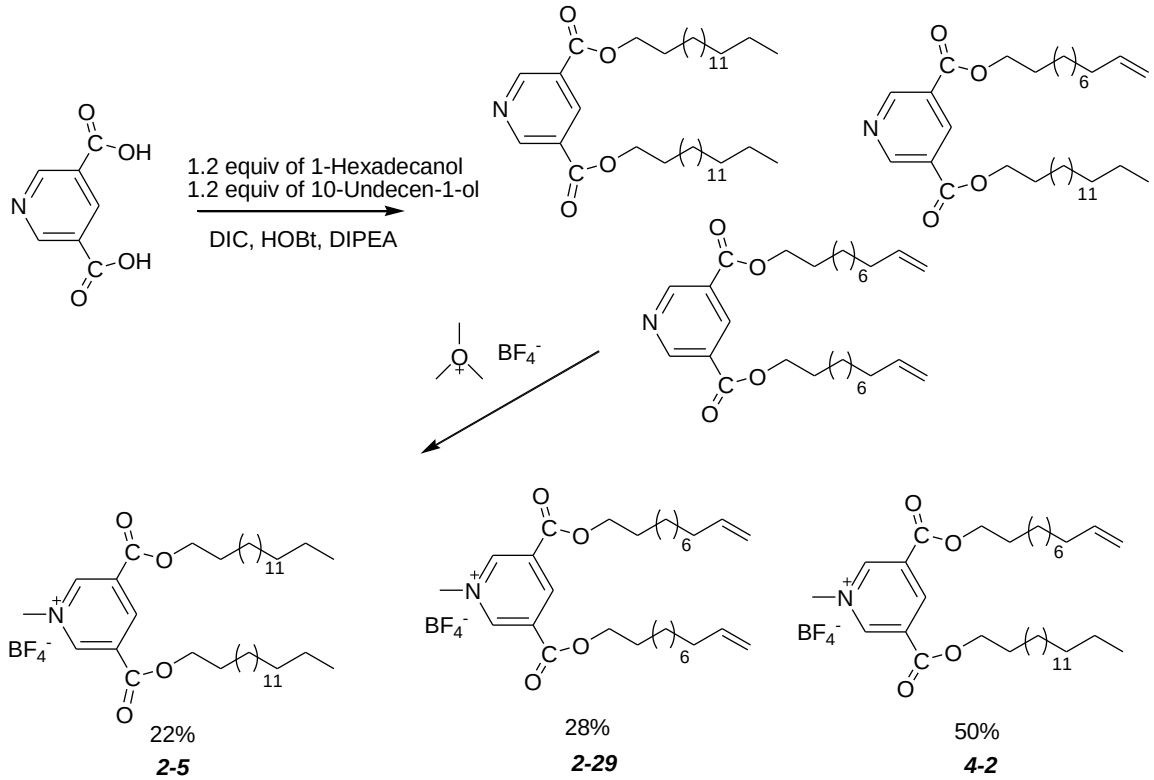

Scheme 3.10-Synthesis of mixed chain lipids for compounds *4-2*, *2-29* and *2-5*.

For the direct determination of the composition of the mixture, ESI-MS analysis was done on standard solutions of the lipids mixture at 0.1, 0.2 and 0.5 mM The relative ratios of ionization intensity were the same at all three concentration, showing that the ionization efficiencies of the three compounds are in a constant ratio and the ion intensity ratios correspond to the composition of the mixture. Comparison of the intensity of peaks in relation to each other gives the percentage of each lipid in the mixture as 22:28:50 for ***2-29***:***2-5***:***4-2***, which was applied in further calculations. Both alcohols were present in the reaction in slight excess, so the larger amount of ***2-29*** reflected a slight preference for the reaction of the shorter alcohol (Scheme 3.10).

Another parallel investigation was carried out by José Mendez to explore an alternative synthesis of pyridinium lipids. In this route the pyridine diacyl chloride was synthesized

from the diacid and then converted to the esters. Using this synthesis another lipid mixture was synthesized in 87% yield. Its composition was determined via the described ESI-MS method to be 16:28:56 for ***2-27***:***2-25***:***4-4*** (Scheme 3.11).

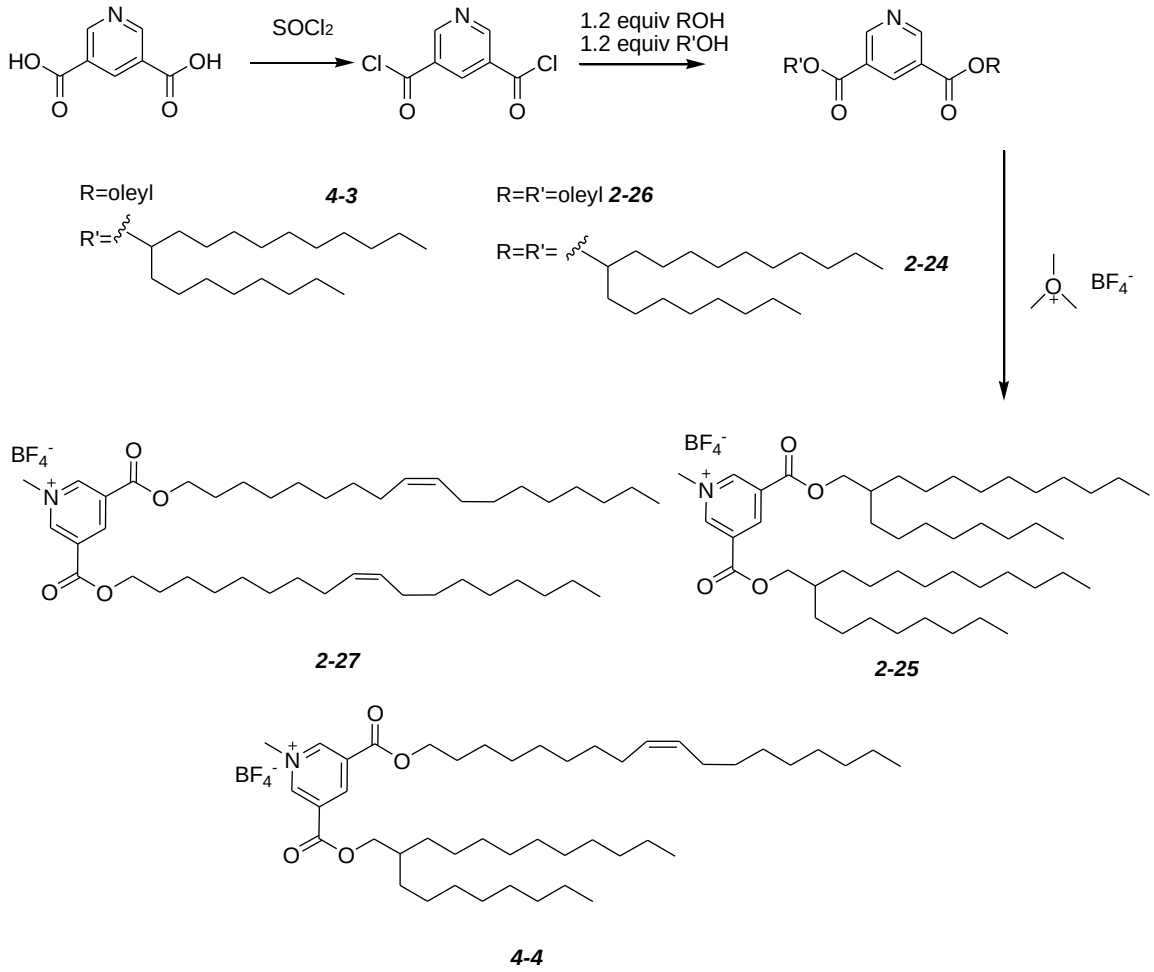

Scheme 3.11-Synthesis of mixed lipid via acylation route.

3.5-Summary

In summary, a series of diester pyridines was synthesized via ester coupling of the pyridine dicarboxycylic acids with various alcohols to yield final lipids with varied properties such as clogP, shape parameter, and miscibility.

The synthesis of the macrocyclic product was successful in synthesis of a 26 membered ring, but not in the larger 36 membered one because of difficulty in removing the

catalyst. The alkylation of synthesized diester pyridines was limited to methylation. Other alkylation attempts were carried out, however they were not successful, due to the high electron deficiency of the diester pyridines making them poor nucleophiles for alkylation reactions and prone to sigma-adduct formation with nucleophilic counter ions.

However, methylation of prepared diester pyridines with a non-nucleophilic counterion resulted in a library of pure, well characterized compounds for further studies to be discussed in upcoming chapters.

Chapter 4: Initial development of a Transfection Index (TI)

The experimental work in this chapter was performed by collaborators and is presented to provide a context for the development of a Transfection Index in order to correlate the results. Samples of the pyridinium lipids made in the previous chapter were sent to collaborators in Qatar at the Premedical Unit, Weill Cornell Medical College to the group of Dr. Mike Pungente. Within the Pungente group Dr. Emile Jubeli, Nada Abdul Khalique, Liji Raju, Ahmed Almeer, Hebatalla Allam, Maryem Al Manaa and Zara Awais formulated the lipoplexes and determined particle sizes, then conducted the gel retardation and DNase I degradation assays, followed by transfection and cytotoxicity bioassays. The small angel X-ray scattering (SAXS) experiments were conducted at the European Synchrotron Radiation Facility in Grenoble, France. Samples were prepared on site by Dr. Michael Pungente, Dr. Emile Jubeli, Nada Abdul Khalique and Liji Raju. The experiments were conducted under the supervision of Prof. David Nicholson, Norwegian University of Science and Technology with the data being analyzed by Dr. Helge Larsen, University of Stavanger, Norway. The development of the Transfection Index was done at the University of Victoria in Canada in Dr. Tom Fyles group.

The contents of this chapter have been published: "Aspects of non-viral gene therapy: Correlation of molecular parameters with lipoplex structure and transfection efficacy in pyridinium-based cationic lipids", Parvizi, Paria; Jubeli, Emile; Raju, Liji; Khalique, Nada Abdul; Almeer, Ahmed; Allam, Hebatalla; Al Manaa, Maryem; Larsen, Helge; Nicholson, David; Pungente, Michael D.; Fyles, Thomas M. *International Journal of Pharmaceutics*, **2014**, *461*, 145-156 (Parts of this chapter are taken from this manuscript With permission of Elsevier).

4.1-Liposome/lipoplex formulation and particle sizing

Liposomes of **diC16:0** (***2-5***) or **diC16:1** (***2-8***) with EPC (commercial cationic lipid) were prepared with co-lipids, cholesterol and DOPE, in a 3:2 ratio of cationic lipid to co-lipid (for completeness the structures are given below in Figure 4.1).

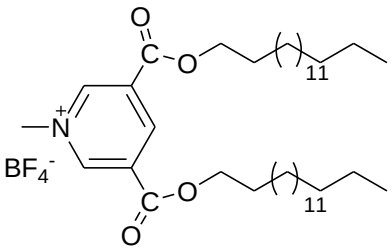

2-5
diC16:0

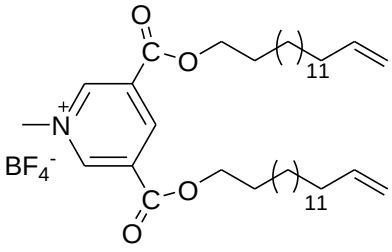

2-8
diC16:1

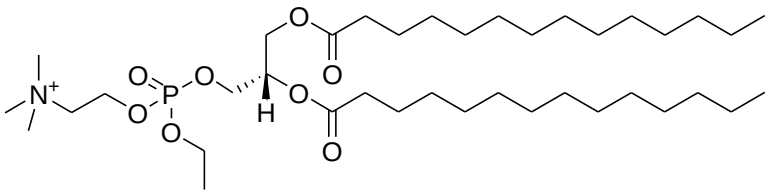

EPC

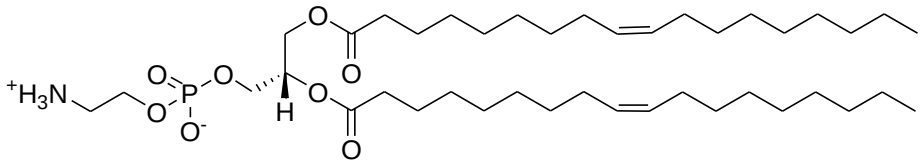

DOPE

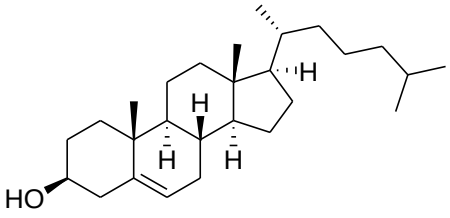

Cholesterol

Figure 4.1-The structures of pyridinium-based cationic lipids, diC16:0 and diC16:1, and commercial lipid, EPC, and co-lipids DOPE and cholesterol.

A thin layer of lipid was prepared by evaporating an ethanol solution of the desired lipid mixture which was then hydrated in buffer and sonicated to yield liposomes. These liposomes were sized using dynamic light scattering (DLS) that indicated diameters in the range d_H = 360–1000 nm, with polydispersity index (PDI) values ranging from 0.3 to 0.6. The liposome and lipoplex size measurements can be found in Appendix C.

The prepared liposomes with varied formulation were combined with negatively charged DNA to form lipoplexes driven by electrostatic interaction between the cationic lipids and DNA. Particle sizes of the lipoplexes were found to be between d_H = 380–3900 nm, with PDI values ranging from 0.2 to 0.8. The larger lipoplex particle sizes with higher PDI values are associated with the highest N/P molar charge ratios, and are believed to be a result of aggregation and fusion of the liposomes during lipoplex formation in the buffer.

4.2-Gel retardation and DNase I degradation assays of lipoplex formulations

The gel retardation assay is used to assess the binding of DNA to liposomes. The data are given in Figure 4.2. These results show that as the charge ratio of the formulation increases, the binding of DNA to the lipoplex improves (Figure 4.2-(A)). The lipoplex formulations of EPC/DOPE and EPC/cholesterol show complete retention at a charge ratio of 3 and higher, whereas the formulation of **diC16:0** and **diC16:1** with either DOPE or cholesterol exhibited complete retention at charge ratio of 5 and above.

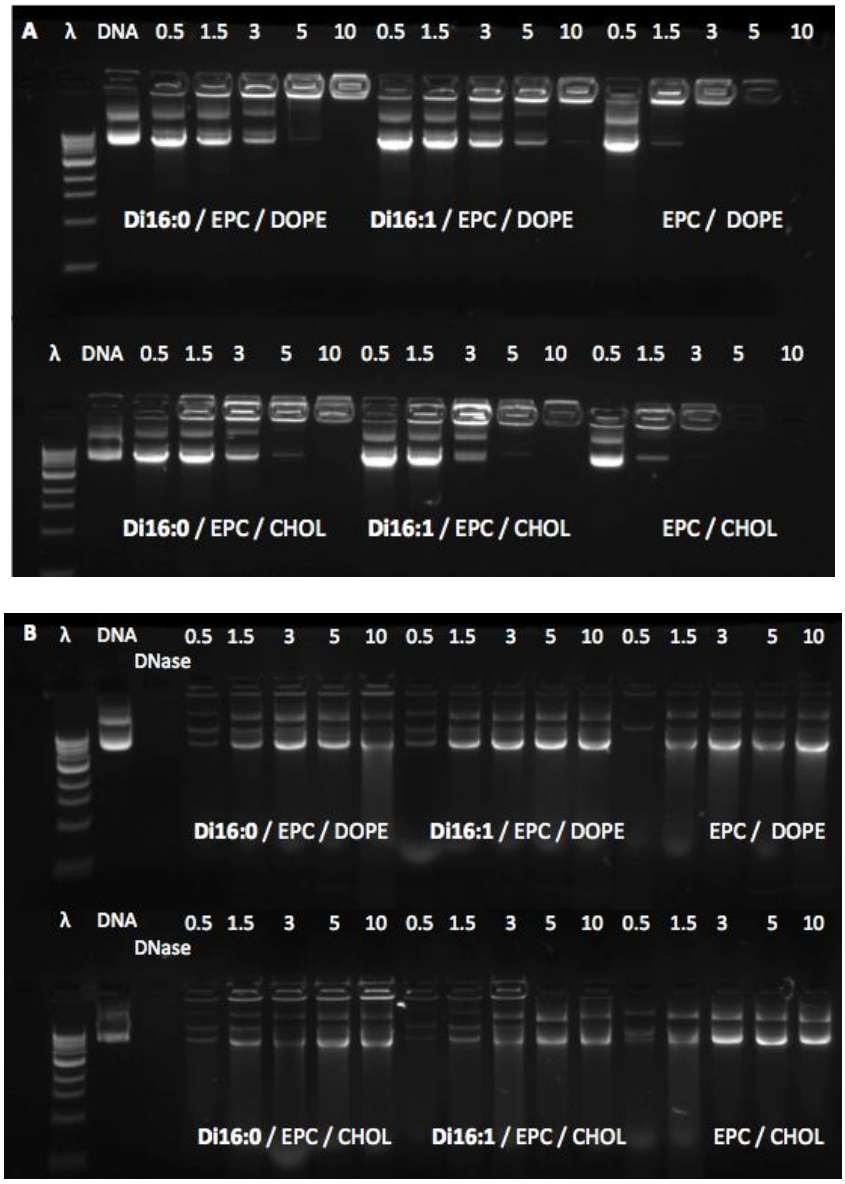

Figure 4.2-(A) Gel retardation assay and (B) DNase I degradation assay of diC16:0 (Di16:0) and diC16:1 (Di16:1) co-formulated with commercial lipid EPC and neutral co-lipid DOPE or cholesterol at molar charge ratios of 0.5 to 10, and run through a 1% agarose gel impregnated with the *p*DNA gel stain, ethidium bromide. Lanes λ and D denote the 1 kb DNA ladder and *p*DNA, respectively.

A DNase I degradation assay was used to determine the accessibility of the lipid-associated DNA toward nucleases. All formulations at charge ratio greater than 0.5 showed comparable DNA protection from nuclease degradation, though formulations

other than EPC/DOPE and EPC/cholesterol, with DOPE showed less degradation compared to formulations with cholesterol as the co-lipid (Figure 4.2-(B)). These assays imply that below a critical value of CR the DNA can easily dissociate from the complex, but there is still some protection afforded to the DNA by the lipoplex.

4.3-Transfection efficiency and cytotoxicity

The transfection efficiency of the synthesized pyridinium lipids **diC16:0** and **diC16:1** with EPC as the co-cationic lipids in formulations with co-lipids DOPE and cholesterol was studied and compared with Lipofectamine 2000^{TM} as a positive control.

To determine the relative gene transfer efficiency, lipoplexes were formed using a plasmid that contained a gene encoding the enzyme, β-galactosidase (β-gal). CHO-K1 cells were chosen based on their common use as a target for transfection. All formulations were tested in three sets of triplicates each (total n = 9; mean ± SE) with the exception of Lipofectamine 2000^{TM}, which was tested in a single triplicate set (n = 3; mean ± SD). β-Galactosidase activity and sample protein concentration were determined 48 h after transfection (Figure 4.3).

All pyridinium lipid formulations showed higher β-galactosidase activity than the cells incubated with free soluble *p*DNA. The results show that formulations with cholesterol as the co-lipid exhibit somewhat better transfection compared to those with DOPE as co-lipid, with the highest activity of **diC16:1**/EPC/Chol formulation at charge ratio 3 which was only 15-20% less efficient than Lipofectamine 2000^{TM}.

Formulations both of pyridinium lipids with EPC and EPC alone with DOPE proved to be less toxic compared to those with cholesterol as the co-lipid. In general, all formulations showed lower toxicity compared to Lipofectamine 2000^{TM}.

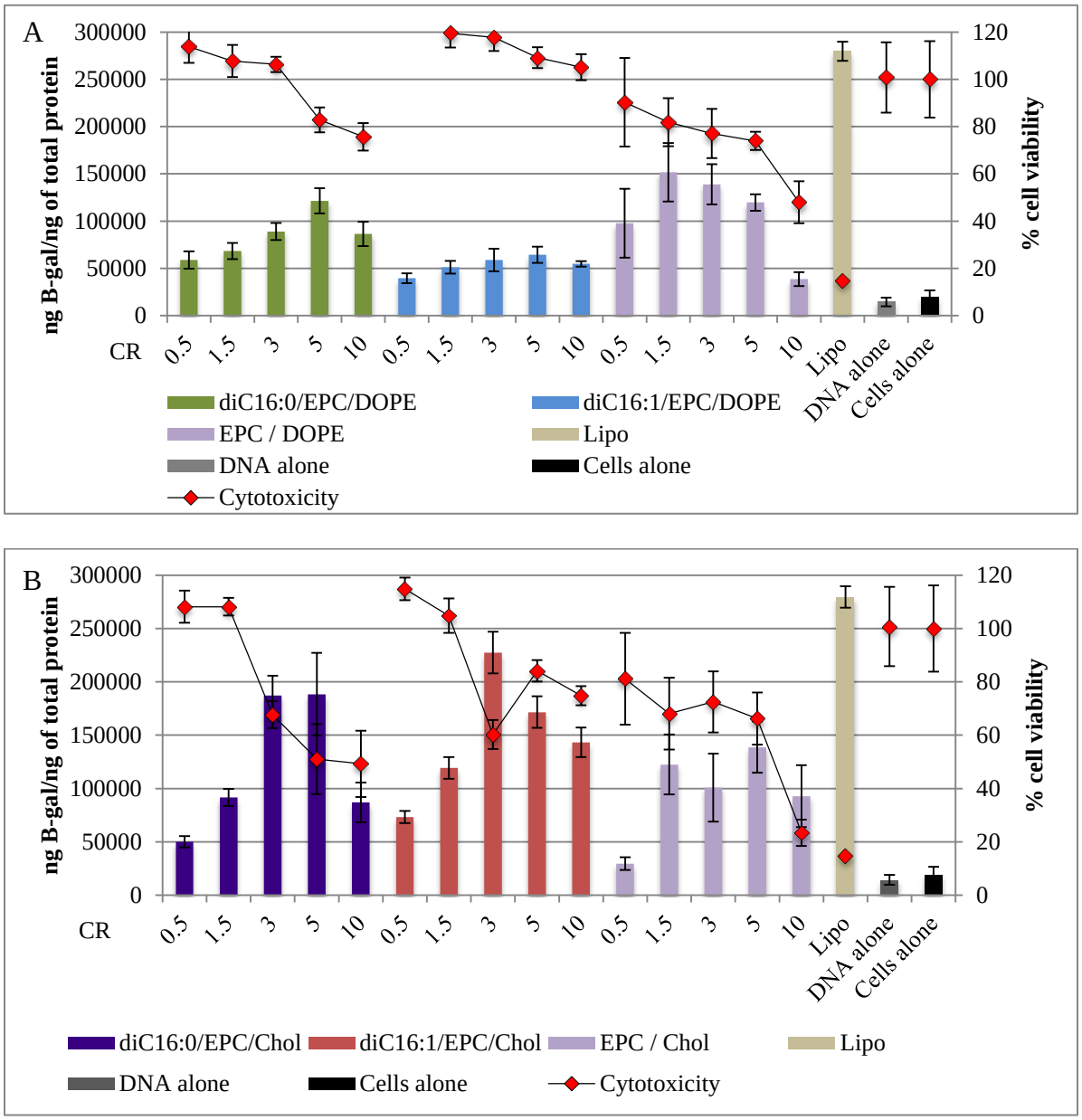

Figure 4.3-Transfection efficiency and cytotoxicity (after 48 h) of synthetic lipids diC16:0 or diC16:1/co-lipid/DNA lipoplexes compared to EPC/co-lipid/DNA at molar charge ratios of 0.5 to 10 (n = 9; mean ± SD) and Lipofectamine 2000™ (Lipo) (n = 3; mean ± SE) as positive controls, and plasmid DNA alone and CHO-K1 cells alone as negative controls (where A: co-lipid = DOPE; and B: co-lipid = cholesterol).

4.4-Fluorescence imaging

Green fluorescent proteins (GFP) expressing plasmids was utilized to visually study and compare the efficacy of the various lipoplex formulations. Cells were incubated with lipoplexes for 4 h then with complete RPMI medium for further 44 h, and finally were imaged using a camera attached to an inverted epifluorescence microscope (Figure 4.4). The formulations with **diC16:0** showed a small number of green cells, exhibiting medium transfection efficiency. However the number of green cells was higher in formulations with cholesterol in comparison to those with DOPE. Formulations with **diC16:1** with DOPE showed a similar efficiency, however when co-formulated with cholesterol, there was a much higher efficiency, shown by the greater number of green cells.

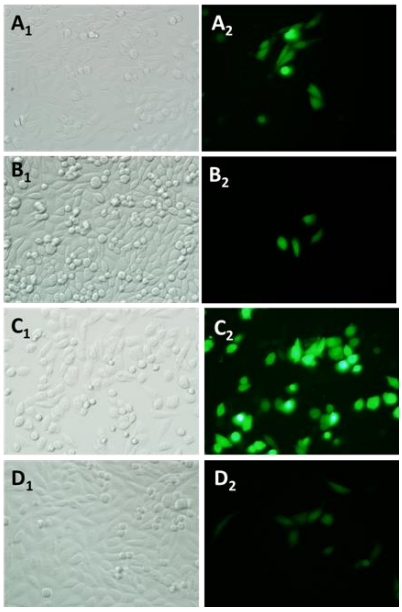

Figure 4.4-Fluorescence images of GFP transfected cells. Transfection achieved with the pyridinium lipoplex formulations diC16:0/EPC/Chol (A), diC16:0/EPC/DOPE (B), diC16:1/EPC/Chol (C), diC16:1/EPC/DOPE (D) in the CHO-K1 cell line at N/P +/-molar charge ratio 3:1. Cells were kept in contact with lipoplexes for 4 h prior to being incubated

for additional 44 h (48 h after initial transfection), and viewed by phase contrast (left panels) and green fluorescent channel (right panels).

4.5-Calculation of molecular parameters

To develop a structure activity relationship, the previously published LI[8b] (lipofection index) was chosen as a starting point (Equation 4.1).

$$LI = CR\ (R/(R+1))(logP_{mix})(logP_{+}/|\Delta logP|) \qquad \textit{Equation 4.1}$$

To calculate the LI the following parameters are required:

CR which is the molar charge ratio of cationic lipids to DNA (N/P), available from the experimental design.

R which is the molar ratio of the neutral lipid to the cationic lipid, available from experimental design.

$ClogP_{mix}$ which is the molar weighted clogP of all lipids and $clogP_{+}$ which is the molar weighted clogP of the cationic lipids. $|\Delta logP|$ is the absolute difference of clogP between the cationic lipid and the neutral lipid. The clogP terms were computed using the built-in function of ACDlab ChemSketch. This function is based on additive structural fragments following the method of Hansch and Leo[37]. The calculated values correctly reflect differential lipophilicity within a homologous series but may be seriously inaccurate in the absolute (Table 4.1).

The parameters above are sufficient to compute LI. Below, this is shown to be inadequate. Considering the importance of the shape of the lipid in the control of phase behaviours and thus potentially of importance in controlling transfection efficiency, a

shape parameter was calculated based on the Kumar and Israelachvili method (Equation 4.2)[28b, 52];

$$S = {V_c}/{(a_0 \times l_c)} \qquad \textbf{\textit{Equation 4.2}}$$

Where V_c is volume of the hydrophobic chains, a_0 is cross-sectional area occupied by the headgroup of the amphiphile and l_c is the critical chain length. As discussed in chapter 1, lipids with $S < 0.5$ (cone shaped) form micelles, cylindrical lipids with $0.7 < S < 1$ form bilayers, and inverted cone lipids with $S > 1$ have a tendency to form inverted phases. In previous work of Israelachvili[29] these parameters have been obtained experimentally. We required these parameters to be calculated directly using the structure of the cationic lipids. We proceeded as follows:

-l_c is calculated from the fully extended length of a saturated polymethylene chain of length n terminated in methyl as 1.54 + 1.265n (units of Å). This equation assumes the chains consist of carbon-carbon single bonds linked at 109˚ bond angles. To account for the presence of *gauche* segments that typically shorten to 80% of the fully extended length[28b], an 80% factor was used. Where necessary by the presence of alkenes in the structure, a C=C double bond length and appropriate bond angles were incorporated as well. The length of cholesterol is taken from previously published work[28b].

-The volume of the chains (V; units of $Å^3$) was calculated by adding the partial molar volume increments for the atoms present in the molecule. This approach reproduced the experimental value of the volume of fatty acids, straight chain alcohols and phospholipids successfully[53]. We also required some additional volume parameters: DNA is assumed to be a rod of 10Å radius with a rise of 3.4Å per base pair which bears two negative charges

per rise. The calculated partial molar volume of water by the method used here is 26.4Å^3/molecule.

-To calculate the headgroup area (a_0; units of Å^2) the partial molar volumes of headgroup atoms were used to calculate the volume of headgroup which was assumed to be a sphere, hence a_0 was the cross-sectional area at the equator of the sphere.

The calculated S, was validated against the S of known pure phospholipid and single-chain amphiphiles. Calculated S is a linear function of experimental S (slope = 1.0; R^2 = 0.98) that differs by a small increment (+0.02 ± 0.03) which is acceptable, considering the experimental results are from a variety of sources. For example, the calculated S for DPPC of 0.83 compares to an experimental S of 0.80 and the calculated S for PE of 1.09 compares to an experimental value of 1.12[28b, 30].

To calculate the S of a mixture, molar weighted values of mixtures of the pure components were used. This weighted averaging process has been applied previously to predict the morphological transitions and phase transition temperatures between micellar, lamellar, and hexagonal phases[9, 10c, 10d, 54]. The precision and accuracy of this method of averaging is unknown; for prediction of lipid phase we report only to the first decimal place (Table 4.1).

All the data in Table 4.1 are calculated as just described from partial molar volumes of atoms and bond lengths and angles, except for the cholesterol data, which were obtained from experimental values measured by Kumar[28b]. Because of difference in structure of cholesterol with other straight chain lipids, we decided here to use the experimental value of S = 1.20 for this lipid. Though in this preliminary analysis of the data for **diC16:0** and **diC16:1**, the Kumar S value may be applicable, it is likely that with a more extensive set

of data, the cholesterol shape parameter should be reconsidered to better reflect its effect in the lipoplex. This issue will be discussed in the next chapter.

Table 4.1 -Molecular structure parameters used to calculate transfection indices

	l_c (Å)[a]	a_0(Å^2)	V_C(Å^3)[a]	S	clogP	l_{lip} (Å)[b]	V_{lip} (Å^3)[b]
Cholesterol*	17.5	19.0	400	1.20	9.8	22.4	462
DOPE	21.8	43.2	950	1.14	14.8	29.2	1163
EPC	17.8	51.1	850	0.94	9.8	25.8	1146
diC16:0	17.4	38.4	866	1.30	12.6	24.3	1066
diC16:1	17.1	38.4	833	1.27	11.4	24.1	1033

[a] Critical length and partial molar volume of the hydrocarbon tails only.
[b] Overall length and partial molar volume of the lipid including the hydrocarbon and the headgroup. The volume includes a chloride counterion (if required).
* Experimental data from Kumar[28b].

4.6-SAXS studies on diC16:0 and diC16:1 lipoplexes

SAXS studies were carried out to determine the morphology of formed lipoplexes based on the electron density maps and d-spacing with **diC16:0** and **diC16:1** at a charge ratio 1.5 (Figure 4.5).

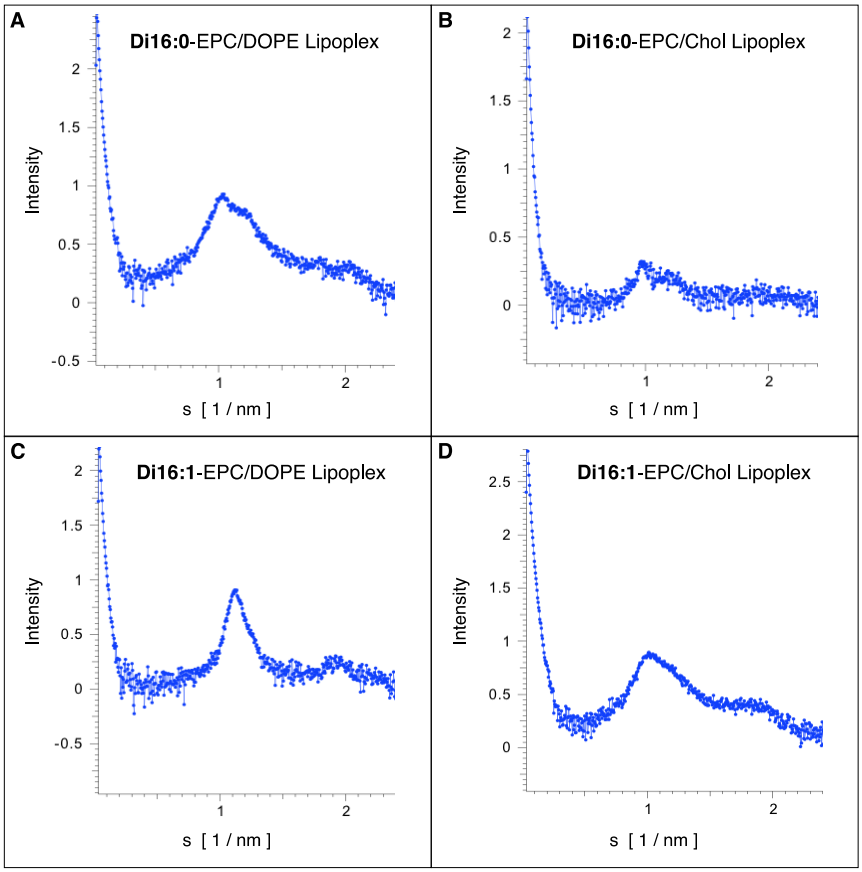

Figure 4.5-Results of SAXS experiments on diC16:0 (Di16:0), (A) and (B) and diC16:1 (Di16:1), (C) and (D) EPC lipid/pDNA lipoplex formulations at (+/-) molar charge ratio 1.5:1 (Abscissa: modulus of the scattering vector. Ordinate: intensity in arbitrary units).

Lipoplexes formed with EPC with either cholesterol or DOPE which form lamellar phases were used as a control. The inverted cone shape lipids (S > 1) form lipoplexes with hexagonal packing, so the S_{mix} of the lipid mixture is calculated to predict the phase of the lipoplex (Table 4.2). All formulation with **diC16:0** and **diC16:1** (except for the

inconclusive result of **diC16:0** with EPC and cholesterol) were in accordance with calculated S_{mix}. Note that this is calculated from the S of pure lipids, where the packing result is from the lipoplexes. Though S_{mix} predicts the phase of the lipoplex correctly, further exploration with lipids of more varied structures and S parameters is required to be able to confirm the generality of these observations.

Table 4.2-Summary of SAXS results for diC16:0 and diC16:1/EPC lipid/pDNA and EPC/DOPE and EPC/Chol lipoplex formulations at (+/-) molar charge ratio 1.5:1. δ refers to the actual packing in each case, with an estimated standard deviation of typically 1Å.

Lipid/DNA Lipoplex	**Packing**	**Lattice Parameter**	**S_{mix}**
diC16:0/EPC/DOPE	hexagonal	δ = 70Å	1.1
diC16:0/EPC/Chol	ND	δ = ND	1.2
diC16:1/EPC/DOPE	hexagonal	δ = 65Å	1.1
diC16:1/EPC/Chol	hexagonal	δ = 71Å	1.1
EPC/DOPE	lamellar	δ = 62Å	0.9
EPC/Chol	lamellar	δ = 62Å	1.0

4.7-Development of a Transfection Index (TI)

The transfection data from Figure 4.3 were correlated to LI (Equation 4.1), using the molar weighted clogP for the mixtures (Figure 4.6). Though there seems to be a maximum, the correlation was not particularly successful and this approach did not produce the bell shape curve of the original study[8b]. This result was perhaps expected, as compounds here are more lipophilic than the steroidal lipids that were considered previously[8b], so the ΔclogP term of Equation 4.1 becomes more substantial and affects the absolute value of LI unrealistically for small structural differences (the ΔclogP appears as a divisor). Note that there is an inherent problem with Equation 4.1 in the ΔclogP term. This term can approach infinity for ΔclogP = 0, when the clogP of the

cationic lipid is the same as the co-lipid. This problem had a small effect in the published work; it has a larger effect with our data.

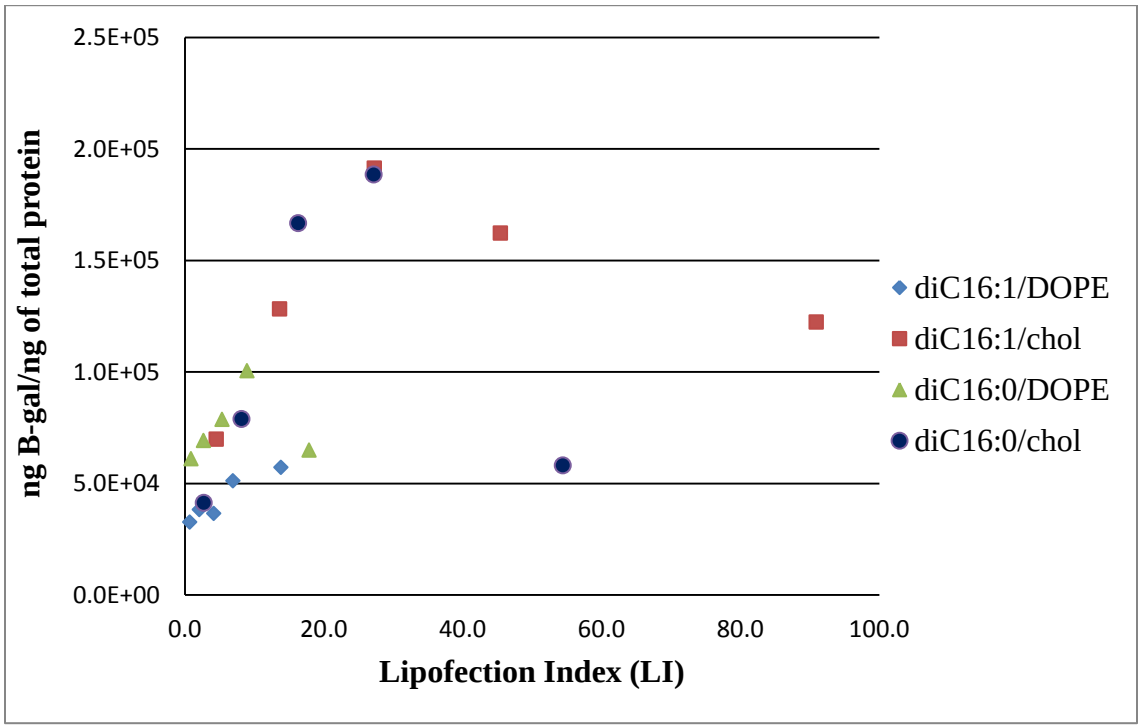

Figure 4.6-Transfection as a function of LI for the lipids diC16:0 and diC16:1.

However looking at the correlation of transfection data with LI, it can be observed that the pattern in Figure 4.3 is repeated here, i.e. there is a maximum that is roughly correlated with the charge ratio of the lipoplex. At an optimum charge ratio, there is an optimum LI. This can be expected as the charge ratio shows the amount of cationic lipid that is available for packing the DNA. At lower CR there may not be enough cationic lipid, so the DNA is packed insufficiently and leads to a defective lipoplex which can release DNA before arriving at the cell as seen in the gel retardation assay results. If there is too much cationic lipid, it may interfere with the formation of the regular hexagonal lattice packing. In the limit of excess lipid the individual DNA molecules will be covered

with a bilayer of lipids which cells might not uptake through endocytosis. Also excess lipids may lead into free liposomes which could rival any formed lipoplex for entering the cell. Thus it is reasonable to suppose that there is an optimum charge ratio where the lattice is perfectly filled and formed.

Once inside the endosome, the lipoplex should unravel and release the nucleic acid cargo. Here the lipids with different shape than those found in bilayer are more likely to disrupt the endosome. In addition the partitioning difference between lipids, can act as a driving force for migration of the lipids from the lipoplex to the endosomal membrane.

This qualitative analysis suggests that there could be three sets of parameters affecting the transfection efficiency:

-a partition term (related to clogP) that determines the endocytosis process and the unravelling of the liposome,

-a shape parameter term (related to S of the lipids) which affects the lipid migration and morphology of the lipoplex, and

-a volume term which relates the experimental terms of the composition of the lipoplex (CR and R) to the volume filling of the lattice.

For predictive purposes none of these terms should involve adjustable or fitting parameters.

We therefore define a transfection index:

TI = *partition term* × *shape term* × *volume term* ***Equation 4.3***

The partition term in LI can be simplified, as the partitioning of the cationic lipids and their difference with clogP of the neutral lipids of the endosome bilayer is the driving force here. So the partition term will be:

$$partition\ term = {clogP_{mix}}/{|\Delta clogP|} = {clogP_{mix}}/{|clogP_{+} - clogP_{0}|}$$

Equation 4.4

$clogP_{mix}$, $clogP_{+}$, and $clogP_{0}$ are the molar weighted clogP for the total mixed lipids, only the cationic lipids, and only the neutral lipids respectively. Note that this equation still suffers from the problem of being infinite when $clogP_{+} = clogP_{0}$.

The effect of shape parameter seems mostly influenced by the S of the cationic lipids (S_{+}; molar weighted average of pyridinium lipid and EPC), as the co-lipids are themselves abundant in the endosome[55], so would not be a destabilizing driving force. So the difference of the shape parameter of the cationic lipids with those of the endosome (S~1) is the effective factor. As this difference increases, it results in a greater perturbation to the lamellar part of the endosomal membrane.

$$shape\ term = |S_{+} - 1| \qquad \textbf{\textit{Equation 4.5}}$$

The volume term relates the filling of a hexagonal lattice to the stoichiometric terms CR (the molar ratio of cationic lipid (N) to DNA (P)) and to R (molar ratio of the cationic lipids to co-lipids). The stoichiometric terms state how much lipid is present and the geometric terms (l_c, V, a_0 of lipids, size of DNA) define the lattice dimensions. We need to compare the volume occupied by the lipids to the required volume to just fill the lattice.

To calculate the volume of the lattice, its geometry should be determined. The lattice is an equilateral triangular prism with DNA cylinders at the corners and a height equivalent to one base pair having a charge of -1 since only half a base pair is included in this unit cell. The number of moles of the lipid in an experiment (n_{exp}) within the unit cell is CR (1+R). The edge length of the triangle is twice the radius of the DNA plus twice the length of a lipid, so the volume of lattice (V_{lat}) can be calculated by these dimensions. The volume of the available lipids (V_{mix}) is just the n_{exp} × molar weighted average volume of the lipids; this is discussed in more detail below. The number of moles of the mixed lipids required to fill the volume of lattice is: $n_{lat} = V_{lat}/ V_{mix}$

For the best survival of the lipoplex in the extracellular medium, the lattice should be at its minimum free energy which is when the lattice is at its optimum filling. At a lower charge ratio, the lattice will have gaps and defects, hence will be unable to protect the DNA. At excess charge ratio, when too many lipids are present, the hexagonal morphology of the lipoplex will be destabilized and there will be enough lipids to partially cover the DNA with tail to tail bilayers (Figure 4.7). The volume of a fully covered cylinder of a lipid bilayer surrounding a DNA can be calculated from the height of a base pair and a radius equal to the radius of the DNA plus twice the length of the lipid. Again the number of the lipids required to fill this cylinder can be calculated as follows; $n_{cyl} = V_{cyl}/ V_{mix}$. Based on the geometry, $n_{lat} < n_{cyl}$.

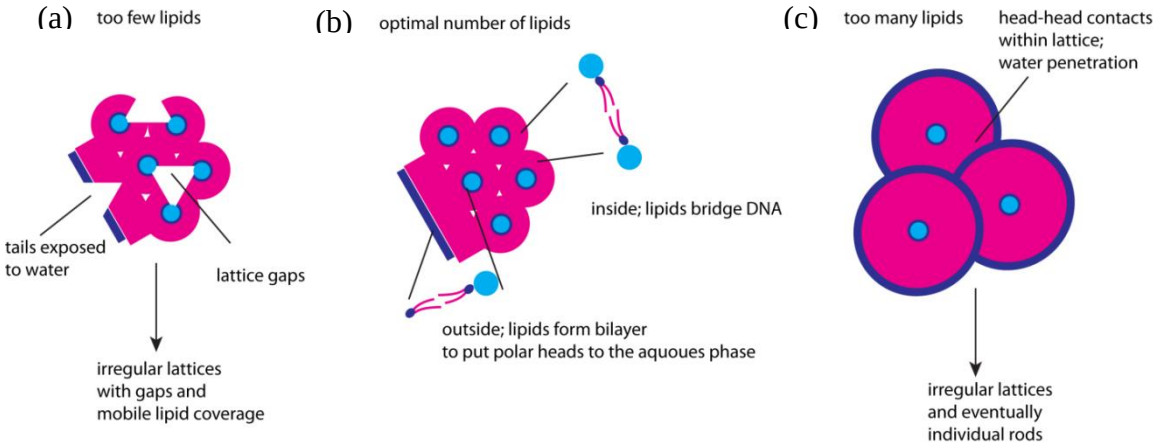

Figure 4.7-Effect of the number of lipids in filling the volume of a hexagonal lattice (a) too few lipids (lower CR), (b) optimum number of lipids and (c) too many lipids (higher CR).

As CR increases, the lattice starts to fill and n_{exp} will increase to n_{lat}. To approximate the extent of lattice filling, a linear function ($f_{lat} = n_{exp}/n_{lat}$) is applied which runs from 0 to 1; if $n_{exp} > n_{lat}$, at the optimum filling of the lattice, $f_{lat} = 1$. As the number of lipids increases, a similar function can be used to determine the filling of the cylinder; $0 < f_{cyl} = n_{exp}/n_{cyl} < 1$. The filling of the lattice is assumed to be favourable for transfection while the filling of the cylinder is assumed to be unfavourable. These two fractional filling terms then define the required volume term.

$$volume\ term = f_{lat} - f_{cyl} = \left({}^{n_{exp}}/_{n_{lat}}\right) - \left({}^{n_{exp}}/_{n_{cyl}}\right);\ n_{exp} < n_{lat}$$

Equation 4.6.a

$$volume\ term = f_{lat} - f_{cyl} = 1 - \left({}^{n_{exp}}/_{n_{cyl}}\right);\ n_{exp} \geq n_{lat}$$

Equation 4.6.b

The required volume V_{mix} is the mole weighted average of the lipid volumes (V_{lip}) which includes the hydrocarbon portion (V_C), the headgroup volume and the volume of any counterion required. Real and simulated lipoplex lattices contain a substantial amount of water; experimental values range from 3–30 moles of water per mole of lipid[10d, 56]. This volume needs to be considered as part of V_{lip}; here 10 mole water/mole lipid is the

chosen amount as this is consistent with the mid-range in previous discussions of this question.

The initial transfection index (TI) values were calculated for the formulations with **diC16:0** and **diC16:1** with co-lipids (Figure 4.8) and correlated to their transfection activity (Figure 4.8). It happens that the values produce a TI range to approximately 1, but this is not required by the method and is fortuitous. The correlation has R^2 of 0.91. The stated goal of "no adjustable parameters" is technically not met as the amount of water in the lattice is unknown. The goodness of fit is relatively insensitive to values between 8 and 20 moles of water/lipid but R^2 degrades to ~ 0.78 outside this range.

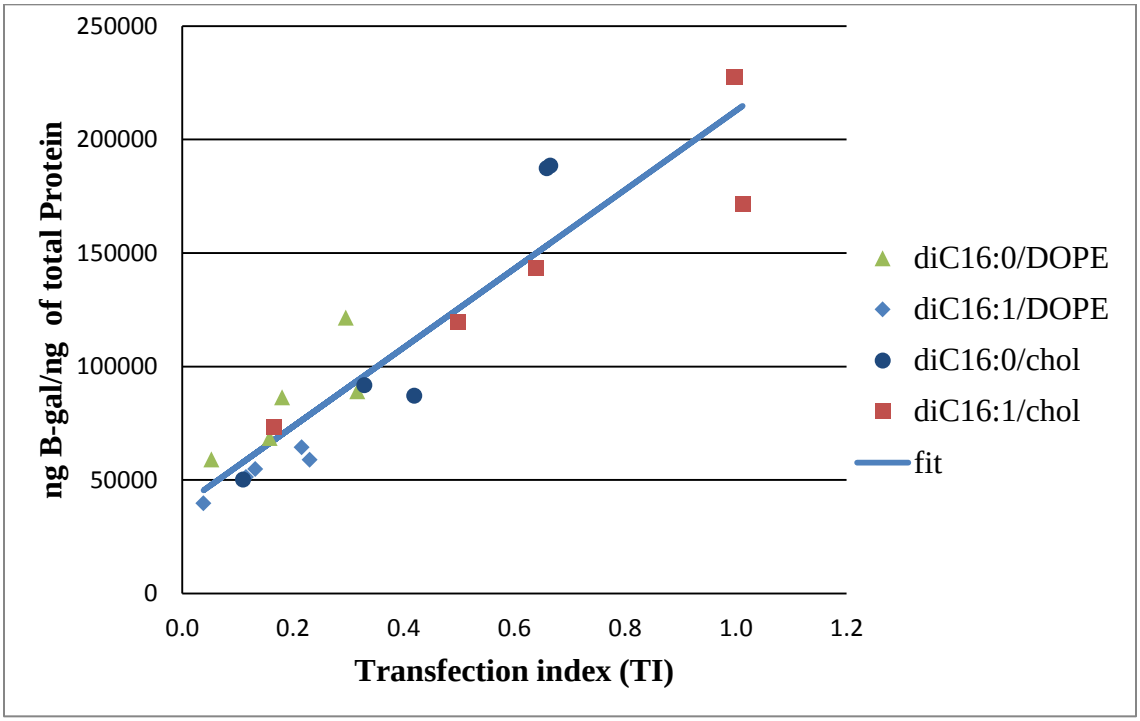

Figure 4.8-Transfection as a function of TI, which includes parameters related to lipid shape and volume filling of a hexagonal lattice, for diC16:0 and diC16:1

4.8-Cytotoxicity of pyridinium lipids

Cationic lipids, essential for transfection are toxic to cells, so it is important to have cationic lipids with as low an inherent toxicity as possible.

As discussed in the introduction, different parameters could potentially affect the toxicity of a mixture of lipids used for transfection. Looking at the toxicity results of studies reported above, a clear dependency can be seen on the CR. As the charge ratio increases, the amount of cationic lipid in each experimental well increases. Even for a well-formed lipoplex it is likely that there will be some extra free lipids which can form aggregates of their own and be disruptive to cells.

ClogP, which represents the partition of the lipid, is another effective factor controlling toxicity. Lipids with a higher clogP have better partitioning into the liposome and are less likely to escape and interact with the membranes of the cell.

The shape parameter of the mixture is potentially another important factor, as it determines the packing of the lipoplex and later on, the releasing of DNA cargo. If the shape is not optimal the lipid can escape the lipoplex to enter into direct cell disruption.

Considering these parameters, a three parameter regression fit was carried out on the experimental cytotoxicity data using the logarithm of normalized cell survival as a measure of the cytotoxicity. The normalization was done with respect to the cell viability in wells which had no DNA or lipids added. In some cases “survival” by this method of up to 120% was observed. The log(survival) values run from about 1 to 2.3 for 60 separate experimental conditions.

The following correlation was observed for the data set:

$$\log(\text{surv}) = (-0.035\pm0.007)\text{CR} + (0.30\pm0.03)\text{clogP}_{\text{mix}} + (5.8\pm0.9)S_{\text{mix}} + (-7.8\pm1.2)$$

Equation 4.7

The quality of the fitting result is given visually in Figure 4.9 in which the calculated log(survival) is plotted as a function the experimental log(survival). A perfect correlation

would be a line of slope 1. Here the toxicity of the linear pyridinium lipids has a generally linear trend with an R^2 of 0.71 for formulations with cholesterol and 0.70 for DOPE. The adjusted R^2 of the three-parameter fit for the full dataset (60 independent observations) is 0.71 with a significance F of 2.1×10^{-15} indicating high confidence in the model. The P-values of the individual coefficients determined are similarly very small. Thus although the experimental data are scattered, the model captures the variance correctly.

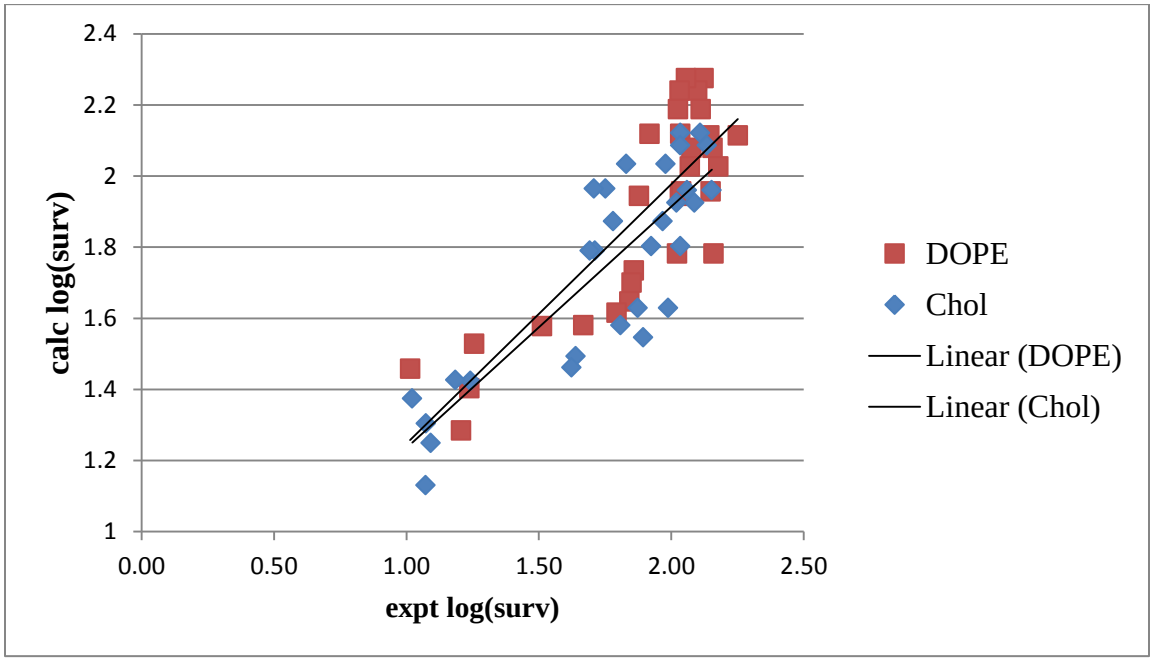

Figure 4.9-Three parameter correlation of toxicity of pyridinium lipids with charge ratio, shape parameter and clogP.

4.9-Summary

A transfection index (TI) was developed using a partition term, a shape term and a term related to the volume filling of the lattice. These parameters were molecular structure parameters which were calculated from the structure of lipids without experimental data. This TI was linearly correlated to transfection activity of synthesized pyridinium lipids,

diC16:0 and **diC16:1** co-formulated with EPC with co-lipids DOPE and cholesterol with an adequate correlation coefficient.

Additional findings of this preliminary work include:

- The most efficient formulation was less toxic than, but comparably effective in transfection to Lipofectamine2000™ (the commercial control). This confirms that pyridinium lipids are well suited to transfection and worthy of further exploration.

- The shape parameter of the lipid mixture was calculated based on molar weighted S of the lipids and appears to be able to predict the morphology of the lipoplex, as observed by the SAXS measurement of the prepared lipoplexes.

These preliminary results encourage further development of the TI as a tool to correlate the structural parameters of non-viral vectors and predict their transfection efficiency. Further application and development based on a more extensive set of lipids will be discussed in chapter 5.

Chapter 5: Further development of a Transfection Index (TI)

The experimental work in this chapter was done by collaborators. Samples of the synthesized pyridinium lipids were sent to collaborators in Qatar at the Premedical Unit, Weill Cornell Medical College to the group of Dr. Mike Pungente. Within the Pungente group Dr. Emile Jubeli, Nada Abdul Khalique, Liji Raju, Ahmed Almeer, Hebatalla Allam, Maryem Al Manaa and Zara Awais formulated the lipoplexes and determined particle sizes, then conducted the gel retardation and DNase I degradation assays, followed by transfection and cytotoxicity bioassays. The small angel X-ray scattering (SAXS) experiments were conducted at the European Synchrotron Radiation Facility in Grenoble, France. Samples were prepared on site by Dr. Michael Pungente, Dr. Emile Jubeli, Nada Abdul Khalique and Liji Raju. The experiments were conducted under the supervision of Prof. David Nicholson, Norwegian University of Science and Technology with the data being analyzed by Dr. Helge Larsen, University of Stavanger, Norway. The development of the Transfection Index was done at University of Victoria in Canada, in the Fyles group. This work is unpublished and the experimental results remain the property of my collaborators.

5.1-Cholesterol shape parameter

Before exploring the transfection index, the cholesterol shape parameter has to be addressed. As mentioned in chapter 4, the TI and toxicity calculation were based on a cholesterol shape parameter from the experimental data calculated by Kumar[28b]. In the work in the previous chapter, the lipid shape parameter is based on the assumption that a_0 is a physical area related solely to the dimensions of the headgroup based on atomic volume increments. This is not the way a_0 is defined in other work on lipid parameters

where it refers to the equilibrium area occupied at an interface and therefore includes a component of electrostatic repulsions between like charges from the headgroups of neighbouring molecules[57]. However in our approach, this distinction did not appear to affect the S, as our calculated values were close to the experimental S values obtained for pure lipids. In the experimental world, a_0 is larger than the physical area occupied by the headgroups, and by similar considerations V is larger than the physical volume of the atoms in the chains. In calculating S, the error in our assumption of equivalence with physical area and volume cancel each other out as the method for calculation of a_0 and V is the same. Our crude approximation appears to work for lipids in general, with the exception of cholesterol where we rely on an experimental value.

Recent computational studies on cholesterol in membranes have showed that the area associated with the headgroup varies with the composition of the membrane and depends on the type of the other lipids present[57-58]. It has been shown that as the amount of cholesterol increases, the headgroup area associated with the cholesterol shrinks. The area of cholesterol in the range of 25-50 mol% is 24Å^2 in DPPC, 21Å^2 in DOPC, and 12Å^2 (!) in POPC[59]. The volume changes as well, so the S is nearly independent of the composition. This shrinkage can occur due to two reasons: 1) as the amount of cholesterol increases it interacts better with lipid to effectively make closer contacts; and 2) it can "sink" into the bilayer phase, thereby cause the headgroup to shrink without altering the volume.

Using one experimental value for cholesterol would be acceptable if it were the only co-lipid we are interested in using, but there will be problems comparing with other lipid

compositions in the liposome. As a result the values for l_c, a_0 and V need to be calculated from the structure as is done with the other lipids.

Considering the structure in Figure 5.1, the apparent length can be approximated by an equivalent alkyl chain of 13 carbons as shown for a calculated length of 17.9Å fully extended. The core is rigid out to C18 and the terminal isopropyl is also rigid, so for simplicity, we could assume this is a rigid object through the full length. There are four rotors in the terminal chain but these are all more restricted than in linear alkyl chains so the usual 80% contraction to accommodate gauche conformations is likely not correct but l_c must be shorter than 17.9Å. The Kumar value of 17.5Å is certainly in line with this logic. The computation studies reported above give values in the range of 17.3-17.5Å. We selected a value of 17.4Å for the l_c of cholesterol.

The hydroxyl group on its own cannot be assumed to be the headgroup, as its area is too small (5.2Å^2). Assuming that the headgroup includes the atoms in the square (Figure 5.1), the headgroup area will increase to 22.7Å^2 which is in line with the experimental work above. However, the S comes out to 1.35 which seems too large.

The object is rigid so the incompressible part is actually wider than the squared carbons. Adding the CH in the circle gives the right sort of width. This gives a_0 = 26.4Å^2, V = 528Å^3. This is also in the zone of the experimental work in DPPC[58b]. Assuming the l_c = 17.4Å and this V and a_0, the S of the cholesterol is estimated to be 1.14. This set of cholesterol structural parameters is used in subsequent correlations.

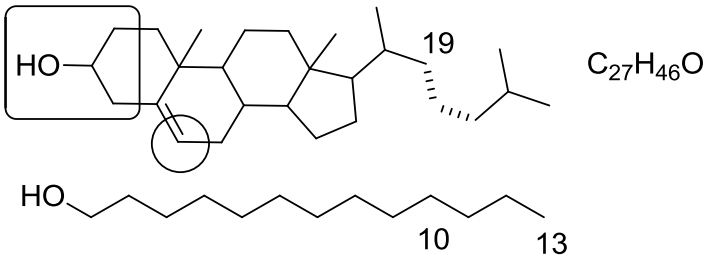

Figure 5.1-Estimation of headgroup and critical chain length of the cholesterol structure.

5.2-The effect of the chain length on the transfection

The TI developed in chapter 4 was built on the following terms, which will be referred to as TI_{PSV} .

TI_{PSV} = *partition term* × *shape term* × *volume fill term* ***Equation 5.1***

$$partition\ term = {logP_{mix}}/{|logP_{+} - logP_{0}|} \qquad \textbf{\textit{Equation 5.2}}$$

$$shape\ term = |S_{+} - 1| \qquad \textbf{\textit{Equation 5.3}}$$

$$volume\ term = f_{lat} - f_{cyl} = \left({n_{exp}}/{n_{lat}}\right) - \left({n_{exp}}/{n_{cyl}}\right);\ n_{exp} < n_{lat}$$

Equation 5.4.a

$$volume\ term = f_{lat} - f_{cyl} = 1 - \left({n_{exp}}/{n_{cyl}}\right);\ n_{exp} \geq n_{lat} \qquad \textbf{\textit{Equation 5.4.b}}$$

The efforts described in the previous chapter mainly addressed the volume filling term which is dominated by the charge ratio. The structure of the pyridinium lipids, **diC16:0** ***(2-5)*** and **diC16:1** ***(2-8)*** studied and used to analyze the transfection are closely related, so the effect of the other two terms for partition and shape were not effectively explored. To explore the effect of the partition term, a series of lipids was synthesized with the same headgroup and linker, but with varied lipophilic part which varied in chain length (Figure 5.2).

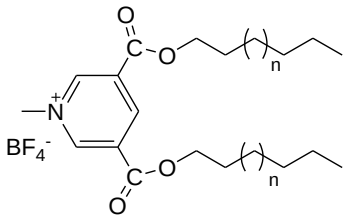

n=7 **diC12:0** ***2-15***
n=9 **diC14:0** ***2-17***
n=11 **diC16:0** ***2-5***
n=13 **diC18:0** ***2-19***
n=15 **diC20:0** ***2-21***

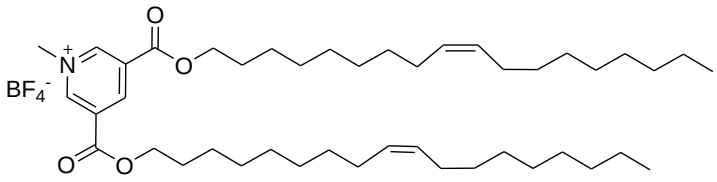

2-27

diC18:1

Figure 5.2-Pyridinium lipids with chain length with C12 to C20 and dioleyl.

These lipids provide a series of compounds with relatively constant S, but with significant variation in clogP (Table 5.1).

Table 5.1-Log P and shape parameter of the lipids with varying chain length and saturation.

Compound Name	**S**	**Log P**
diC12:0	1.2	8.3
diC14:0	1.2	10.5
diC16:0	1.2	12.6
diC18:0	1.2	14.7
diC18:1	1.2	13.7
diC20:0	1.2	16.8

5.2.1-Transfection efficiency and cytotoxicity

Liposome, lipoplex and transfection experiments were conducted using the protocols discussed in the previous chapter. Pyridinium lipids were formulated with EPC and a co-lipid (cholesterol or DOPE) in a molar ratio of 1.5:1.5:2 as liposomes and then mixed with plasmid DNA at one charge ratio, CR = 3. Gel retardation assays established that all lipoplexes only partially bound DNA but the DNase assay showed good protection of the DNA by the lipoplexes. The results are closely similar to those for the C16 lipids discussed in Chapter 4. The results can be found in the Appendix C. The transfection efficiency and cytotoxicity were measured for the synthesized pyridinium lipids **diC12:0**

to **diC20:0** (three sets of triplicates) and included Lipofectamine 2000™ (single triplicate set) as the control (Figure 5.3).

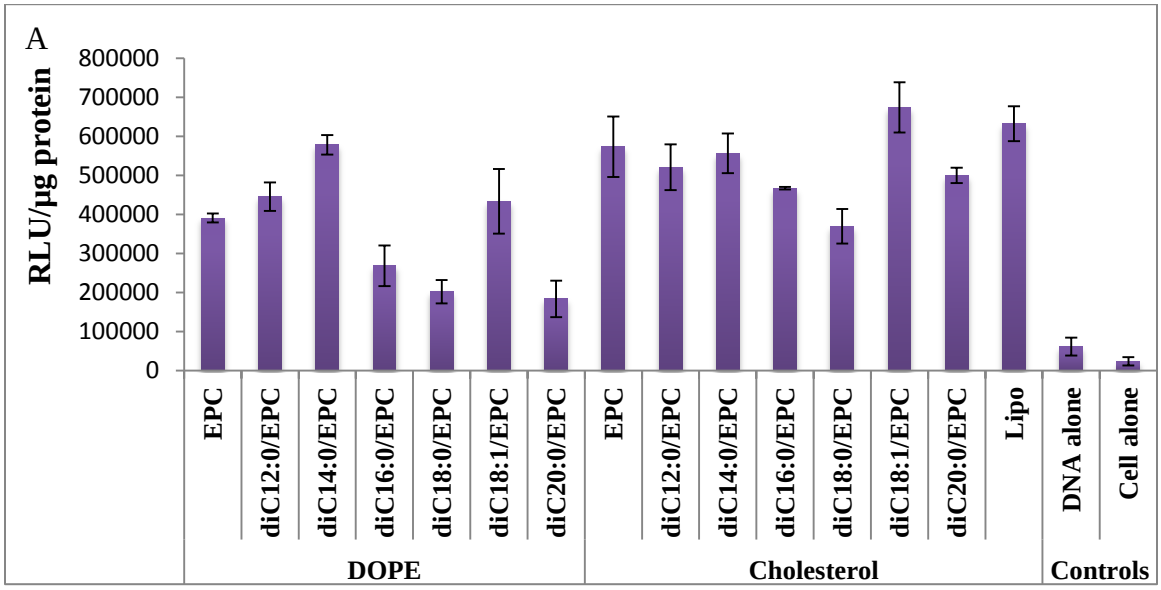

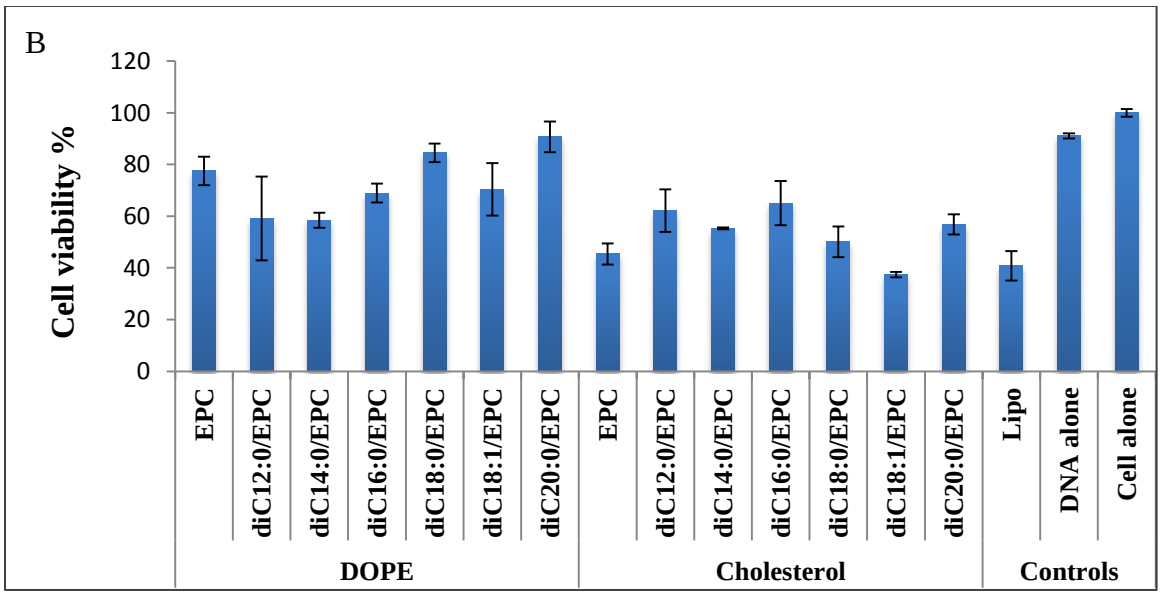

Figure 5.3-Transfection efficiency as luminescence readings of β-galactosidase (A) and cytotoxicity (B) (after 48 h) of synthetic lipid diC12:0 to diC20:0/co-lipid/DNA lipoplexes compared to EPC/co-lipid/DNA at molar charge ratios of 3 and Lipofectamine 2000™ (Lipo) as positive controls, and plasmid DNA alone and CHO-K1 cells alone as negative controls.

All pyridinium lipid formulations showed higher activity than the cells incubated with free soluble *p*DNA. The results have shown that formulations with cholesterol as the co-

lipid has demonstrated better transfection compared to those with DOPE, however these cholesterol formulations proved more toxic in comparison to those of DOPE formulations. The highest activity is that of the **diC18:1**/EPC/Chol formulation at charge ratio 3 which has the same efficiency compared to Lipofectamine2000^{TM}, and with comparable toxicity.

5.2.2-SAXS studies on the prepared lipoplexes

SAXS studies were performed on the lipoplexes prepared with pyridinium lipids co-formulated with EPC and co-lipids, DOPE and cholesterol, at two charge ratios 1.5 (Table 5.2) and 3 (Data in Appendix C).

In a majority of cases at CR = 1.5 the sample was sufficiently organized to generate useful experimental data and these samples showed a hexagonal packing. This is the predicted result based on the calculated S_{mix} of the lipids. The formulation with **diC20:0** and DOPE gave no SAXS signal and in the cholesterol formulation the scattering could not be fit to a model. It is possible that the lipoplexes were not formed correctly with this very hydrophobic lipid. Additional experiments on liposome formation with **diC20:0** will be discussed in section 5.2.1.

Table 5.2-Summary of SAXS results for pyridinium lipids/EPC lipid/pDNA and EPC/DOPE and EPC/Chol lipoplex formulations at (+/-) molar charge ratio 1.5:1. δ refers to the actual packing in each case, with an estimated standard deviation of typically 1Å.

Cationic lipids	Co-Lipid	Packing	Lattice Parameter	S_{mix}
diC12:0/EPC	DOPE	**Hexagonal?**	δ = 63Å	1.1
diC14:0/EPC	DOPE	**Hexagonal?**	δ = 69Å	1.1
diC16:0/EPC	DOPE	**Hexagonal**	δ = 68Å	1.1
diC18:0/EPC	DOPE	**Hexagonal**	δ = 76-84Å	1.1
diC18:1/EPC	DOPE	**Hexagonal**	δ = 68Å	1.1
diC12:0/EPC	Cholesterol	**Hexagonal?**	δ = 80Å	1.1
diC14:0/EPC	Cholesterol	**Hexagonal**	δ = 84Å	1.1
diC16:0/EPC	Cholesterol	**Hexagonal?**	δ = 75-90Å	1.1
diC18:0/EPC	Cholesterol	**Indeterminate**	δ = ND	1.1
diC18:1/EPC	Cholesterol	**Hexagonal**	δ = 82Å	1.1
diC20:0/EPC	Cholesterol	**Indeterminate**	δ = ND	1.1

5.2.3-Correlation of transfection efficiency with TI and its further development

The transfection activity of pyridinium lipids with DOPE and cholesterol as co-lipids does not correlate with initial transfection index (TI_{PSV}) developed in the previous chapter (Figure 5.4). The transfection efficiency of formulations with cholesterol as the co-lipid is scattered with no trend and those with DOPE are negatively correlated with TI_{PSV}. Clearly the TI_{PSV} correlation developed in chapter 4 is accidental and misses some essential features of the underlying processes involved in the transfection.

One parameter in the previous developed TI_{PSV} which should be reconsidered, is the partition term ($clogP_{mix}$ / $|clogP_{+} - clogP_{o}|$), as this term could be infinite if $clogP_{+} = clogP_{o}$. However this cannot be the only incorrect feature responsible for the lack of correlation of TI_{PSV} with transfection of pyridinium lipids in Figure 5.4.

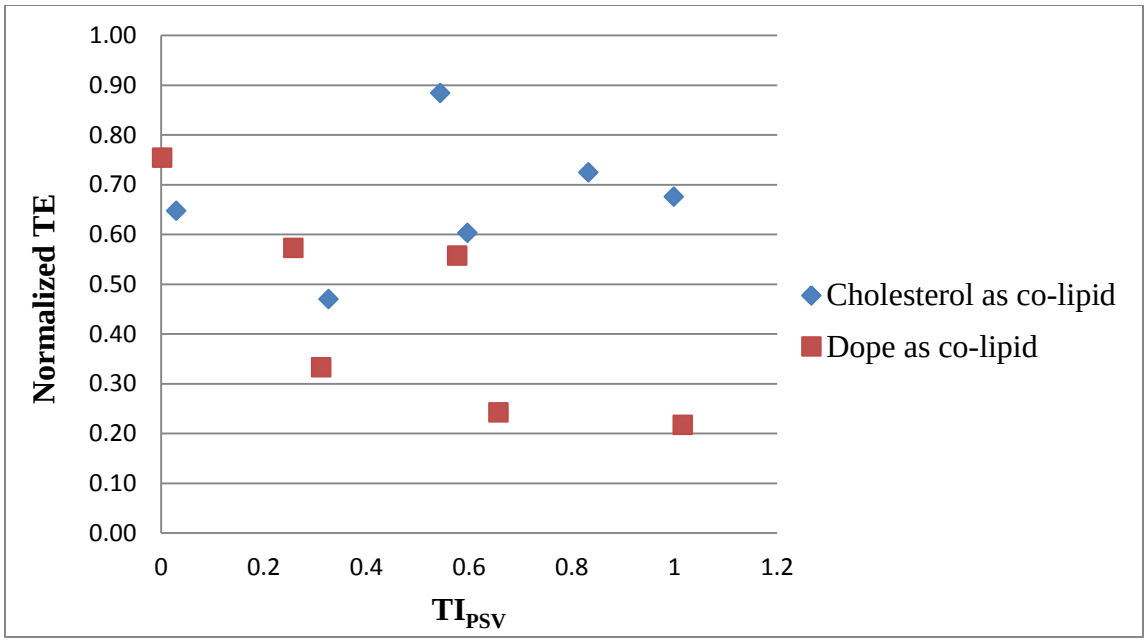

Figure 5.4-Transfection results of pyridinium lipids with chain length C12 to C20 as function of TI_{PSV} with co-lipids DOPE and Cholesterol.

To adjust the partition term, and to use a function that will be a maximum at one, a new term can be defined as follows:

$$\textit{Partition term} = (1/(\text{clogP}_{mix} - |\text{clogP}_{+} - \text{clogP}_{mix}|)) \qquad \textit{Equation 5.5}$$

Any case of interest will have clogP_{mix} and clogP_{+} as positive values so this function will not suffer from the problems of the previous version. Substitution of this form into the initial TI_{PSV} makes essentially no difference to the goodness of fit of the correlations with the **diC16:0** and **diC16:1** lipids in chapter 4. Similarly, it makes no improvements to the lack of correlation with the series of cationic lipids considered here.

Taking a closer look at the transfection activity of **diC12:0** to **diC20:0** with DOPE and cholesterol as the co-lipids, it was seen that **diC14:0** had the highest transfection efficiency among the saturated lipids (Figure 5.5). The sequence is clearest with DOPE as co-lipid where 14:0 > 12:0 > 16:0 > 18:0 > 20:0. The same sequence applies in the cholesterol series except for **C20:0**. As noted in the SAXS data there may be a problem

with formulations involving this compound (section 5.2.1). If this is the underlying sequence of activity then no linear transformation of clogP will reproduce this sequence as clogP increases linearly with carbon number. The points for the unsaturated **diC18:1** lie well above those for the saturated **diC18:0** but the effect is different with the different co-lipids cholesterol and DOPE.

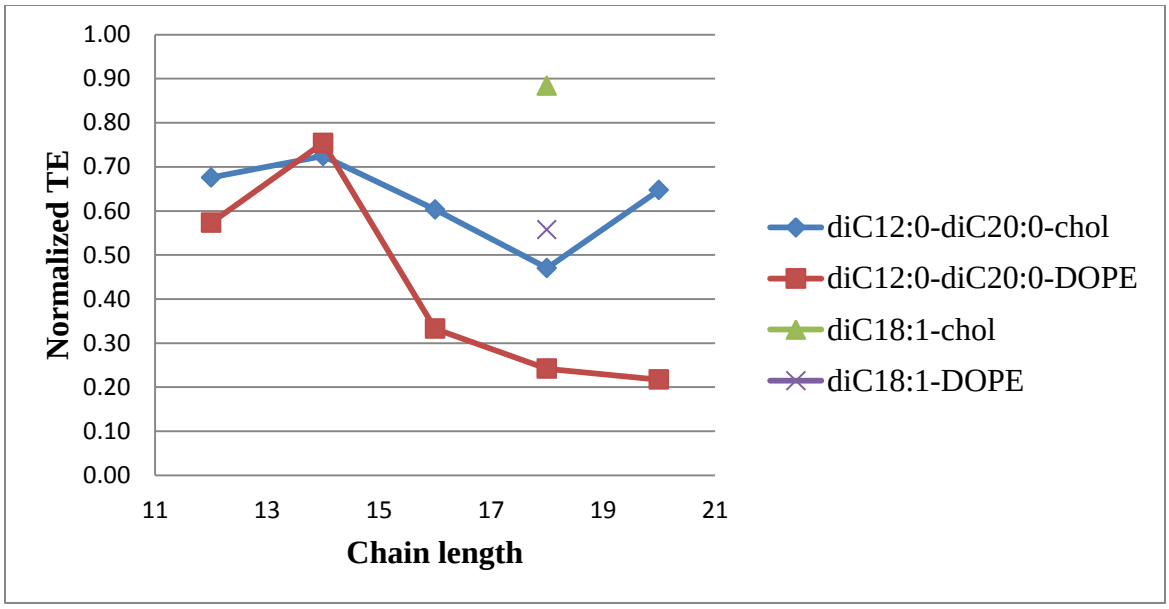

Figure 5.5-Transfection activity of lipids diC12:0 to diC20:0 as a function of the number of carbons in the chains.

Recall that the structure of the lipophilic part of EPC has two straight chains of 14 carbons. The peak at **diC14:0** suggests that chain-length matching of the pyridinium lipid with the EPC may be important. More generally, perhaps matching of the physico-chemical properties of the EPC/co-lipid mixture by the cationic lipid controls important parameters in the transfection. Two physical properties of lipid mixtures are directly influenced by chain length. One property is the melting behaviour of the pure lipids which scales directly with the number of carbons[31]. Another parameter of lipid mixtures is the miscibility of components which is directly related to chain-length mismatching in

simple cases[32]. Both these factors (fluid state and miscibility) would play a role as the lipids migrate from the lipoplex to the endosomal membrane.

When a pure lipid in a lamellar gel state is heated, it will undergo a phase transition first in the disorder of the chains; as the temperature increases, the disorder increases. When the chains are disordered, the volume must increase, resulting in a ripple phase. Further temperature increase will result in a second phase transition where the disorder in the headgroups occurs. When both the chains and the head-groups are melted, the lipid will be in a lamellar fluid phase. The required energy for melting and hence T_m depends on the entropy and the enthalpy of the system. Both these parameters depend on the length of the chains[31]. Based on these studies the minimum chain length for lipids to have this type of phase transition behaviour is about nine carbons.

In pure lipids, headgroups, chain-branching, and chain unsaturation with cis double bonds will affect the T_m. Not only does the presence of a cis double bond affect the chain melting, but its position in the chain can alter the melting temperature. The largest effect has been observed in oleyl chains, where the cis double bond is at position nine with a terminal eight carbon chain. Effectively, lipids with oleyl chains behave as if they were very short and therefore are fluid at low temperatures. DSPC melts at 54°C, whereas addition of the cis double bond at C9 in DOPC will decrease the T_m to -21°C[31,32].

However, real lipid mixtures are not ideal and the phase changes are not as clearly defined as in pure lipids. A common feature of a mixture of dissimilar lipids is the existence of different phases that co-exist. In a gel phase the lipids exchange only slowly. In a fluid phase some mixing of components between different phases can occur depending on the temperature[15b, 27, 60].

Previous studies which have investigated transfection and the lipid phase behaviour concurrently have shown that the T_m of a binary lipid mixture of two EPCs with saturated C14 and C16 chains plays a critical role in affecting the transfection efficiency. When the mixture composition has a T_m that is very close to the temperature of the cell culture medium where the transfection experiment is conducted (37°C) there is a dramatic increase in transfection efficiency. This is attributed to the enhanced mobility of lipids at the phase transition temperature which results from inevitable defects as the structured phase melts[15b].

Considering the formulations in this study, all have EPC (C14 chains) as the co-cationic lipid. We therefore see EPC as the reference point for considering phase behaviours. There have been various studies on the melting temperature and phase behaviour of EPC lipids[14b,27,15a]. The lipid EDPPC (EPC with 16 carbons) has a T_m of 40ºC, which is in a convenient range for calorimetric work, making it better studied. The T_m of the EPC used in the present study (EDMPC with 14 carbon chain) is 24ºC[60]. The phase behaviour of EPC lipids with co-lipids showed that T_m of these systems are not significantly changed upon on introduction of DNA and the formation of the lipoplex[14b,60]. Formulations where lipids of a similar chain structure are mixed form a lower-melting eutectic, which indicates the effect of good miscibility of the lipids.

The EPC lipids have been shown to form such a lower-melting eutectic and their lipoplexes have a lamellar phase. At a temperature that the system is fluid, a good interaction between the lipids and DNA has been demonstrated.

Another study by Koynova and MacDonald[15b], has shown that a binary mix of cationic lipids has higher transfection efficiency compared to a single cationic lipid. The cause is

believed to be the formation of domains with different conformations, which will lead to packing defects which in turn enhance the fusogenicity (ability to fuse with the endosomal membrane and mix lipid components). They also showed if the lipid mixture undergoes solid-liquid crystalline phase transition at the temperature of the transfection experiment, transfection efficiency was much higher[8a].

In the formulations in the present study, there is a ternary mixture of EPC, pyridinium lipid and the co-lipid at 3:2 mole ratio of cationic lipid to co-lipid. At a 3:2 ratio of EPC and co-lipid as a binary mixture, the S_{mix} of the lipoplex is below 1. Addition of pyridinium lipid shifts S_{mix} to 1.1 for linear pyridinium lipids. At the final composition in the presence of pyridinium lipids, the phase is known to be hexagonal, however whether it is in a fluid phase or a gel phase or a mixture of co-existing domains has not been determined and cannot be calculated[31].

The T_m of a 3:2 EPC/cholesterol mixture can be estimated to be around 20ºC based on published data for a 1:1 mixture which is only a few degrees of melting point depression relative to the pure lipid[27]. DOPE has a greater melting point depression effect. Added DOPE (1:1) lowers the T_m of EDPPC from 41°C to ~ 22°C. If the same effect applied for EDMPC (EPC with C14 chains) then the T_m of 24ºC for the pure compound would be depressed to about 5ºC.

Engbert has measured the melting point of the pyridinium lipids **diC14:0**, **diC16:0** and **diC18:0** as pure compounds using DSC[39a]. The T_m values are higher than corresponding PCs of the same chain length but following the same trend, of increasing melting point in proportion to the carbons in the chains (Figure 5.6).

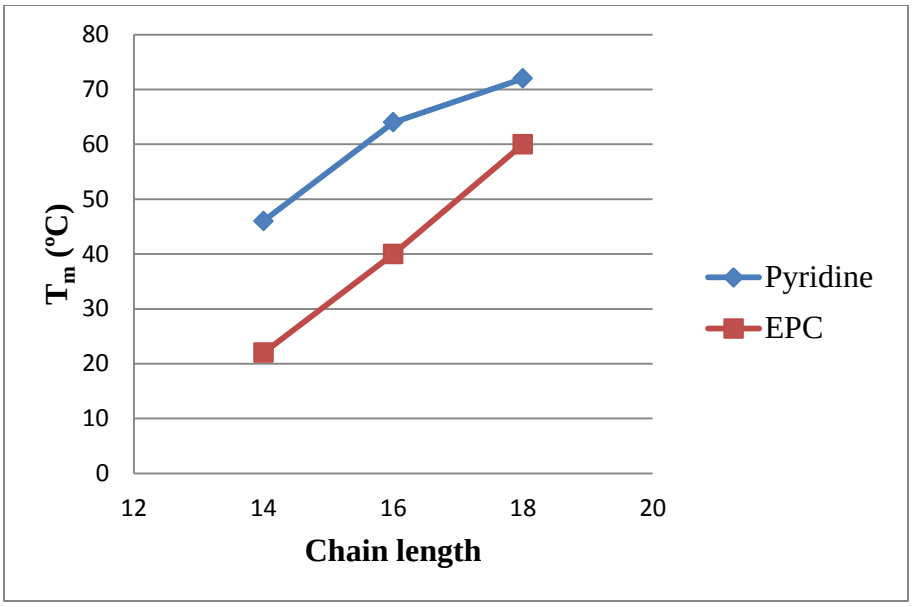

Figure 5.6-T_m of pyridinium lipids and PC lipids as a function of the number of carbons in the chains[39a,14b,15a].

While it is not possible to predict the phase diagram of the ternary systems used here, it can be concluded that as the T_m of the pure pyridinium lipid increases, the T_m of the system overall will increase. Low-melting lipids will certainly form a lipoplex with a melting temperature below the experimental transfection temperature. A high-melting lipid will result in increasing the T_m of the system from the initial value of a binary EPC/co-lipid mixture to some higher value. This might result in a single phase or the formation of separate domains where they may or may not be melted fully.

The experimental temperature of the transfection activity measurement of these lipids is 37°C. At this temperature four different types of mixtures could exist for a given pyridinium lipid/EPC/co-lipid system based on the independent behaviours of T_m and component miscibility:

1) If the T_m of the pure pyridinium lipid is lower than 37°C and the chains of the pyridinium are highly miscible in the EPC/co-lipid binary mixture then it is

likely this leads to formation of a lipoplex having only one hexagonal phase with melted chains. In such a mixture lipids can diffuse through the phase and there is likely no lipid-phase barrier to migration of the pyridinium lipid to the endosomal membrane. This is likely the case for **diC12:0**/EPC/cholesterol and **diC18:1**/EPC/DOPE.

2) If the T_m of the pyridinium lipid is lower than 37°C, but the structure of the pyridinium chains does not allow a good mixing with the EPC/co-lipid binary system, then it is likely that this system will consist of co-existing fluid phases, where the pyridinium rich phase is an inverted phase and the other phase could be inverted phase or lamellar. These conditions are not as favourable as the previous case, as there are kinetic barriers to de-mix the pyridinium lipids to allow the penetration into the endosomal membrane. An example for this system is **diC18:1**/EPC/Cholesterol.

3) If the T_m of the pure pyridinium lipid is higher than 37°C and the pyridinium chain structures allow a good mixing with the EPC/co-lipid binary fluid phase, it is likely that a ternary lower-melting phase will form. This will be a hexagonal phase which will enhance the transfection. **DiC14:0**/EPC/Cholesterol is a possible formulation of this type of system.

4) If the T_m of the pure pyridinium is higher than 37°C and the pyridinium chain structures are not miscible with the EPC/co-lipid fluid phase, it is likely that there will be two phases in this system. One may be a pyridinium-rich gel phase where the chains are not melted and is probably an inverted phase. The other phase will be EPC/co-lipid with none or a very little pyridinium in dissolved in

the fluid phase. This system would not be ideal for transfection, as there will be a kinetic and thermodynamic barrier for melting and de-mixing the pyridinium lipids before diffusing into the endosomal membrane. Pyridinium lipids with longer chains such as **diC20:0** and **diC18:0** will likely form such systems with either co-lipid cholesterol or DOPE.

The role of co-lipids in formation of the aforementioned systems is not completely clear. However it can be assumed that cholesterol will have a more pronounced effect compared to DOPE. Cholesterol decreases the T_m of the EPC/cholesterol system only a small amount but broadens the transition which indicates that the size of the phase that is melting is getting smaller[27]. So EPC/cholesterol must consist of two mixed lamellar phases, one a regular bilayer of EPC with 14 carbon chains possibly with a fixed amount of cholesterol and the other a cholesterol rich phase. Upon introduction of pyridinium lipids to either of these phases, the chain length of the pyridinium lipid will be an important factor, as it will affect the chain mixing greatly.

In the EPC/DOPE system the T_m of the system is low, so the system is in one fluid phase. Upon addition of the pyridinium lipid, the system will be less affected than in the cholesterol case and it will be more tolerant to adding the pyridinium lipids, even those of somewhat mismatched length.

This qualitative analysis suggests that for prediction of transfection efficiency, terms representing the T_m and chain mixing should be included in TI. These terms could be derived from the number of carbons in the chains.

When considering the effect of T_m, it can be presumed if the chains melt below the 37°C, there will not be an adverse effect on the transfection. However as the chain

lengthens and T_m increases to above 37°C, this effect becomes influential. So there is a critical number of carbons in the chain below which this melting term will be 1 and above it the carbon number will affect the transfection inversely. For a straight saturated chain it can be defined as:

Chain melting term = $1/(nC - critical\ value)$; for nC > critical value ***Equation 5.6.a***

Chain melting term = 1 ; for nC < critical value ***Equation 5.6.b***

Where nC is the number of independent rotors in the chain. For a saturated chain this is 2 less than the total chain length.

In lamellar systems, lipids of different length do not come to a meeting point at the bilayer mid-plane point. If the system consists of lipids with chains of 14 carbon length, the most miscible lipid to be added will be of the same length, even with a different headgroup. However as the chains are melting and the phase of the system changes from the gel phase, the chain motion will be affected as well as the length of the lipids. The chain motion depends on the conformation of chains, so if the chains are of similar conformation, they will be miscible and if not, the mismatch will cause the formation of separate phases. The conformation can be determined by looking at the rotations in the chains; the more rotors in the chain, the more states are accessible. For straight chain lipids, the number of rotors is the number of carbons minus the end methyl group bond, so it is (nC-2)[31-32].

To develop a term for the transfection index which reflects this chain mixing behaviour and which correlates to the number of carbons, we again focus on a critical number of carbons in the base mixture to which a pyridinium lipid is added. The chain mixing term will be unfavourable when chains are short, maximum at the critical value and

unfavourable as the chain lengthens. For lipids with saturated straight chains such a term can be defined as:

Chain mixing term = $1/|nC - critcial\ value'|$ ***Equation 5.7***

where the critical value may be different from the critical value in the chain melting term.

As noted above, nC is the number of independent rotors in the chain. To determine the nC, for straight saturated chains this number is 2 less than the total chain length, so for EPC this is 12. In a case that there are two chains with different length, this number will be the average of two chains.

For an unsaturated chain with a terminal alkene, one of the rotors of the saturated chain is frozen, so the value of nC is one less than the total chain length.

For chains where the alkene bond is in the middle of the chain, we need to consider the number of rotors on either side of the cis double bond. It is known for pure lipids that the extrapolation of melting behaviour gives an intercept of 8 carbons[31]. In a chain of fixed length e.g. C18 the position of the cis double bond controls the melting temperature from the minimum of the rotors associated with 8 carbons to a maximum close to that of a saturated C18 when the double bond is terminal. This behaviour directly correlates with the number of rotors in the longest possible segment. Here, the shorter part of the chain doesn't affect the melting temperature and the longer part is the one in control of the melting behaviour. We assume the same thing applies in pyridinium lipids. Specifically for **diC18:1** (with oleyl chain) nC = 8 is assumed.

By analogy, the nC of lipids with branched chains will be given by the longest chain of rotors. Cholesterol behaves less like a chain and more like a diluent to reduce the

cooperative length of the phase transition. The l_c of cholesterol that is used here is 17.4Å which is the same length as **diC16:0**, so from a melting point and mixing view; it can be assumed that cholesterol behaves as if it were a saturated C16 compound.

The critical values should encompass the EPC and the co-lipid of the base binary mixture. This can be determined as we have done with other mixtures by calculating a molar weighted average nC of the EPC and the co-lipid, when there is no pyridinium lipids present. This value will be 10.2 for EPC/DOPE systems and 12.8 for EPC/cholesterol systems.

With the additional terms a refined transfection index (TI_{PSVMM}) is developed as follows:

TI_{PSVMM} = *partition term* × *shape term* × *volume fill term* × *mixing term* × *melting term*

Equation 5.8

where the terms are given above in equations 5.3-5.7.

However, calculation of the melting term and mixing term shows that for the lipids of interest in the transfection process, these two terms are essentially the same. The main effective parameters in the mixing term is the length of the chains in the lipid and number of rotors, which are the same parameters affecting the melting of the lipids and are already considered in the melting term. This led to the less complicated transfection index, TI_{PSVM} as follows:

TI_{PSVM} = *partition term* × *shape term* × *volume fill term* × *melting term*

Equation 5.9

The transfection efficiency of the dataset given in Figure 5.3 correlated with the new TI_{PSVM} is shown in Figure 5.7, where $R^2 = 0.59$. It happens that TI_{PSVM} produces values

that are in the range of 0.005-0.01. For convenience the directly determined TI_{PSVM} are multiplied by 100. The correlation is a significant improvement in comparison to Figure 5.4. It can be concluded from observing of the effect of the incorporation of the chain melting term in TI_{PSVM} that this parameter plays a key role in transfection. There are no adjustable parameters in TI_{PSVM} except for the assumed number of water molecules in the lattice. The same data does not correlate ($R^2 < 0.2$) if the chain melting term is replaced by the chain mixing term proposed above (Equation 5.7). Similarly, a five-parameter TI_{PSVMM} that includes both chain mixing and chain melting terms gives a poor correlation with the data. The four-parameter TI_{PSVM} appears to be appropriate at this stage.

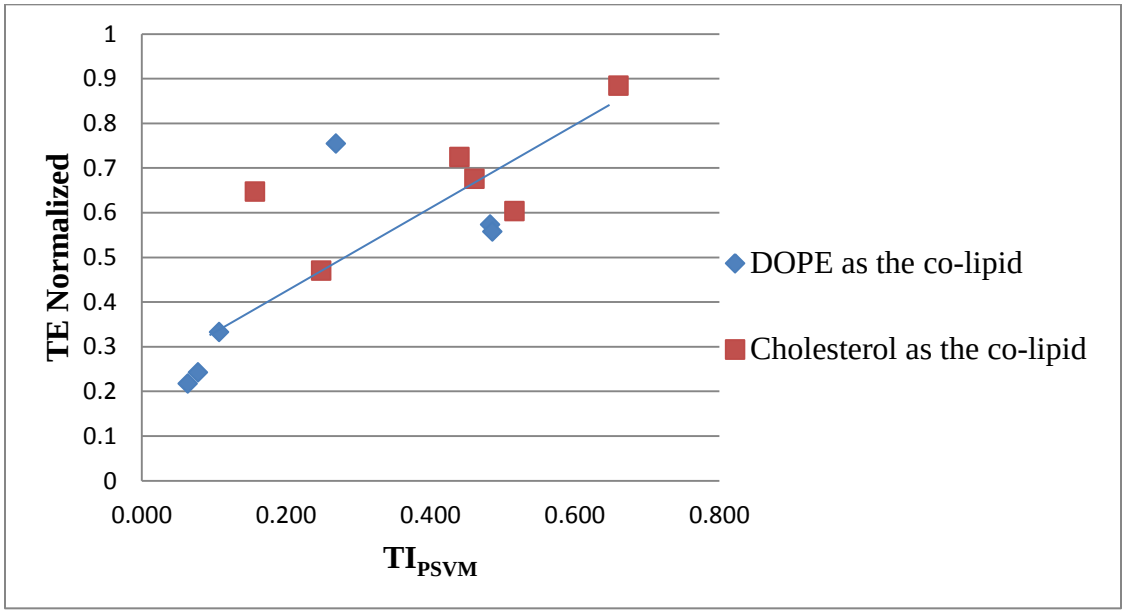

Figure 5.7-Transfection as a function of TI_{PSVM} of the synthesized pyridinium lipids with chain length C12-C20 with co-lipids DOPE and cholesterol which includes shape, partition, filling, melting and mixing terms.

5.2.4-Toxicity of pyridinium lipids

The toxicity of these lipids was studied with the results of previous obtained data and a three parameter regression fit was again carried out (Figure 5.8).

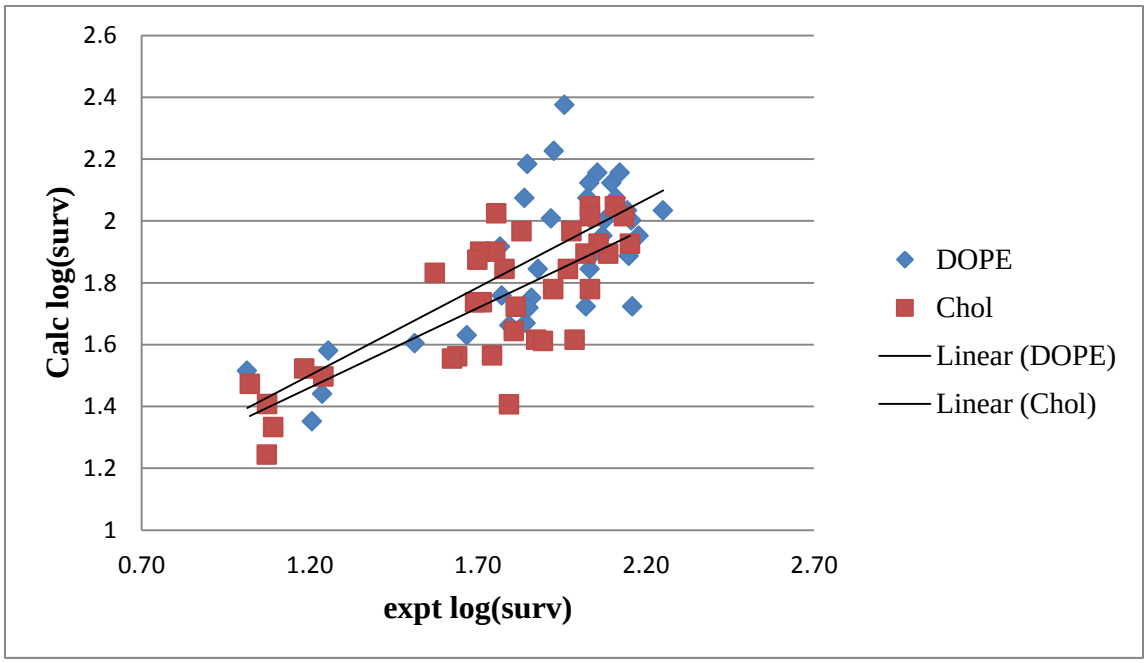

Figure 5.8-Three parameter correlation of toxicity of pyridinium lipids with charge ratio, shape parameter and clogP.

The following correlation was observed for the data set:

log (surv) = (-0.033±0.008) CR + (0.22±0.03) clogPmix + (4.4±0.9) Smix + (-5.4±1.2)

Equation 5.10

The quality of the fit is shown visually in Figure 5.8 where the calculated log (survival) is plotted as a function the experimental log (survival). A perfect correlation would be a line of slope 1. Here the toxicity of the straight-chain pyridinium lipids reveals a linear trend with an R^2 of 0.58 for formulations with cholesterol and 0.52 for formulations containing DOPE. The adjusted R^2 of the three-parameter fit for the full dataset (71 independent observations) is 0.57 with a significance F of 2.5×10^{-12}, indicating high

confidence in the model for a more extensive set of data. The P-values of the individual coefficients determined are similarly very small. Thus although the experimental data is scattered, the model captures the variance correctly.

5.3-The effect of shape parameter on the transfection efficiency

Another interesting characteristic of the cationic lipids is their shape parameter. As discussed in previous chapters, the shape of the cationic lipid plays a key role in destabilizing the endosomal membrane and the release of DNA cargo. To this point, the pyridinium lipids utilized have had relatively similar values of S in the region of 1.2. These values are large with respect to most natural lipids, but it is possible to design lipids with very high S values. To investigate the effect of extreme values of S on transfection, and on the quality of TI_{PSVM} as a parameter to correlate transfection efficiency, two sets of lipids were synthesized with isomeric alkyl chains containing the same number of carbons, but one with straight chains and the other branched. The lipids **diisoC9:0** and **dibrC20:0** were synthesized from readily available branched alcohols (Figure 5.9). The gene transfection efficiency of these lipids lies well away from the optimal activity found with the straight chain lipids, discussed earlier in this chapter. As such, they test the limits of the TI_{PSVM} at both the short-chain/low clogP and long-chain/high clogP extremes.

Branching in the lipid hydrophobic chains causes the shape parameter to increase from 1.17 to 1.67 in the C9 lipids and from 1.23 to 2.16 in the C20 lipids. To study the transfection efficiency, lipoplexes were formulated from the synthesized pyridinium lipids with EPC and co-lipids, DOPE and cholesterol, using directly comparable experimental protocols to those employed previously. For a more direct addressing the

shape parameter, a series of blends of pure lipids, **diC18:1** and **dibrC20:0** were prepared. Blends were made with composition of 50:50, 66:34 and 85:15 of **dibrC20:0**:**diC18:1** with increasing S from 1.70, 1.85 and 2.03.

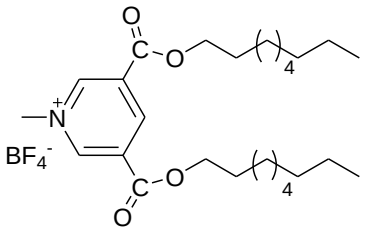

2-11
diC9:0
S=1.17

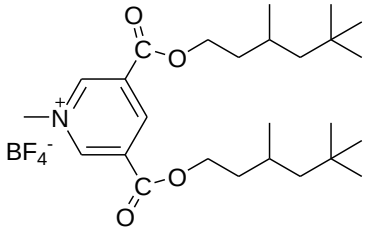

2-23
diisoC9:0
S=1.67

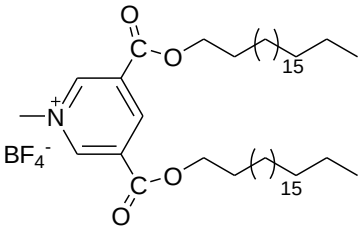

2-21
diC20:0
S=1.23

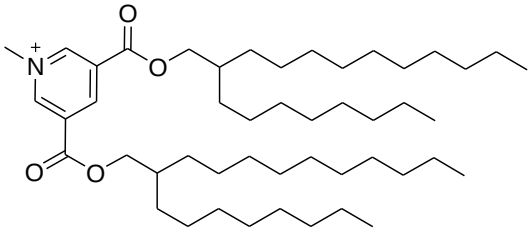

2-25
dibrC20:0
S=2.16

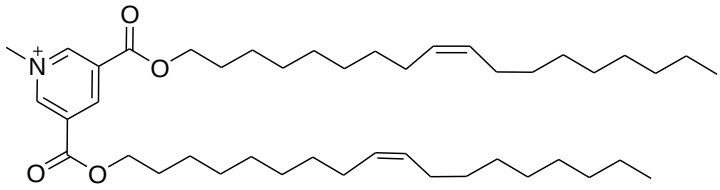

2-27
diC18:1
S=1.25

Figure 5.9-Synthesized pyridinium lipids, diC9:0, diisoC9:0, diC20:0, dibrC20:0 and diC18:1.

5.3.1-Transfection efficiency of diC9:0 and diisoC9:0

Liposome and lipoplex formation and analysis, together with transfection and cytotoxicity assays were conducted using the protocols discussed in the previous chapter. Pyridinium lipids were formulated with EPC and a co-lipid (cholesterol or DOPE) in a molar ratio of 1.5:1.5:2 as liposomes and then mixed with plasmid DNA at varying N/P molar charge ratios. Gel retardation assays established that neither **diC9:0** or **diisoC9:0** were very effective in binding to DNA and the DNase assay generally showed a quite poor protection of the DNA by the lipoplexes. The results can be found in the Appendix C.

The transfection efficiency and toxicity of the synthesized pyridinium lipids, **diC9:0** and **diisoC9:0** with EPC as the co-cationic lipid in formulations with co-lipids DOPE or cholesterol (preformed three times in triplicates) were assessed against the Lipofectamine 2000^{TM} (single triplicate set) as the positive control (Figure 5.10 and 5.11).

Those formulations containing pyridinium lipids with cholesterol as co-lipid showed poor transfection at all charge ratios (Figure 5.10). Formulations of **diC9:0**/EPC/DOPE were more efficient than **diisoC9:0**/EPC/cholesterol, and similar to the activity of EPC/DOPE formulations with the exception of **diisoC9:0**/EPC/DOPE at CR = 1.5 which had the highest activity in the dataset. The poor transfection observed with cholesterol as co-lipid is substantially less than that of EPC/cholesterol alone. This implies that theses pyridinium lipids when formulated with cholesterol give rise to some other morphologies or compositions which are particularly poor for transfection.

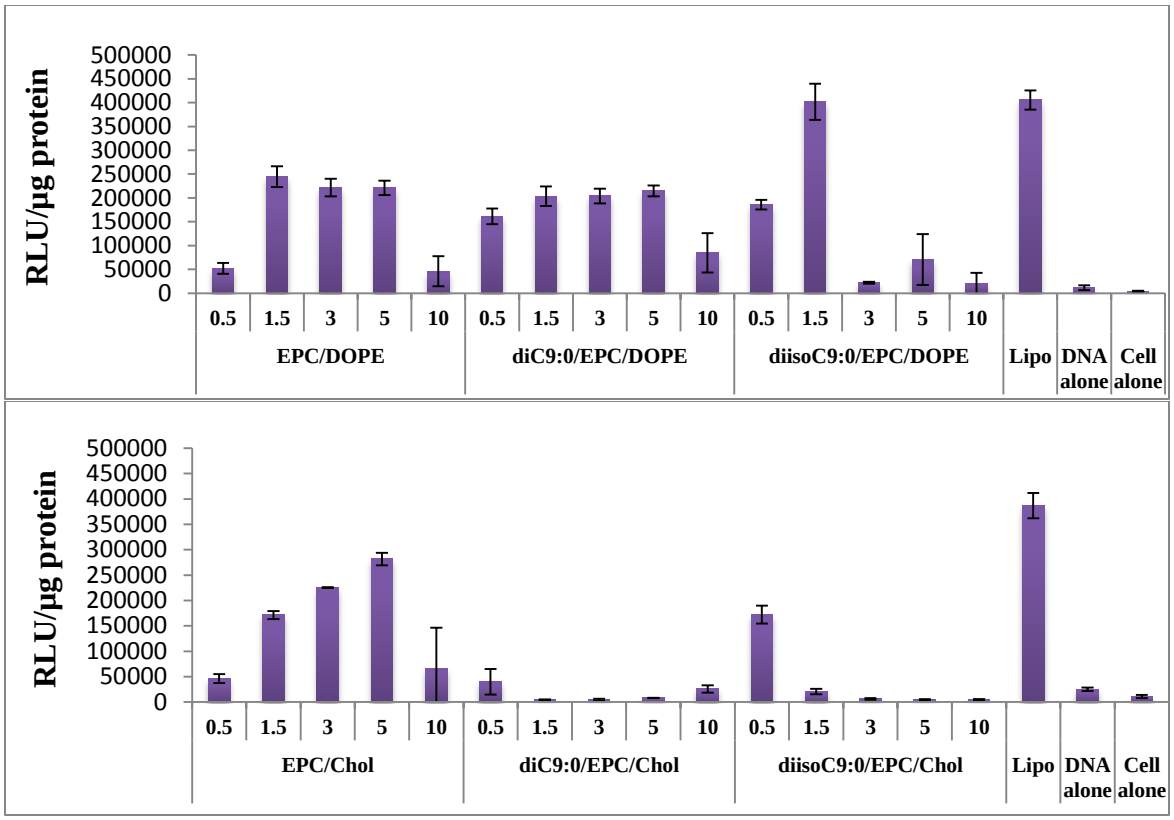

Figure 5.10-Transfection efficiency as luminescence readings of β-galactosidase (after 48 h) of diC9:0 and diisoC9:0/co-lipid/DNA lipoplexes compared to EPC/co-lipid/DNA at molar charge ratios of 0.5 to 10 and Lipofectamine 2000™ (Lipo) (n = 9; mean ± SD) as positive controls, and plasmid DNA alone and CHO-K1 cells alone as negative controls.

The toxicity of these short-chain pyridinium lipids with the exception of **diC9:0**/EPC/DOPE is high as expected for the low value of clogP = 5.11. Formulations of either **diC9:0** or **diisoC9:0** with cholesterol had high toxicity. Formulations of **diC9:0** with DOPE have similar toxicity to EPC/DOPE, whereas the toxicity of **diisoC9:0** formulations in DOPE are high and increase as the charge ratio increases, also in line with the previous correlation.

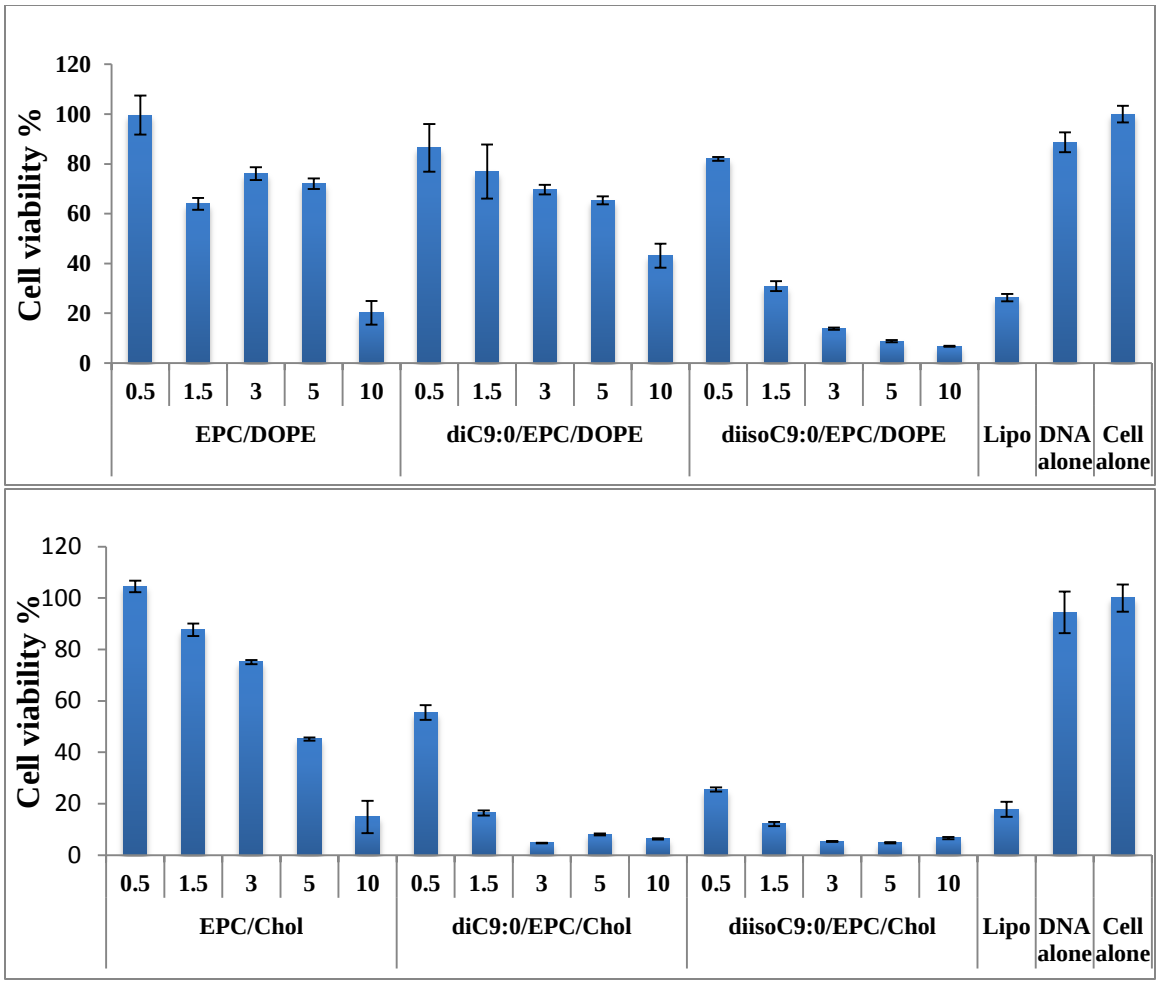

Figure 5.11-Cytotoxicity (after 48 h) of diC9:0 and diisoC9:0/co-lipid/DNA lipoplexes compared to EPC/co-lipid/DNA at molar charge ratios of 0.5 to 10 and Lipofectamine 2000™ (Lipo) (n = 9; mean ± SD) as positive controls, and plasmid DNA alone and CHO-K1 cells alone as negative controls

SAXD studies were performed on the lipoplexes prepared with the C9 pyridinium lipids and co-lipids, DOPE and cholesterol at two charge ratio 1.5 and 3 (Table 5.3).

All formulations with cholesterol at both CR showed lamellar packing, despite the calculated value of S_{mix} greater than one in all cases. Formulations of **diC9:0** with DOPE at lower charge ratio have lamellar packing, however as the CR increases, the packing is

observed to change to hexagonal. Formulations of **diisoC9:0** with DOPE at both CR showed hexagonal packing, which was expected because of the higher S of this lipid.

Table 5.3-Summary of SAXD results for pyridinium lipids/EPC lipid/pDNA and EPC/DOPE and EPC/Chol lipoplex formulations at (+/-) molar charge ratio 1.5:1 and 3:1. δ refers to the actual packing in each case, with an estimated standard deviation of typically 1Å.

Cationic lipids	Co-Lipid	CR	Packing	Lattice Parameter	S_{mix}
diC9:0/EPC	DOPE	1.5	Lamellar	δ = 63Å	1.1
diisoC9:0/EPC	DOPE	1.5	Hexagonal	δ = 68Å	1.2
diC9:0/EPC	DOPE	3	Lam/Hexagonal	δ = 64Å	1.1
diisoC9:0/EPC	DOPE	3	Hexagonal	δ = 68Å	1.2
diC9:0/EPC	Cholesterol	1.5	Lamellar	δ = 68Å	1.1
diisoC9:0/EPC	Cholesterol	1.5	Lamellar	δ = 66-85Å	1.3
diC9:0/EPC	Cholesterol	3	Lamellar	δ = 71Å	1.1
diisoC9:0/EPC	Cholesterol	3	Lamellar	δ = 70Å	1.3

Formulations of both pyridinium lipids with cholesterol have low activity compared the EPC/cholesterol and the SAXD data show lamellar phases are formed. Considering the poor transfection of these formulations, it is likely that the pyridinium lipids destabilize the EPC/Chol phase and form another phase which, though it is lamellar, is different from EPC/cholesterol alone. This phase must contain pyridinium lipids and has very poor transfection efficiency.

Formulations of **diC9:0** with DOPE as the co-lipid show similar transfection and toxicity as the EPC/DOPE binary formulation. Looking at the SAXD result, at lower charge ratios the **diC9:0** lipoplex has lamellar packing but as the CR increases from 1.5 to 3 the packing changes from lamellar to hexagonal. **DiisoC9:0** formulations with DOPE in general have lower transfection, and higher toxicity as the charge ratio increases. As previously discussed, EPC/DOPE systems are probably more tolerant to the introduction

of the pyridinium lipid as an impurity. It is likely that **diC9:0** could partition into EPC/DOPE to some extent and be less exposed to the cell and so less toxic. The **diisoC9:0**, because of the structure of chains would disturb the packing even in a tolerant EPC/DOPE matrix, would lower the transfection efficiency, and increase the toxicity due to losses into the medium.

These transfection data cannot be correlated with TI_{PSVM} to investigate the effect of shape parameter, since formulations are either lamellar, or inactive, or too toxic and in some cases all three.

5.3.2-Transfection efficiency of diC20:0 and dibrC20:0

Liposome and lipoplex formation and analysis, together with transfection and cytotoxicity assays were conducted using the protocols discussed in the previous chapter. Pyridinium lipids were formulated with EPC and a co-lipid (cholesterol or DOPE) in a molar ratio of 1.5:1.5:2 as liposomes and then mixed with plasmid DNA at varying charge ratios. Gel retardation assays established that DNA binding was better at a charge ratio greater than 5 for **diC20:0** and 10 for **dibrC20:0**. The DNase assay generally showed a similar protection of the DNA by the lipoplexes at charge ratio greater than 5. The results can be found in the Appendix C.

The transfection efficiency and toxicity of the synthesized pyridinium lipids, **diC20:0** and **dibrC20:0** with EPC as the co-cationic lipids in formulations with co-lipids DOPE and cholesterol (three sets of triplicates) has been studied and compared with Lipofectamine 2000^{TM} (single sets of triplicates) as the control (Figure 5.12 and 5.13).

Formulations of **dibrC20:0** showed similar transfection with both co-lipids (Figure 5.12). However, **diC20:0** revealed comparable transfection to **dibrC20:0** with cholesterol

as co-lipid, but significantly reduced transfection compared to **dibrC20:0** with DOPE as co-lipid.

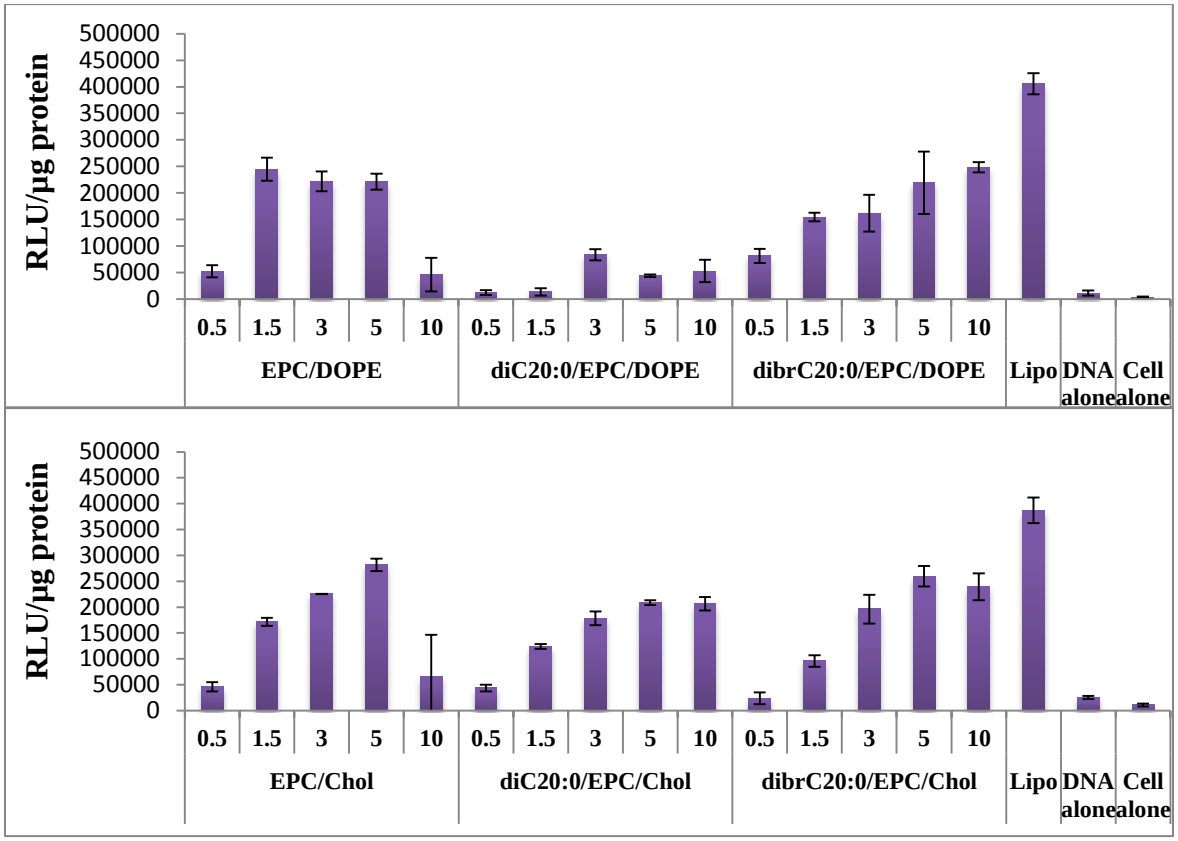

Figure 5.12-Transfection efficiency as luminescence readings of β-galactosidase (after 48 h) of diC20:0 and dibrC20:0/co-lipid/DNA lipoplexes compared to EPC/co-lipid/DNA at molar charge ratios of 0.5 to 10 and Lipofectamine 2000™ (Lipo) (n=9; mean ± SD) as positive controls, and plasmid DNA alone and CHO-K1 cells alone as negative controls.

Formulations of both **diC20:0** and **dibrC20:0** with cholesterol or DOPE had similar toxicity to the binary EPC/co-lipid formulations (Figure 5.13). In general these pyridinium compounds showed a charge ratio dependent toxicity at the lower charge ratios. This is in line with the previous toxicity correlation with clogP and with S.

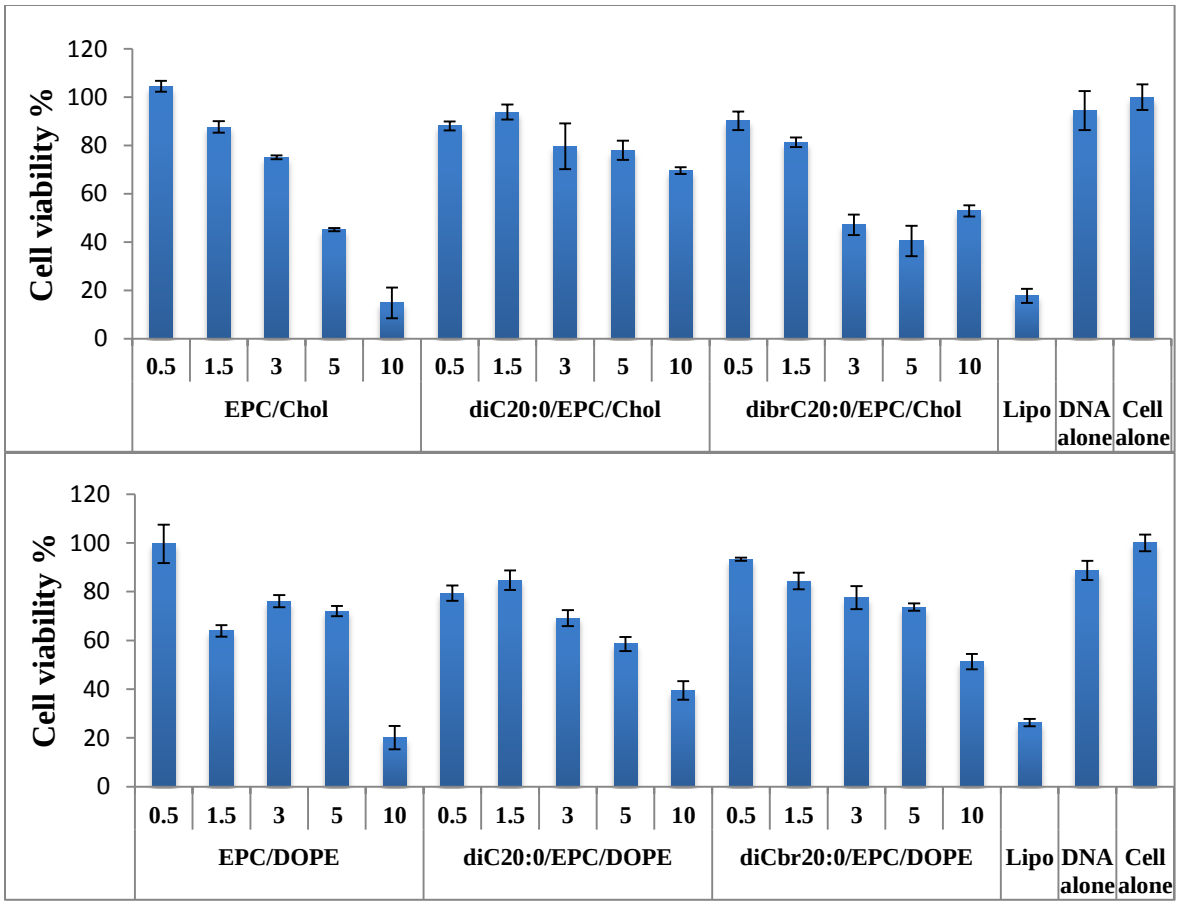

Figure 5.13-Cytotoxicity (after 48 h) of diC20:0 and dibrC20:0/co-lipid/DNA lipoplexes compared to EPC/co-lipid/DNA at molar charge ratios of 0.5 to 10 and Lipofectamine 2000™ (Lipo) (n = 9; mean ± SD) as positive controls, and plasmid DNA alone and CHO-K1 cells alone as negative controls.

SAXD studies were attempted on the lipoplexes prepared with lipids **diC20:0** and **dibrC20:0** and co-lipids, DOPE and cholesterol at two charge ratio 1.5 and 3.

None of the formulations of **diC20:0** and **dibrC20:0** gave a clear SAXD result on the packing. As a result we can assume a hexagonal phase lipoplex but we have no experimental confirmation. The data is found in Appendix C.

Looking at the transfection results of **diC20:0** and **dibrC20:0** correlated with CR (Figure 5.12), it can be seen that binary EPC/co-lipid formulations have similar activity.

Formulations of both pyridinium lipids with cholesterol have similar activity compared the EPC/cholesterol, except at CR = 10. **DiC20:0**/EPC/DOPE revealed the lowest transfection at all charge ratios. This is in line with expectation as the high T_m of this lipid in the EPC/DOPE mixture could lead to coexisting phases in which the pyridinium compound is not available for migration from the lipoplex and therefore has low transfection efficiency.

The transfection as a function of charge ratio for formulations involving **dibrC20:0** is unlike previous cases. Usually there is a maximum about CR 3 and earlier this was associated with a lattice filling process. However at low charge ratios (0.5–5) the transfection is similar to binary EPC/co-lipid but increases significantly at charge ratio 10. This suggests that if there is a lattice filling occurring, it requires a large amount of added lipid to achieve. These are very hydrophobic lipids and it is possible that because of low solubility of these lipids only a small amount is actually transferred to the liposomes during the lipid hydration stage. Visual observation of the liposome formation process confirms this suggestion and the collaborators struggled to get the C20 pyridinium lipids into lipoplexes.

To further investigate the potential losses of **dibrC20:0**, an experiment was carried out, comparing the hydration and partitioning of EPC/**dibrC20:0** and EPC/**diC16:0** binary mixtures, using ESI-MS with tetrbutylammonium as an internal standard to assess if fractionation and/or loss occur. The pyridinium lipids in 1:1 ratio to EPC were dissolved in a chloroform stock solution where they are all very soluble. Analysis of an aliquot of this solution with a known added standard gave spectra that showed strong ions for the parent cationic lipids and the standard. The ion intensity of each peak in the mixture was

measured and compared, using the ion intensity of the tetrabutylammonium ion as the reference. Then the stock solution was evaporated to form a thin layer of lipids and the layer was hydrated with water as occurs in the first stage of liposome formation. After sonication of this solution, an aliquot plus a known amount of standard was analysed as previously. The ion intensities of the lipids were again compared with the ion intensity of the tetrabutylammonium standard. The sets of experiments are conveniently compared as given in Table 5.4 which sets the intensity of the initial pyridinium ion from the chloroform stock solution = 100.

The results clearly showed that though there is a significant loss of pyridinium lipids on transfer from an organic stock solution to a dispersion in an aqueous phase in comparison to EPC, the loss of **dibrC20:0** is much greater than the loss of **diC16:0.** It is likely that during liposome formation at lower charge ratios where there is a smaller amount of the pyridinium lipid present, the hydration might not pick up the pyridinium lipids into the aqueous dispersion solution. In these experiments a residue of lipid film on the wall of the glass container was evident. Since a lower amount of the pyridinium lipid than expected is transferred to the liposome this has the effect of making the actual charge ratio lower than the CR based on the initial mixture of lipids.

Table 5.4-Comparison of ESI-MS ion intensity of dibrC20:0/EPC and diC16:0/EPC from an initial chloroform stock solution and a dispersion in water

Compound	**%EPC**	**%diC16:0**
diC16:0 stock $CHCl_3$	64	100
diC16:0 water dispersion	49	14
Compound	**%EPC**	**%dibrC20:0**
dibrC20:0 stock $CHCl_3$	67	100
dibrC20:0 water dispersion	35	0.06

To summarize: this attempt to explore the influence of lipid shape at the extremes of the range of the lipid series was not very successful. The C9 isomers were quite inactive and only one formulation (**disoC9:0**/EPC/DOPE) showed any significant activity. As interesting as this result might be, it does not provide a general test of TI_{PSVM} and the shape parameter. At the lipophilic end of the sequence there were signs of interesting activity, particularly for **dibrC20:0** at high charge ratios, but this cannot be used as a test of shape parameter and TI_{PSVM} as there is evidence of significant loss of these lipophilic lipids with the consequence that the true charge ratio in the lipoplex is unknown and the calculated TI_{PSVM} is thus in error.

5.3.3-Transfection efficiency of blends of lipids diC18:1 and dibrC20:0

In an attempt to generate lipoplexes with high values of S yet containing material at the composition of the stocks mixed, we explored the use of blends of two pure compounds. **Blend 50** (50:50 of **dibrC20:0**:**diC18:1)**, **blend 66** (66:34 of **dibrC20:0**:**diC18:1)** and **blend 85** (85:15 of **dibrC20:0**:**diC18:1)** were prepared. Liposome, lipoplex and transfection experiments were conducted using the protocols discussed in the previous chapter. Pyridinium lipids were formulated with EPC and a co-lipid (cholesterol or DOPE) in a molar ratio of 1.5:1.5:2 as liposomes and then mixed with plasmid DNA at varying charge ratios. Gel retardation assays established that all blends are similar in binding to DNA and in the DNase assay generally showed a similar protection of the DNA by the lipoplexes at the charge ratio greater than 5. The results can be found in the Appendix C.

The transfection efficiency and toxicity of the blends of synthesized pyridinium lipids, **blend 50, blend 66** and **blend 85** with EPC as the co-cationic lipids in formulations with

co-lipids DOPE and cholesterol (three sets of triplicates) has been studied and compared with Lipofectamine 2000™ (single triplicate set) as the control (Figure 5.14 and 5.15).

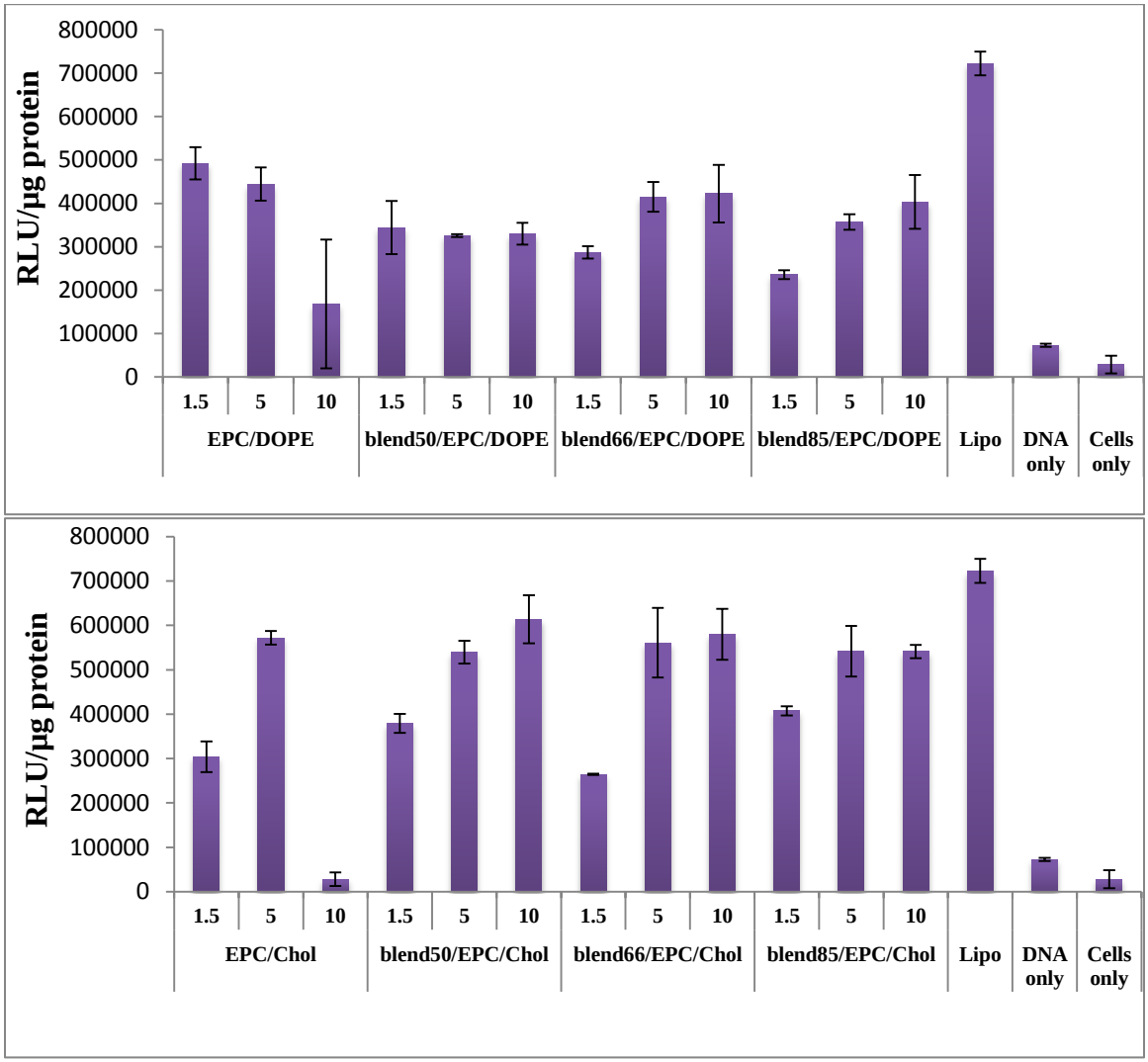

Figure 5.14-Transfection efficiency as luminescence readings of β-galactosidase (after 48 h) of blend 50, blend 66 and blend 85/co-lipid/DNA lipoplexes compared to EPC/co-lipid/DNA at molar charge ratios of 1.5, 5, 10 and Lipofectamine 2000™ (Lipo) (n = 9; mean ± SD) as positive controls, and plasmid DNA alone and CHO-K1 cells alone as negative controls.

The transfection results of the blends (Figure 5.14) showed that the transfection efficiency in blends is better with cholesterol rather than DOPE. The toxicity of these lipids is shown in Figure 5.15; the formulations with DOPE are generally less toxic than

those with cholesterol.

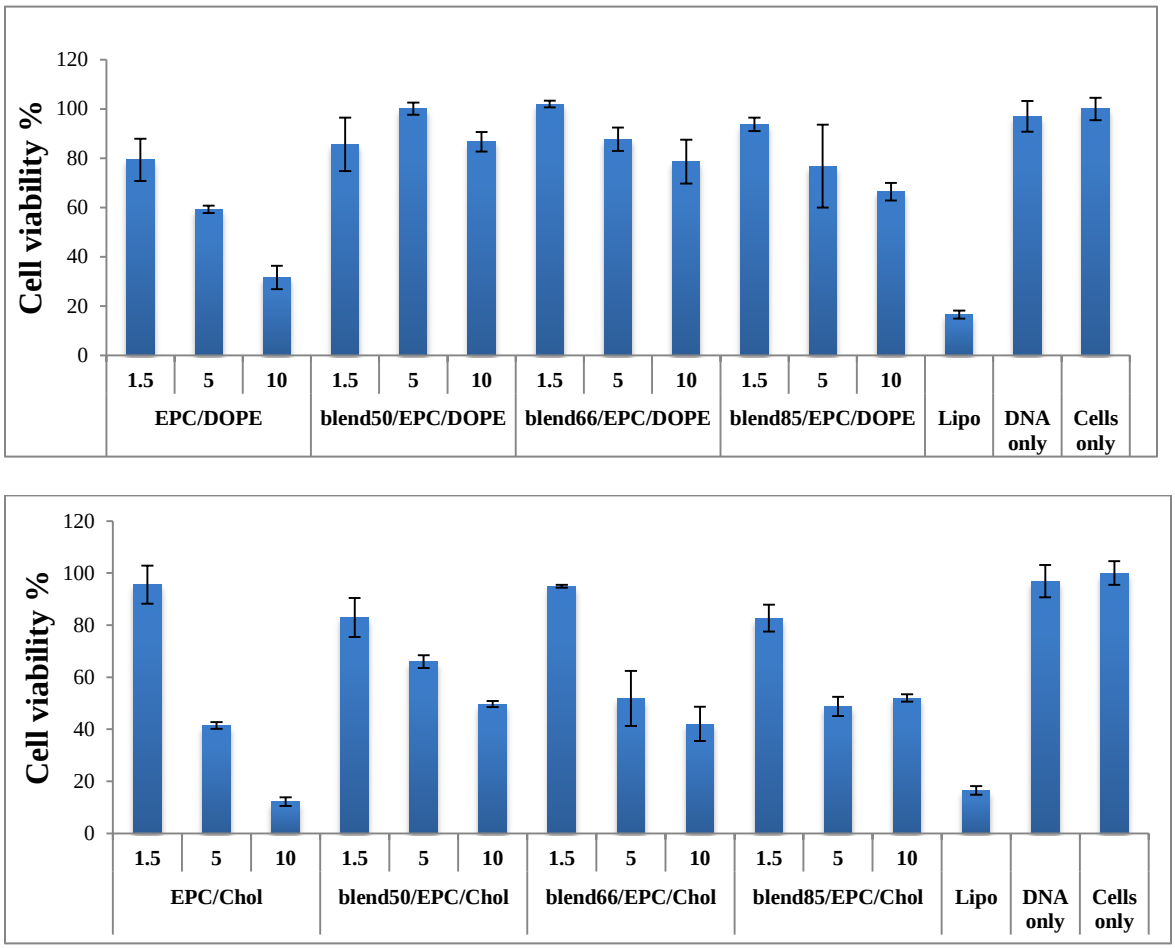

Figure 5.15-Cytotoxicity (after 48 h) of blend 50, blend 66 and blend 85/co-lipid/DNA lipoplexes compared to EPC/co-lipid/DNA at molar charge ratios of 1.5, 5, 10 and Lipofectamine 2000™ (Lipo) (n = 9; mean ± SD) as positive controls, and plasmid DNA alone and CHO-K1 cells alone as negative controls.

SAXD studies were attempted on the lipoplexes prepared with blends of the pyridinium lipids formulations with EPC and co-lipids, DOPE and cholesterol at two charge ratios 1.5 and 3. The Data is in Appendix C.

The formulations of **blend 50** gave a lamellar packing. However, as the amount of **dibrC20:0** in the blend increases, the SAXD result is indeterminate, which we believe is

because of the presence of **dibrC20:0**. As a result we can assume a hexagonal phase lipoplex but we have no experimental confirmation.

When we attempted the correlation of the transfection results with TI_{PSVM}, the data were scattered and the fit was poor (Figure 5.16).

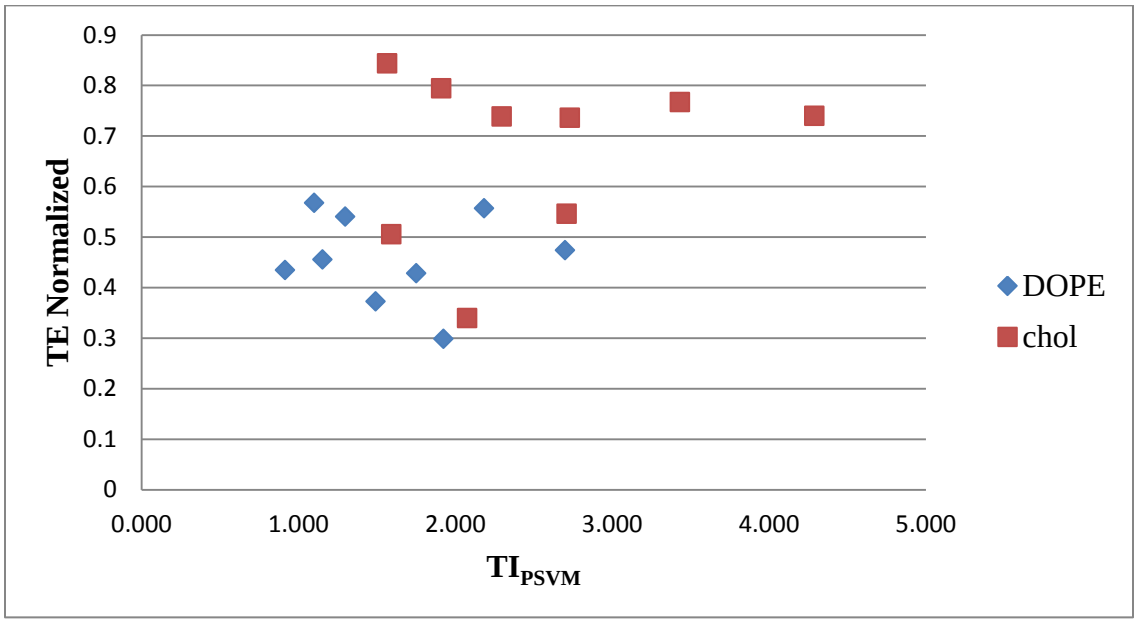

Figure 5.16-Transfection as a function of TI_{PSVM} of the blends of synthesized pyridinium lipids, blend 50, blend 66 and blend 85 with co-lipids DOPE and cholesterol.

After looking at the results of these experiments, it can be concluded that the shape of the lipid is important as an effective parameter in the transfection. However, looking deeper into the TI_{PSVM} , it was seen that the molecular parameters that are used to calculate the shape parameter, a_0, V_c and l_c, are the same parameters applied in the calculation of the volume filling term, and these two terms are not independent from each other. The volume filling terms seems to be the more fundamental, so we explored a TI where the shape parameter was omitted from TI_{PSVM}. This resulted in a simpler transfection index, TI_{PVM} as follows:

TI_{PVM} = *partition term* × *volume fill term* × *melting term* ***Equation 5.11***

Correlation of the transfection results of the blends with TI_{PVM} is shown in Figure 5.17, showing a slightly better correlation with some trend in the data, but this is not very persuasive. Poor fractionation of **dibrC20:0** is possible in these experiments and may be the origin of the scatter.

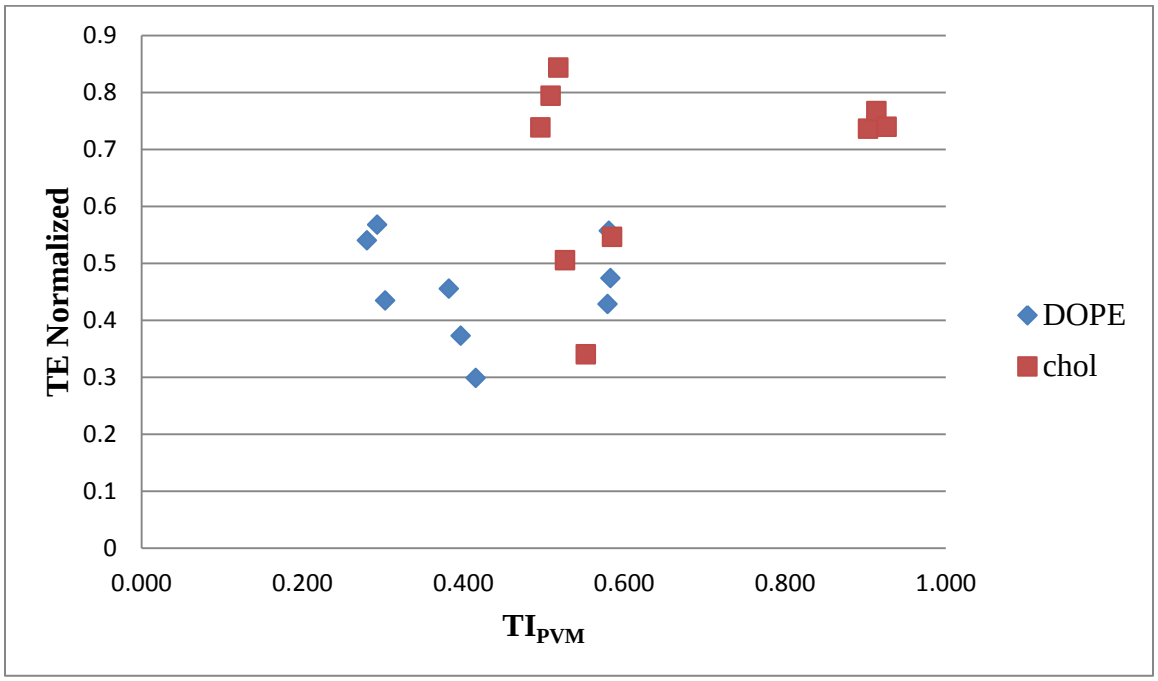

Figure 5.17-Transfection as a function of TI_{PVM} of the blends of synthesized pyridinium lipids, blend 50, blend 66 and blend 85 with co-lipids DOPE and cholesterol.

5.4-Comparison of transfection efficiency of synthesized ternary lipids and binary blend of pure lipids

In order to generate a sample of lipids with a high S yet an acceptable formation of liposomes on hydration we considered the synthesis of mixed-chain lipids. In addition, it is likely that lipids with two different chains enhance the transfection efficiency by favouring lower melting phases. To study the effect of this kind of lipid mixture a ternary lipid mixture of **diC18:1** ***(2-27)***, **dibrC20:0** ***(2-25) and*** **(C18:1)(brC20:0)** ***(4-4)*** was synthesized and the composition of the mixture was determined with ESI-MS as

described in chapter 3 (Figure 5.18). Here the **dibrC20:0** is present but at a much lower concentration than in the experiments of the previous section. At the same time, the S_{mix} of the lipids is high.

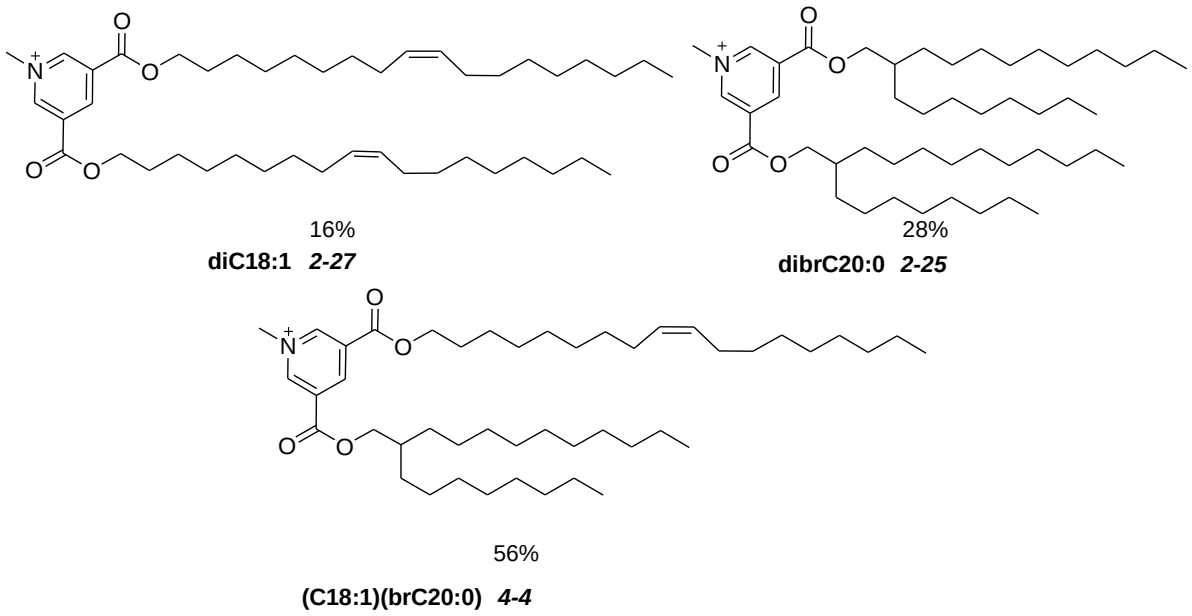

Figure 5.18-The ternary mixture of diC18:1 (2-27), dibrC20:0 (2-25) and (C18:1)(brC20:0) (4-4) and the composition of the mixture

We were also interested to compare the activity of this mixture with that of a binary blend of pure lipids, **diC18:1** ***(2-27)*** and **dibrC20:0** ***(2-25)***, in ratio of 32% to 68%. The composition of blend was calculated to give the same shape parameter as the ternary mixture, so the molecular parameters of the mixture and the blend were similar.

The transfection efficiency and toxicity of the synthesized pyridinium lipids, ternary mixture and binary blend of the lipids with EPC as the co-cationic lipids in formulations with co-lipids DOPE and cholesterol (three sets of triplicates) has been studied and compared with Lipofectamine 2000^{TM} (single sets of triplicates) as the control (Figure 5.19 and 5.20).

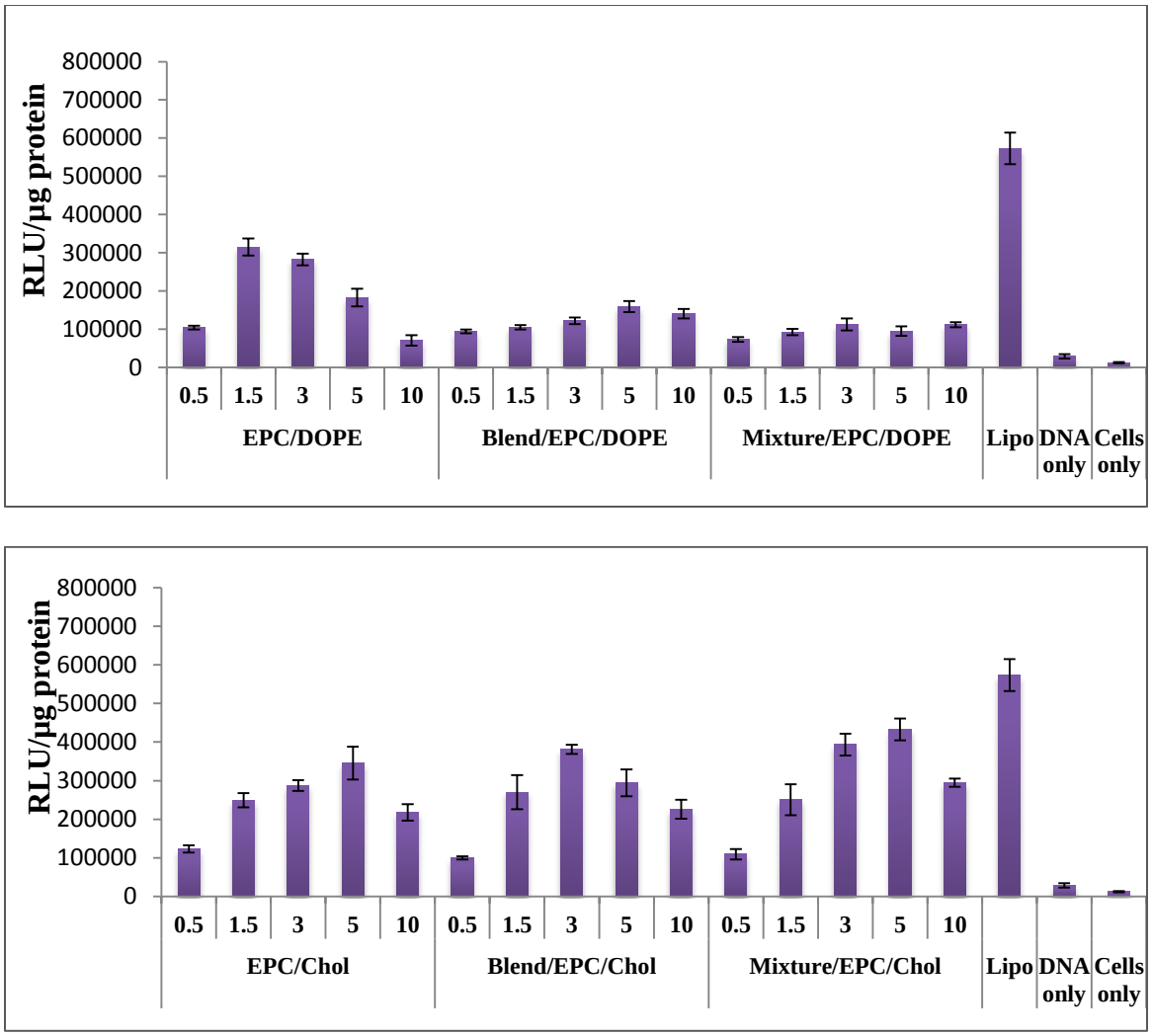

Figure 5.19-Transfection efficiency as luminescence readings of β-galactosidase (after 48 h) of the ternary mixture and binary blend of lipids/co-lipid/DNA lipoplexes compared to EPC/co-lipid/DNA at molar charge ratios of 0.5 to 10 and Lipofectamine 2000™ (Lipo) (n = 9; mean ± SD) as positive controls, and plasmid DNA alone and CHO-K1 cells alone as negative controls.

The transfection efficiency of the ternary mixture and binary blend are similar, however the transfection with DOPE as co-lipid is quite poor and is much lower than EPC/DOPE. The transfection with cholesterol as the co-lipid is consistent with EPC/chol, only slightly greater with the mixture.

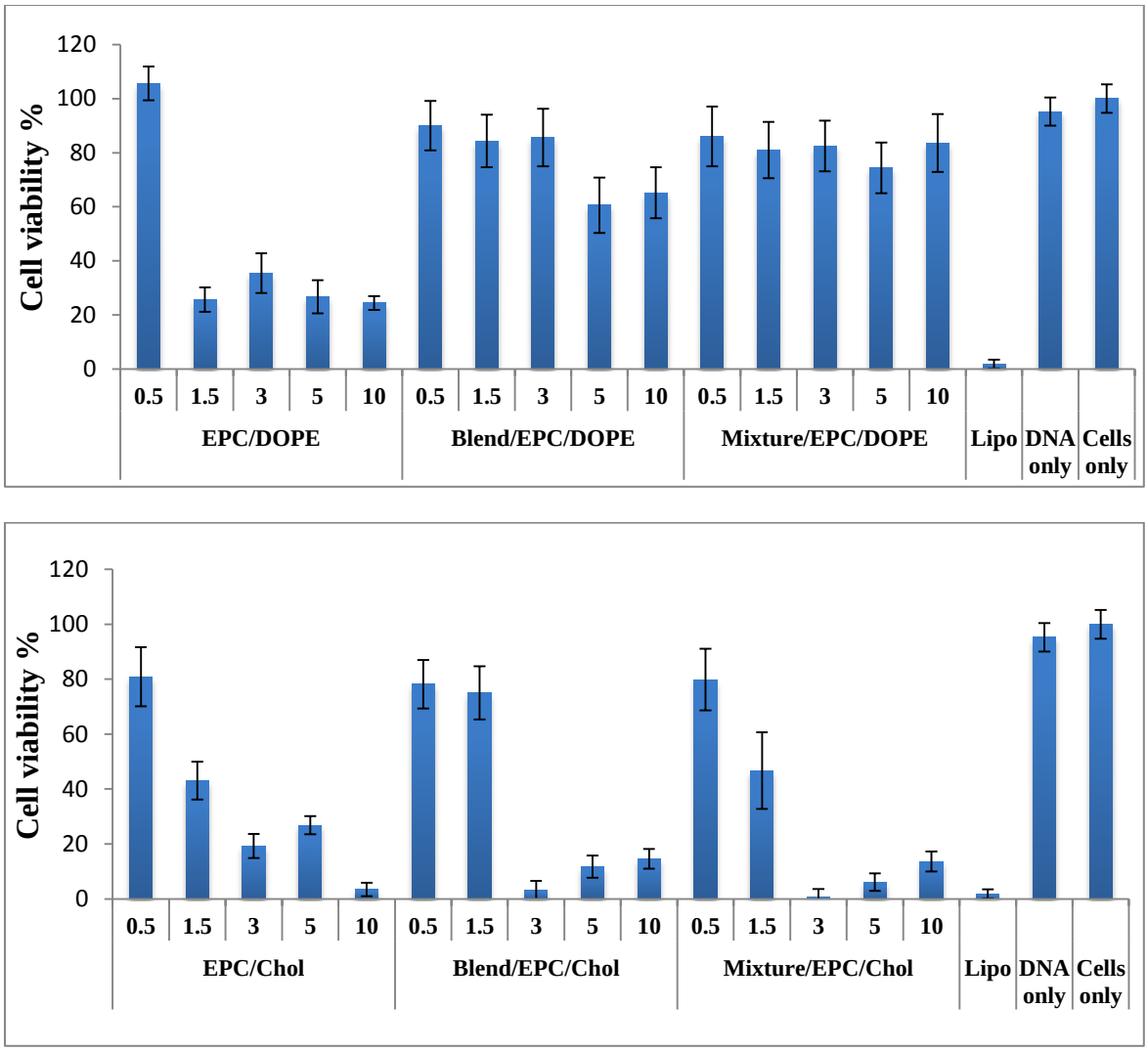

Figure 5.20-Cytotoxicity (after 48 h) of the ternary mixture and binary blend of lipids/co-lipid/DNA lipoplexes compared to EPC/co-lipid/DNA at molar charge ratios of 0.5 to 10 and Lipofectamine 2000™ (Lipo) (n = 9; mean ± SD) as positive controls, and plasmid DNA alone and CHO-K1 cells alone as negative controls.

SAXD studies were attempted on the lipoplexes prepared with pyridinium lipids, EPC and co-lipids, DOPE and cholesterol at two charge ratio 1.5 and 3. None of the formulations of the mixture and the blend gave a clear result on the packing. The data is in the Appendix C.

Looking at the toxicity of these lipids, there is a significant increase in all formulations with cholesterol at charge ratio greater than 1.5, similar for both the mixture and blend. The toxicity of all formulation with DOPE was low, which is in line with their low transfection.

Comparing the transfection of the blends (two pure components) with the synthesized mixture in Figure 5.21, it can be seen that the transfection efficiency of these lipids is essentially the same, demonstrating that a mixture of of pure lipids with close molecular parameters, the efficiency is similar.

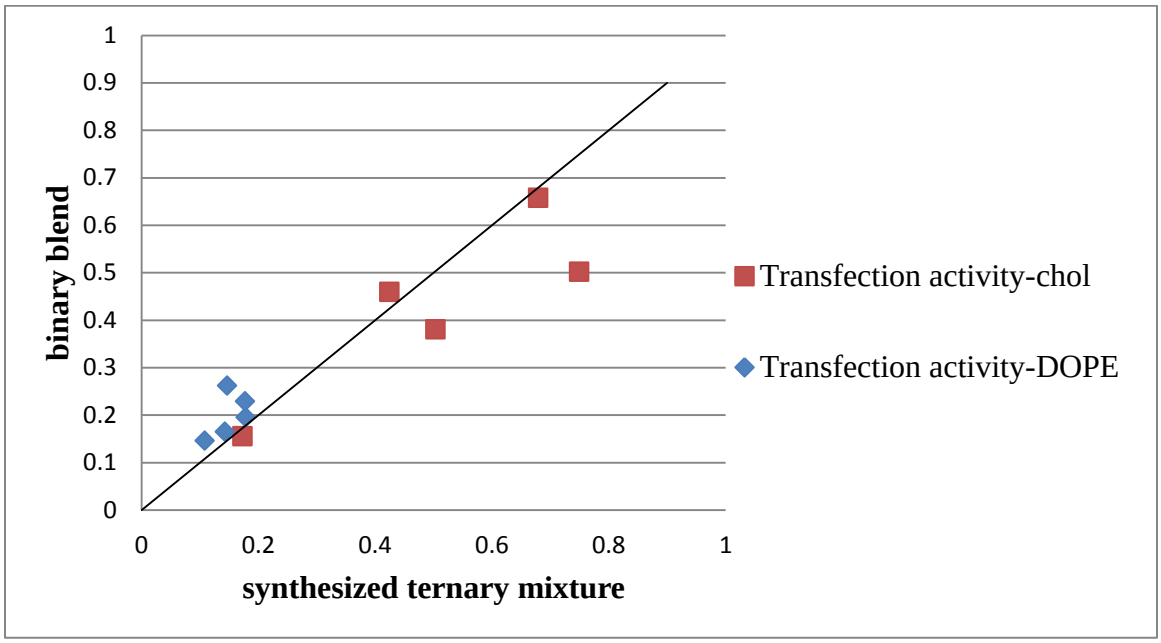

Figure 5.21-Comparison of transfection efficiency of ternary mixture of lipids diC18:1, dibrC20:0, (C18:1)(brC20:0) and binary blend of diC18:1 and dibrC20:0.

For investigating the similarity in TI_{PVM}, the transfection data gave a better correlation for the formulations with cholesterol as the co-lipid (R^2 = 0.84) (Figure 5.22). The fit using formulations that include DOPE gave a poor correlation (R^2 = 0.21), which can be related to the unknown phase of the lipoplex. The merged dataset (cholesterol plus

DOPE) gave an overall correlation with $R^2 = 0.63$. The cholesterol data gave a good fit of which confirms that TI_{PVM} is based on molecular parameters that are relevant to transfection.

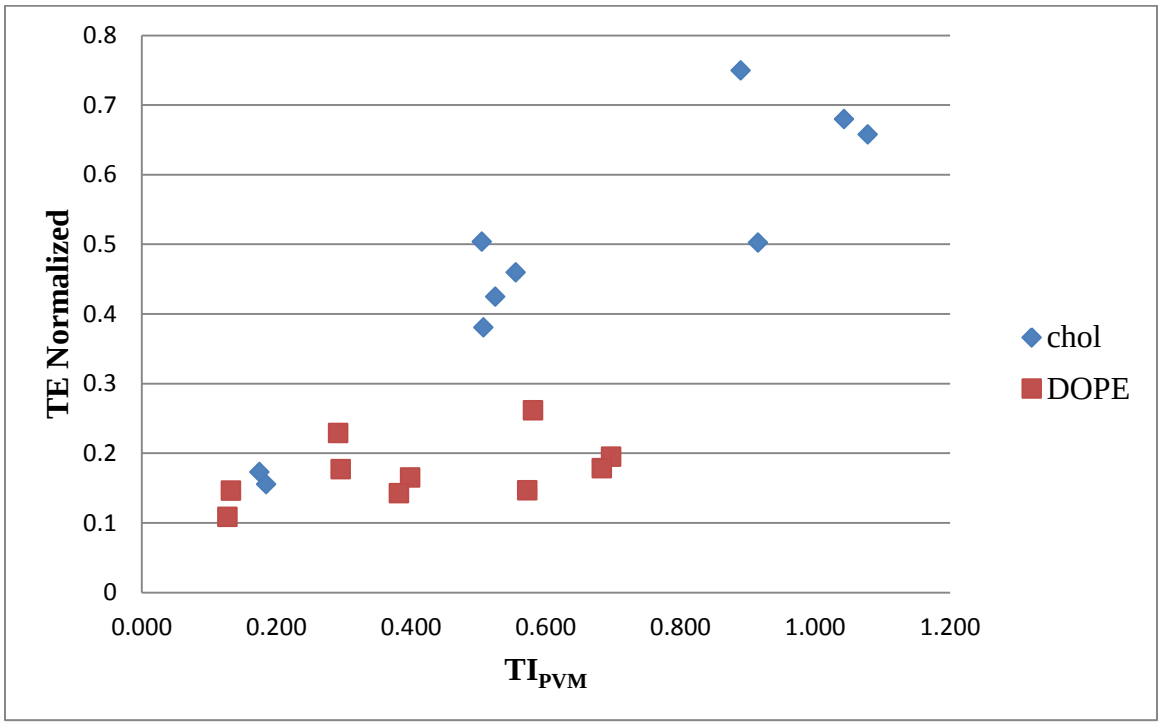

Figure 5.22-Transfection as a function of TI_{PVM} of the blends of synthesized pyridinium lipids, blend 50, blend 66 and blend 85 with co-lipids DOPE and cholesterol.

5.5-Effective parameters in the transfection efficiency

The correlations discussed to this point have involved single experiments that are performed in triplicate. The experiments are limited to about 30 independent treatments within an experiment to allow triplicates within a single 96-well plate. At this point we have several independent experiments and a refined TI_{PVM}. Within each experiment TI_{PVM} gives the best correlation of any of the alternatives that have been explored. The question is whether this index can unify independent transfection experiments. To study the effect of the developed TI_{PVM}, a correlation was carried out on the total available transfection results. This includes all the data discussed in the previous sections of this

chapter and the data of chapter 4. The result is shown in Figure 5.23. The correlation, independent of the co-lipid, showed an acceptable fit of R^2 = 0.57. This confirms that TI_{PVM} is based on the developed parameters which are dependent on the molecular parameters.

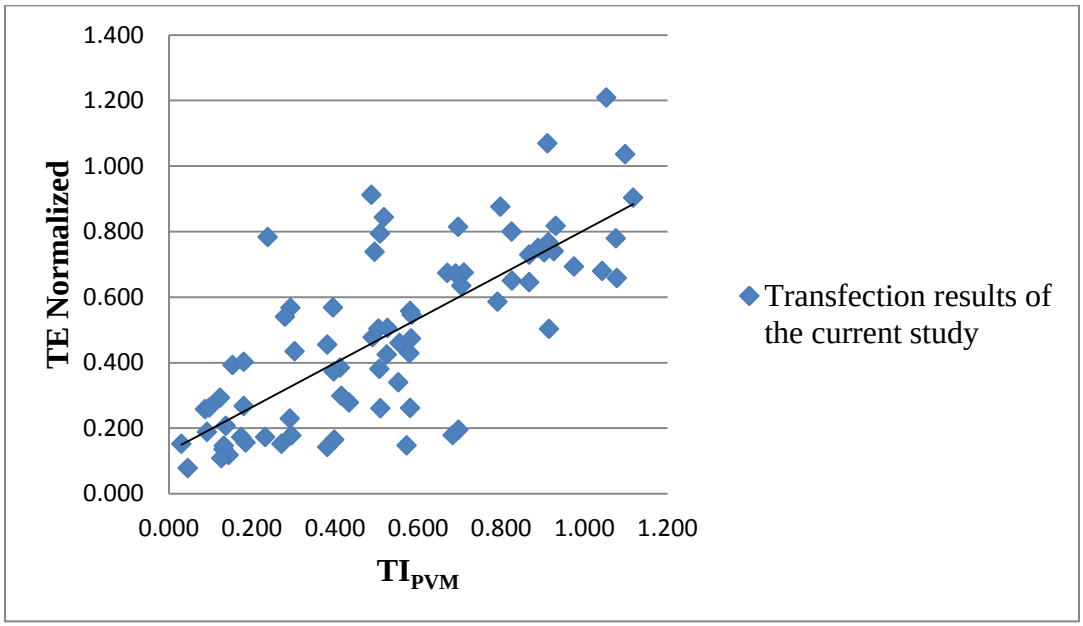

Figure 5.23-Transfection as a function of TI_{PVM} of the total transfection results of the current study.

5.6-Summary

Pyridinium lipids of varied chain length were studied to further investigate the prediction ability of TI_{PSV} developed in the previous chapter. Poor correlation of the transfection efficiency of these pyridinium lipids, led to modifying the TI_{PSV}. From the transfection data it appeared that the T_m and miscibility of the pyridinium lipids could have a considerable effect on the transfection. For lipids with straight chains, both of these properties can be correlated to the number of carbons in the chain. There is a critical number of carbons which is different for each T_m and miscibility, where both of these terms will have an optimum and deviation from this value will decrease the

transfection efficiency. Using these terms, a modified TI_{PSVM} was developed and correlation of the transfection results gave an acceptable fit.

A QSAR study was performed on the toxicity of lipids studied, relating the cytotoxicity to charge ratio, $clogP_{mix}$ and S_{mix}.

Looking at the effect of shape parameter on the transfection efficiency, analogues of pyridinium lipids of C9 (**diC9:0** and **diisoC9:0**) and C20 (**diC20:0** and **dibrC20:0**) were studied. The results of C20 analogues suggested there is a limited transfer and extensive fractionation of these lipids into the liposomes and the lipoplex because of their poor solubility. However when at a higher charge ratio some of the **dibrC20:0** incorporates into the lipoplex, it enhances the transfection significantly in comparison to EPC/co-lipid formulations. C9 analogues had poor miscibility with the EPC/co-lipid phase because of shorter chains. At lower charge ratios, the small amount of these lipids improved the transfection efficiency. However as the charge ratio increases, these lipids prefer to form aggregates on their own, which not only decreases the transfection but increases the toxicity.

For a more direct investigation of increasing shape parameter, a series of blends of **blend 50** (50:50 of **dibrC20:0**:**diC18:1)**, **blend 66** (66:34 of **dibrC20:0**:**diC18:1)** and **blend 85** (85:15 of **dibrC20:0**:**diC18:1)** was studied. With these data, TI_{PSVM} gave poor correlation. Although the shape parameter is an effective factor in the transfection process and is essential to predict the formation of hexagonal lipoplexes, it is not independent of the volume filling term, as the same molecular parameters are used for their calculation. This led to development of a simpler transfection index TI_{PVM},

correlating the transfection to partition, volume filling and chain melting all derived from molecular parameters of the lipids.

Comparison of the synthesized ternary mixture of lipids and a binary blend of pure lipids with similar molecular parameters, showed that the transfection efficiency depends on the molecular parameters of the lipids and when these lipid parameters are similar, lipoplexes derived from these lipids will exhibit similar transfection efficiencies.

Finally, correlation of all the transfection results obtained from the various synthetic pyridinium lipids studied with TI_{PVM} showed an acceptable fit, confirming the dependency of transfection on the identified parameters.

Chapter 6: Conclusions, future directions and significance

The goal outlined at the start of this study was to develop a "pre-QSAR" transfection index (TI) to relate the in vitro transfection efficiency to molecular parameters of the lipids used as the non-viral vector, and to the stoichiometric parameters of the liposomes and lipoplexes in the transfection experiment. In parallel, this study investigated the toxicity of these cationic lipids with a goal to determine the effective molecular parameters that could be adjusted to lower the toxicity. Based on the TI and cytotoxicity models, it should be possible to design a high-activity cationic lipid as a non-viral vector for delivery of nucleic acid with optimum transfection efficiency and low toxicity.

To achieve this goal, a series of diester pyridines was synthesized via ester coupling of pyridine dicarboxycylic acid with various alcohols to yield final lipids (with yields ranging from 16% to 84%) with varied structural properties such as clogP, lipid shape parameter, and chain length and branching. Methylation of the prepared diester pyridines with a non-nucleophilic counterion resulted in a library of pure, well characterized compounds.

A preliminary transfection index (TI_{PSV}) was developed:

$$TI_{PSV} = \textit{partition term} \times \textit{shape term} \times \textit{volume fill term} \qquad \textbf{Equation 6.1}$$

These terms were derived from molecular structure parameters which were in turn calculated from the structure of lipids without experimental data. The partition term refers to the difference in clogP of cationic lipids and neutral lipid of the endosome, which is the driving force in destabilizing the endosomal membrane. The shape parameter, (the difference between shape parameter of the cationic lipids and that of the neutral lipids in the endosome given a value of 1) is the effective factor in releasing the

nucleic acid inside the cell. The lattice filling term reflects how well the lattice of nucleic acid and lipids is packed. At the optimum number of lipids, which is dependent on charge ratio of cationic lipids to DNA and the ratio between the cationic lipids and co-lipids, the free energy of the lattice is at the minimum and the nucleic acid is well protected by the lipids. This TI was linearly correlated to transfection activity of synthesized pyridinium lipids, **diC16:0** and **diC16:1** co-formulated with EPC with co-lipids DOPE and cholesterol with an adequate correlation coefficient. The shape parameter of the lipid mixture was calculated based on molar weighted S of the lipids in the mixture and appears to be able to predict the morphology of the lipoplex, as observed by the SAXS measurement of the prepared lipoplexes. A QSAR study was done on the toxicity of studied lipids, relating the cytotoxicity to charge ratio, $clogP_{mix}$ and S_{mix}.

To further investigate and develop the TI, and to study the effect of the partitioning and shape parameter of these lipids, additional sets of experiments were carried out.

Pyridinium lipids of varied chain length were studied to further investigate the prediction ability of TI developed in the previous chapter. Poor correlation of the transfection efficiency of these pyridinium lipids, led to modifying the TI. It was suggested that the chain melting and the miscibility of the pyridinium lipids have a considerable effect on the transfection. When the melting temperature of the lipids is lower than the temperature of the experiment, the mixture will be at a fluid phase. Lipids with higher T_m will be in a gel phase. Depending on how well the cationic lipid is mixed with EPC/co-lipid system, the phase of the system will be different. It has been reported that in systems with melting temperature close to the temperature of the experiment, the transfection efficiency increases. In lipids with straight chains, both of these properties

can be correlated to the number of carbons in the chain. We assumed that there is a critical number of carbons for the lipid mixture, where both of these terms will reach an optimum and that deviation of this value will decrease the transfection efficiency. Using these terms, a TI_{PSVMM} was proposed as follows:

TI_{PSVMM} = *partition term* × *shape term* × *volume fill term* × *mixing term* × *melting term*

Equation 6.2

However, calculating the mixing and melting term showed that for lipids that are used experimentally, these two term are essentially the same, as they both relate to the number of rotors in the chains and the chain length. The melting term is good representative of these two parameters, as it has a more significant effect on the transfection. This led to development a less complex transfection index, TI_{PSVM} as follow:

TI_{PSVM} = *partition term* × *shape term* × *volume fill term* × *melting term*

Equation 6.3

The TI_{PSVM} was correlated to the transfection results to give an acceptable fit. A QSAR study was done on the toxicity of these additional lipids, confirming the relation between the cytotoxicity to charge ratio, $clogP_{mix}$ and S_{mix}, on a more extensive set of data.

Looking at the effect of shape parameter on the transfection efficiency, analogues of pyridinium lipids of C9 (**diC9:0** and **diisoC9:0**) and C20 (**diC20:0** and **dibrC20:0**) were studied. The results from the C20 analogues suggested there is a limited transfer of these lipids into the liposomes and the lipoplex because of their poor solubility. However at higher charge ratios some of the **dibrC20:0** incorporates into the lipoplex where it enhances the transfection significantly in comparison to EPC/co-lipid formulations. C9 analogues had poor miscibility with EPC/co-lipid phase because of shorter chains. At

lower charge ratios, the small amount of these lipids improved the transfection efficiency but as the charge ratio increased these lipids preferred to form lamellar aggregates of unknown composition which not only decreases the transfection but increases the toxicity.

A more direct study was done on a series of blends in ratio of 50:50, 66:34 and 85:15 of **dibrC20:0**:**diC18:1** for investigation of the effect of the shape parameter. The correlation with TI_{PSVM} was poor for this experiment. It was observed that, the shape parameter is not independent of the volume filling term since the same molecular parameters are used for their calculation. This led to development of a simpler transfection index TI_{PVM}, correlating the transfection to partition, melting and molecular parameters of the lipids.

TI_{PVM} = *partition term* × *volume fill term* × *melting term*

Equation 6.4

Comparison of the synthesized ternary mixture of lipids and a binary blend of pure lipids, with similar molecular parameters showed the transfection depends only on the molecular parameters of the lipids and when these parameters are similar, they will have close transfection efficiency at the same charge ratio.

A correlation between the total transfection results in this study and the developed TI_{PVM}, showed an acceptable fit, confirming the dependency on the developed parameters. This three parameter transfection index is relatively simple and the three terms can be computed directly from the structure of lipids and lipoplex preparation terms.

In summary, we were able to develop a transfection index (TI_{PVM}) to predict and correlate the transfection activity for cationic lipids with methyl pyridinium headgroups with esters as the linkers. Based on these results, an optimized pyridinium lipid for this system will have the methyl pyridinium headgroup, esters as the linker, and two different chains, one straight saturated chain of C14 and another with a branched chain, each branch of a length close to C14, so that the average length of chains is close to C14, which has been shown to be an optimum chain length in mixtures containing EPC. The S_{mix} of such a species formulated with EPC and cholesterol or DOPE will be around 1.6 which will enhance the transfection (Figure 6.1).

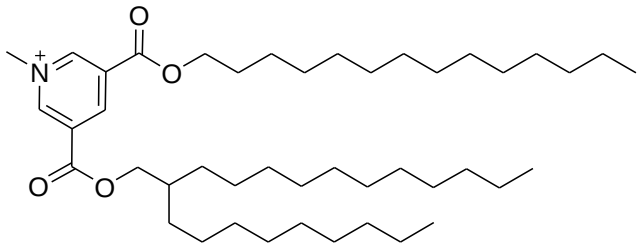

Figure 6.1-Structure of an optimized lipid with nC = 14 and S_{mix} ~ 1.6.

This compound can be synthesized and used as a ternary mixture, however based on our similar results on transfection efficiency of binary blend of pure lipids and ternary synthesized mixture, the optimized transfection could also be achieved with a binary blend of two pure pyridinium lipids, one with two straight saturated chain of C14 and other with two branched chain, with average chain length of C14.

The developed TI_{PVM}, though relatively efficient for the current study, still is short of what is required in a global sense.

One of the future directions to follow the current study is to investigate the effect of the headgroup on the TI_{PVM} for cationic lipids. The variation of headgroup not only will affect the shape parameter significantly, but also the charge density of the cationic lipid, a

parameter that is known to affect the transfection efficiency and toxicity of the lipids. It is possible that additional factors may need to be considered to incorporate features which were missed in this study due to the constant pyridinium headgroup.

To investigate the effect of the headgroup, a series of compounds could be synthesized from the parent compound in Figure 6.2. The amine group can be manipulated to give a library compounds with the same lipophilic part and ester, but varied headgroups with different charge density and total charge. The transfection results of these lipids can be used for investigation of TI_{PVM} and the effect of variation headgroup on the transfection.

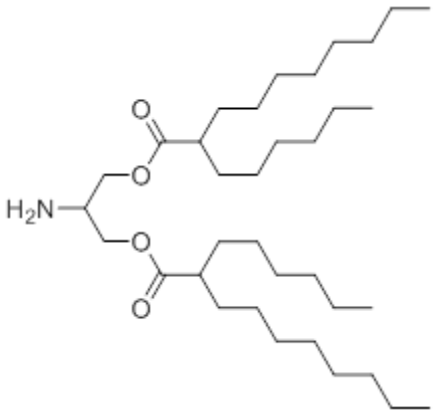

Figure 6.2-The proposed parent compound for investigation of the effect of the headgroup.

In addition, these transfection studies were performed using one cell line and the medium did not include serum so the effect of that variable on lipoplex stability is not yet explored. However, that is less likely to play a direct role, as serum components would be expected to have non-specific interactions with the lipids that should be accommodated within the clogP terms already considered.

Another limitation of this study is that the results are based on batch assays with roughly 30 treatments/batch. For a QSAR study, varied cell line and an extensive set of compounds are required to study the effect of structural variables on the transfection.

Also it is important that they will be handled in a way that allows the data to be compared across a much wider range of conditions.

In conclusion, a transfection index was developed to predict the transfection efficiency in vitro. The effective molecular parameters of the cationic lipids in the transfection process were identified and correlated. It is hoped that the current study helps with further understanding of the transfection of nucleic acids as a bio-medical tool and enables a goal oriented design and synthesis of cationic lipids with high transfection and low toxicity. This predictive tool can be studied and further developed to be applied to gene transfection, helping the progress of gene therapy as the alternative cure for many genetic diseases.

Bibliography

1. Tresset, G., The multiple faces of self-assembled lipidic systems. *PMC biophysics* **2009,** *2* (1).
2. Mintzer, M. A.; Simanek, E. E., Nonviral Vectors for Gene Delivery. *Chemical Reviews* **2009,** *109* (2), 259-302.
3. Wirth, T.; Parker, N.; Yla-Herttuala, S., History of gene therapy. *Gene* **2013,** *525* (2), 162-169.
4. Yang, J.; Liu, H. M.; Zhang, X., Design, preparation and application of nucleic acid delivery carriers. *Biotechnology Advances* **2014,** *32* (4), 804-817.
5. Chan, C. L.; Ewert, K. K.; Majzoub, R. N.; Hwu, Y. K.; Liang, K. S.; Leal, C.; Safinya, C. R., Optimizing cationic and neutral lipids for efficient gene delivery at high serum content. *The Journal of Gene Medicine* **2014,** *16* (3-4), 84-96.
6. Gene Therapy Clinical Trials Worldwide Database. *The Journal of Gene Medicine* **2014**.
7. Verma, I. M.; Somia, N., Gene therapy - promises, problems and prospects. *Nature* **1997,** *389* (6648), 239-242.
8. (a) Koynova, R.; Tenchov, B., Cationic phospholipids: structure-transfection activity relationships. *Soft Matter* **2009,** *5* (17), 3187-3200; (b) Gruneich, J. A.; Diamond, S. L., Synthesis and structure-activity relationships of a series of increasingly hydrophobic cationic steroid lipofection reagents. *The Journal of Gene Medicine* **2007,** *9* (5), 381-391; (c) Ewert, K. K.; Zidovska, A.; Ahmad, A.; Bouxsein, N. F.; Evans, H. M.; McAllister, C. S.; Samuel, C. E.; Safinya, C. R., Cationic Liposome-Nucleic Acid Complexes for Gene Delivery and Silencing: Pathways and Mechanisms for Plasmid DNA and siRNA. In *Nucleic Acid Transfection*, Bielke, W.; Erbacher, C., Eds. 2010; Vol. 296, pp 191-226.
9. Koynova, R.; Tenchov, B., Cationic Lipids: Molecular Structure/Transfection Activity Relationships and Interactions with Biomembranes. In *Nucleic Acid Transfection*, Bielke, W.; Erbacher, C., Eds. Springer-Verlag Berlin: Berlin, 2010; Vol. 296, pp 51-93.
10. (a) Rehman, Z. U.; Zuhorn, I. S.; Hoekstra, D., How cationic lipids transfer nucleic acids into cells and across cellular membranes: Recent advances. *Journal of Controlled Release* **2013,** *166* (1), 46-56; (b) Zidovska, A.; Evans, H. M.; Ahmad, A.; Ewert, K. K.; Safinya, C. R., The Role of Cholesterol and Structurally Related Molecules in Enhancing Transfection of Cationic Liposome-DNA Complexes. *Journal of Physical Chemistry B* **2009,** *113* (15), 5208-5216; (c) Zuhorn, I. S.; Engberts, J.; Hoekstra, D., Gene delivery by cationic lipid vectors: overcoming cellular barriers. *European Biophysical Journal* **2007,** *36* (4-5), 349-362; (d) Seddon, J. M., Structure of the inverted hexagonal (HII) phase, and non-lamellar phase transitions of lipids. *Biochimica Et Biophysica Acta* **1990,** *1031* (1), 1-69.
11. (a) Koynova, R.; Wang, L.; MacDonald, R. C., An intracellular lamellar–nonlamellar phase transition rationalizes the superior performance of some cationic lipid transfection agents. *Proceedings of the National Academy of Sciences* **2006,** *103* (39), 14373-14378; (b) Zuhorn, I. S.; Bakowsky, U.; Polushkin, E.; Visser, W. H.; Stuart, M.

C. A.; Engberts, J.; Hoekstra, D., Nonbilayer phase of lipoplex-membrane mixture determines endosomal escape of genetic cargo and transfection efficiency. *Molecular Therapy* **2005,** *11* (5), 801-810.
12. Wasungu, L.; Hoekstra, D., Cationic lipids, lipoplexes and intracellular delivery of genes. *Journal of Controlled Release* **2006,** *116* (2), 255-264.
13. Tarahovsky, Y. S.; Koynova, R.; MacDonald, R. C., DNA release from lipoplexes by anionic lipids: Correlation with lipid mesomorphism, interfacial curvature, and membrane fusion. *Biophysical Journal* **2004,** *87* (2), 1054-1064.
14. (a) Tenchov, B. G.; Wang, L.; Koynova, R.; MacDonald, R. C., Modulation of a membrane lipid lamellar–nonlamellar phase transition by cationic lipids: A measure for transfection efficiency. *Biochimica et Biophysica Acta (BBA) - Biomembranes* **2008,** *1778* (10), 2405-2412; (b) Koynova, R.; MacDonald, R. C., Cationic O-ethylphosphatidylcholines and their lipoplexes: phase behavior aspects, structural organization and morphology. *Biochimica et Biophysica Acta (BBA) - Biomembranes* **2003,** *1613* (1–2), 39-48.
15. (a) Koynova, R.; MacDonald, R. C., Lipid transfer between cationic vesicles and lipid–DNA lipoplexes: Effect of serum. *Biochimica et Biophysica Acta (BBA) - Biomembranes* **2005,** *1714* (1), 63-70; (b) Koynova, R.; Wang, L.; MacDonald, R. C., Synergy in Lipofection by Cationic Lipid Mixtures: Superior Activity at the Gel−Liquid Crystalline Phase Transition. *The Journal of Physical Chemistry B* **2007,** *111* (27), 7786-7795.
16. de Lima, M. C. P.; Neves, S.; Filipe, A.; Duzgunes, N.; Simoes, S., Cationic liposomes for gene delivery: From biophysics to biological applications. *Current Medicinal Chemistry* **2003,** *10* (14), 1221-1231.
17. Floch, V.; Loisel, S.; Guenin, E.; Herve, A. C.; Clement, J. C.; Yaouanc, J. J.; des Abbayes, H.; Ferec, C., Cation substitution in cationic phosphonolipids: A new concept to improve transfection activity and decrease cellular toxicity. *Journal of Medicinal Chemistry* **2000,** *43* (24), 4617-4628.
18. (a) Pijper, D.; Bulten, E.; Šmisterová, J.; Wagenaar, A.; Hoekstra, D.; Engberts, Jan B. F. N.; Hulst, R., Novel Biodegradable Pyridinium Amphiphiles for Gene Delivery. *European Journal of Organic Chemistry* **2003,** *2003* (22), 4406-4412; (b) Kuiper, J. M.; Buwalda, R. T.; Hulst, R.; Engberts, J. B. F. N., Novel pyridinium surfactants with unsaturated alkyl chains: aggregation behavior and interactions with metyl orange in aqueous solution. *Langmuir* **2001,** *17*, 5216-5224; (c) Meekel, A. A. P.; Wagenaar, A.; Smisterova, J.; Kroeze, J. E.; Haadsma, P.; Bosgraaf, B.; Stuart, M. C. A.; Brisson, A.; Ruiters, M. H. J.; Hoekstra, D.; Engberts, J., Synthesis of pyridinium amphiphiles used for transfection and some characteristics of amphiphile/DNA complex formation. *European Journal of Organic Chemistry* **2000,** (4), 665-673; (d) Zhu, L.; Lu, Y.; Miller, D. D.; Mahato, R. I., Structural and Formulation Factors Influencing Pyridinium Lipid-Based Gene Transfer. *Bioconjugate Chemistry* **2008,** *19* (12), 2499-2512.
19. Lv, H.; Zhang, S.; Wang, B.; Cui, S.; Yan, J., Toxicity of cationic lipids and cationic polymers in gene delivery. *Journal of Controlled Release* **2006,** *114* (1), 100-109.
20. Yingyongnarongkul, B.-e.; Radchatawedchakoon, W.; Krajarng, A.; Watanapokasin, R.; Suksamrarn, A., High transfection efficiency and low toxicity

cationic lipids with aminoglycerol-diamine conjugate. *Bioorganic & Medicinal Chemistry* **2009,** *17* (1), 176-188.
21. (a) Karmali, P. P.; Chaudhuri, A., Cationic Liposomes as non-viral carriers of gene medicines: Resolved issues, open questions, and future promises. *Medicinal Research Reviews* **2007,** *27* (5), 696-722; (b) Ghosh, Y. K.; Visweswariah, S. S.; Bhattacharya, S., Nature of linkage between the cationic headgroup and cholesteryl skeleton controls gene transfection efficiency. *Febs Letters* **2000,** *473* (3), 341-344.
22. (a) Li, S.-D.; Huang, L., Non-viral is superior to viral gene delivery. *Journal of Controlled Release* **2007,** *123* (3), 181-183; (b) Gao, X.; Huang, L., Cationic liposome-mediated gene transfer. *Gene Therapy* **1995,** *2* (10), 710-722.
23. (a) Guo, X.; Szoka, F. C., Chemical approaches to triggerable lipid vesicles for drug and gene delivery. *Accounts of Chemical Research* **2003,** *36* (5), 335-341; (b) Nagasaki, T.; Taniguchi, A.; Tamagaki, S., Photoenhancement of transfection efficiency using novel cationic lipids having a photocleavable spacer. *Bioconjugate Chemistry* **2003,** *14* (3), 513-516.
24. Kish, P.; Kim, J. S.; Roessler, B.; Campbell, S.; Hilfinger, J., Bile acid conjugates improve the oral bioavailability of the neurominidase inhibitor zanamivir. *Antiviral Research* **2007,** *74* (3), A45-A46.
25. Felgner, J. H.; Kumar, R.; Sridhar, C. N.; Wheeler, C. J.; Tsai, Y. J.; Border, R.; Ramsey, P.; Martin, M.; Felgner, P. L., Enhanced gene delivery and mechanism studies with a novel series of cationic lipid formulations. *Journal of Biological Chemistry* **1994,** *269* (4), 2550-2561.
26. Soltan, M. K.; Ghonaim, H. M.; El Sadek, M.; Abou Kull, M.; El-Aziz, L. A.; Blagbrough, I. S., Design and Synthesis of N-4,N-9-Disubstituted Spermines for Non-viral siRNA Delivery - Structure-Activity Relationship Studies of siFection Efficiency Versus Toxicity. *Pharmaceutical Research* **2009,** *26* (2), 286-295.
27. Koynova, R.; MacDonald, R. C., Mixtures of Cationic Lipid O-Ethylphosphatidylcholine with Membrane Lipids and DNA: Phase Diagrams. *Biophysical Journal* **2003,** *85* (4), 2449-2465.
28. (a) Carnie, S.; Israelachvili, J. N.; Pailthorpe, B. A., Lipid packing and transbilayer asymmetries of mixed lipid vesicles. *Biochimica Et Biophysica Acta* **1979,** *554* (2), 340-357; (b) Kumar, V. V., Complementary molecular shapes and additivity of the packing parameter of lipids. *Proceedings of the National Academy of Sciences U.S.A* **1991,** *88* (2), 444-448.
29. Israelachvili, J. N.; Mitchell, D. J.; Ninham, B. W., Theory of self-assembly of lipid bilayers and vesicles. *Biochimica Et Biophysica Acta* **1977,** *470* (2), 185-201.
30. Marsh, D., Nonlamellar packing parameters for diacylglycerols. *Biophysical Journal* **1997,** *72* (6), 2834-2836.
31. Heimberg, T., *Thermal Biophysics of Membranes*. Wiley-VCH: Weinheim, 2007.
32. Marsh, D., Structural and thermodynamic determinants of chain-melting transition temperatures for phospholipid and glycolipids membranes. *Biochimica et Biophysica Acta (BBA) - Biomembranes* **2010,** *1798* (1), 40-51.
33. Hansch, C.; Leo, A., Substitution constants for correlation analysis in chemistry and biology. 1979; p V+339P-V+339P.

34. Teixeira, A. L.; Falcao, A. O., Structural Similarity Based Kriging for Quantitative Structure Activity and Property Relationship Modeling. *Journal of Chemical Information and Modeling* **2014,** *54* (7), 1833-1849.
35. Horobin, R. W.; Weissig, V., A QSAR-modeling perspective on cationic transfection lipids. 1. Predicting efficiency and understanding mechanisms. *The Journal of Gene Medicine.* **2005,** *7* (8), 1023-1034.
36. MacDonald, R. C.; Ashley, G. W.; Shida, M. M.; Rakhmanova, V. A.; Tarahovsky, Y. S.; Pantazatos, D. P.; Kennedy, M. T.; Pozharski, E. V.; Baker, K. A.; Jones, R. D.; Rosenzweig, H. S.; Choi, K. L.; Qiu, R. Z.; McIntosh, T. J., Physical and biological properties of cationic triesters of phosphatidylcholine. *Biophysical Journal* **1999,** *77* (5), 2612-2629.
37. Hansch, C.; Leo, A., *Substituent Constants for Correlation Analysis in Chemistry and Biology*. John Wiley and Sons: New York, 1979; p 18-43.
38. Ahmad, A.; Evans, H. M.; Ewert, K.; George, C. X.; Samuel, C. E.; Safinya, C. R., New multivalent cationic lipids reveal bell curve for transfection efficiency versus membrane charge density: lipid-DNA complexes for gene delivery. *The Journal of Gene Medicine* **2005,** *7* (6), 739-748.
39. (a) Pijper, D.; Bulten, E.; Smisterova, J.; Wagenaar, A.; Hoekstra, D.; Engberts, J.; Hulst, R., Novel biodegradable pyridinium amphiphiles for gene delivery. *European Journal of Organic Chemistry* **2003,** (22), 4406-4412; (b) Sutterlin, H.; Alexy, R.; Kummerer, K., The toxicity of the quaternary ammonium compound benzalkonium chloride alone and in mixtures with other anionic compounds to bacteria in test systems with *Vibrio fischeri* and *Pseudomonas putida*. *Ecotoxicology and Environmental Safety* **2008,** *71*, 498-505.
40. Pinnaduwage, P.; Schmitt, L.; Huang, L., Use of a quaternary ammonium detergent in liposome mediated DNA transfection of mouse L-cells. *Biochimica Et Biophysica Acta* **1989,** *985* (1), 33-37.
41. Kiriya, D.; Chang, H. C.; Kitagawa, S., Molecule-based valence tautomeric bistability synchronized with a macroscopic crystal-melt phase transition. *Journal of the American Chemical Society* **2008,** *130* (16), 5515-5522.
42. Moszynski, J. M.; Fyles, T. M., Synthesis and ion transport activity of oligoesters containing an environment-sensitive fluorophore. *Organic & Biomolecular Chemistry* **2011,** *9* (21), 7468-7475.
43. Konarev, P. V.; Volkov, V. V.; Sokolova, A. V.; Koch, M. H. J.; Svergun, D. I., PRIMUS: a Windows PC-based system for small-angle scattering data analysis. *Journal of Applied Crystallography* **2003,** *36*, 1277-1282.
44. Wolfram Research, I., *Mathematica*. Version 8.0 ed.; Wolfram Research, Inc.: Champaign, Illinois, 2010.
45. Kuwabe, S.; Torraca, K. E.; Buchwald, S. L., Palladium-catalyzed intramolecular C-O bond formation. *Journal of the American Chemical Society* **2001,** *123* (49), 12202-12206.
46. March, J., Smith, Michael, *March's advanced organic chemistry : reactions, mechanisms, and structure*. Wiley: New York, 2001.
47. Rossi, R. A.; Pierini, A. B.; Penenory, A. B., Nucleophilic substitution reactions by electron transfer. *Chemical Reviews* **2003,** *103* (1), 71-167.

48. Hon, Y. S.; Wong, Y. C.; Chang, C. P.; Hsieh, C. H., Tishchenko reactions of aldehydes promoted by diisobutylaluminum hydride and its application to the macrocyclic lactone formation. *Tetrahedron* **2007,** *63* (46), 11325-11340.
49. Baldwin, J. E.; Spring, D. R.; Atkinson, C. E.; Lee, V., Efficient synthesis of the sponge alkaloids cyclostellettamines A-F. *Tetrahedron* **1998,** *54* (44), 13655-13680.
50. Jiang, A. J.; Zhao, Y.; Schrock, R. R.; Hoveyda, A. H., Highly Z-Selective Metathesis Homocoupling of Terminal Olefins. *Journal of the American Chemical Society* **2009,** *131* (46), 16630-+.
51. Watarai, N.; Kawasaki, H.; Azumaya, I.; Yamasaki, R.; Saito, S., Synthesis, structure and catalytic activity of macrocyclic NHC Pd pincer complexes. *Heterocycles* **2009,** *79*, 531-548.
52. Israelachvili, J. N.; Mitchell, D. J., Model for packing of lipids in bilayer membranes. *Biochimica Et Biophysica Acta* **1975,** *389* (1), 13-19.
53. Durchschlag, H.; Zipper, P., Calculations of the partial volume of organic compounds and polymers. In *Ultracentrifugation*, Lechner, M. D., Ed. Dr Dietrich Steinkopff Verlag: Berlin 33, 1994; Vol. 94, pp 20-39.
54. Hui, S. W.; Sen, A., Effects of lipid packing on polymorphic phase behavior and membrane properties. *Proceedings of the National Academy of Sciences* **1989,** *86* (15), 5825-5829.
55. (a) Kobayashi, T.; Beuchat, M. H.; Chevallier, J.; Makino, A.; Mayran, N.; Escola, J. M.; Lebrand, C.; Cosson, P.; Gruenberg, J., Separation and characterization of late endosomal membrane domains. *Journal of Biological Chemistry* **2002,** *277* (35), 32157-32164; (b) Sobo, K.; Chevallier, J.; Parton, R. G.; Gruenberg, J.; van der Goot, F. G., Diversity of Raft-Like Domains in Late Endosomes. *Plos One* **2007,** *2* (4).
56. (a) Sen, A.; Hui, S. W., Direct measurement of headgroup hydration of polar lipids in inverted micelles. *Chemistry and Physics of Lipids* **1988,** *49* (3), 179-184; (b) Bennett, M. J.; Aberle, A. M.; Balasubramaniam, R. P.; Malone, J. G.; Malone, R. W.; Nantz, M. H., Cationic lipid-mediated gene delivery to murine lung: Correlation of lipid hydration with in vivo transfection activity. *Journal of Medicinal Chemistry* **1997,** *40* (25), 4069-4078; (c) Corsi, J.; Hawtin, R. W.; Ces, O.; Attard, G. S.; Khalid, S., DNA Lipoplexes: Formation of the Inverse Hexagonal Phase Observed by Coarse-Grained Molecular Dynamics Simulation. *Langmuir* **2010,** *26* (14), 12119-12125.
57. Nagarajan, R., Molecular packing parameter and surfactant self-assembly: The neglected role of the surfactant tail. *Langmuir* **2002,** *18* (1), 31-38.
58. (a) Hofsass, C.; Lindahl, E.; Edholm, O., Molecular dynamics simulations of phospholipid bilayers with cholesterol. *Biophysical Journal* **2003,** *84* (4), 2192-2206; (b) Falck, E.; Patra, M.; Karttunen, M.; Hyvonen, M. T.; Vattulainen, I., Lessons of slicing membranes: Interplay of packing, free area, and lateral diffusion in phospholipid/cholesterol bilayers. *Biophysical Journal* **2004,** *87* (2), 1076-1091.
59. Pandit, S. A.; Chiu, S. W.; Jakobsson, E.; Grama, A.; Scott, H. L., Cholesterol packing around lipids with saturated and unsaturated chains: A simulation study. *Langmuir* **2008,** *24* (13), 6858-6865.
60. Montis, C.; Sostegni, S.; Milani, S.; Baglioni, P.; Berti, D., Biocompatible cationic lipids for the formulation of liposomal DNA vectors. *Soft Matter* **2014,** *10* (24), 4287-4297.

Appendix A: experimental details

Appendix A: experimental details

General procedures for synthesis

Most chemicals and solvents were used as received from known suppliers, except THF and DMF which were dried and distilled before use. Compounds were purified by column chromatography using silica gel 60.

NMR spectra were collected on a Bruker AC300 (300 MHz) or Bruker Avance (500 MHz) instrument. Proton (^{1}H) chemical shift are reported in part per million (ppm, δ scale), referenced with residual proton shift of $CDCl_3$ (7.26). The ^{1}HNMR results are reported as shift, multiplicity (s = singlet, d = doublet, t = triplet, m = multiple, br= broad), integration and J value (Hz). ^{13}CNMR are reported in part per million and are referenced to carbon resonance of $CDCl_3$ (77.23). ESI-Mass spectra were recorded on a Waters MicroMass Q-TOF instrument running in positive ion mode. Elemental analysis was done at Canadian Microanalytical Service Ltd.

Ether coupling:

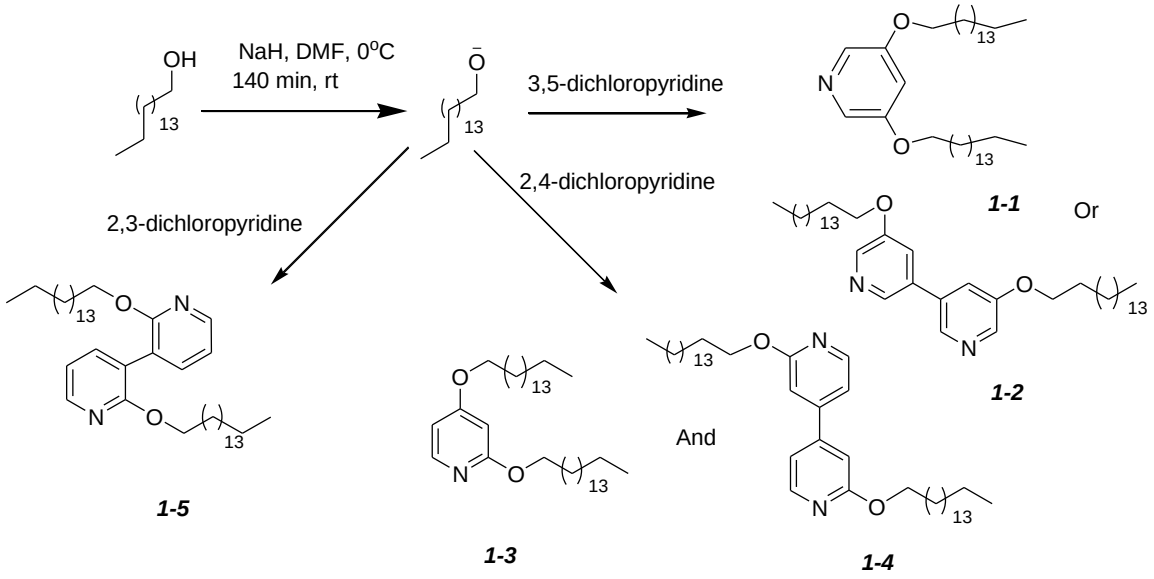

Scheme A.1-Ether coupling for synthesis of compounds *1-1* to *1-5*.

To an anhydrous suspension[41] (Scheme A.1) of 1 equivalent (relative to the alcohol) of NaH (60% in oil) in distilled DMF in a round bottom flask, alcohol was added at 0°C and the solution was stirred for 140 min at room temperature. Dichloropyridine was added and the mixture was stirred for 60 h at 120^{o}C. The reaction was quenched by adding water, and the product was extracted with DCM (4 times), and then washed with water (twice) and saturated $NaHCO_3$ (3 times) and dried over sodium sulphate. The crude product was purified by column chromatography on silica gel, using ether/hexanes as eluent.

Synthesis of diether pyridine *1-1*

Ether coupling conditions: To an anhydrous suspension of NaH (60% in oil) (1.724 g) in 75 ml of distilled DMF, hexadecanol (40.2 mmol, 9.753 g) was added at 0°C, stirred for 140 min, then dichloropyridine (5.2 mmol, 0.7600 g) was added and stirred for 60 h at 85°C and then following standard work up, the crude was recrystallized in Ethanol to give 0.550 g of ***1-1*** (19% yield) as a white solid. NMR ($CDCl_3$) ^{1}H δ: 7.91 (d, J=3Hz, 2H), 6.72 (m, 1H), 3.98 (t, J=15 Hz, 4H), 1.79 (m, 4H), 1.26 (br S, 50H), 0.88(br t, 6H).

Synthesis of diether bipyridine *1-2*

Ether coupling conditions: NaH (60% in oil) (12.5 mmol, 0.765 g) in 25 ml of distilled DMF, hexadecanol (12.5 mmol, 3.025 g) and dichloropyridine (5 mmol, 0.740 g). Then following standard work up, the crude was purified by column chromatography on silica gel, using 15% ether/hexanes as eluent to yield white solid, 0.727 g (26%). NMR ($CDCl_3$) ^{1}H δ: 8.19 (br s, 4H), 7.19 (t, J=6 Hz, 2H), 3.99 (t, J=12Hz, 4H), 1.80 (m, 4H), 1.26 (br, 57H), 0.88 (br t, 6H). ^{13}C δ: 155.5, 140.5, 136.2, 131.8, 121.0, 68.8, 31.9, 29.67, 25.9, 22.7, 14.1.

Synthesis of diether bipyridines *1-3* and *1-4*

Ether coupling conditions: NaH (60% in oil) (30.0 mmol, 1.199 g) in 25 ml of distilled DMF, hexadecanol (25 mmol, 6.061 g) and dichloropyridine (10 mmol, 1.479 g). Then following standard work up, the crude was purified by column chromatography on silica gel, using 15% ether/hexanes as eluent to yield white solid, to give ***1-3*** first 0.143 g (2.5%). NMR ($CDCl_3$) ^1H δ: 7.94 (d, J=6 Hz, 1H), 6.42 (m, 1H), 6.17 (m, 1H), 4.24 (t, J=12 Hz, 2H), 3.95 (t, J=12Hz, 2H), 1.74 (m, 4H), 1.25 (br s, 57H), 0.88 (br t, 6H). ^{13}C δ: 147.3, 106.3, 94.4, 67.9, 66.8, 31.9, 29.3, 26.0, 25.9, 22.7, 14.1. Elemental analysis: Calculated: C: 79.36%, H: 12.42%, N: 2.5% found: C: 79.33%, H: 12.42%, N: 2.84%.

And then ***1-4***, as a white solid, 0.329 g (5.2%). NMR ($CDCl_3$) ^1H δ: 8.16 (d, J=6 Hz, 2H), 6.82 (m, 2H), 6.74 (m, 2H), 3.99 (t, J=15 Hz, 4H), 1.79 (m, 4H), 1.25 (br, 57H), 0.88 (br t, 6). ^{13}C δ: 166.8, 152.6, 150.2, 110.1, 109.8, 68.6, 31.9, 29.5, 28.7, 25.8, 22.7, 14.1. Elemental analysis: Calculated: C: 79.19%, H: 11.39%, N: 4.40% found: C: 70.86%, H: 10.66%, N: 3.93%.

Synthesis of diether bipyridine *1-5*

Ether coupling conditions: NaH (60% in oil) (40 mmol, 1.587 g) in 75 ml of distilled DMF, hexadecanol (40.2 mmol, 9.750 g) and dichloropyridine (5.12 mmol, 0.758 g). Then following standard work up, the crude was purified by column chromatography on silica gel, using 15% ether/hexanes as eluent to yield white solid, 2.533g (43%). NMR ($CDCl_3$) ^1H δ: 8.04 (m, 2H), 7.62 (dd, 2H), 6.82 (m, 2H), 4.36 (t, 4H, 12), 1.82 (m, 4H), 1.26 (br s, 26H), 0.88 (br t, 6H). ^{13}C δ: 159.4, 144.6, 138.1, 118.3, 116.9, 67.0, 31.9, 29.5, 28.8, 25.9, 22.7, 14.1.

Synthesis of *2-1*

THP protection conditions[42]: Dihydropyran (1.2 equiv., 12 mmol, 1.013 g) and *p*-toluene sulfonic acid (0.1 equiv., 1mmol, 0.195 g) was added to a solution of 11-bromo-1-undecanol (10 mmol, 2.510 g) in DCM (12 ml) at 0°C and the mixture was stirred at room temperature for 2.5 h, monitored by TLC (silica, eluent at 5% ether/hexanes). Once complete the reaction mixture was washed with sat. $NaHCO_3$ (twice), water (twice) and sat. NaCl (twice), dried over anhydrous sodium sulfate and concentrated under vacuum. The crude product was purified by column chromatography on silica gel, (eluent at 5% ether/hexanes) to yield 2.123 g (63%) of ***2-1*** as a white solid. NMR ($CDCl_3$) ^{1}H δ: 4.58 (m, 1H), 3.87(m, 1H), 3.54 (m, 1H), 3.48 (m, 1H), 3.38 (m, 3H), 0.86-1.83 (m, 72H), ^{13}C δ: 98.9, 67.7, 62.5, 34.6, 30.8, 29.5, 28.2, 26.2, 25.5, 22.6, 19.7. Compared to known compound[49].

^{1}H δ (200 MHz, $CDCl_3$): 4.56 (dd, J=3 Hz, 1H), 3.66-3.91 (m, 2H), 3.39 (t, J=7 Hz, 2H), 3.30-3.53 (m, 2H), 1.53-1.90 (m, 24H), ^{13}C δ (200 MHz, $CDCl_3$): 98.8, 67.6, 62.3, 34.0, 32.8, 30.7, 29.7, 29.4, 28.7, 28.1, 26.2, 25.5, 19.7.

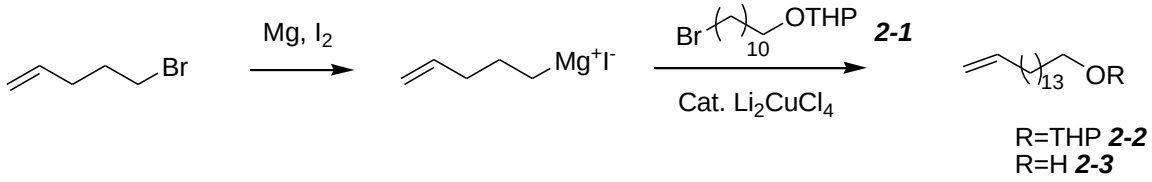

Scheme A.2-Synthesis for compounds *2-1-2-3*.

Synthesis of *2-2*

Grignard coupling conditions (Scheme A.2)[48]: To a solution of 5-bromo pentene (0.087 mL, 0.74 mmol) in anhydrous THF (0.5 mL) magnesium powder (212 mg, 8.65 mmol) and a catalytic amount of iodine under nitrogen was added. After the reaction starts, the remaining 5-bromo pentene (0.45 mL, 3.76 mmol) in 1.5 mL of THF was added dropwise and the reaction mixture was then refluxed for 2 h and then cooled to -78°C. To this gignard reagent solution was added a solution of 2-(11-bromo-undecyloxy)-tetrahydropyran (***2-1***) (0.771 g, 2.295 mmol) in 1.5 mL of THF followed by lithium tetrachlorocuprate solution (0.689 mmol, 6.88 mL, 0.3 M in THF). The mixture was stirred at -78°C overnight. The reaction was quenched with 1 N aqueous ammonium chloride solution and extracted with EtOAc. The organic layer was dried over magnesium sulfate and concentrated and which was purified by column chromatography on silica gel, (eluent at 5% ether/hexanes) to yield 0.653 g of a white solid. NMR ($CDCl_3$) ^1H δ: 5.83 (m, 1H), 4.91 (m, 2H) 4.58 (m, 1H), 3.87 (m, 1H), 3.53 (m, 1H), 3.48 (m, 1H), 3.38 (m, 1H), 2.03 (m, 2H), 1.26-1.71 (br s, 36H), 0.88 (br t, 0H, exp 0.50H). ^{13}C δ: 139.27, 114.0, 98.8, 67.7, 62.3, 33.8, 30.7, 29.6, 28.9, 26.2, 25.2, 19.6.

Compared to known compound[48]:

NMR ($CDCl_3$, 400 MHz) ^1H δ: 1.26–1.39 (m, 22H), 1.49–1.61 (m, 6H), 1.69–1.75 (m, 1H), 1.79–1.87 (m, 1H), 2.01–2.07 (m, 2H), 3.38 (dt, J¼=9.6 and 6.7 Hz, 1H), 3.47–3.53 (m, 1H), 3.74 (dt, J¼=9.6 and 7.0 Hz, 1H), 3.85–3.90 (m, 1H), 4.58 (dd, J¼=4.4 and 2.6 Hz, 1H), 4.91–5.02 (m, 2H), 5.77–5.87 (m, 1H); NMR ($CDCl_3$, 100 MHz) ^{13}C δ: 19.6, 25.5, 26.2, 28.9, 29.1, 29.45, 29.47, 29.56, 29.57, 29.6, 29.7, 30.7, 33.8, 62.2, 67.6, 98.7, 114.0, 139.1

Synthesis of *2-3*

THP removal[42]: pTsOH (0.3 equiv, 9.8 mmol, and 1.875 g) was added to a solution of THP protected product amassed from experiments as noted above (32.8 mmol, 13.194 g) in 6 ml of 90:10 v/v CH_3OH: DCM, which was stirred at rt for 5 h, and monitored by TLC (silica, eluent at 1% ethyl acetate /hexanes). Once complete, the reaction was diluted with DCM, washed with H_2O (once), saturated $NaHCO_3$ (twice), and saturated NaCl (once), then dried over sodium sulfate and concentrated under vacuum. NMR ($CDCl_3$) ^1H δ: 5.81 (m, 1H), 4.94 (m, 2H), 3.63 (m, 2H, exp 2.40H), 2.03 (m, 2H), 1.54 (m, 4H), 1.26 (m, 26H), 0.88 (br t, 0H, exp 0.56 H). ^{13}C δ: 139.27, 114.05, 98.84, 63.09, 32.80, 29.59, 28.94, 25.72, 14.00.

Compared to known compound:

^{1}HNMR ($CDCl_3$, 400 MHz) δ: 1.20 (br, 1H), 1.26–1.39 (m, 22H), 1.53–1.60 (m, 2H), 2.01–2.07 (m, 2H), 3.64 (td, J¼=6.5 and 5.4 Hz, 2H), 4.91–5.02 (m, 2H), 5.77–5.85 (m, 1H); ^{13}C NMR (CDCl3, 100 MHz) δ: 25.7, 28.9, 29.1, 29.4, 29.5, 29.58, 29.62, 32.7, 33.8, 62.9, 114.0, 139.2.

Ester coupling (Scheme A.3)[42]:

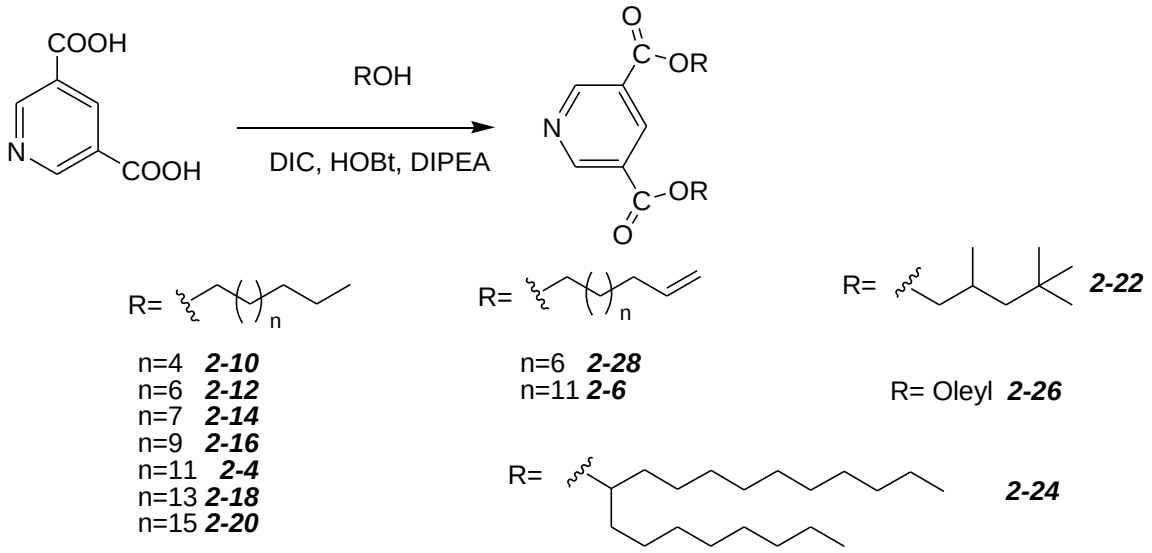

Scheme A.3-Ester coupling for synthesis of 3,5-dialkyloate pyridine.

To a solution of 1 equivalent of 3,5-pyridinedicarboxylic acid (Scheme A3) in relation to 2.4 equivalent of the alcohol in THF were added 2.4 eq. of DIC, HOBt and *N,N*-diisopropylethyl amine. The reaction was sealed under an atmosphere of N_2, and stirred for 24 h at room temperatures. Once complete, the reaction was filtered to remove DIU, and diluted with DCM. The organic phase was extracted with phosphate buffer (pH = 3) (twice), water (twice) 10% NaCl (twice) and rinsed with sat. NaCl (once), dried with anhydrous sodium sulfate, and concentrated under vacuum. The crude product was purified by column chromatography on silica gel, using ether/hexanes as eluent.

Synthesis of diC16:0 pyridine *(2-4)*

Ester coupling conditions: 1 equivalent of 3,5-pyridinedicarboxylic acid (1.000 g, 5.98 mmol), 2.4 equivalents of *N,N*-diisopropyl carbodiimide (DIC) (1.811 g, 14.3 mmol), 2.4

equivalents of hydroxybenzotriazole (HOBt; 2.198 g, 14.3 mmol), 2.4 equivalents of 1-hexadecanol (3.473 g, 14.3 mmol) and 2.4 equivalents of *N*,*N*-diisopropylethyl amine (DIPEA; 1.854 g, 14.3 mmol) were stirred in THF at rt for 24 h. Standard work-up and purification by silica gel chromatography , using 15% ether/hexanes as eluent, yields ***2-4*** as a white solid, 2.16 g (59%). NMR ($CDCl_3$) ^{1}H δ: 9.35 (d, J=3 Hz, 2H), 8.85 (t, J=3 Hz, 1H), 4.38 (t, J=12 Hz, 4H), 1.82 (m, 4H), 1.25 (m, 52H), 0.88 (br t, 6H). ^{13}C δ: 164.7, 154.1, 137.9, 126.3, 65.9, 31.9, 29.5, 28.6, 25.9, 22.6, 14.1. MS (+ve ESI): calc'd for $C_{39}H_{70}NO_4^+$ = 616.5 amu, obtained = 616.7 amu.

Synthesis of mixed diC16:1/(C16:1)(C11:0) pyridines (*2-6*/*2-7*)

Ester coupling conditions: 1 equivalent of 3,5-pyridinedicarboxylic acid (1.000 g, 5.98 mmol), 2.4 equivalents of *N*,*N*-diisopropyl carbodiimide (DIC) (1.811 g, 14.3 mmol), 2.4 equivalents of hydroxybenzotriazole (HOBt; 2.198g, 14.3 mmol), 2.4 equivalents of ***2-3*** (3.444 g, 14.3 mmol) and 2.4 equivalents of *N*,*N*-diisopropylethyl amine (DIPEA; 1.854 g, 14.3 mmol, 2.4 equiv) were stirred in THF at rt for 24 h. Standard work-up and purification by silica gel chromatography , using 15% ether/hexanes as eluent, yields ***2-6*** in 90% and ***2-7*** in 10% as a white solid, 1.48 g (57%). NMR ($CDCl_3$) ^{1}H δ: 9.36 (d, J=3 Hz, 2H), 8.85 (t, J=6 Hz, 1H), 5.83 (m, 2H, exp 1.75), 4.94 (m, 4H), 4.38 (t, 4H, 15), 2.05 (m, 4H), 1.82 (m, 4H), 1.25 (m, 47H), 0.88 (br t, 0H, exp 1.48 H). ^{13}C δ: 164.4, 154.0, 139.2, 137.9, 126.3, 114.1, 65.9, 33.7, 31.8, 29.5, 29.1, 28.9, 28.6, 25.9, 22., 14.0. MS (+ve ESI): calc'd for ***(2-6)*** $C_{39}H_{66}NO_4^+$ = 612.49 amu, obtained = 612.21 amu. calc'd for ***(2.7)*** $C_{34}H_{58}NO_4^+$ = 544.4 amu, obtained = 544.8 amu.

Synthesis of diC9:0 pyridine (*2-10*)

Ester coupling conditions: 1 equivalent of 3,5-pyridinedicarboxylic acid (0.835 g, 5 mmol), 2.4 equivalents of *N*,*N*-diisopropyl carbodiimide (DIC) (1.514 g, 12 mmol), 2.4 equivalents of hydroxybenzotriazole (HOBt; 1.620 g, 12 mmol), 2.4 equivalents of 1-nonaol (1.731 g, 12 mmol) and 2.4 equivalents of *N*,*N*-diisopropylethyl amine (DIPEA; 1.550 g, 12 mmol) were stirred in THF at rt for 24 h. Standard work-up and purification by silica gel chromatography , using 15% ether/hexanes as eluent, yields ***2-10*** as a white solid, 1.777 g (84%). NMR ($CDCl_3$) ^{1}H δ: 9.35 (d, J=3 Hz, 2H), 8.85 (t, J=6 Hz, 1H), 4.38 (t, J=15 Hz, 4H) , 1.82 (m, 4H), 1.25 (m, 28 H), 0.88 (m, 6H). ^{13}C δ: 164.4, 154.0, 137.8, 126.2, 65.9, 31.7, 29.5, 28.0, 25.9, 22.5, 14.1. MS (+ve ESI): calc'd for $C_{25}H_{42}NO_4^+$ = 420.3 amu, obtained = 420.1 amu.

Synthesis of diC11:0 pyridine (*2-12*)

Ester coupling conditions: 1 equivalent of 3,5-pyridinedicarboxylic acid (0.835 g, 5 mmol), 2.4 equivalents of *N*,*N*-diisopropyl carbodiimide (DIC) (1.564 g, 12 mmol), 2.4 equivalents of hydroxybenzotriazole (HOBt; 1.840 g, 12 mmol), 2.4 equivalents of 1-undecanol (2.068 g, 12 mmol) and 2.4 equivalents of *N*,*N*-diisopropylethyl amine (DIPEA; 1.854 g, 12 mmol) were stirred in THF at rt for 24 h. Standard work-up and purification by silica gel chromatography , using 15% ether/hexanes as eluent, yields ***2-12*** as a white solid, 1.235 g (51%) .NMR ($CDCl_3$) ^{1}H δ: 9.35 (d, J=3 Hz, 2H), 8.85 (t, J=6 Hz, 1H), 4.38 (t, J=15 Hz, 4H), 1.79 (m, 4H), 1.26 (m, 36H), 0.87 (br t, 6H). ^{13}C δ: 164.3, 154.50, 138.4, 126.6, 66.1, 31.8, 29.3, 28.5, 25.9, 22.6, 14.0. MS (+ve ESI): calc'd for $C_{29}H_{50}NO_4^+$ = 476.3 amu, obtained = 476.6 amu.

Synthesis of diC12:0 pyridine (*2-14*)

Ester coupling conditions: 1 equivalent of 3,5-pyridinedicarboxylic acid (0.835 g, 5 mmol), 2.4 equivalents of *N*,*N*-diisopropyl carbodiimide (DIC) (1.564 g, 12 mmol), 2.4 equivalents of hydroxybenzotriazole (HOBt; 1.840 g, 12 mmol), 2.4 equivalents of 1-dodecanol (2.238 g, 12 mmol) and 2.4 equivalents of *N*,*N*-diisopropylethyl amine (DIPEA; 1.854 g, 12 mmol) were stirred in THF at rt for 24 h. Standard work-up and purification by silica gel chromatography , using 15% ether/hexanes as eluent, yields ***2-14*** as a white solid, 1.01 g (40%). NMR ($CDCl_3$) ^{1}H δ: 9.36 (d, J=3 Hz, 2H), 8.85 (t, J=6 Hz, 1H), 4.39 (t, J=15 Hz, 4H), 1.80 (m, 4H), 1.27 (m, 36H), 0.88 (br t, 6H). ^{13}C δ: 164.5, 154.0, 137.9, 126.5, 65.9, 31.8, 29.3, 28.6, 25.9, 22.6, 14.0. MS (+ve ESI): calc'd for $C_{31}H_{54}NO_4^+$ = 504.7 amu, obtained = 504.4 amu.

Synthesis of diC14:0 pyridine (*2-16*)

Ester coupling conditions: 1 equivalent of 3,5-pyridinedicarboxylic acid (0.835 g, 5 mmol), 2.4 equivalents of *N*,*N*-diisopropyl carbodiimide (DIC) (1.564 g, 12 mmol), 2.4 equivalents of hydroxybenzotriazole (HOBt; 1.840 g, 12 mmol), 2.4 equivalents of 1-tetradecanol (2.5750 g, 12 mmol) and 2.4 equivalents of *N*,*N*-diisopropylethyl amine (DIPEA; 1.854 g, 12 mmol) were stirred in THF at rt for 24 h. Standard work-up and purification by silica gel chromatography , using 15% ether/hexanes as eluent, yields ***2-16*** as a white solid, 0.732 g (26%) .NMR ($CDCl_3$) ^{1}H δ: 9.36 (br s, 2H), 8.87 (t, J=3 Hz, 1H) , 4.39 (t, J=15 Hz, 4H) , 1.79 (m, 4H), 1.26 (m, 48H), 0.89 (br t, 6H). ^{13}C δ: 164.5, 154.0, 137.9, 126.3, 65.9, 31.8, 29.4, 28.6, 25.9, 22.6, 14.0. MS (+ve ESI): calc'd for $C_{35}H_{62}NO_4^+$ = 560.4 amu, obtained = 560.4amu.

Synthesis of diC18:0 pyridine (*2-18*)

Ester coupling conditions: 1 equivalent of 3,5-pyridinedicarboxylic acid (0.835 g, 5 mmol), 2.4 equivalents of *N*,*N*-diisopropyl carbodiimide (DIC) (1.564 g, 12 mmol), 2.4 equivalents of hydroxybenzotriazole (HOBt; 1.840 g, 12 mmol), 2.4 equivalents of 1-octadecanol (3.245 g, 12 mmol) and 2.4 equivalents of *N*,*N*-diisopropylethyl amine (DIPEA; 1.854 g, 12 mmol) were stirred in THF at rt for 24 h. Standard work-up and purification by silica gel chromatography , using 15% ether/hexanes as eluent, yields ***2-18*** as a white solid, 1.09 g (32%). NMR ($CDCl_3$) ^{1}H δ: 9.34 (br s, 2H), 8.83 (t, J=3 Hz, 1H), 4.36 (t, J=12 Hz, 4H), 1.78 (m, 4H), 1.23 (m, 64H), 0.89(br t, 6H). ^{13}C δ: 164.5, 154.0, 137.9, 126.3, 65.9, 31.9, 29.4, 28.6, 25.9, 22.6, 14.0. MS (+ve ESI): calc'd for $C_{43}H_{78}NO_4^+$ = 672.5 amu, obtained = 672.4 amu.

Synthesis of diC20:0 pyridine (*2-20*)

Ester coupling conditions: 1 equivalent of 3,5-pyridinedicarboxylic acid (0.334 g, 1.2 mmol), 2.4 equivalents of *N*,*N*-diisopropyl carbodiimide (DIC) (0.363 g, 2.88 mmol), 2.4 equivalents of hydroxybenzotriazole (HOBt; 0.735 g, 2.88 mmol), 2.4 equivalents of 1-eicosanol (0.373 g, 2.88 mmol) and 2.4 equivalents of *N*,*N*-diisopropylethyl amine (DIPEA; 1.854 g, 2.88 mmol) were stirred in THF at rt for 24 h. Standard work-up and purification by silica gel chromatography , using 15% ether/hexanes as eluent, yields ***2-20*** as a white solid, 0.308 g (35%) . NMR ($CDCl_3$) ^{1}H δ: 9.36 (d, J=3 Hz, 2H), 8.85 (t, J=6 Hz, 1H), 4.38 (t, J=12 Hz, 4H), 1.80 (m, 4H), 1.26 (m, 72 H), 0.88 (br t, 6H). ^{13}C δ: 164.5, 154.0, 137.9, 126.3, 65.9, 31.9, 29.4, 28.6, 25.9, 22.6, 14.0. MS (+ve ESI): calc'd for $C_{47}H_{86}NO_4^+$ = 728.5 amu, obtained = 728.7 amu.

Synthesis of diisoC9:0 pyridine (*2-22*)

Ester coupling conditions: 1 equivalent of 3,5-pyridinedicarboxylic acid (0.835 g, 5 mmol), 2.4 equivalents of *N*,*N*-diisopropyl carbodiimide (DIC) (1.564 g, 12 mmol), 2.4 equivalents of hydroxybenzotriazole (HOBt; 1.840 g, 12 mmol), 2.4 equivalents of 3,5,5-trimethylhexan-1-ol (1.731 g, 12 mmol) and 2.4 equivalents of *N*,*N*-diisopropylethyl amine (DIPEA; 1.854 g, 12 mmol) were stirred in THF at rt for 24 h. Standard work-up and purification by silica gel chromatography , using 15% ether/hexanes as eluent, yields ***2-22*** as a colorless oil, 1.233 g (58%). NMR ($CDCl_3$) ^{1}H δ: 9.34 (d, J=3 Hz, 2H), 8.83 (t, J=3 Hz, 1H), 4.41 (t, J=15 Hz, 4H), 1.83 (m, 6H), 0.90-1.63 (m, 30H). ^{13}C δ: 164.4, 154.0, 137.8, 126.2, 64.3, 50.9, 37.7, 31.0, 29.3, 27.2, 26.2, 22.5. MS (+ve ESI): calc'd for $C_{25}H_{42}NO_4^+$ = 420.3 amu, obtained = 420.2 amu.

Synthesis of dibrC20:0 pyridine (*2-24*)

Ester coupling conditions: 1 equivalent of 3,5-pyridinedicarboxylic acid (0.835 g, 5 mmol), 2.4 equivalents of *N*,*N*-diisopropyl carbodiimide (DIC) (1.564 g, 12 mmol), 2.4 equivalents of hydroxybenzotriazole (HOBt; 1.840 g, 12 mmol), 2.4 equivalents of nonadecan-9-ol (3.583 g, 12 mmol) and 2.4 equivalents of *N*,*N*-diisopropylethyl amine (DIPEA; 1.854 g, 12 mmol) were stirred in THF at rt for 24 h. Standard work-up and purification by silica gel chromatography , using 15% ether/hexanes as eluent, yields ***2-24*** as a colorless oil, 2.144 (67%). NMR ($CDCl_3$) ^{1}H δ: 9.35 (d, J=3 Hz, 2H), 8.84 (t, J=3 Hz, 1H), 4.28 (d, J=6 Hz, 4H), 1.80 (m, 2H), 1.27 (m, 64H), 0.87 (br t, 12H). ^{13}C δ: 164.5, 154.0, 137.8, 126.3, 68.5, 37.4, 31.8, 31.3, 29.5, 26.7, 22.6, 14.0. MS (+ve ESI): calc'd for $C_{47}H_{86}NO_4^+$ = 728.5 amu, obtained = 728.5 amu.

Synthesis of diC18:1 pyridine (*2-26*)

Ester coupling conditions: 1 equivalent of 3,5-pyridinedicarboxylic acid (0.835 g, 5 mmol), 2.4 equivalents of *N*,*N*-diisopropyl carbodiimide (DIC) (1.564 g, 12 mmol), 2.4 equivalents of hydroxybenzotriazole (HOBt; 1.840g, 12 mmol), 2.4 equivalents of Oleyl alcohol (3.220 g, 12 mmol) and 2.4 equivalents of *N*,*N*-diisopropylethyl amine (DIPEA; 1.854 g, 12 mmol) were stirred in THF at rt for 24 h. Standard work-up and purification by silica gel chromatography , using 15%ether/hexanes as eluent, yields ***2-26*** as a colorless oil, 0.537g (16%). NMR ($CDCl_3$) ^{1}H δ: 9.35 (d, J=3 Hz, 2H), 8.85 (t, J=6 Hz, 1H, 6), 5.36 (m, 4H), 4.38 (t, J=12 Hz, 4H), 2.00 (m, 8H), 1.79 (m, 4H), 1.27 (m, 48H), 0.90 (br t, 6H). ^{13}C δ: 164.5, 154.0, 137.9, 129.9, 129.7, 126.3, 65.9, 32.5, 31.8, 29.3, 28.6, 27.1, 25.9, 22.6, 14.0. MS (+ve ESI): calc'd for $C_{47}H_{74}NO_4^+$ = 668.5 amu, obtained = 668.4 amu.

Synthesis of diC11:1 pyridine (*2-28*)

Ester coupling conditions: 1 equivalent of 3,5-pyridinedicarboxylic acid (0.835 g, 5 mmol), 2.4 equivalents of *N*,*N*-diisopropyl carbodiimide (DIC) (1.564 g, 12 mmol), 2.4 equivalents of hydroxybenzotriazole (HOBt; 1.840 g, 12 mmol), 2.4 equivalents of 10-undecen-1-ol (2.043 g, 12 mmol) and 2.4 equivalents of *N*,*N*-diisopropylethyl amine (DIPEA; 1.854 g, 12 mmol) were stirred in THF at rt for 24 h. Standard work-up and purification by silica gel chromatography , using 15% ether/hexanes as eluent, yields ***2-28*** as a colorless oil, 1.069 g (45%). NMR ($CDCl_3$) ^{1}H δ: 9.36 (d, J=3 Hz, 2H), 8.85 (t, J=6 Hz, 1H), 5.76 (m, 2H), 4.97 (m, 4H), 4.38 (t, J=15 Hz, 4H), 2.03 (m, 4H), 1.82 (m, 4H), 1.31 (m, 28 H). ^{13}C δ: 164.5, 154.0, 139.1, 137.9, 128.3, 114.1, 65.9, 33.7, 29.4, 29.3, 29.2, 29.0, 28.8, 28.5, 25.9. MS (+ve ESI): calc'd for $C_{29}H_{46}NO_4^+$ = 472.3 amu, obtained = 472.5 amu.

Synthesis of (C16:0)(C11:1) pyridine (*4-1*)

Ester coupling conditions: 1 equivalent of 3,5-pyridinedicarboxylic acid (0.835 g, 5 mmol), 2.4 equivalents of *N*,*N*-diisopropyl carbodiimide (DIC) (1.564 g, 12 mmol), 2.4 equivalents of hydroxybenzotriazole (HOBt; 1.840 g, 12 mmol), undecen-1-ol (1.022 g, 6 mmol), 1.2 equivalents of 1-hexadecanol (1.4593 g, 6 mmol) and 2.4 equivalents of *N*,*N*-diisopropylethyl amine (DIPEA; 1.854 g, 12 mmol) were stirred in THF at rt for 24 h. Standard work-up and purification by silica gel chromatography , using 15% ether/hexanes as eluent, yields 1.0395 g of white solid which was later determined via ESI mass spectroscopy of methylated analogues to contain 22% of ***2-4***, 28% of ***2-28*** and 50% of ***4-1***. NMR ($CDCl_3$) ^{1}H δ: 9.35 (d, J=3 Hz, 2H), 8.84 (t, J=6 Hz, 1H), 5.79 (m, 1H), 4.95 (m, 2H), 4.37 (t, J=15 Hz, 4H), 2.00 (m, 2H), 1.79 (m, 4H), 1.27 (m, 38H), 0.87 (br t, 3H). ^{13}C δ: 164.5, 149.2, 154.0, 139.1, 137.9, 126.3, 114.1, 65.9, 33.7, 31.8, 29.3, 28.8, 25.9, 22.9, 14.0. MS (+ve ESI): calc'd for (2-4) $C_{39}H_{70}NO_4^+$ = 616.5 amu, obtained = 616.7 amu. calc'd for (2.28) $C_{29}H_{46}NO_4^+$ = 472.3 amu, obtained = 472.5 amu, calc'd for (4-1) $C_{34}H_{58}NO_4^+$ = 544.8 amu, obtained = 544.8 amu.

Methylation reaction (Scheme A.4):

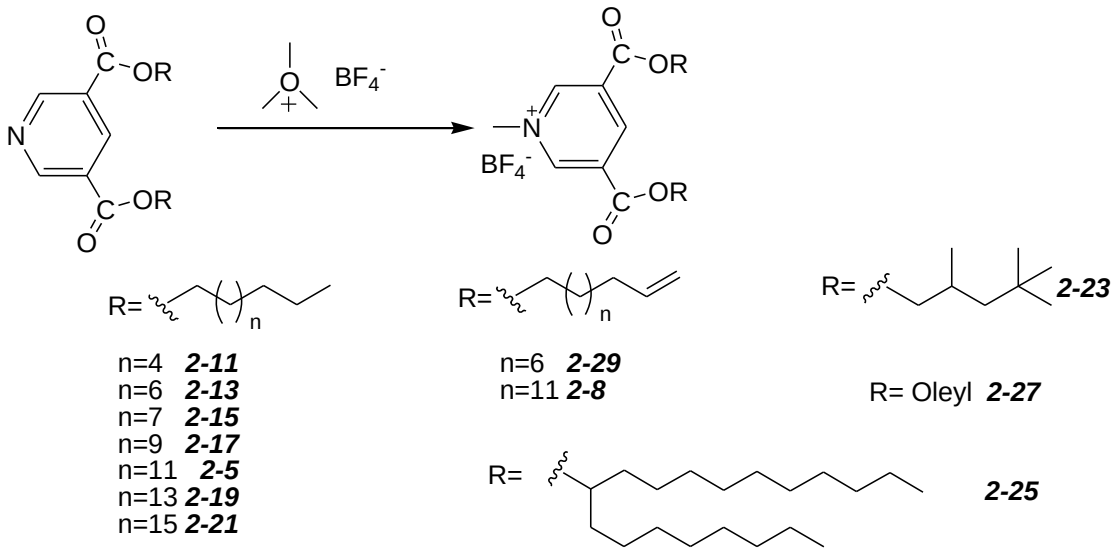

Scheme A.4-Methylation reaction for synthesis of 3,5-dialkyloate methyl pyridinium.

To a solution of 1 equivalent of compound in DCM (Scheme A.4), 1 equivalent of trimethyloxoniumtetrafluoroborate was added and stirred at room temperature overnight. Then it was concentrated in vacuum to give the tetrafluoroborate salt of compound in quantative yield.

Synthesis of diC16:0 (*2-5*)

Methylation conditions: To a solution of ***2-4*** (200 mg, 0.326 mmol) in DCM, trimethyloxoniumtetrafluoroborate (0.0482 g, 0.326 mmol) was added and the mixture was stirred at room temperature overnight. Concentration in vacuum gave white solid in quantitative yield. Known was mixed with σ-adducts[18a], here the pure compound is reported: NMR ($CDCl_3$) ^{1}H δ: 9.39 (m, 3H), 4.69 (s, 3H), 4.38 (t, J=15 Hz, 4H), 1.82 (m, 4H), 1.26 (br s, 51H), 0.86 (br t, 6H). ^{13}C δ: 160.6, 149.4, 131.6, 68.1, 50.2, 32.1, 29.7, 28.5, 26.0, 22.9, 14.3. MS (+ve ESI): calc'd for $C_{40}H_{72}NO_4^+$ = 630.5 amu, obtained = 630.7 amu.

Synthesis of diC16:1/(16:1)(11:0) (*2-8*/*2-9*)

Methylation conditions: To a solution of ***2-6/2-7*** (200 mg, 0.326 mmol) in DCM, trimethyloxoniumtetrafluoroborate (0.0482 g, 0.326 mmol) was added and the mixture was stirred at room temperature overnight. Concentrated in vacuum gave ***2-8/2-9*** (90%/10%) as a white solid in quantitative yield. NMR ($CDCl_3$) ^{1}H δ: 9.39 (m, 3H), 5.80 (m, 2H), 4.94 (m, 4H) 4.68 (s, 3H), 4.47 (t, 4H, J=12 Hz, exp 4.48H), 2.05 (m, 4H), 1.83 (m, 4H), 1.27 (br s, 50H), 0.88 (br t, 0H, exp 1.07H). ^{13}C δ: 160.6, 149.4, 145.0, 139.4, 131.6, 114.2, 68.1, 50.3, 34.0, 29.7, 28.5, 25.9. MS (+ve ESI): calc'd for ***(2-8)*** $C_{40}H_{68}NO_4^+$ = 626.51 amu, obtained = 626.67 amu, calc'd for ***(2-9)*** $C_{35}H_{60}NO_4^+$ = 558.4 amu, obtained = 558.6 amu.

Synthesis of diC9:0 (*2-11*)

Methylation conditions: To a solution of ***2-10*** (100 mg, 0.238 mmol) in DCM, trimethyloxoniumtetrafluoroborate (0.0352 g, 0.238 mmol) was added and the mixture was stirred at room temperature overnight. Concentration in vacuum gave white solid in quantitative yield. NMR ($CDCl_3$) ^{1}H δ: 9.37 (m, 3H), 4.62 (s, J=15 Hz, 3H), 4.43 (t, 4H) 1.80 (m, 4H), 1.27 (br s, 28H), 0.87 (br t, 6H). ^{13}C δ: 160.5, 149.3, 144.3, 131.1, 67.4, 49.9, 33.8, 29.4, 28.4, 25.7, 22.6, 14.0. MS (+ve ESI): calc'd for $C_{26}H_{44}NO_4^+$ = 434.3 amu, obtained = 434.1 amu.

Synthesis of diC11:0 (*2-13*)

Methylation conditions: To a solution of ***2-1*** (100 mg, 0.210 mmol) in DCM, trimethyloxoniumtetrafluoroborate (0.0311 g, 0.210 mmol) was added and the mixture was stirred at room temperature overnight. Concentration in vacuum gave white solid in quantitative yield. NMR ($CDCl_3$) ^{1}H δ: 9.37 (m, 3H), 4.68 (s, 3H), 4.51 (t, J=15 Hz, 4H) 1.80 (m, 4H), 1.27 (br s, 36H), 0.87(br t, 6H). ^{13}C δ: 160.8, 149.5, 147.7, 144.6, 131.3,

67.7, 50.2, 29.5, 28.5, 25.9, 22.6, 14.0. MS (+ve ESI): calc'd for $C_{30}H_{52}NO_4^+$ = 490.3 amu, obtained = 490.5 amu.

Synthesis of diC12:0 (*2-15*)

Methylation conditions: To a solution of ***2-14*** (200 mg, 0.398 mmol) in DCM, trimethyloxoniumtetrafluoroborate (0.0587 g, 0.398 mmol) was added and the mixture was stirred at room temperature overnight. Concentration in vacuum gave white solid of in quantitative yield. NMR ($CDCl_3$) ^{1}H δ: 9.29 (m, 3H), 4.64 (s, 3H), 4.43 (t, J=12 Hz, 4H), 1.81 (m, 4H), 1.26 (br s, 36H), 0.88 (br t, 6H). ^{13}C δ: 160.3, 149.2, 144.7, 131.4, 67.9, 50.1, 31.8, 29.6, 28.3, 25.7, 22.6, 14.0. MS (+ve ESI): calc'd for $C_{32}H_{56}NO_4^+$ = 518.4 amu, obtained = 518.6 amu.

Synthesis of diC14:0 (*2-17*)

Methylation conditions: To a solution of ***2-16*** (200 mg, 0.358 mmol) in DCM, trimethyloxoniumtetrafluoroborate (0.0529 g, 0.358 mmol) was added and the mixture was stirred at room temperature overnight. Concentration in vacuum gave white solid in quantitative yield. NMR ($CDCl_3$) ^{1}H δ: 9.34 (m, 3H), 4.87 (s, 3H), 4.45 (t, J=15 Hz, 4H), 1.83 (m, 4H), 1.27 (br s, 48H), 0.89 (br t, 6H). ^{13}C δ: 160.4, 149.2, 144.6, 131.3, 67.8, 50.0, 31.9, 29.6, 28.3, 25.7, 22.6, 14.0. MS (+ve ESI): calc'd for $C_{36}H_{64}NO_4^+$ = 574.4 amu, obtained = 574.4 amu.

Synthesis of diC18:0 (*2-19*)

Methylation conditions: To a solution of ***2-18*** (100 mg, 0.149 mmol) in DCM, trimethyloxoniumtetrafluoroborate (0.0220 g, 0.149 mmol) was added and the mixture was stirred at room temperature overnight. Concentration in vacuum gave white solid in quantitative yield. NMR ($CDCl_3$) ^{1}H δ: 9.38 (m, 3H), 4.63 (s, 3H), 4.42 (t, 4H), 1.80 (m,

4H), 1.27 (br s, 64H), 0.88 (br t, 6H). ^{13}C δ: 160.5, 149.3, 144.4, 131.2, 67.7, 49.9, 31.9, 29.3, 28.4, 25.7, 22.6, 14.0. MS (+ve ESI): calc'd for $C_{44}H_{80}NO_4^+$ = 686.6 amu, obtained = 686.5 amu.

Synthesis of diC20:0 (*2-21*)

Methylation conditions: To a solution of ***2-20*** (100 mg, 0.134 mmol) in DCM, trimethyloxoniumtetrafluoroborate (0.0199 g, 0.134 mmol) was added and the mixture was stirred at room temperature overnight. Concentration in vacuum gave white solid in quantitative yield. NMR ($CDCl_3$) ^{1}H δ: 9.39 (m, 3H), 4.64 (s, 3H), 4.43 (t, J=15 Hz, 4H), 1.82 (m, 4H), 1.26 (br s, 72H), 0.88 (br t, 6H). ^{13}C δ: 160.4, 149.2, 144.4, 131.3, 67.8, 49.8, 31.9, 29.3, 28.3, 25.7, 22.6, 14.0. MS (+ve ESI): calc'd for $C_{48}H_{88}NO_4^+$ = 742.6 amu, obtained = 742.4 amu.

Synthesis of diisoC9:0 (*2-23*)

Methylation conditions: To a solution of ***2-22*** (100 mg, 0.238 mmol) in DCM, trimethyloxoniumtetrafluoroborate (0.0353 g, 0.238 mmol) was added and the mixture was stirred at room temperature overnight. Concentration in vacuum gave colorless oil in quantitative yield. NMR ($CDCl_3$) ^{1}H δ: 9.37 (m, 3H), 4.61 (s, 3H), 4.44 (t, J=12 Hz, 4H), 1.83 (m, 6H), 1.0-1.30 (m, 30H). ^{13}C δ: 160.6, 149.3, 144.1, 131.1, 66.3, 50.9, 49.9, 37.3, 31.0, 29.3, 26.3, 22.4. M S (+ve ESI): calc'd for $C_{26}H_{44}NO_4^+$ = 434.3 amu, obtained = 434.1 amu.

Synthesis of dibrC20:0 (*2-25*)

Methylation conditions: To a solution of ***2-24*** (200 mg, 0.247 mmol) in DCM, trimethyloxoniumtetrafluoroborate (0.0406 g, 0.247 mmol) was added and the mixture was stirred at room temperature overnight. Concentration in vacuum gave colorless oil in

quantitative yield. NMR ($CDCl_3$) ^{1}H δ: 9.37 (m, 3H), 4.68 (s, 3H), 4.36 (d, J=6 Hz, 4H), 1.84 (m, 2H), 1.26 (br s, 64H), 0.87 (br t, 12H). ^{13}C δ: 160.5, 149.3, 144.2, 147.4, 131.2, 129.9, 70.0, 50.3, 37.3, 31.8, 31.2, 29.5, 26.6, 22.4, 14.0. MS (+ve ESI): calc'd for $C_{48}H_{88}NO_4^+$ = 742.6 amu, obtained = 742.6 amu.

Synthesis of diC18:1 (*2-27*)

Methylation conditions: To a solution of ***2-26*** (124 mg, 0.185 mmol) in DCM, trimethyloxoniumtetrafluoroborate (0.0274 g, 0.185 mmol) was added and the mixture was stirred at room temperature overnight. Concentration in vacuum gave colorless oil in quantitative yield. NMR ($CDCl_3$) ^{1}H δ: 9.42 (m, 3H), 5.34 (m, 4H), 4.62 (s, 3H), 4.42 (t, J=12 Hz, 4H), 2.00 (m, 8H), 1.80 (m, 4H), 1.30 (br s, 48H), 0.87 (br t, 6H). ^{13}C δ: 160.5, 149.3, 144.4, 131.2, 129.9, 129.7, 126.3, 67.4, 49.9, 32.5, 31.8, 29.2, 28.4, 27.2, 26.7, 25.7, 22.6, 14.0. MS (+ve ESI): calc'd for $C_{44}H_{76}NO_4^+$ = 682.5 amu, obtained = 682.4 amu.

Synthesis of diC11:1 (*2-29*)

Methylation conditions: To a solution of ***2-28*** (217 mg, 0.460 mmol) in DCM, trimethyloxoniumtetrafluoroborate (0.0680 g, 0.460 mmol) was added and the mixture was stirred at room temperature overnight. Concentration in vacuum gave colorless oil in quantitative yield. NMR ($CDCl_3$) ^{1}H δ: 9.39 (m, 3H), 5.80 (m, 2H), 4.94 (m, 4H), 4.65 (s, 3H), 4.41 (t, J=12 Hz, 4H) , 2.03 (m, 4H), 1.81 (m, 4H), 1.30 (m, 28H). ^{13}C δ: 160.7, 149.5, 144.7, 139.4, 131.5, 114.3, 67.6, 50.2, 34.0, 29.3, 28.5, 28.5, 25.9. MS (+ve ESI): calc'd for $C_{30}H_{48}NO_4^+$ = 486.3 amu, obtained = 486.5 amu.

Synthesis of cycloC20 (*3-5*)

Methylation conditions: To a solution of ***3-4*** (40 mg, 0.090 mmol) in DCM, trimethyloxoniumtetrafluoroborate (0.0136 g, 0.090 mmol) was added and the mixture was stirred at room temperature overnight. Concentration in vacuum gave colorless oil in quantitative yield. NMR ($CDCl_3$) ^{1}H δ: 9.40 (br s, 2H), 9.17 (m, 1H), 5.343 (m, 2H), 4.46 (s, 3H), 4.44 (t, 4H), 1.98 (m, 4H), 1.79 (m, 4H), 1.29 (m, 24H). ^{13}C δ: 160.7, 149.5, 143.7, 131.1, 130.5, 130.0, 67.6, 49.9, 32.2, 29.0, 28.3, 26.9. MS (+ve ESI): calc'd for $C_{27}H_{41}NO_4^+$ = 458.3 amu, obtained = 458.2 amu.

Synthesis of (C16:0)(C11:1) (*4-2*)

Methylation conditions: To a solution of ***4-1*** (200 mg, 0.367 mmol) in DCM, trimethyloxoniumtetrafluoroborate (0.0543 g, 0.367 mmol) was added and the mixture was stirred at room temperature overnight. Concentration in vacuum gave colorless oil in quantitative yield which was later determined via ESI mass spectroscopy method of methylated analogues to contain 22% of ***2-5***, 28% of ***2-29*** and 50% of ***4-2***. NMR ($CDCl_3$) ^{1}H δ: 9.39 (m, 3H), 5.80 (m, 2H), 4.94 (m, 4H), 4.66 (s, 3H), 4.42 (t, J=15 Hz, 4H), 2.00 (m, 4H), 1.79 (m, 4H), 1.27 (m, 38H), 0.88 (br t, 1.5H). ^{13}C δ: 164.4, 149.2, 139.1, 131.4, 114.1, 67.8, 50.0, 33.7, 31.9, 29.3, 28.8, 25.7, 22.6, 14.0. MS (+ve ESI): calc'd for ***(2-5)*** $C_{40}H_{72}NO_4^+$ = 630.55 amu, obtained = 630.47 amu. calc'd for ***(2.29)*** $C_{30}H_{48}NO_4^+$ = 486.3 amu, obtained = 486.3 amu, calc'd for ***(4-2)*** $C_{35}H_{60}NO_4^+$ = 558.4 amu, obtained = 558.4 amu.

Synthesis of (C18:1)(brC20:0) (*4-4*)

Methylation conditions: To a solution of ***4-3*** (200 mg, 0.286 mmol) in DCM, trimethyloxoniumtetrafluoroborate (0.0424 g, 0.286 mmol) was added and the mixture was stirred at room temperature overnight. Concentration in vacuum gave colorless oil in

quantitative yield which was determined via ESI mass spectroscopy method to contain 28% of ***2-25***, 16% of ***2-27*** and 56% of ***4-4***. NMR ($CDCl_3$) ^1H δ: 9.35 (m, 3H), 5.35 (m, 2H), 4.68 (s, 3H), 4.42 (m, 4H), 3.49 (m, 0H, exp. 2H), 2.00 (m, 8H), 1.27 (m, 67H), 0.88 (br t, 10 H). ^{13}C δ: 160.5, 149.2, 144.1, 131.2, 129.9, 129.7, 126.3, 70.4, 58.5, 50.1, 37.2, 31.0, 29.3, 27.2, 26.7, 22.6, 14.0. MS (+ve ESI): calc'd for ***(2-25)*** $C_{48}H_{88}NO_4^+$ = 742.6 amu, obtained = 742.6 amu, calc'd for ***(2.27)*** $C_{44}H_{76}NO_4^+$ = 682.5 amu, obtained = 682.4 amu, calc'd for ***(4-4)*** $C_{46}H_{82}NO_4^+$ = 712.6 amu, obtained = 712.3 amu.

Ring closing Metathesis reaction (Scheme A.5):

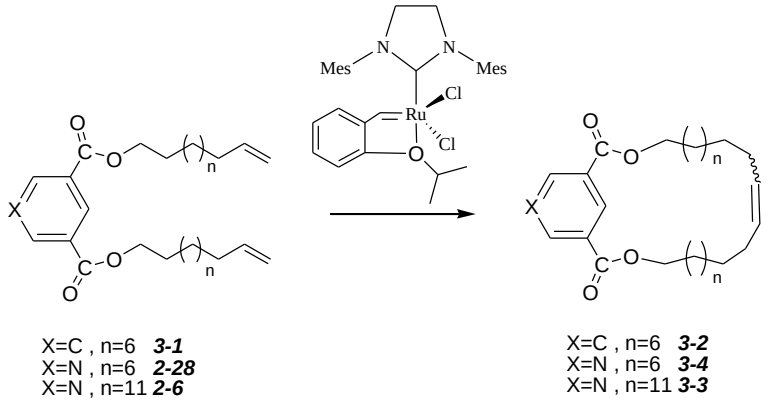

Scheme A.5-RCM reaction for synthesis of compounds *3-2-3-4* with the Hoveyda-grubbs 2nd generation catalyst.

Synthesis of *3-1*

To a mixture of resorcinol (1.653 g, 15 mmol) in acetone (75 ml) , 11-bromo-undece-1-ene (10.505 g, 45 mmol) and potassium carbonate (5.197 g, 37.5 mmol) were added and refluxed for 72h. The reaction mixture was evaporated and then 100 ml of water was added, the organic phase was extracted with EtOAc (3 times), then washed with water (twice), 3M NaOH solution (3 times) and dried over sodium sulphate. The crude product was purified by column chromatography on silica gel, using 10% ether/hexanes as eluent to give 2.496 g (80%) of ***3-1*** as a white solid. NMR ($CDCl_3$) ^1H δ: 7.15 (t, J=12 Hz, 1H),

6.47 (m, 3H), 5.83 (m, 2H), 4.97 (m, 4H), 3.93 (t, J=12 Hz, 4H), 2.03(m, 4H), 1.79 (m, 4H), 1.31 (m, 24H). ^{13}C δ: 160.3, 139.2, 129.7, 114.1, 106.6, 101.4, 67.9, 33.7, 29.4, 29.3, 29.1, 28.9, 26.0.

Synthesis of *3-2*

Ring closing metathesis conditions: To a solution of ***3-1*** (0.207 g, 0.5 mmol) in toluene (10 ml), 3% of Hoveyda-grubbs 2ndgeneration catalyst (0.0094 g, 0.015 mmol) was added and stirred at 70°C for 5 days. The solvent was removed under reduced pressure and the crude product was purified by column chromatography on silica gel, using DCM as eluent to give 0.149 g (77%) of ***3-1*** as an off white solid. NMR ($CDCl_3$) ^{1}H δ: 7.15 (t, J=12 Hz, 1H), 6.46 (m, 3H), 5.41 (m, 2H), 3.92 (t, J=15 Hz, 4H), 1.97 (m, 4H), 1.29-1.87 (m, 28H). ^{13}C δ: 160.3, 130.3, 129.7, 106.6, 101.4, 67.9, 32.2, 29.2, 26.8.

Synthesis of *3-3*

Ring closing metathesis conditions: To a solution of ***2-6*** (0.100 g, 0.164 mmol) in toluene (3 ml), 3% of Hoveyda-grubbs 2ndgeneration catalyst (0.0031 g, 0.005 mmol) was added and stirred at 70°C for 3 days. The solvent was removed under reduced pressure and the crude product was purified by column chromatography on silica gel, using 10% ether/hexanes as eluent to give 12 mg of product with residual catalyst. NMR ($CDCl_3$) ^{1}H δ: 9.37 (d, J=3 Hz, 2H), 8.85 (t, 1H, 3), 5.37 (m, 2H), 4.41 (t, J=15 Hz, 4H), 1.97 (m, 4H), 1.25-1.82 (m, 70H), 0.88 (t, 0H, exp 1.61H). ^{13}C δ: 164.8, 154.2, 138.1, 130.4, 126.2, 65.9, 32.3, 29.2, 26.0.

Synthesis of cycloC20 pyridine (*3-4*)

Ring closing metathesis conditions: To a solution of ***2-28*** (0.236 g, 0.5 mmol) in toluene (10 ml), 5% of Hoveyda-grubbs 2nd generation catalyst (0.0031 g, 0.0025 mmol)

was added and stirred at 70°C for 72 h. The solvent was removed under reduced pressure and the crude product was purified by column chromatography on silica gel, using 10% ether/hexanes as eluent to give 40 mg (18% yield) as a white solid of product with residual catalyst. NMR ($CDCl_3$) ^{1}H δ: 9.36 (br s, 2H), 8.78 (m, 1H), 5.33 (m, 2H), 4.41 (m, 4H), 1.96 (m, 4H), 1.81 (m, 4H), 1.28-1.60 (m, 24H). ^{13}C δ: 160.3, 149.7, 143.6, 131.1, 130.5, 130.1, 67.6, 32.4, 29.2, 28.5, 26.1. MS (+ve ESI): calc'd for $C_{27}H_{41}NO_4^+$ = 444.3 amu, obtained = 444.2 amu.

Synthesis of (18:1)(brC20:0) (*4-3*)

Done by Jose Mendez Campos: To 1 equivalent of 3,5-pyridinedicarboxylic acid (0.835 g, 5 mmol) (Scheme A.6), thionyl chloride (8.4 g, 70 mmol) was added. The solution was reflux for 24 h under N_2 to yield pyridine-3,5-dicarboyl dichloride. The residual thionyl chloride was removed under reduced pressure and then the remaining product was dissolved in DCM (20 ml). 1.2 equivalent of nonadecan-9-ol (1.791 g, 6 mmol) and 1.2 equivalents of oleyl alcohol (1.610 g, 6 mmol) were added and the reaction solution was refluxed for 3 h. The solvent was removed under reduced pressure and then the residue was dissolved in ether (50 ml) and washed with 4M NaOH, dried over sodium sulphate and the crude product was purified by silica gel chromatography, using 15% ether/hexanes as eluent, yields 3.099g of colorless oil which was determined via ESI mass spectroscopy method of the methylated product to contain 28% of ***2-24***, 16% of ***2-26*** and 56% of ***4-3***. NMR ($CDCl_3$) ^{1}H δ: 9.34 (d, 2H, 3), 8.83 (t, J=3 Hz, 1H), 5.34 (m, 4H), 4.36 (t, J=18 Hz, 4H), 2.00 (m, 8H), 1.82 (m, 4H), 1.25 (m, 52H), 0.86 (br t, 9H). ^{13}C: δ 164.5, 154.0, 139.3, 137.9, 126.3, 114.1, 65.9, 33.7, 31.8, 29.6, 28.8, 28.6, 25.9, 22.6, 14.0. MS (+ve ESI): calc'd for (***2-24***) $C_{47}H_{86}NO_4^+$ = 728.65 amu, obtained =

728.53 amu, calc'd for (***2.26***) $C_{47}H_{74}NO_4^+$ = 668.55 amu, obtained = 668.42 amu, calc'd for **(*4-3*)** $C_{45}H_{80}NO_4^+$ = 698.6 amu, obtained = 698.7 amu.

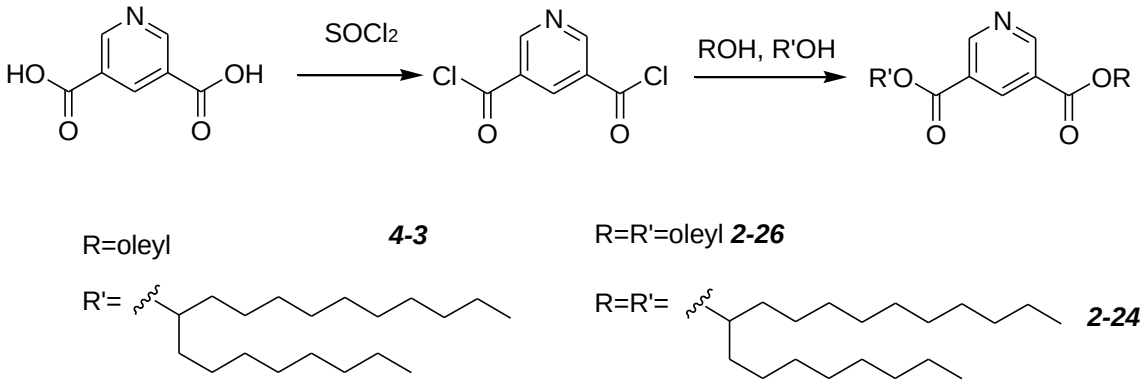

Scheme A.6-Synthesis via acylation reaction for synthesis of mixture of *2-24, 2-26* & *4-3*

General methods for calculation of molecular parameters, and plotting/fitting of data

The equations used to determine the molecular structure parameters of lipids, and used to calculate transfection indices are described in the text. The table below summarizes these parameters. Experimental data on transfection and cytotoxicity (Appendix C) was assigned an experiment number as it was received and the data was formatted in Excel then exported to a database in Access. Subsets of data for analysis were selected using Access queries and exported to an Excel spreadsheet. This spreadsheet was then used to set the stoichiometric parameters of the formulation, the lipid properties were pulled from another spreadsheet similar to the Table A.1 below in the workbook using LOOKUP functions, and the input terms of the transfection indices were calculated. Plotting and the statistical tools of Excel were used to explore the derived correlations.

Bibliography for Appendix A:

1. Kiriya, D.; Chang, H. C.; Kitagawa, S., Molecule-based valence tautomeric bistability synchronized with a macroscopic crystal-melt phase transition. *Journal of the American Chemical Society* **2008,** *130* (16), 5515-5522.
2. Moszynski, J. M.; Fyles, T. M., Synthesis and ion transport activity of oligoesters containing an environment-sensitive fluorophore. *Organic & Biomolecular Chemistry* **2011,** *9* (21), 7468-7475.
3. Baldwin, J. E.; Spring, D. R.; Atkinson, C. E.; Lee, V., Efficient synthesis of the sponge alkaloids cyclostellettamines A-F. *Tetrahedron* **1998,** *54* (44), 13655-13680.
4. Hon, Y. S.; Wong, Y. C.; Chang, C. P.; Hsieh, C. H., Tishchenko reactions of aldehydes promoted by diisobutylaluminum hydride and its application to the macrocyclic lactone formation. *Tetrahedron* **2007,** *63* (46), 11325-11340.
5. Pijper, D.; Bulten, E.; Šmisterová, J.; Wagenaar, A.; Hoekstra, D.; Engberts, Jan B. F. N.; Hulst, R., Novel biodegradable pyridinium amphiphiles for gene delivery. *European Journal of Organic Chemistry* **2003,** (22), 4406-4412.

Table A.1-Molecular parameters used in the calculation of transfection indices:

Compound name	M Wt g/mol	l_c Å	a_0 Å^2	V Å^3	S	logP	l_{tot} Å	V_{tot} Å^3	nC
chol	386	17.4	28	545	1.14	9.9	23.3	654	16
EPC	743	17.9	54	876	0.90	9.8	26.2	1179	12
DOPE	744	18.7	45	967	1.14	14.8	26.3	1198	8
diC9:0	434	10.3	42	506	1.17	5.1	17.6	712	8
diisoC9:0	434	7.2	42	506	1.67	4.0	14.5	712	8
diC11:1	486	12.0	42	593	1.18	6.3	19.3	798	8
diC11:0	490	12.3	42	614	1.19	7.3	19.6	819	9
diC12:0	518	13.3	42	668	1.20	8.3	20.6	872	10
diC14:0	574	15.3	42	775	1.21	10.5	22.6	979	12
diC16:0	630	17.4	42	883	1.22	12.6	24.6	1086	14
diC16:1	626	17.4	42	862	1.19	11.6	24.6	1066	13
diC18:0	686	19.4	42	990	1.23	14.7	26.7	1193	16
diC18:1	682	18.7	42	969	1.25	13.7	26.0	1173	8
(C16:1)(C11:0)	556	14.7	42	728	1.19	9.4	22.0	932	11
diC20:0	742	21.4	42	1097	1.23	16.8	28.7	1300	18
dibrC20:0	744	12.3	42	1108	2.16	16.5	19.6	1311	10
CycloC20	458	12.3	42	539	1.05	3.4	19.6	745	
(C16:0)(C11:1)	558	14.7	42	738	1.20	9.4	22.0	942	11.5
(C18:1)(brC20:0)	712	15.5	42	1033	1.60	15.1	22.8	1236	9
diC16:1 mix	619	17.1	42	849	1.19	11.4	24.4	1052	12.8
(C18:1)(brC20:0)mix	716	15.1	42	1044	1.70	14.9	22.4	1247	8.8
(18:1)(br20:0)blend0.32/0.68	724	14.3	42	1063	1.87	15.6	21.6	1266	9.4
(18:1)(br20:0)blend50	713	15.5	42	1039	1.70	15.1	22.8	1242	9
(18:1)(br20:0)blend66	722	14.5	42	1061	1.85	15.5	21.7	1264	9.3
(18:1)(br20:0)blend85	734	13.3	42	1087	2.03	16.1	20.5	1290	9.7

Appendix B: Supporting information for synthesis

[1]HNMR for compound ***1-1***

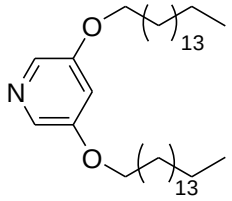

1-1

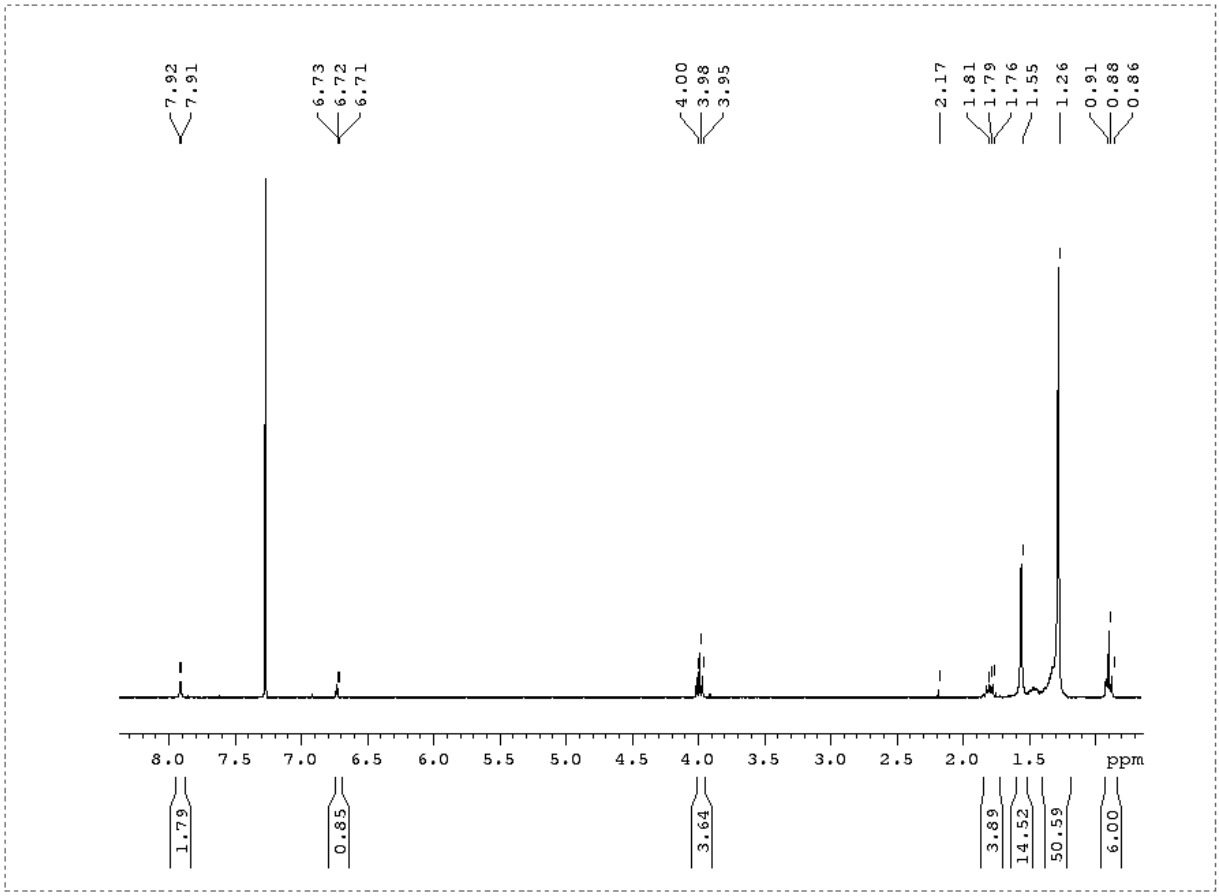

^{1}HNMR for compound ***1-2***

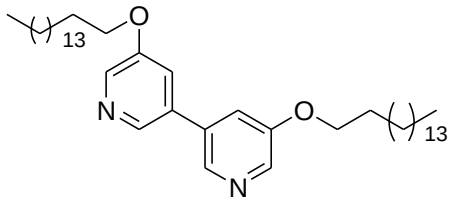

1-2

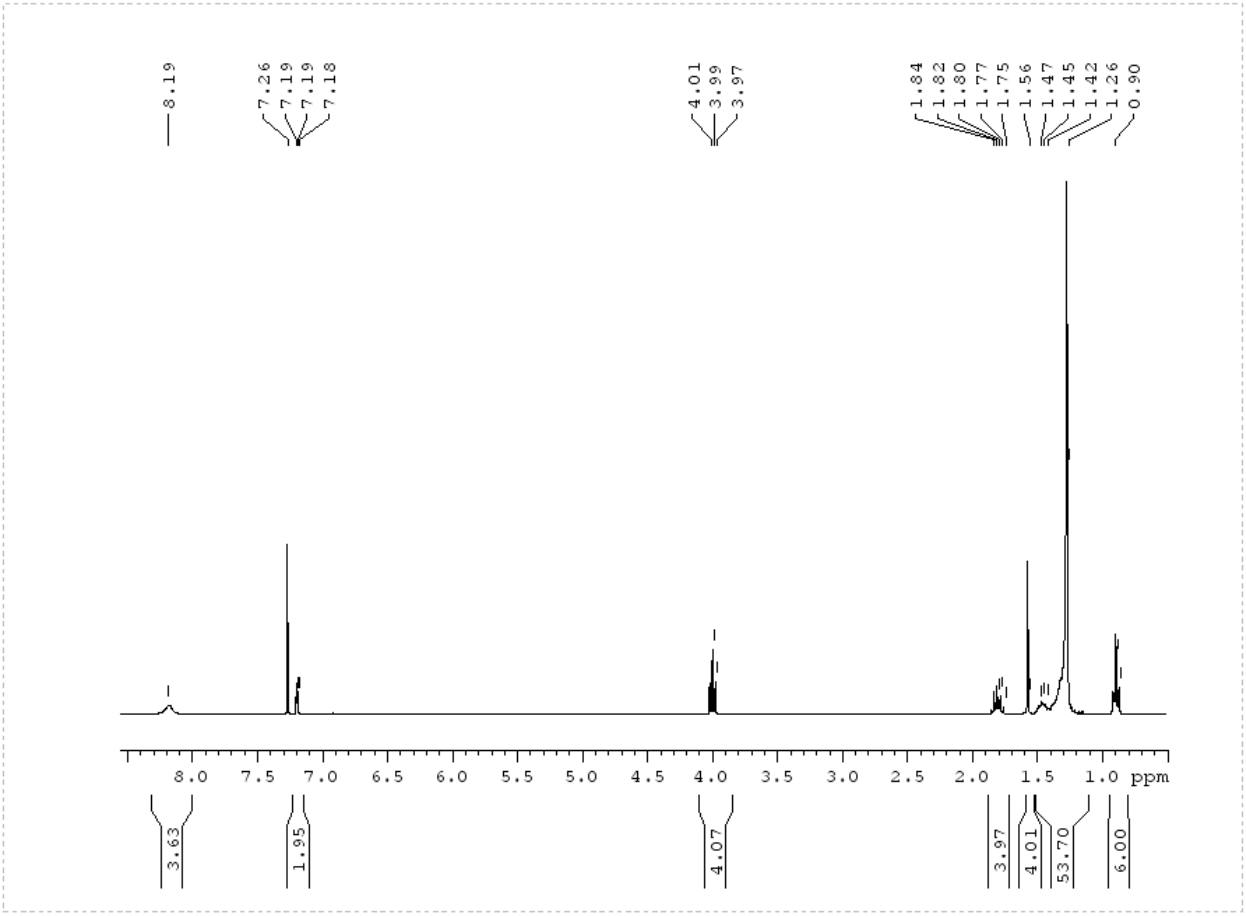

^{13}CNMR for compound ***1-2***

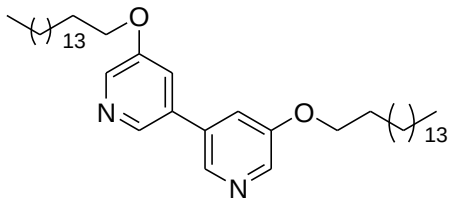

1-2

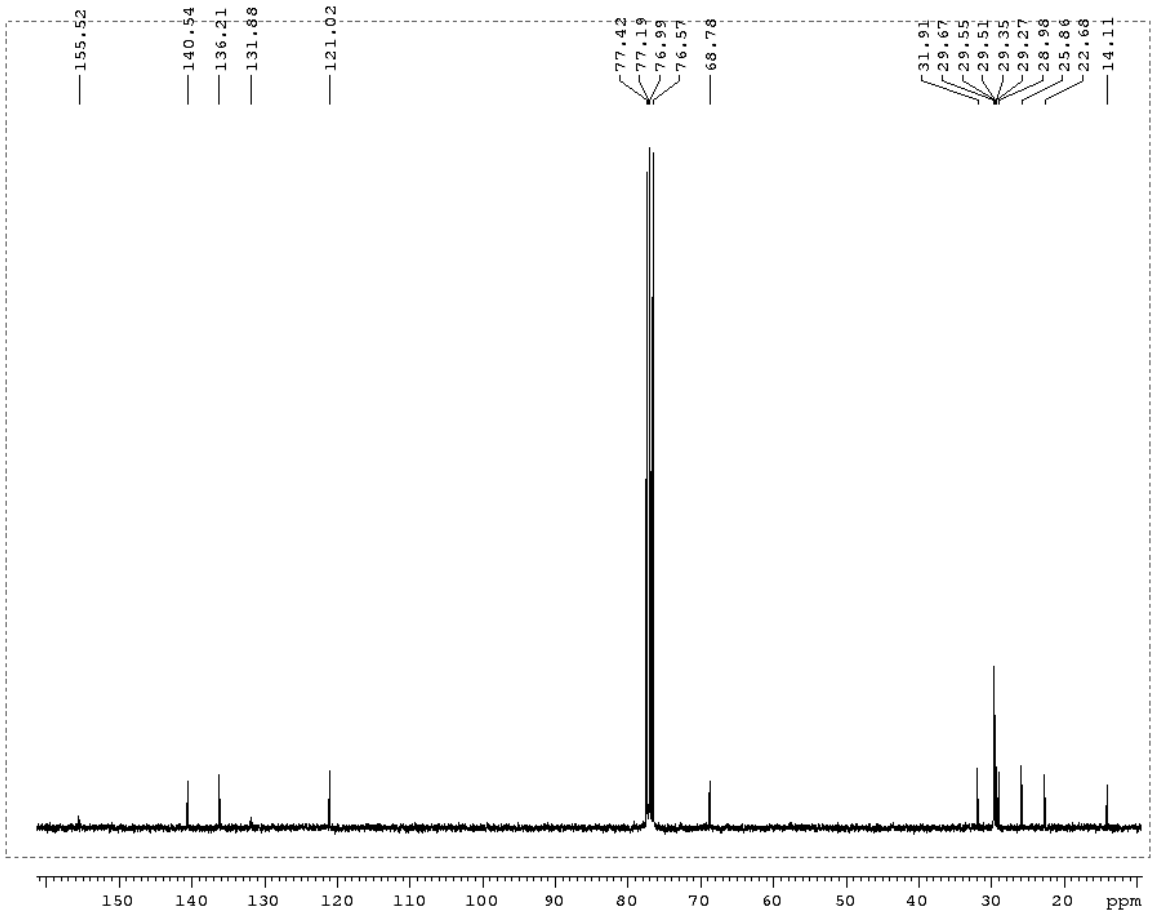

[1]HNMR for compound ***1-3***

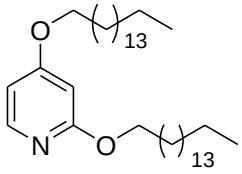

1-3

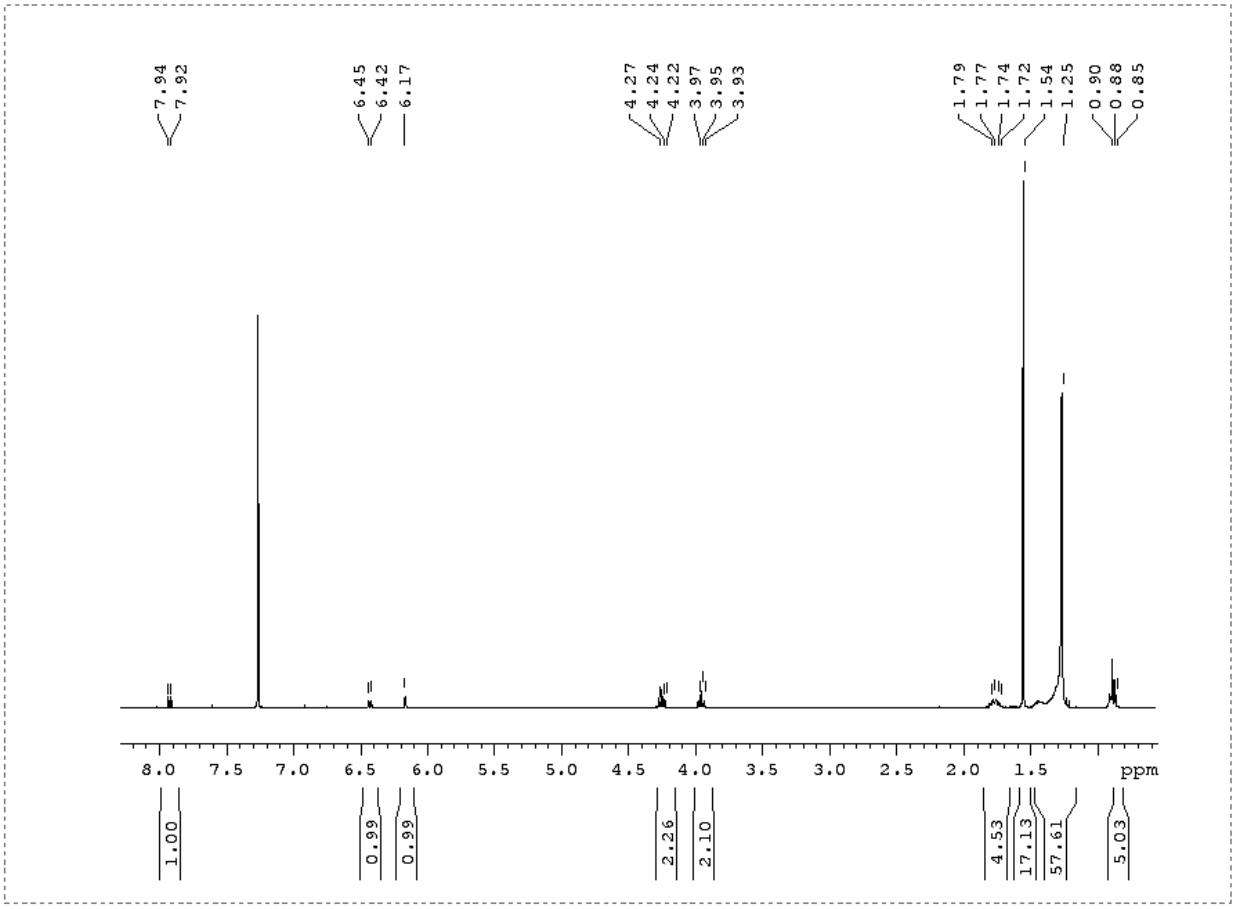

^{13}CNMR for compound ***1-3***

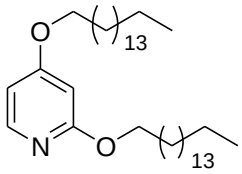

1-3

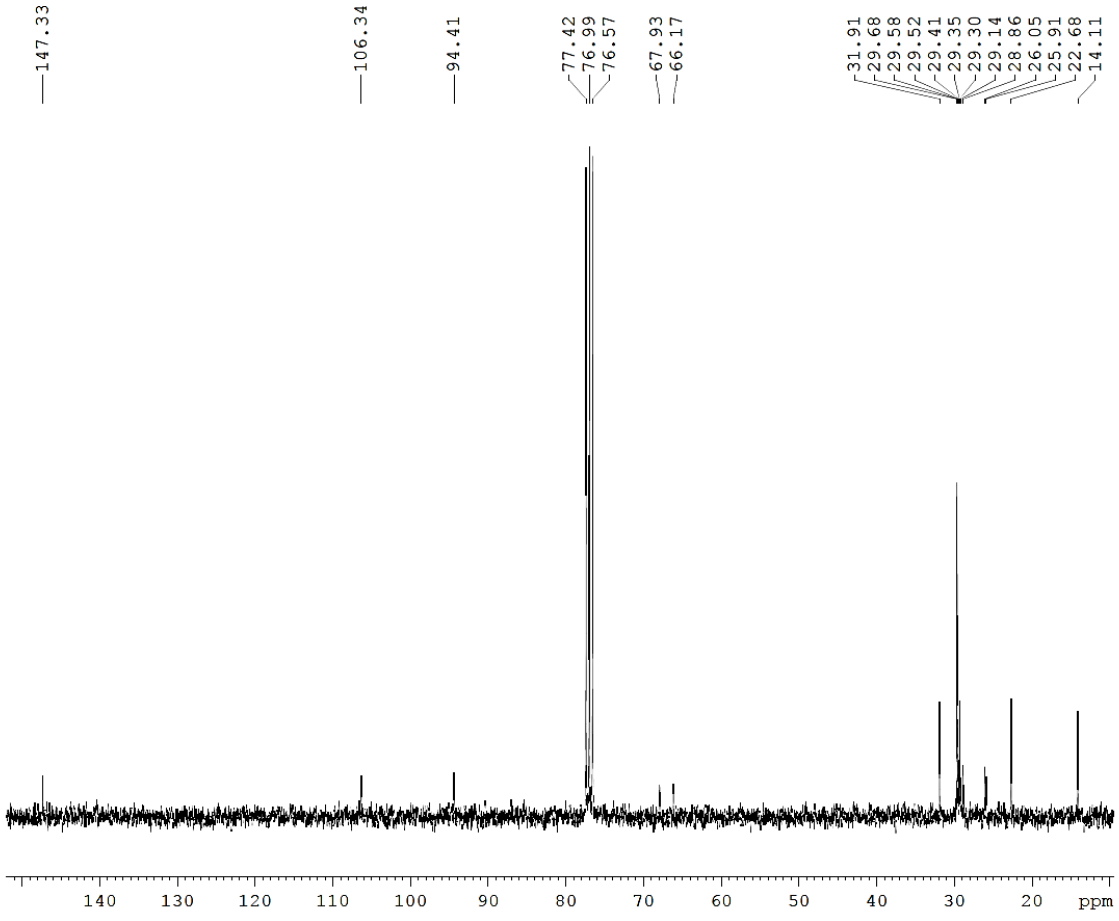

^{1}HNMR for compound ***1-4***

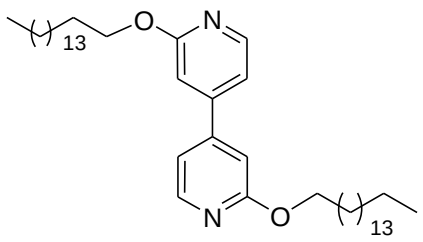

1-4

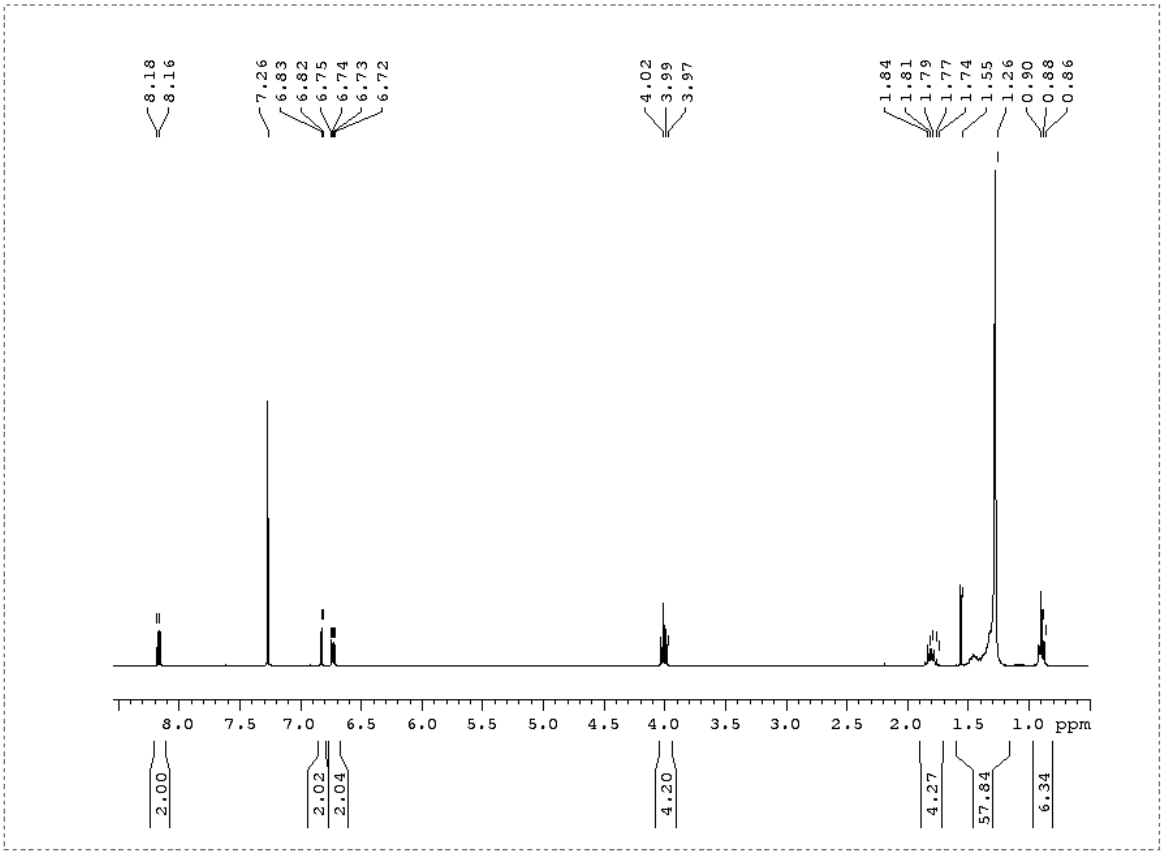

^{13}CNMR for compound ***1-4***

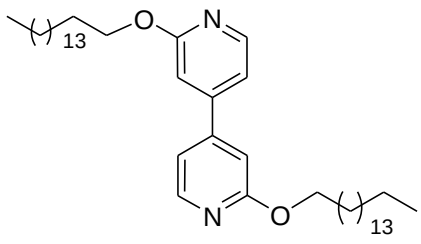

1-4

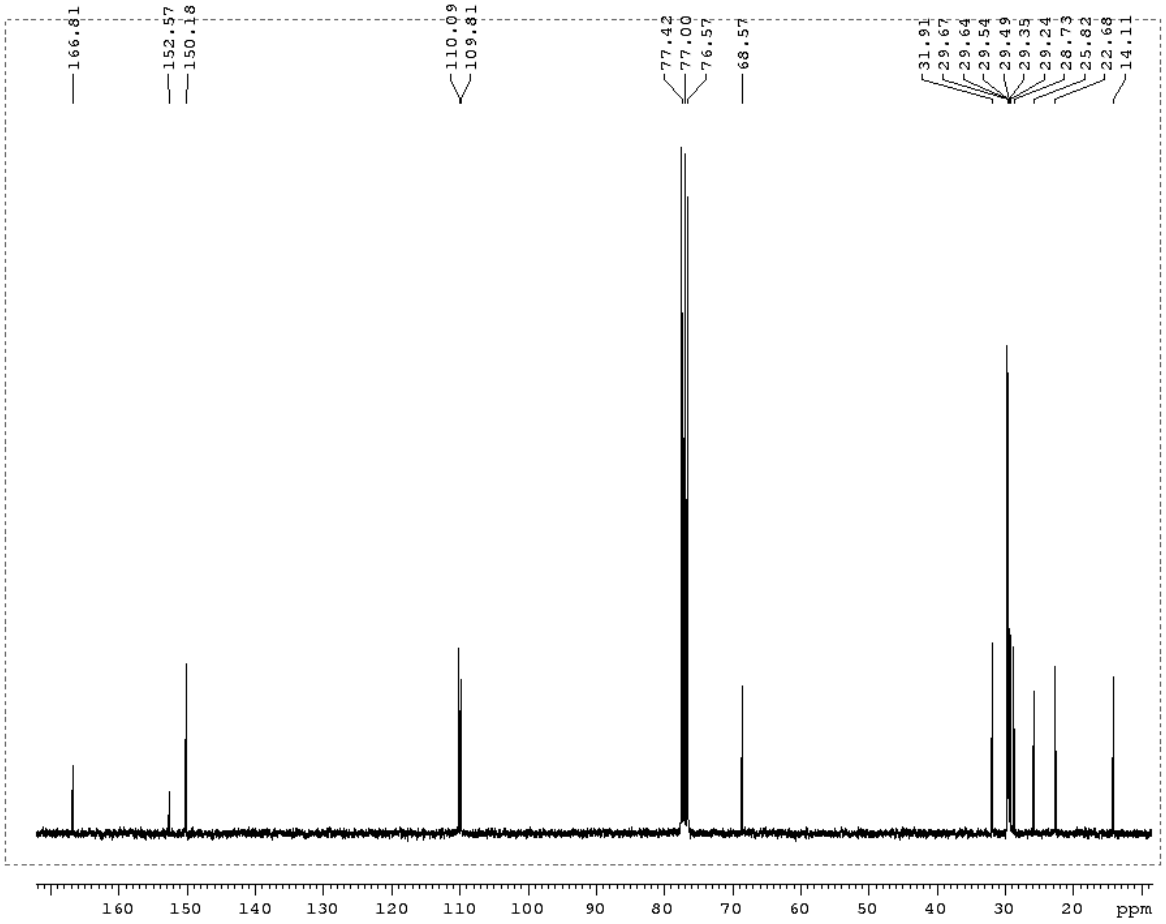

^{1}HNMR for compound ***1-5***

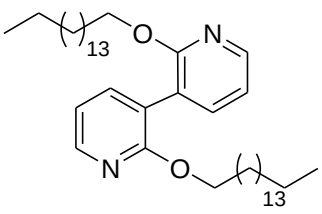

1-5

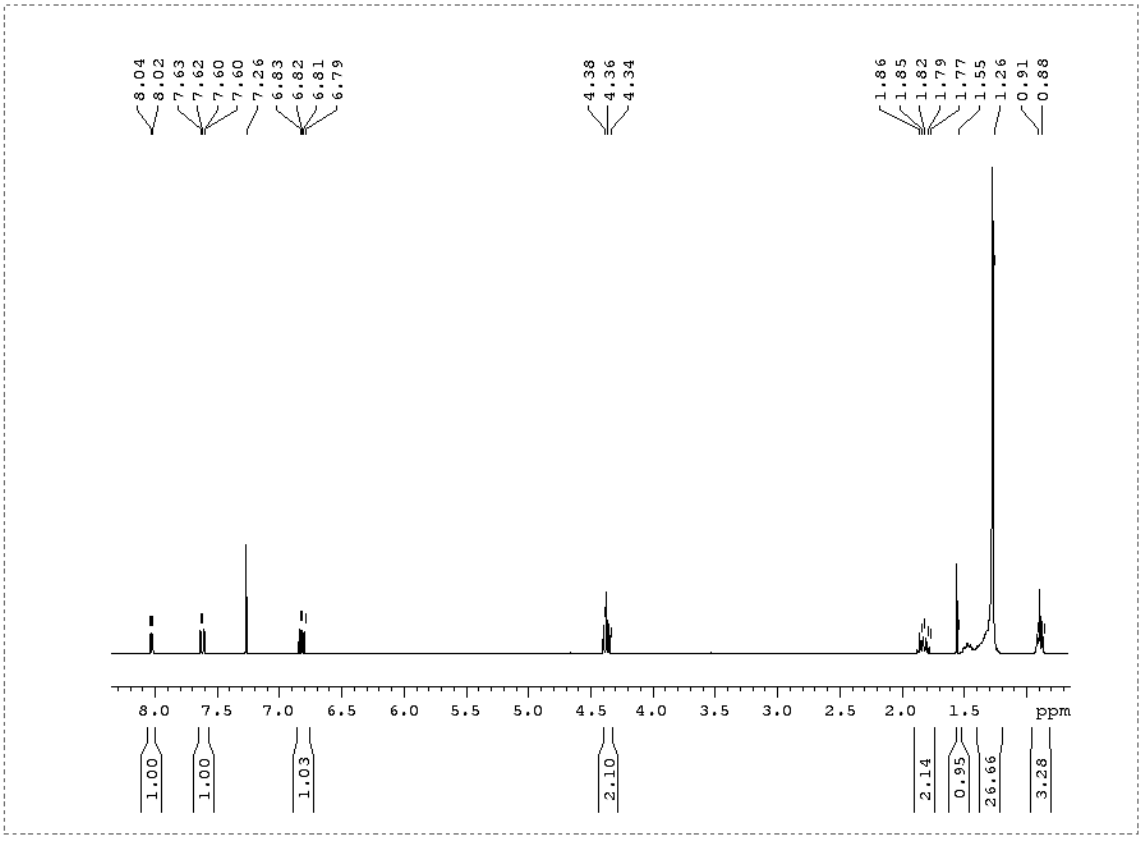

^{13}CNMR for compound ***1-5***

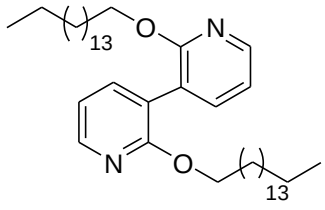

1-5

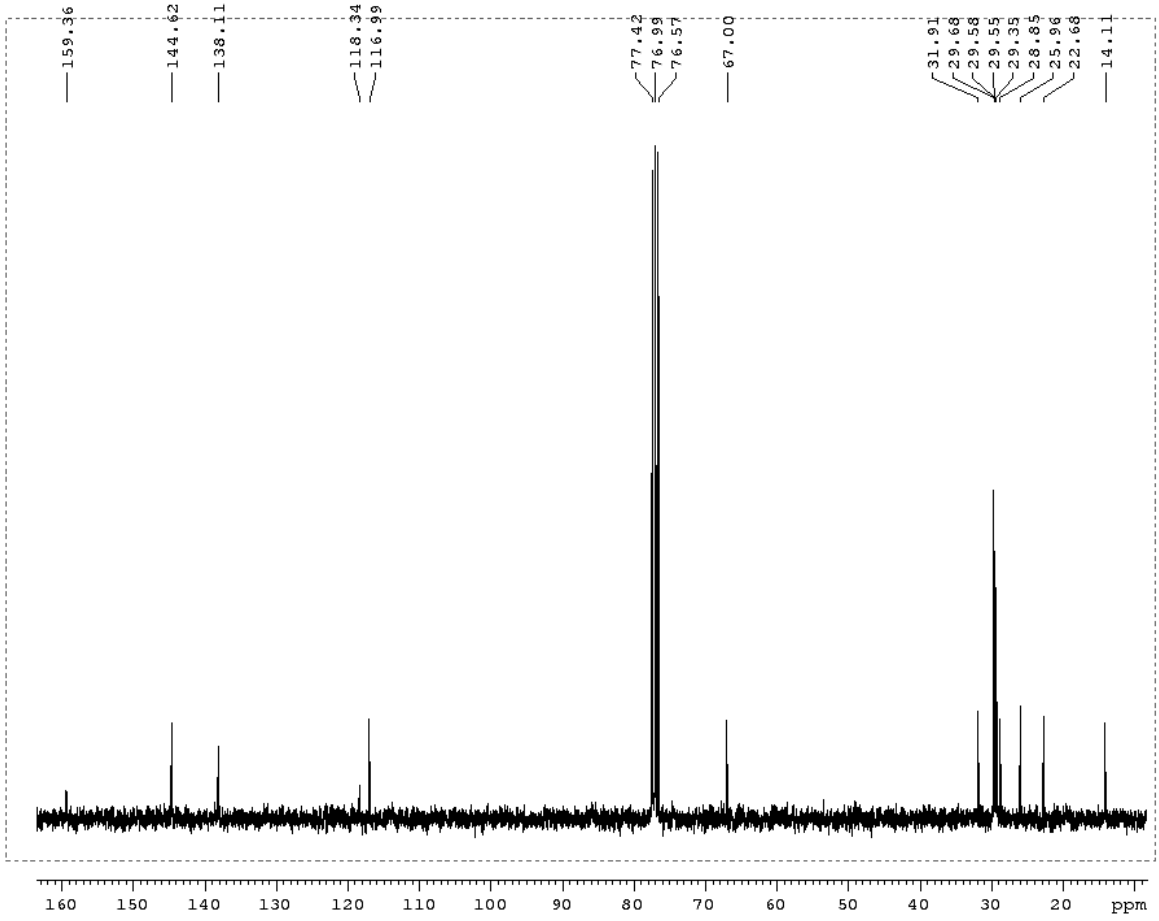

^{1}HNMR for compound ***2-1***

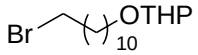

2-1

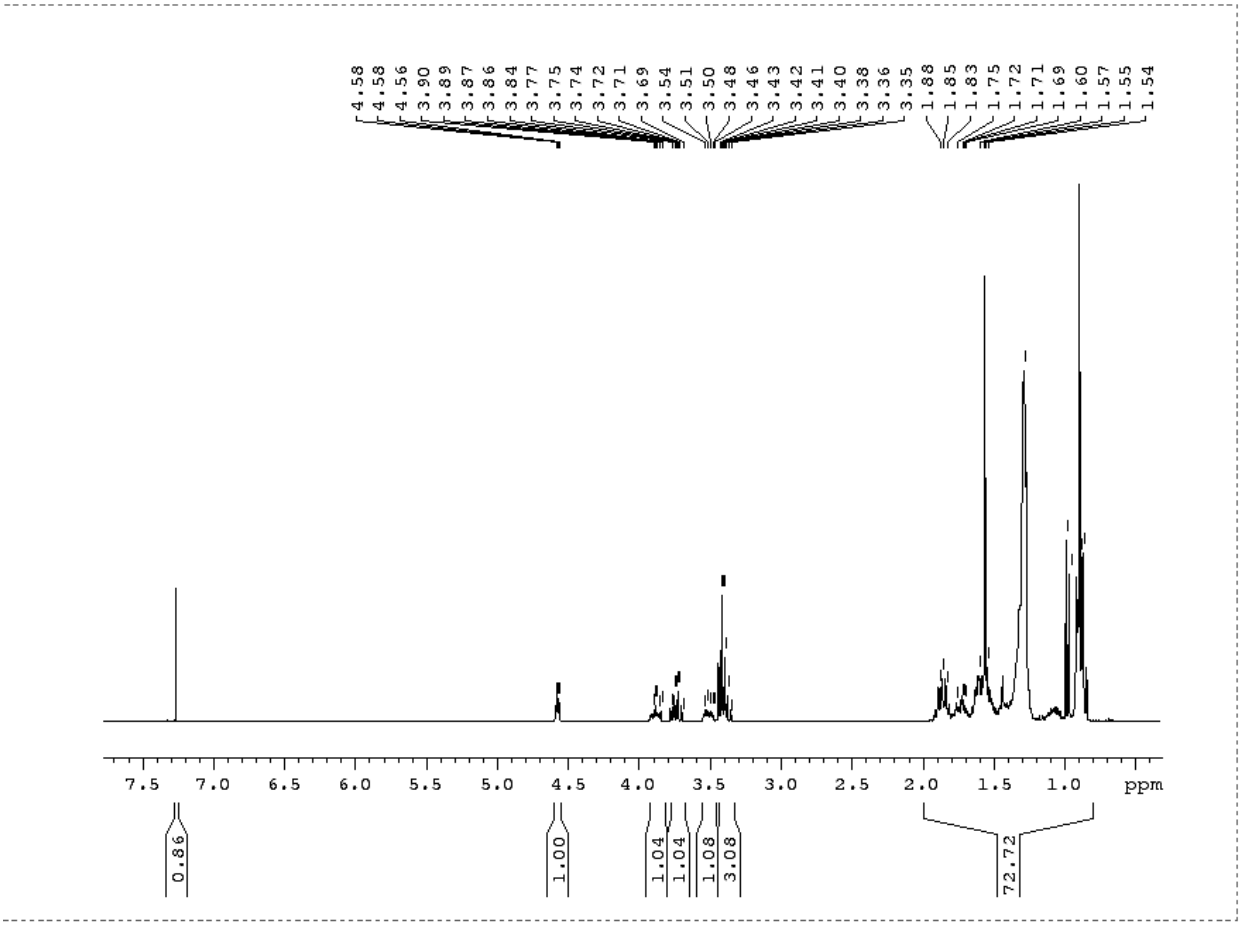

^{13}CNMR for compound ***2-1***

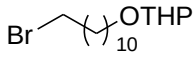

2-1

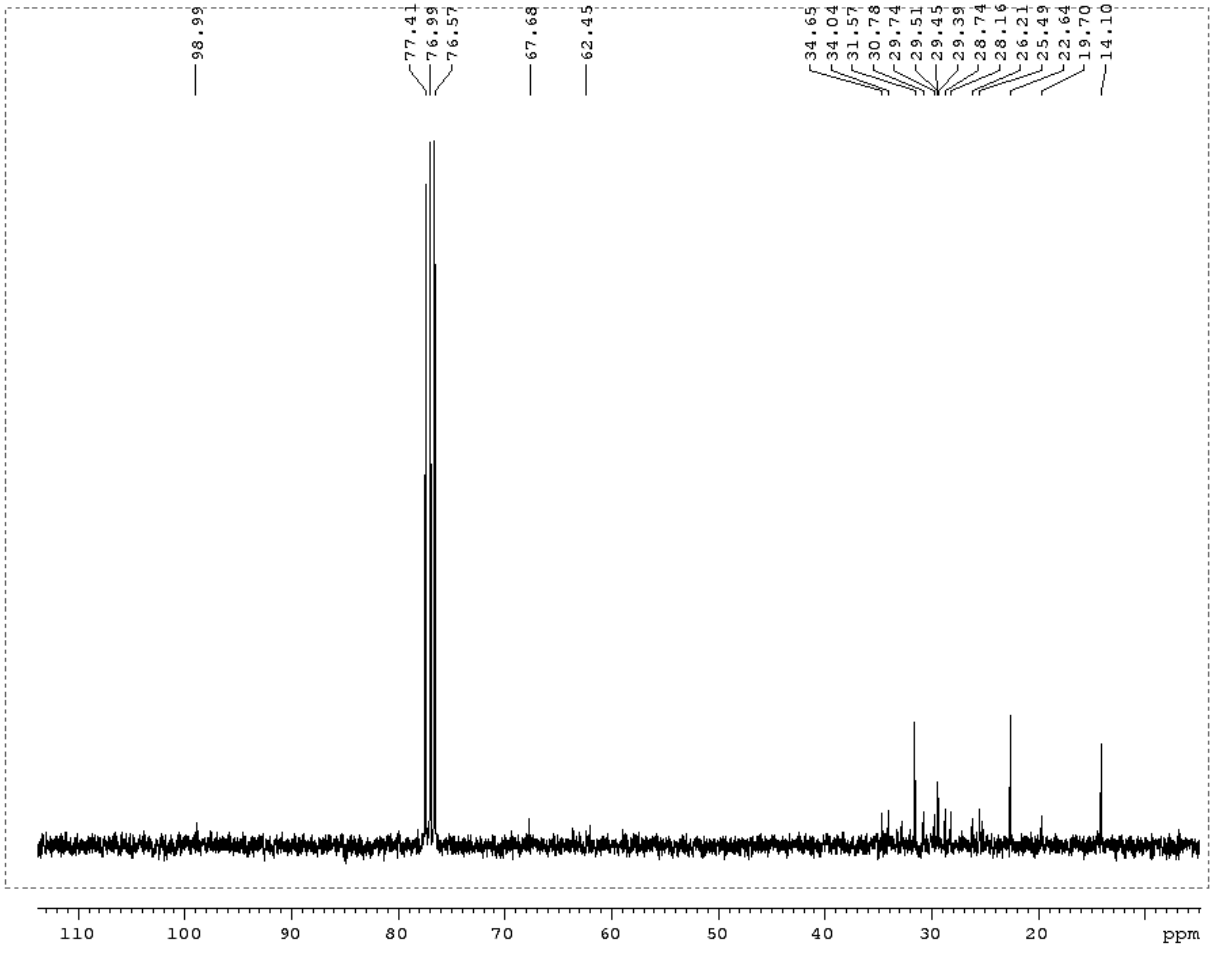

^{1}HNMR for compound ***2-2***

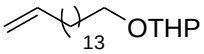

2-2

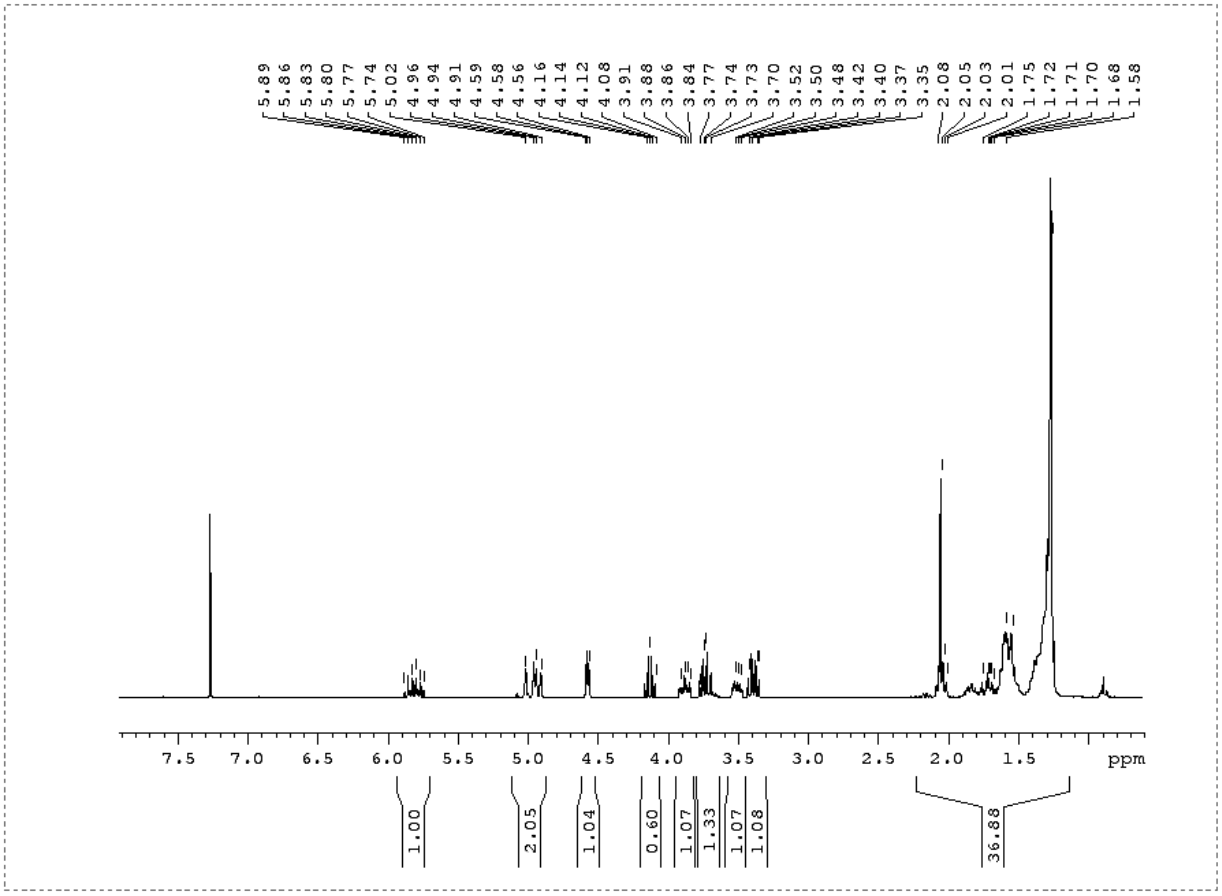

^{13}CNMR for compound ***2-2***

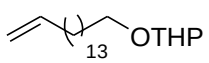

2-2

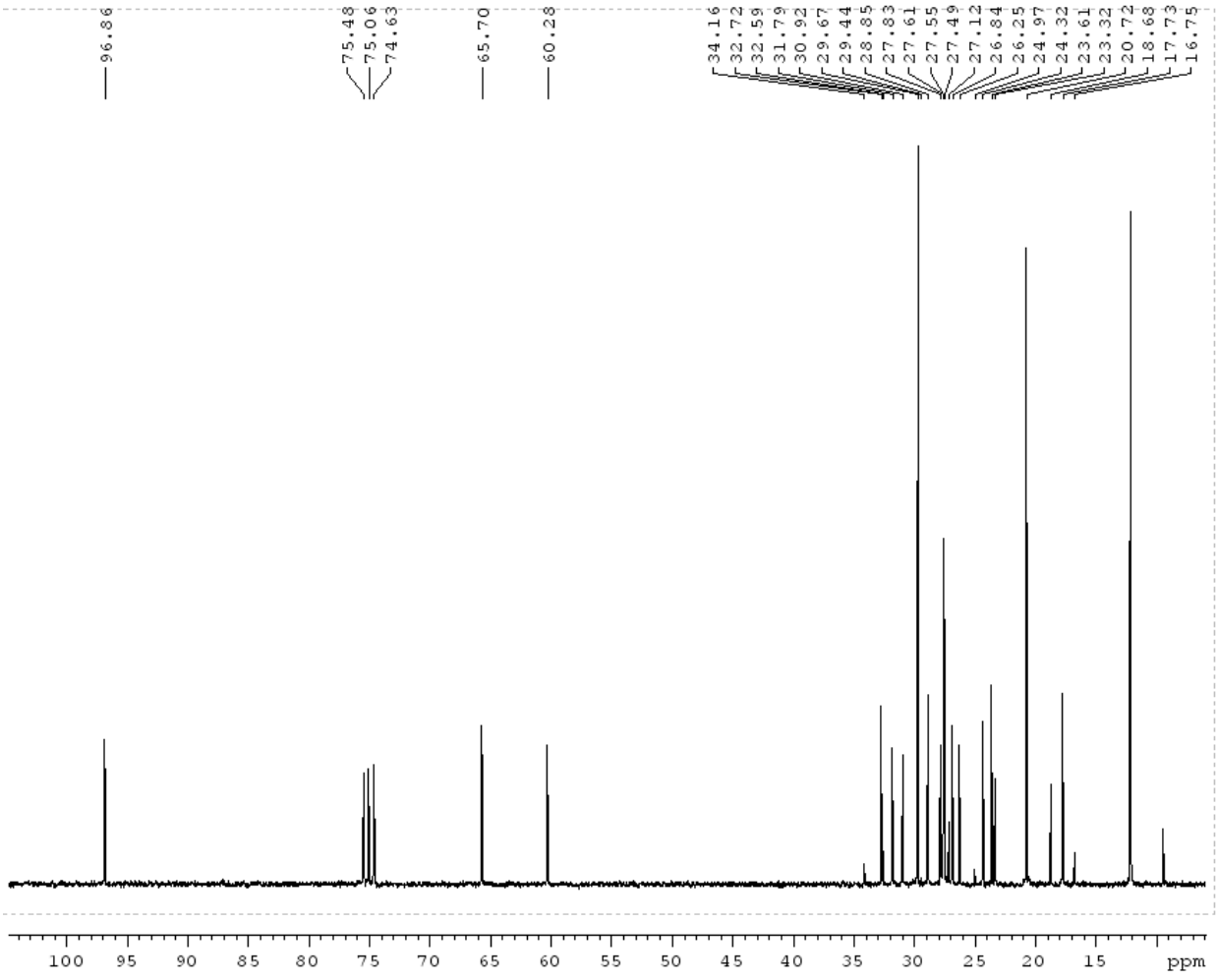

^{1}HNMR for compound ***2-3***

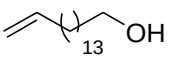

2-3

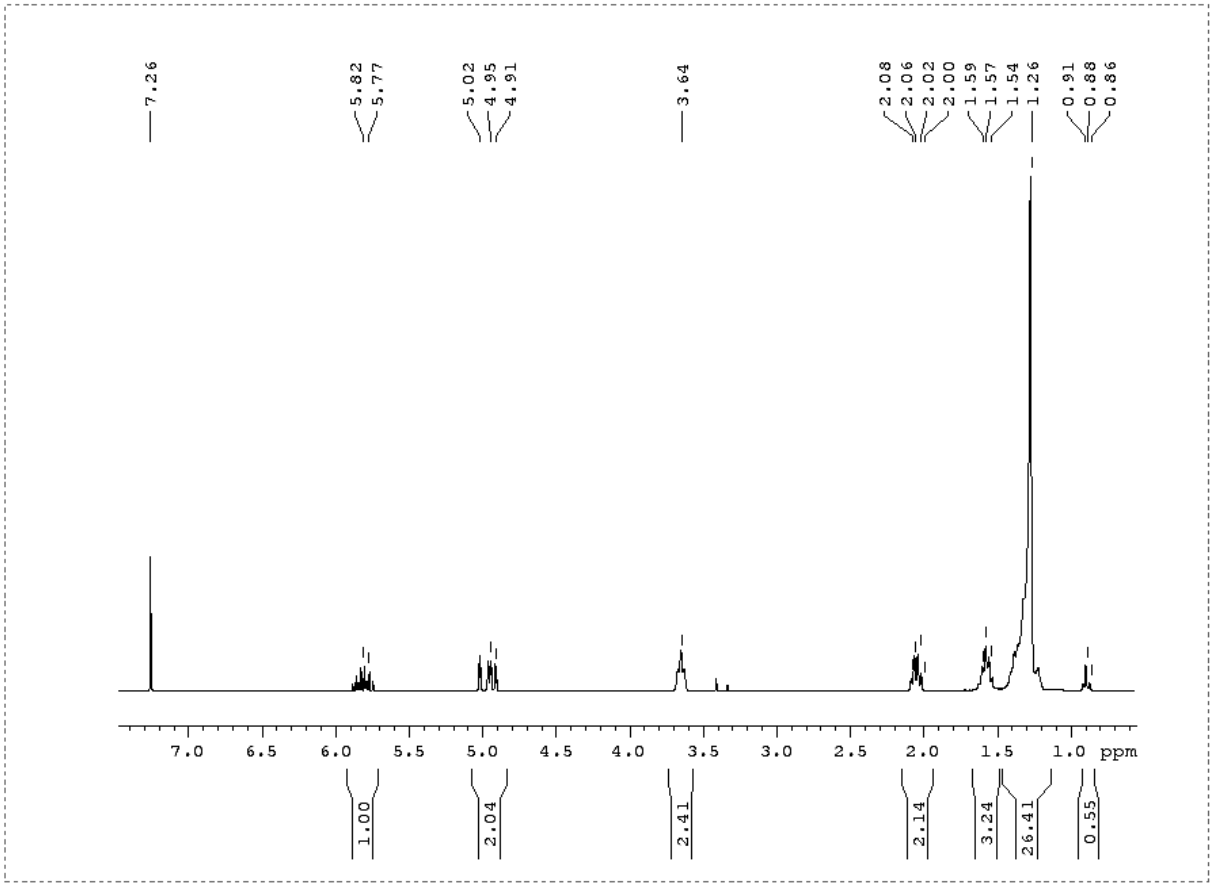

^{13}CNMR for compound ***2-3***

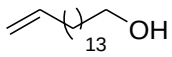

2-3

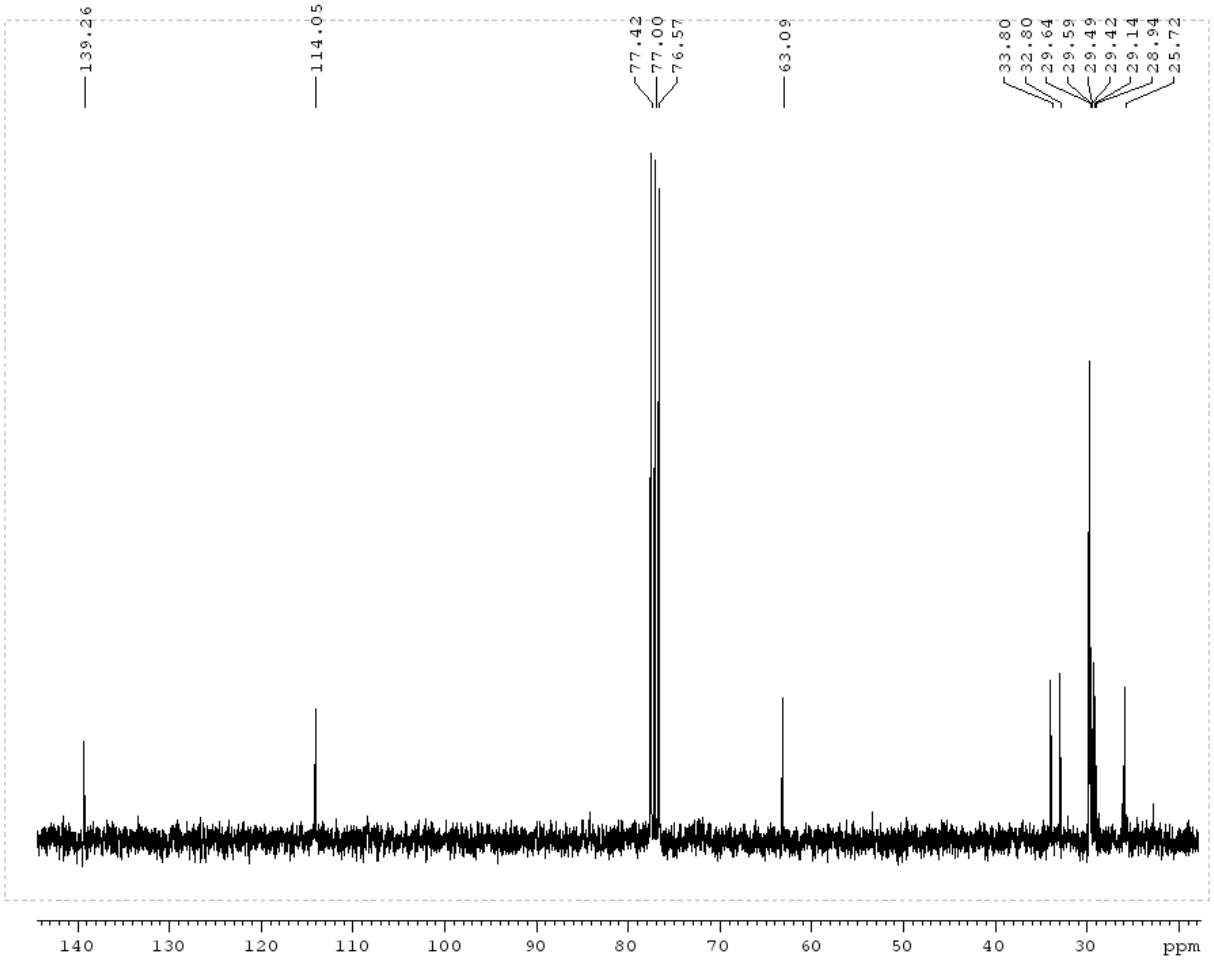

^{1}HNMR for compound ***2-4***

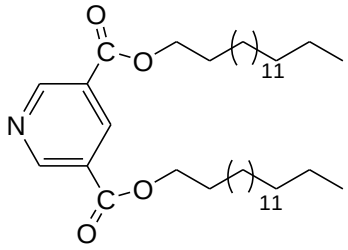

2-4

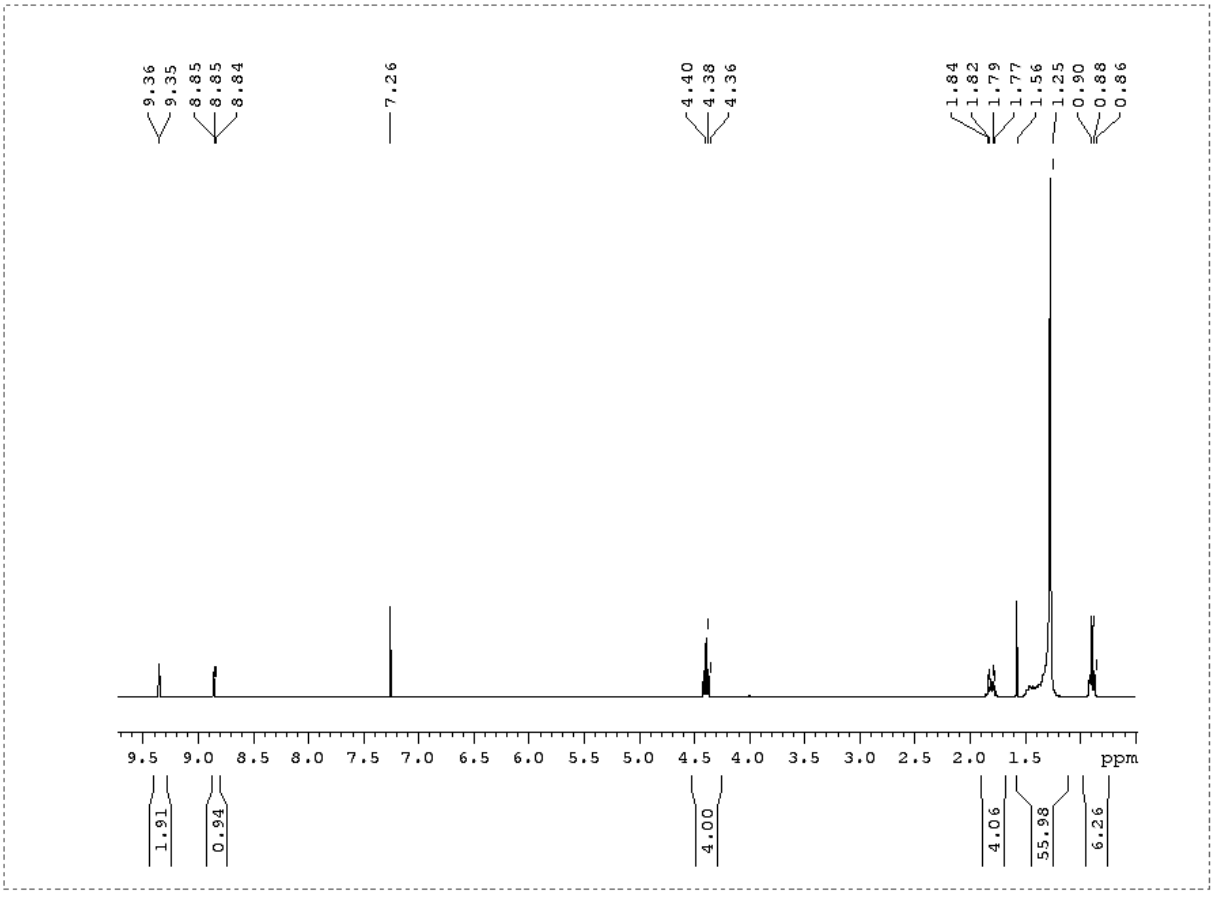

^{13}CNMR for compound ***2-4***

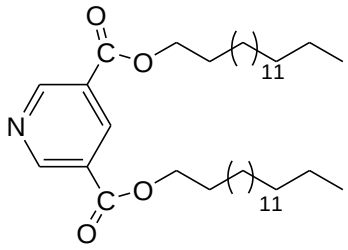

2-4

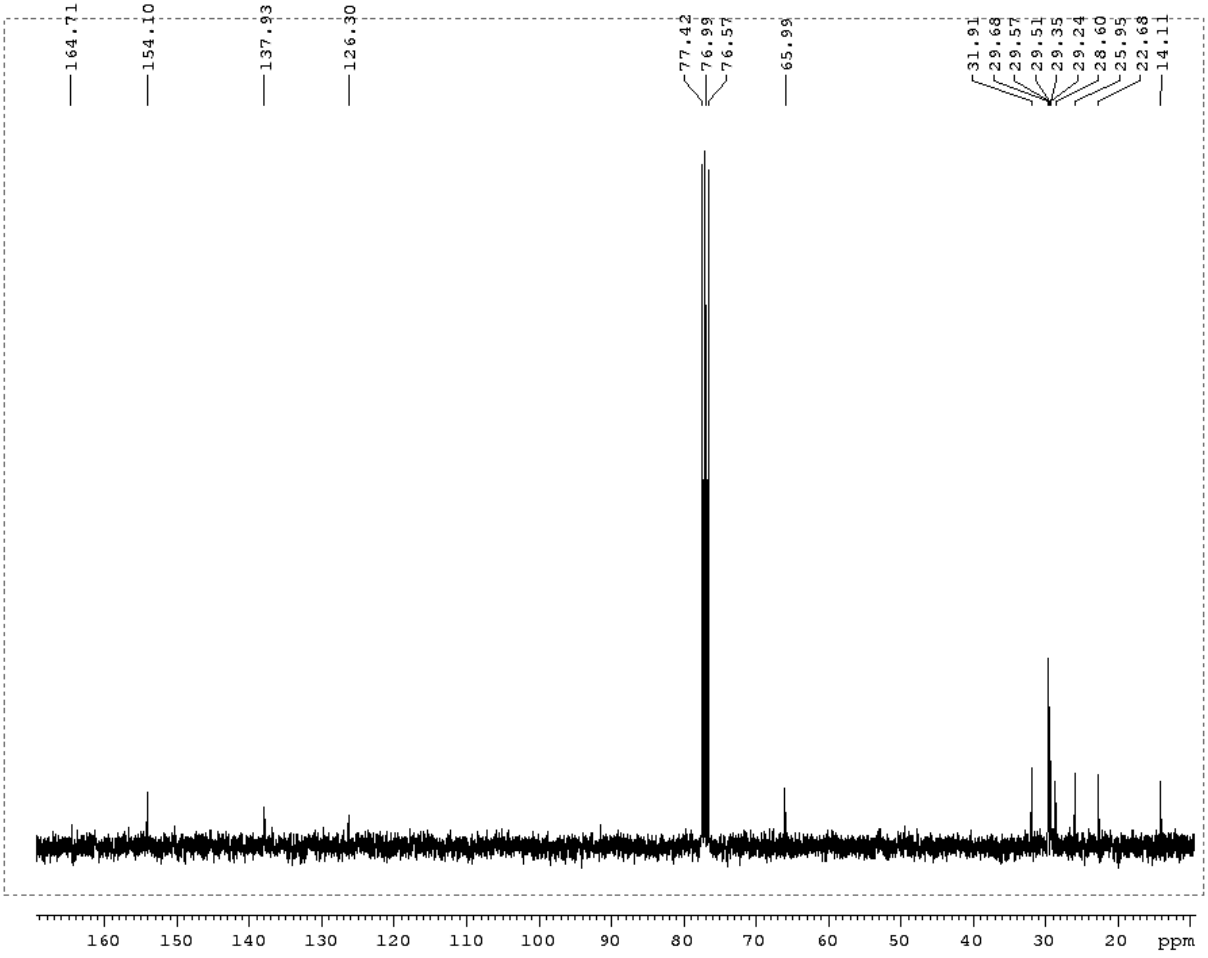

^{1}HNMR for compound ***2-5***

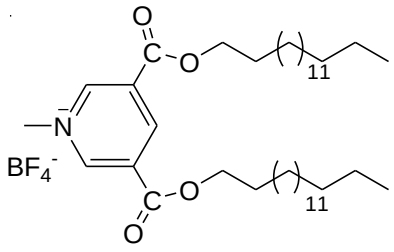

2-5
diC16:0

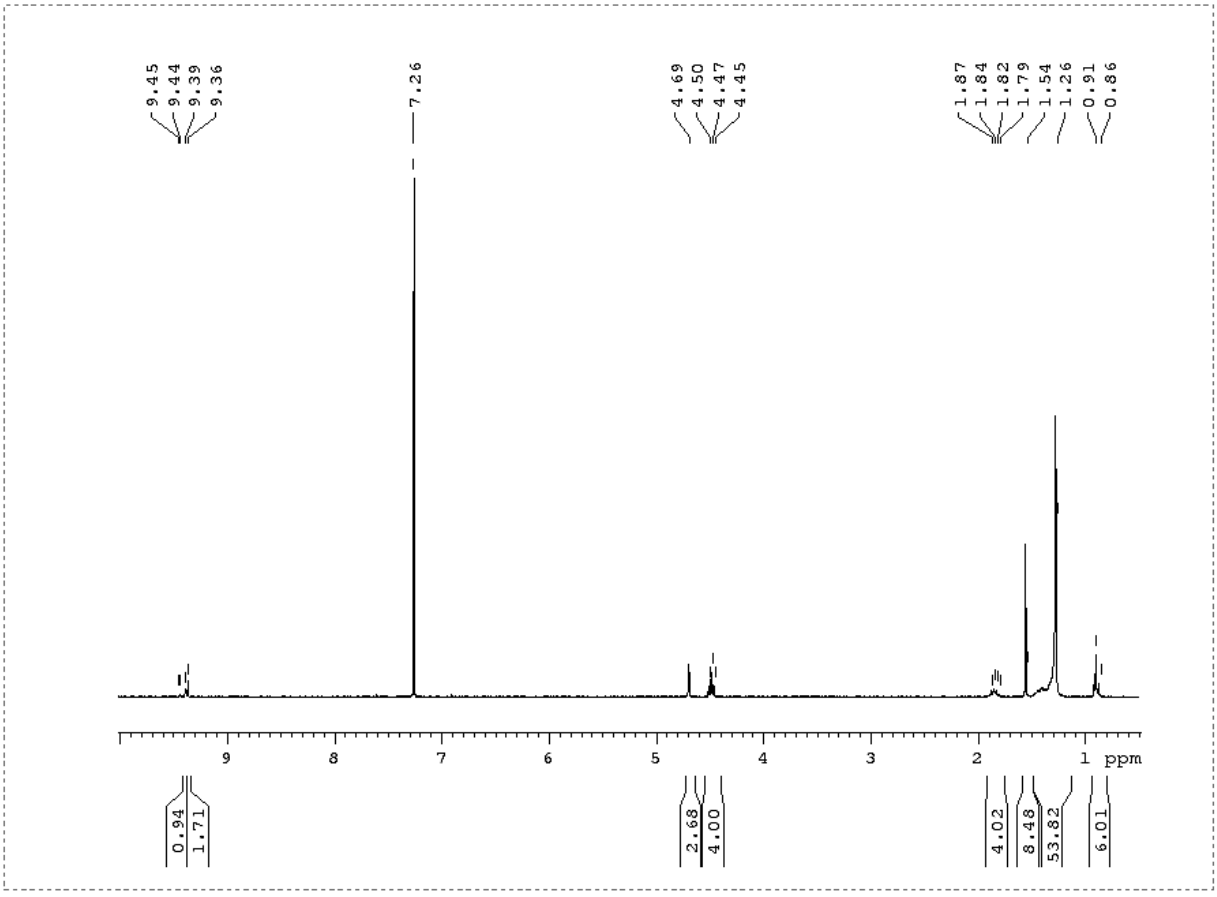

^{13}CNMR for compound ***2-5***

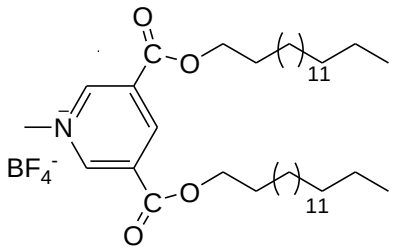

2-5

diC16:0

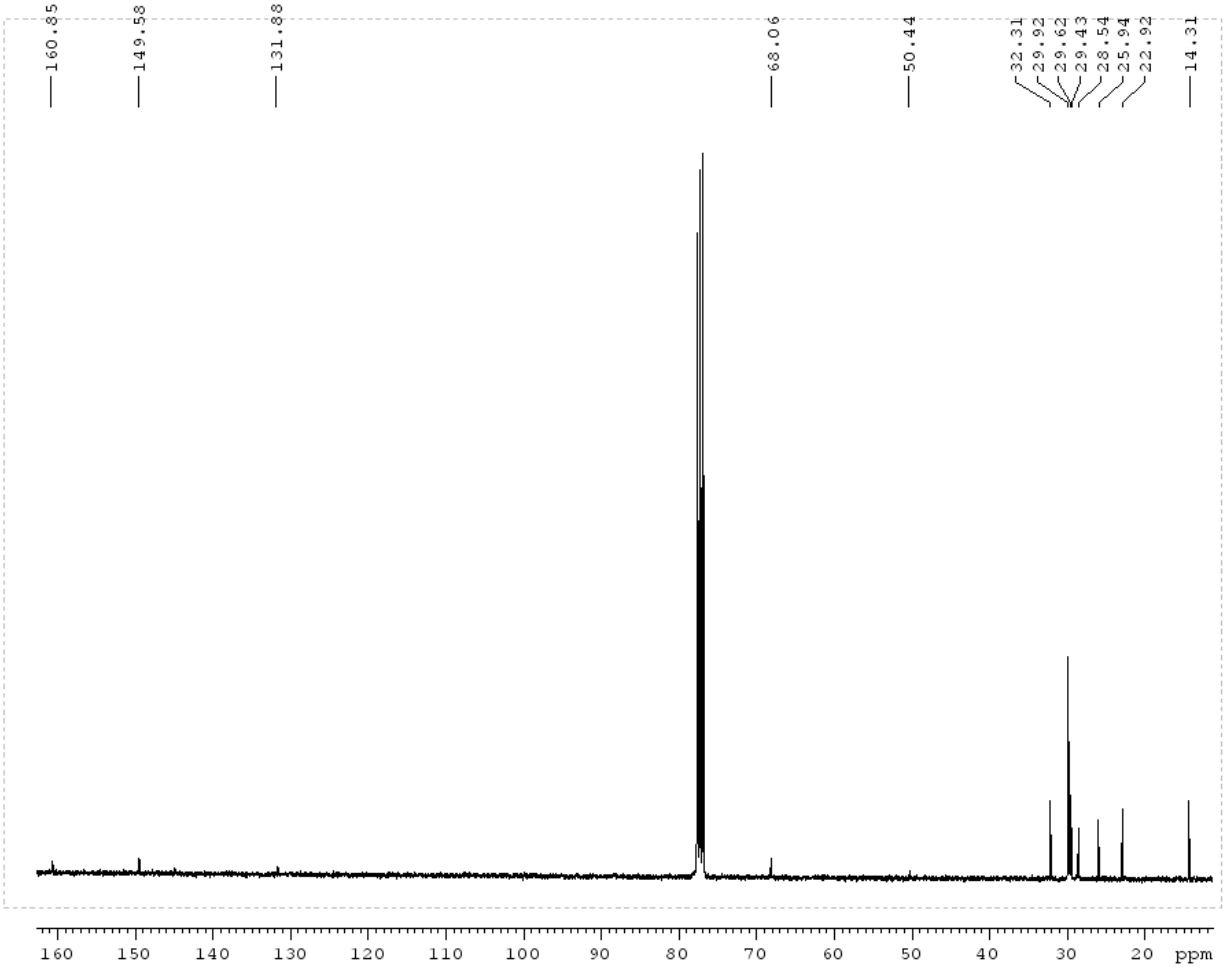

^{1}HNMR for compound ***2-6***/***2-7***

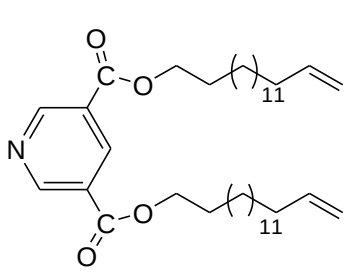

2-6

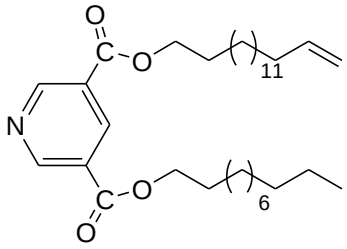

2-7

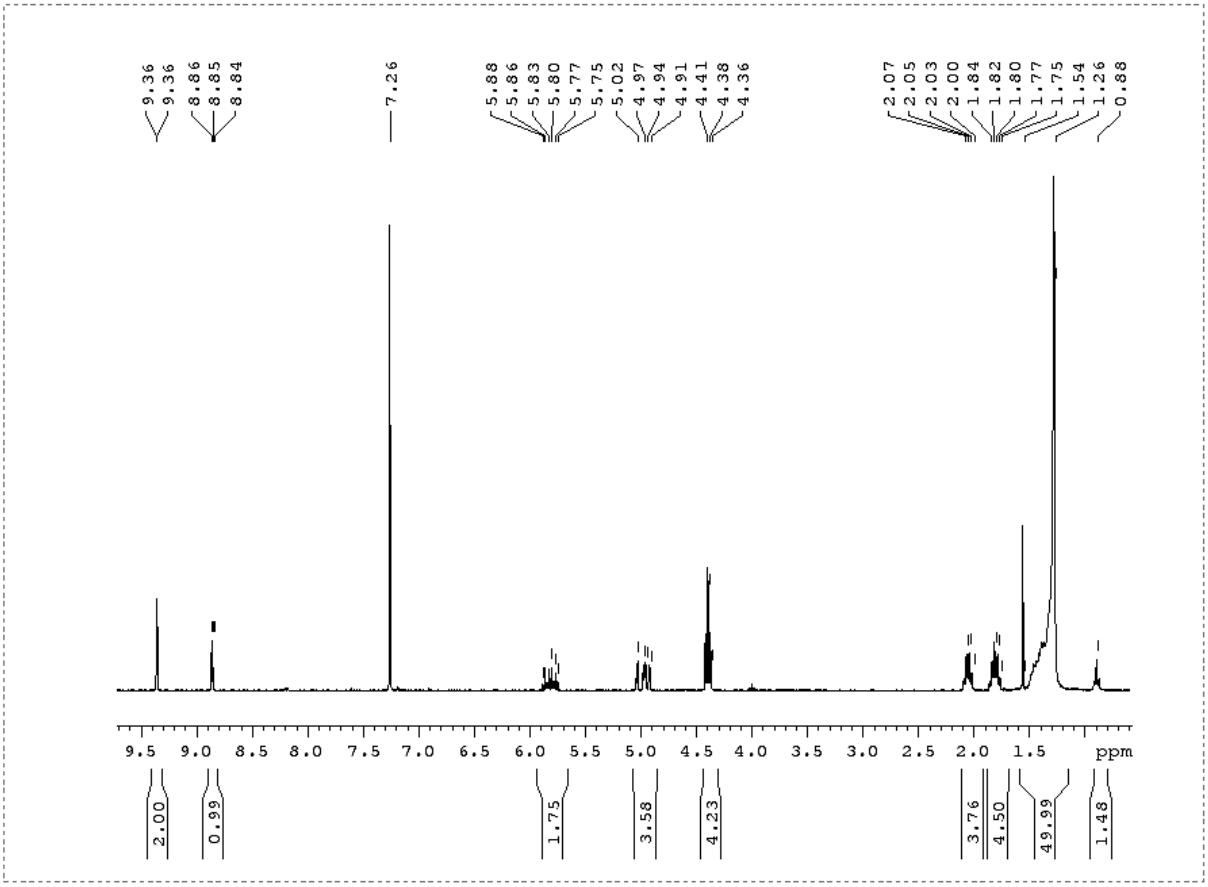

^{13}CNMR for compound ***2-6***/***2-7***

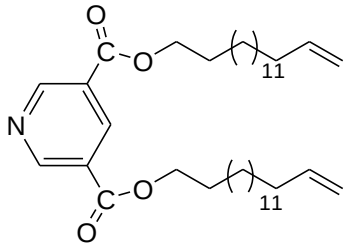

2-6

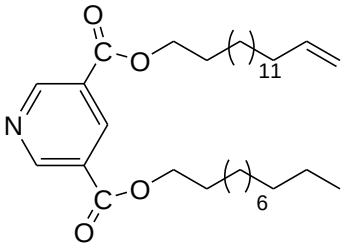

2-7

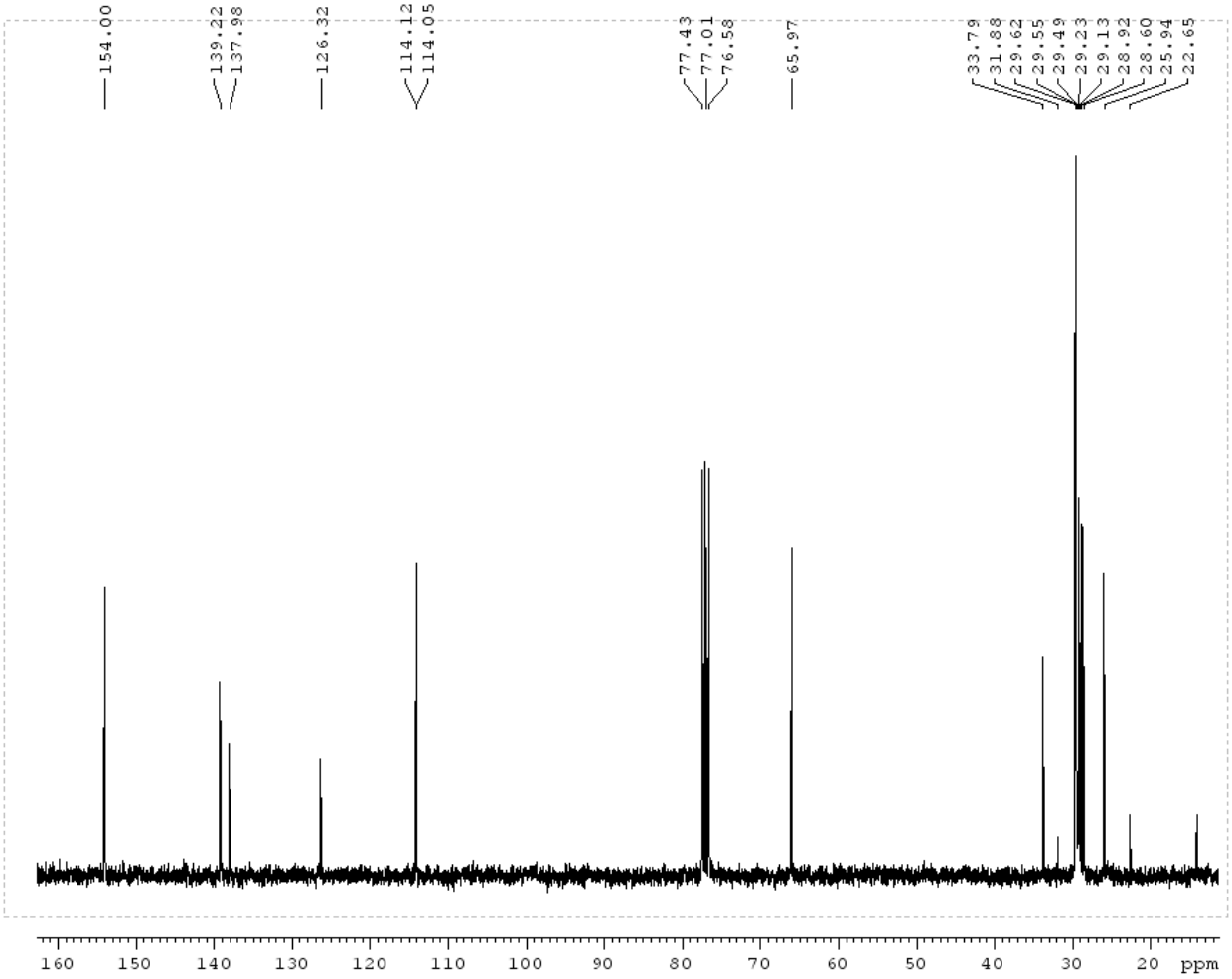

^{1}HNMR for compound ***2-8***/***2-9***

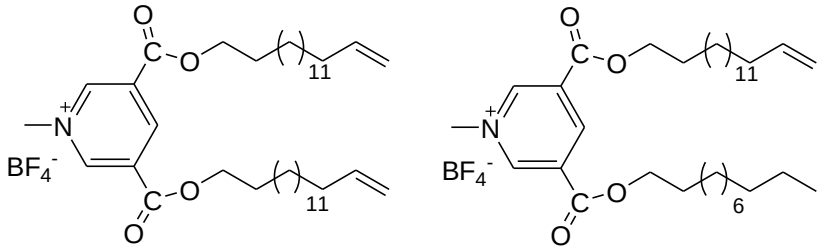

2-8

diC16:1

2-9

(C16:1)(C11:0)

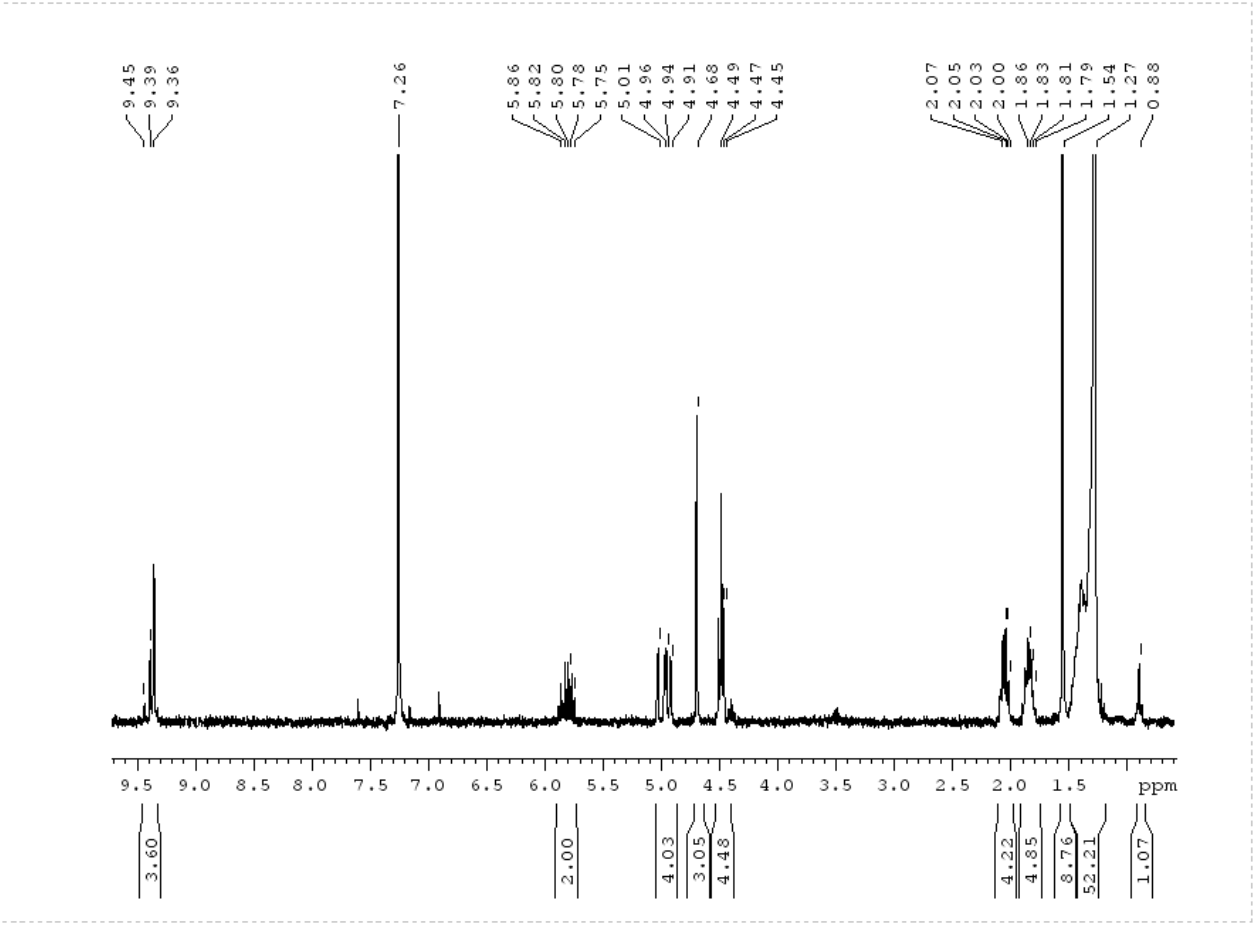

^{13}CNMR for compound ***2-8***/***2-9***

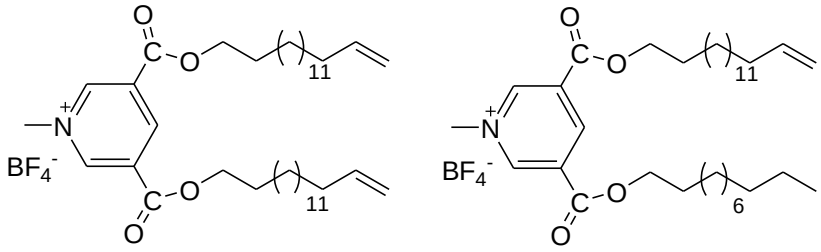

2-8

diC16:1

2-9

(C16:1)(C11:0)

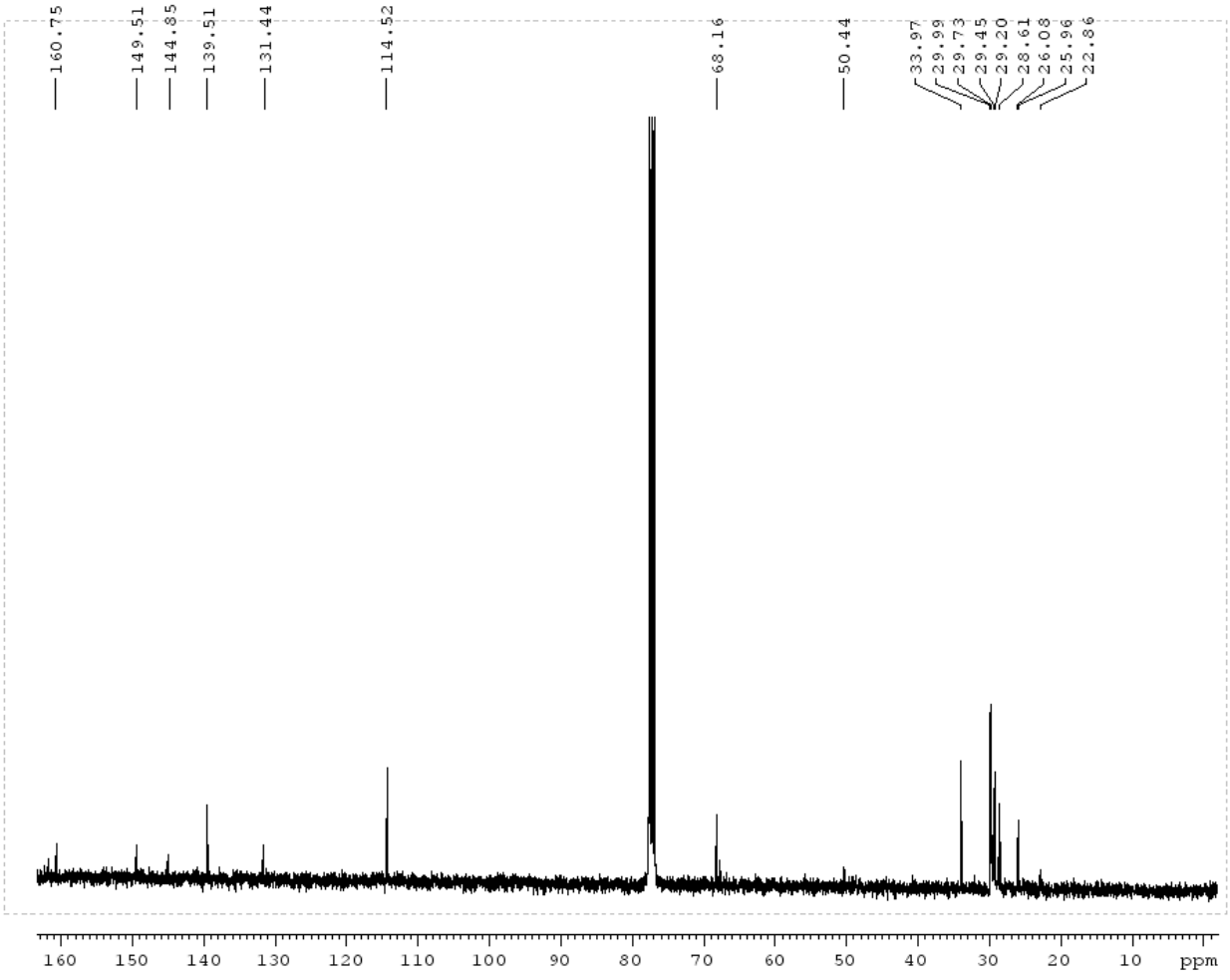

^{1}HNMR for compound ***2-10***

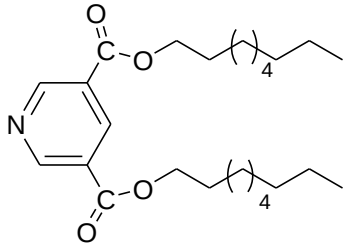

2-10

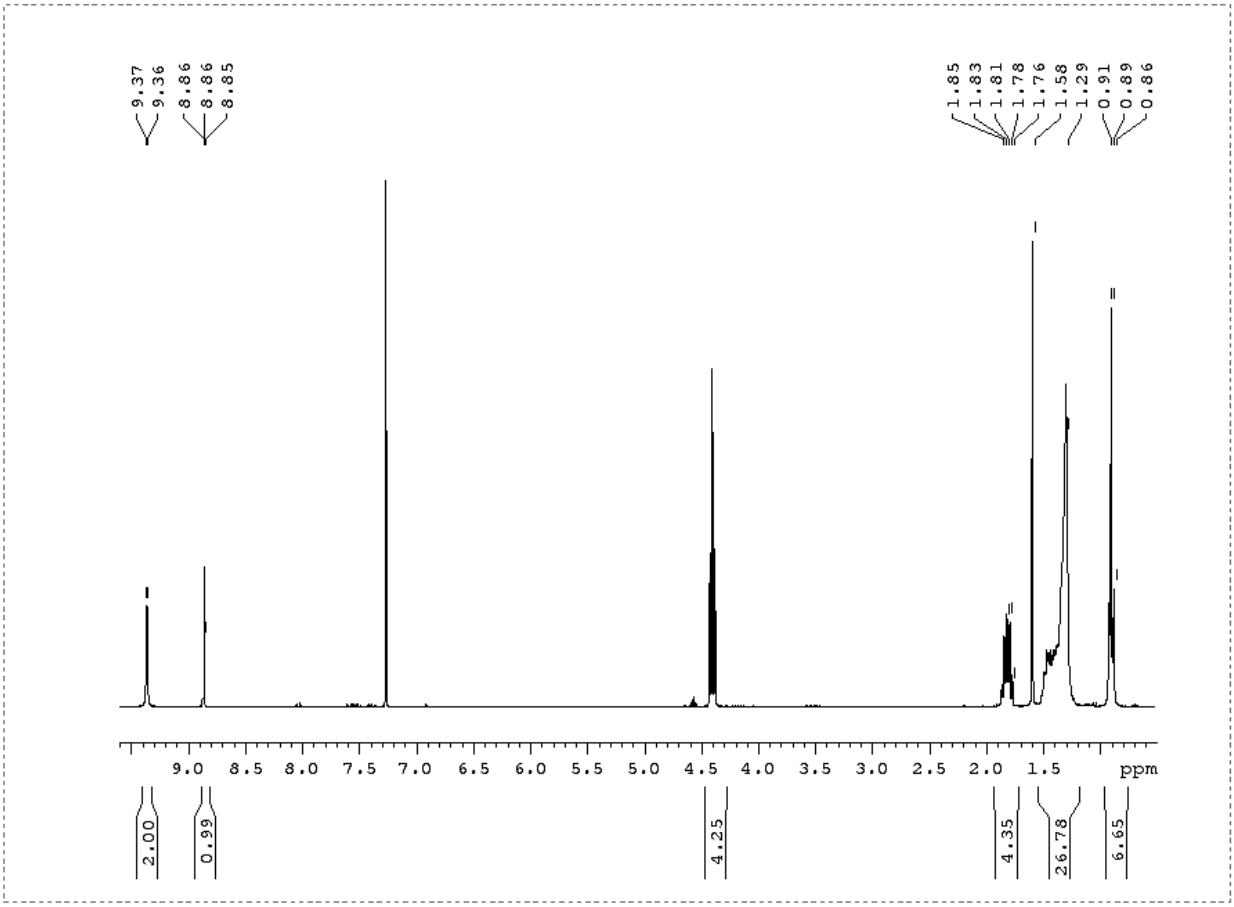

^{13}CNMR for compound ***2-10***

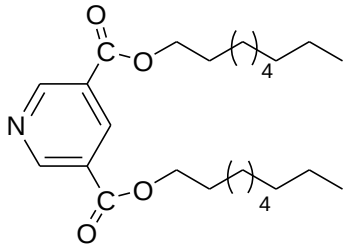

2-10

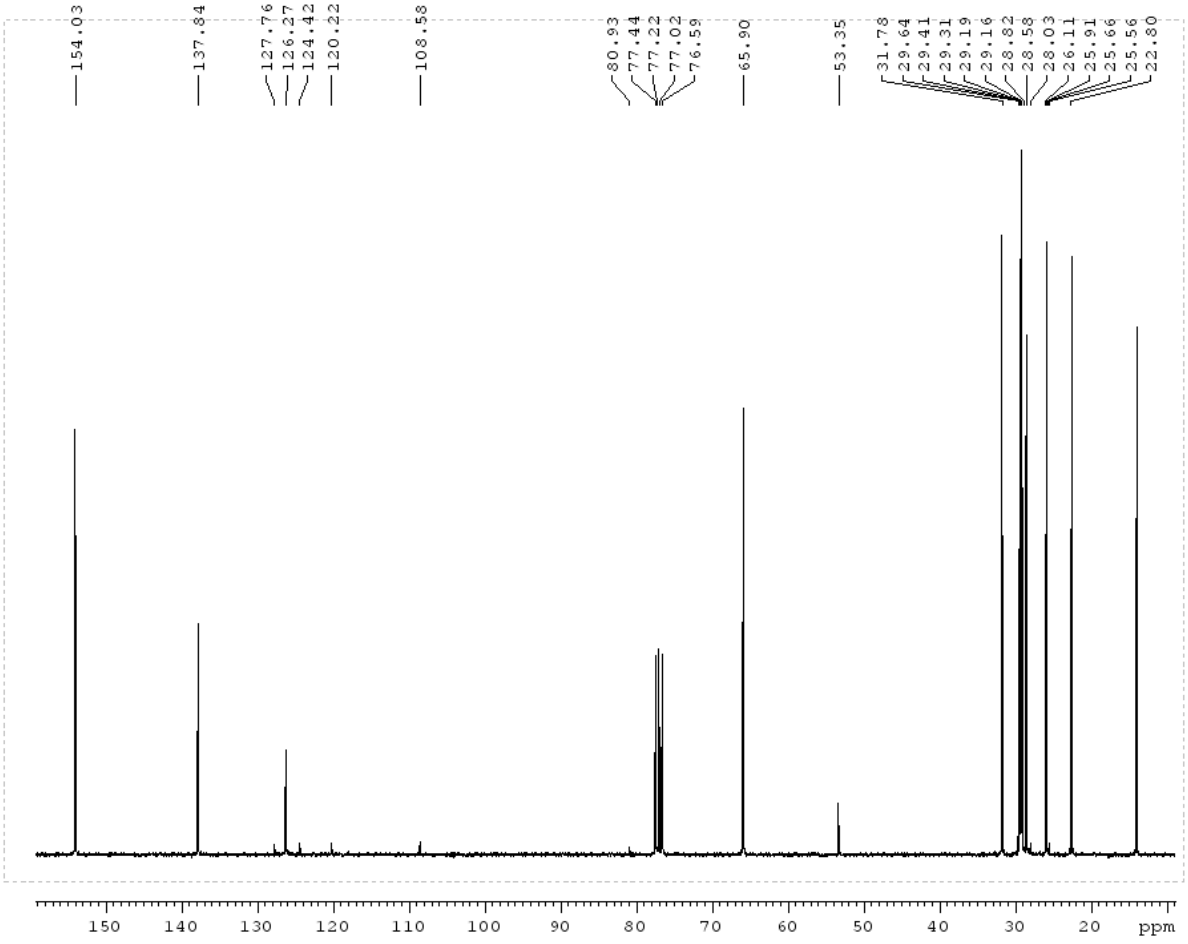

^{1}HNMR for compound ***2-11***

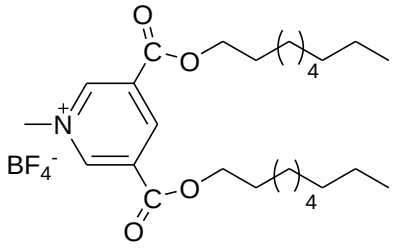

2-11
diC9:0

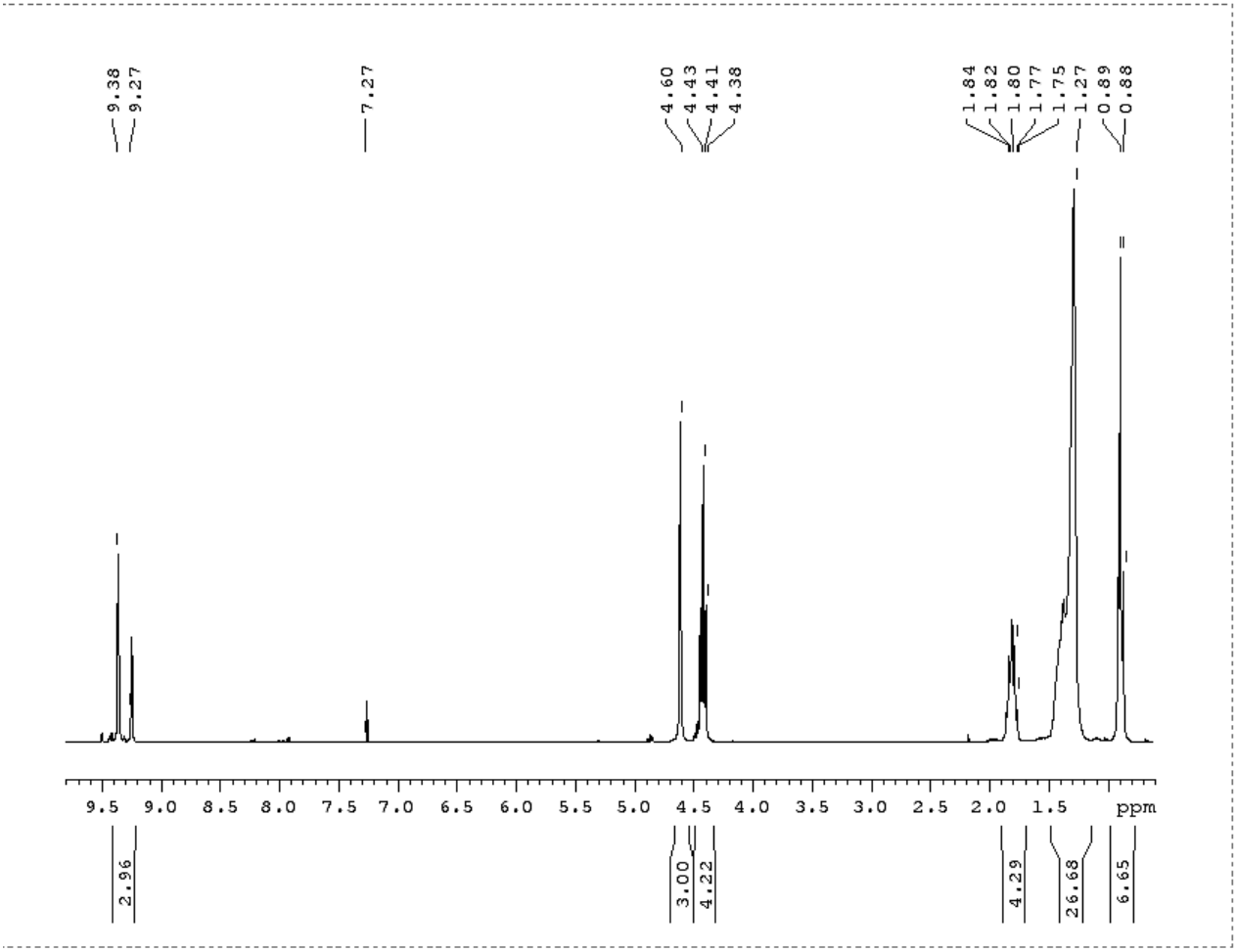

^{13}CNMR for compound ***2-11***

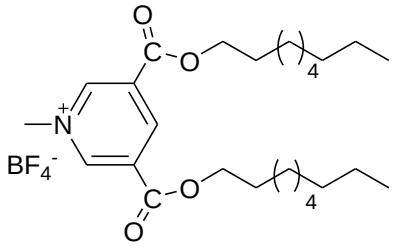

2-11

diC9:0

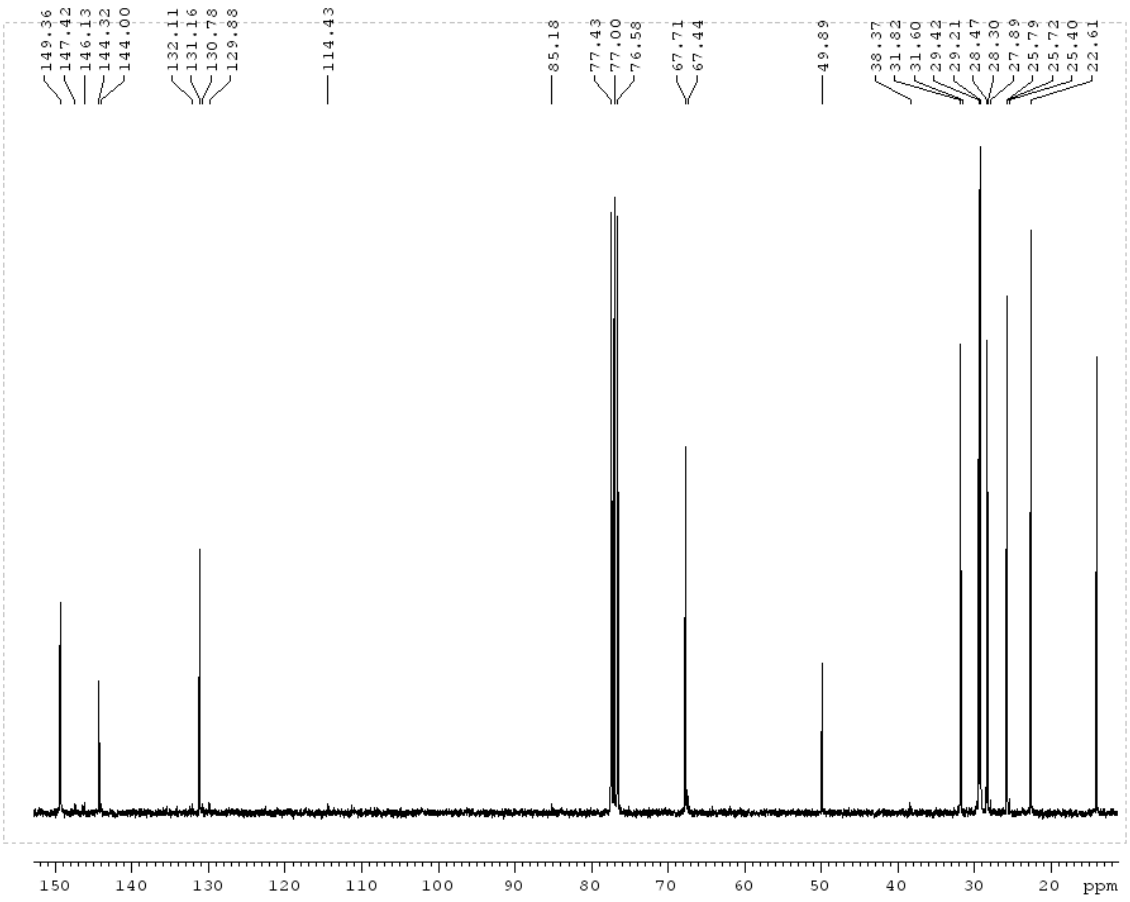

^{1}HNMR for compound ***2-12***

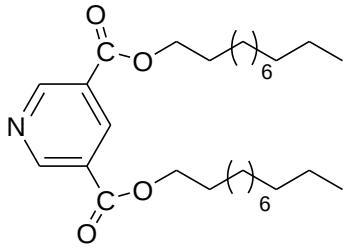

2-12

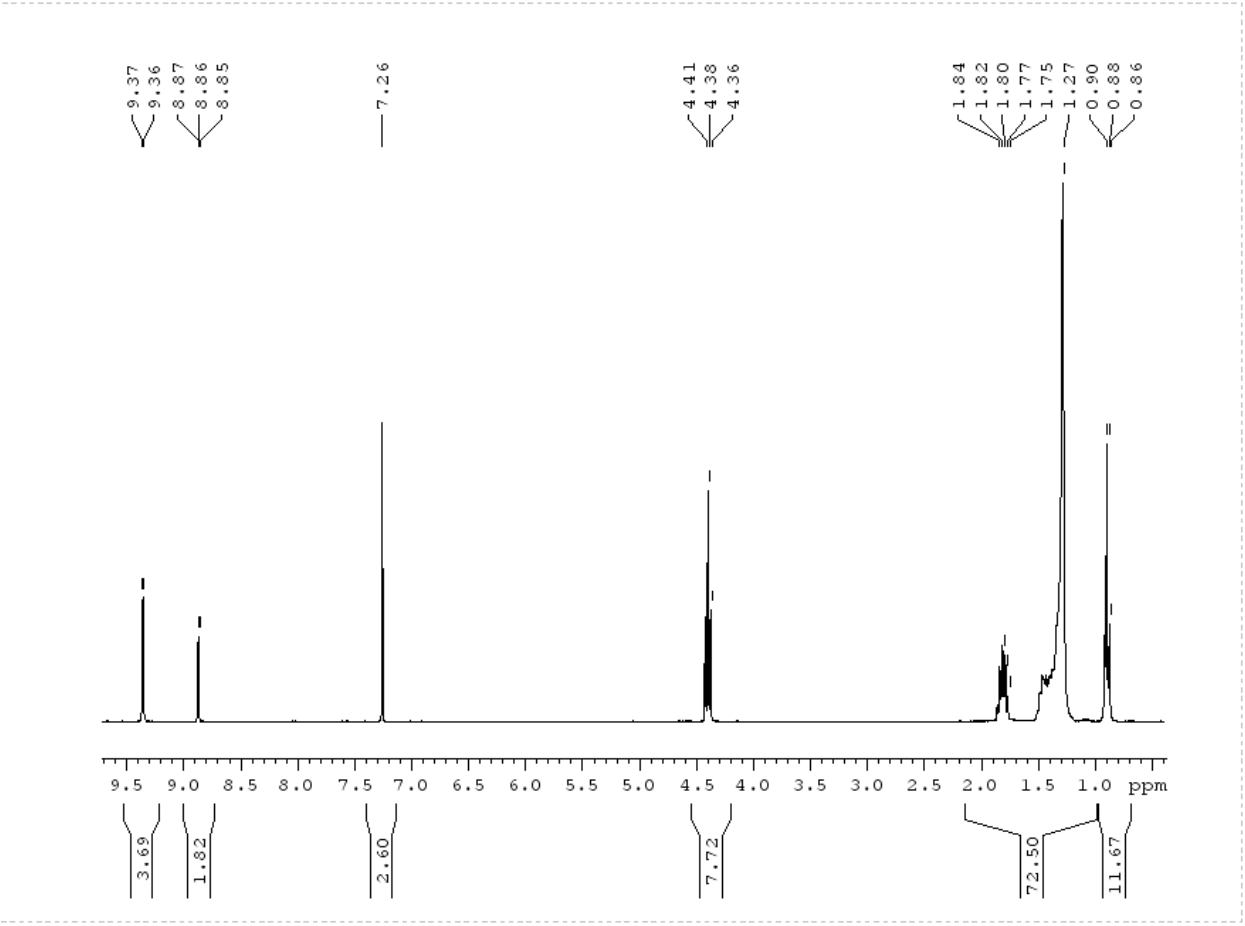

^{13}CNMR for compound ***2-12***

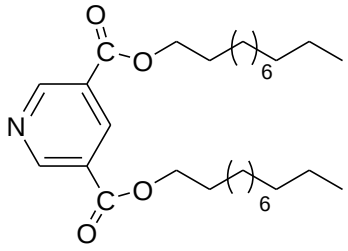

2-12

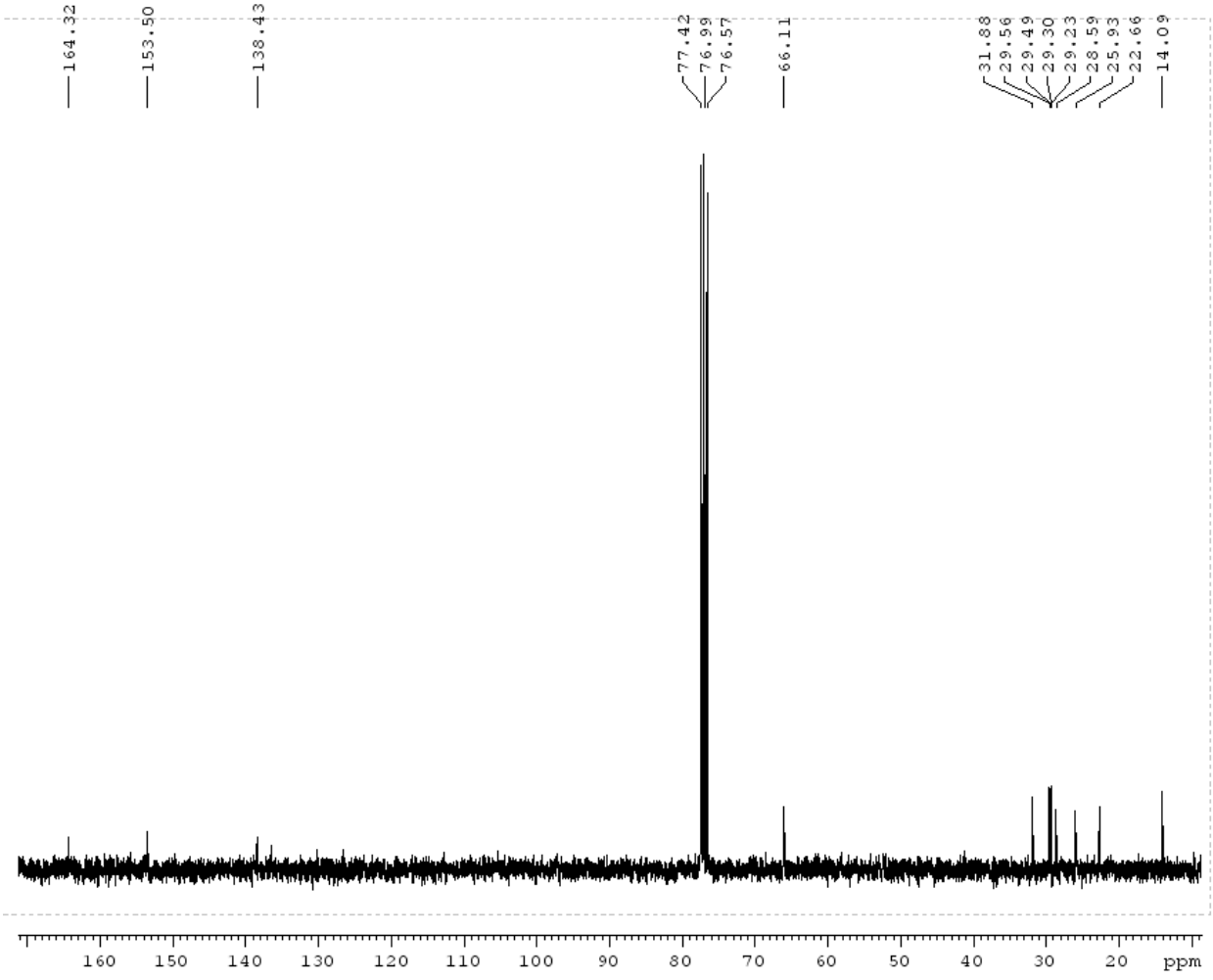

^{1}HNMR for compound ***2-13***

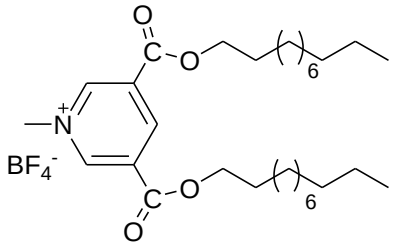

2-13

diC11:0

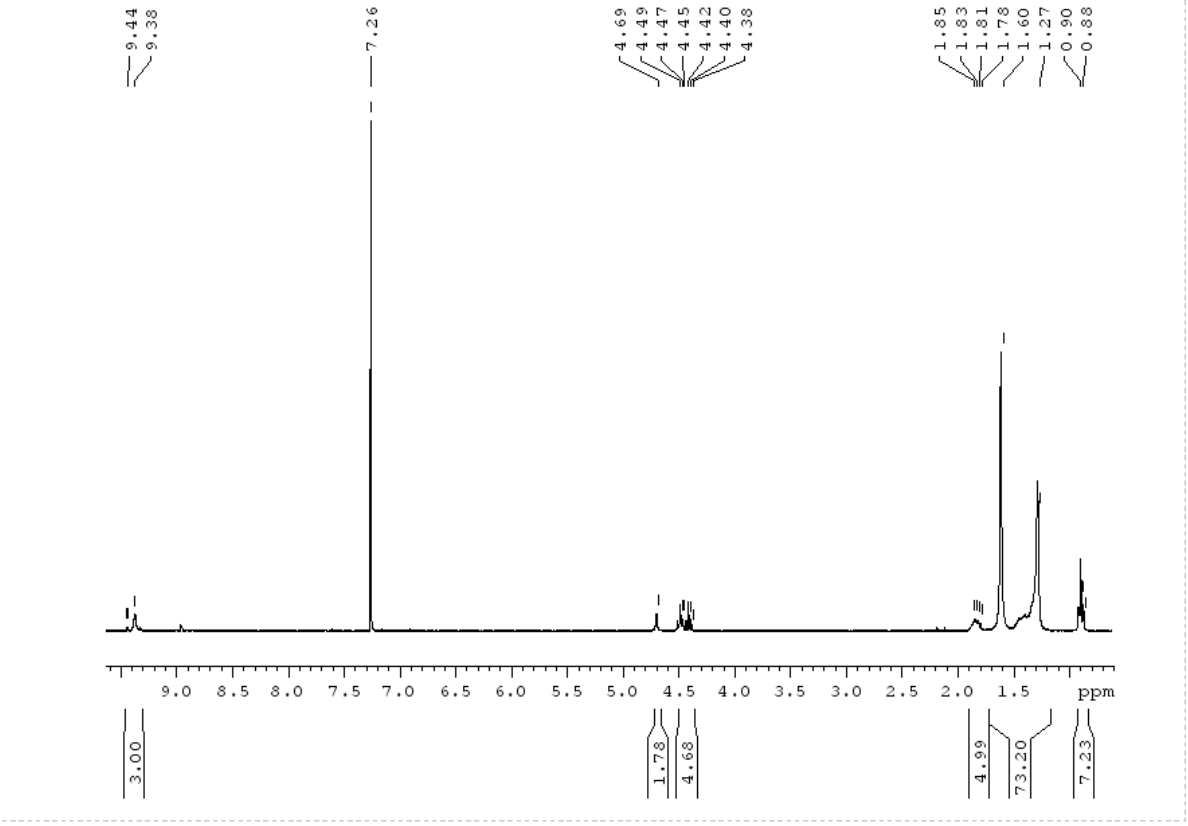

^{13}CNMR for compound ***2-13***

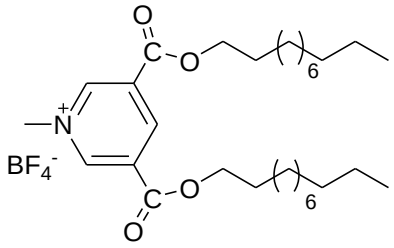

2-13

diC11:0

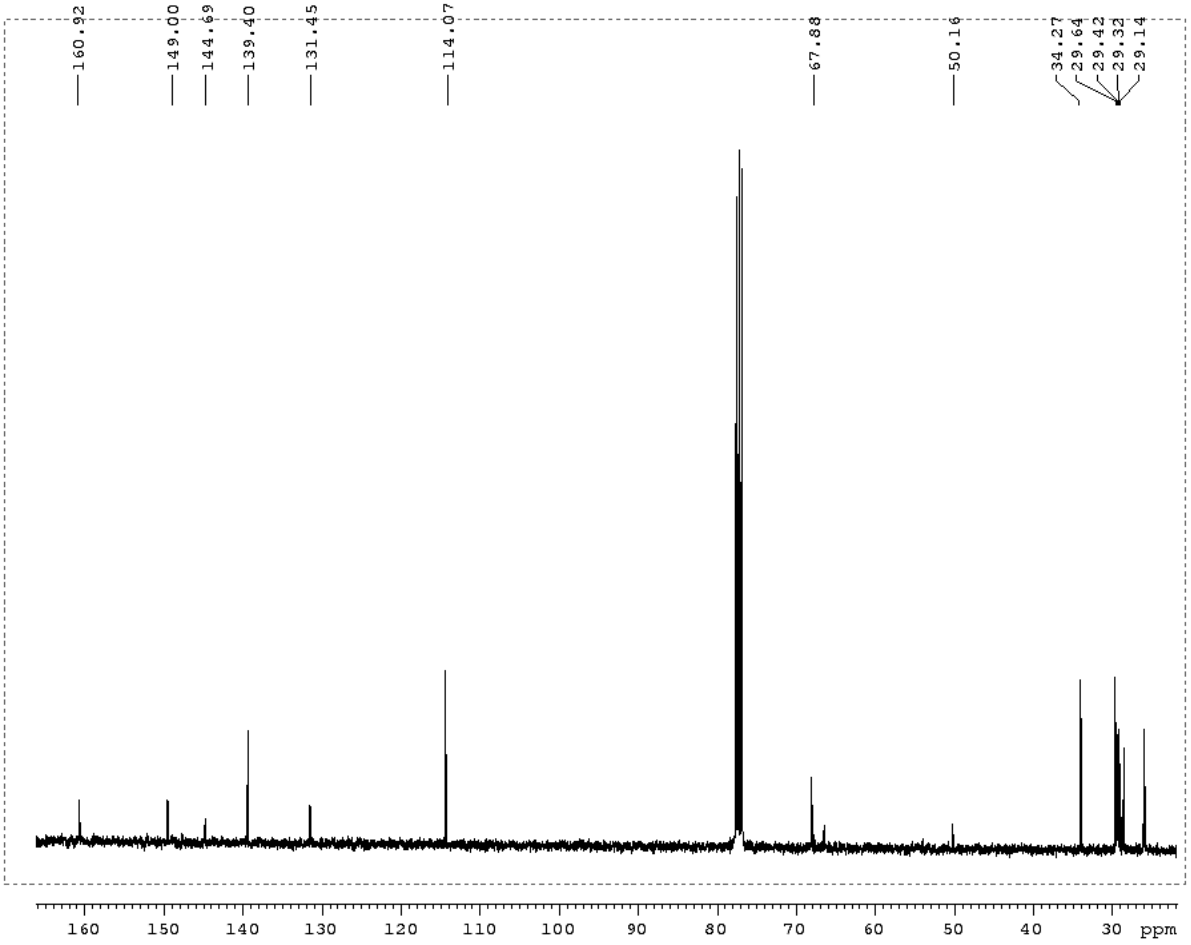

^{1}HNMR for compound ***2-14***

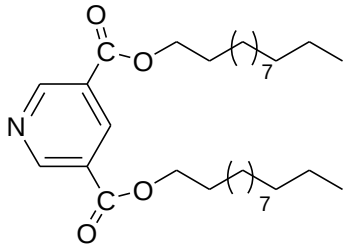

2-14

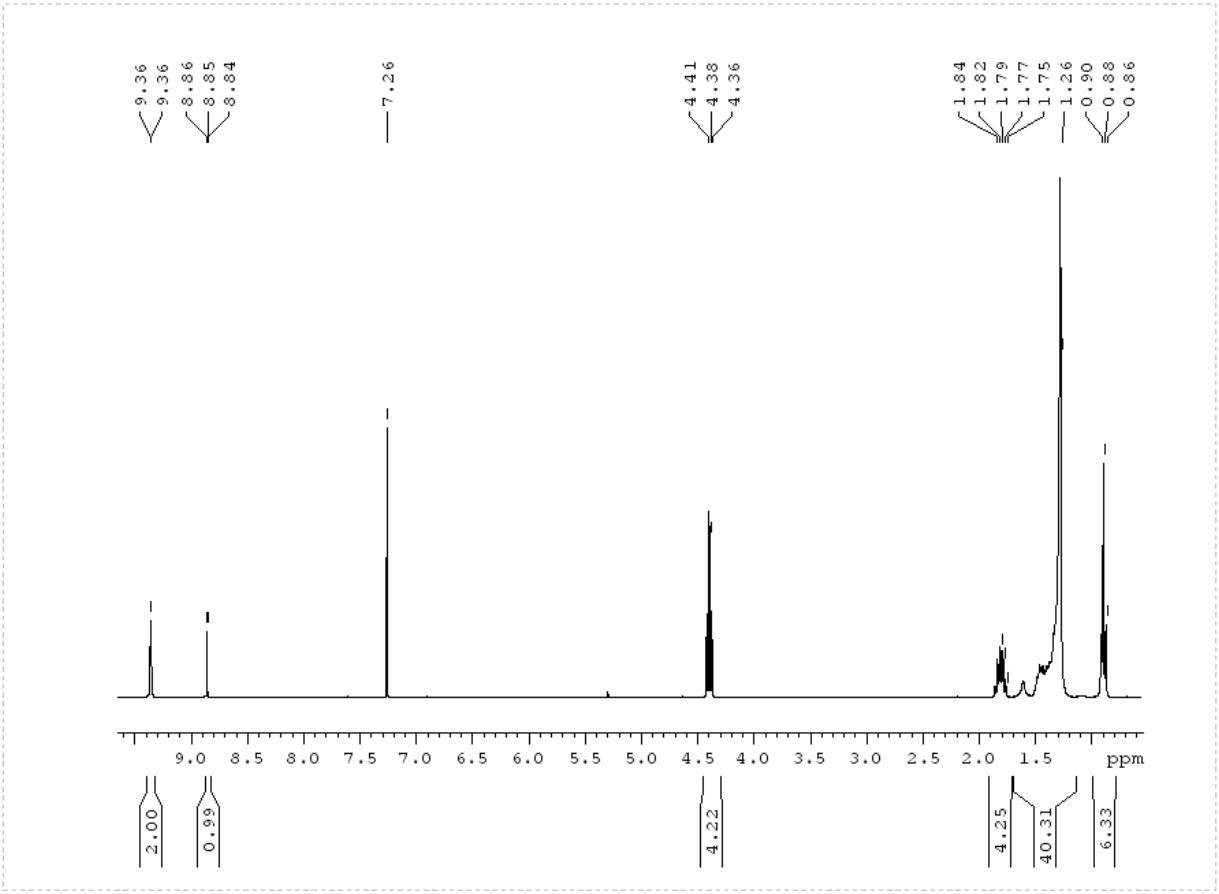

^{13}CNMR for compound ***2-14***

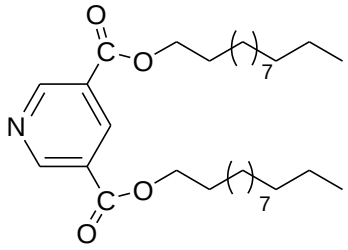

2-14

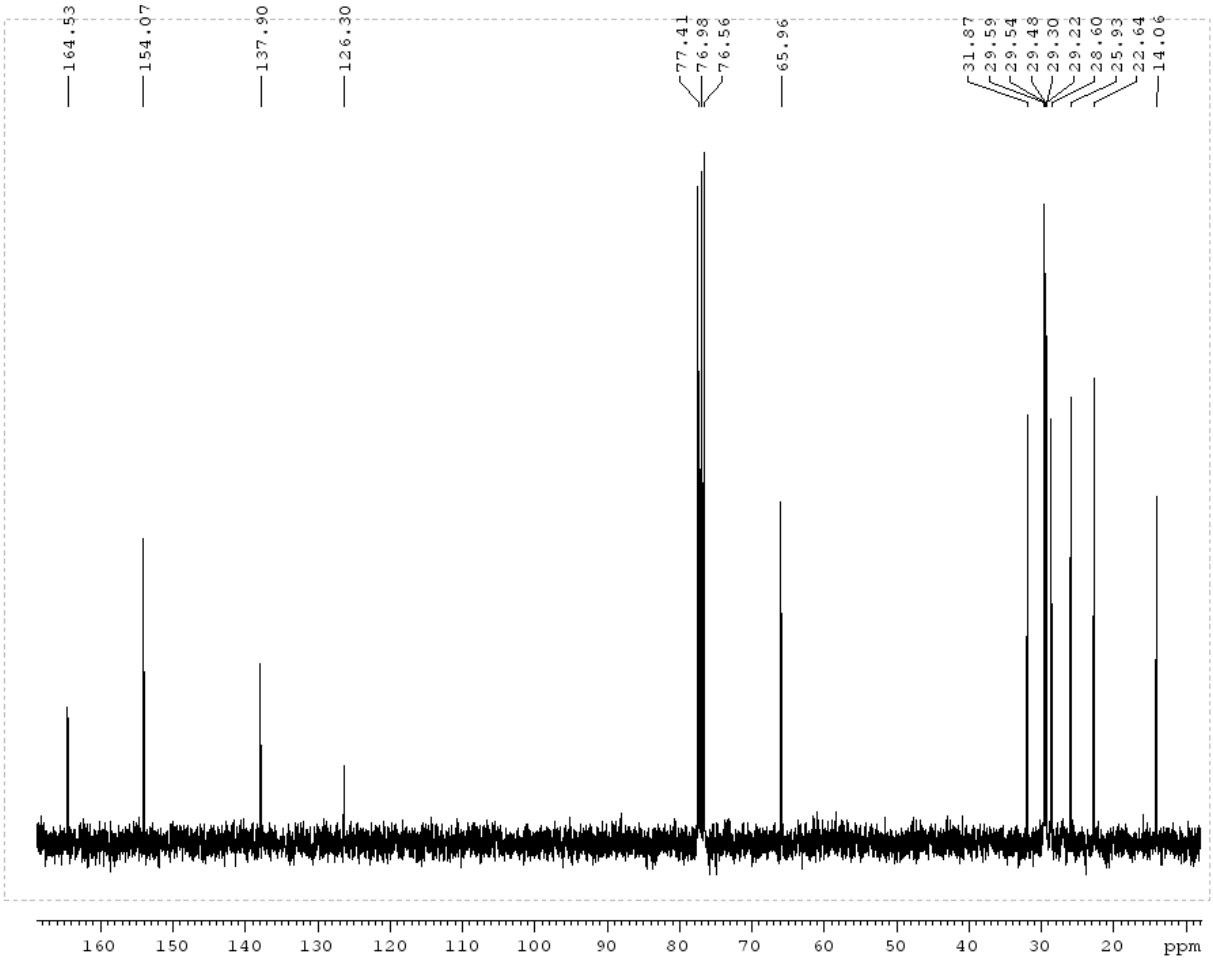

^{1}HNMR for compound ***2-15***

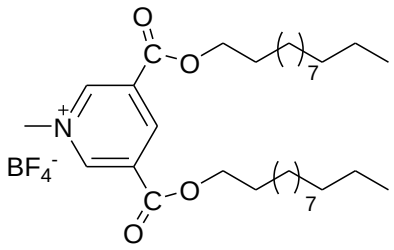

2-15

diC12:0

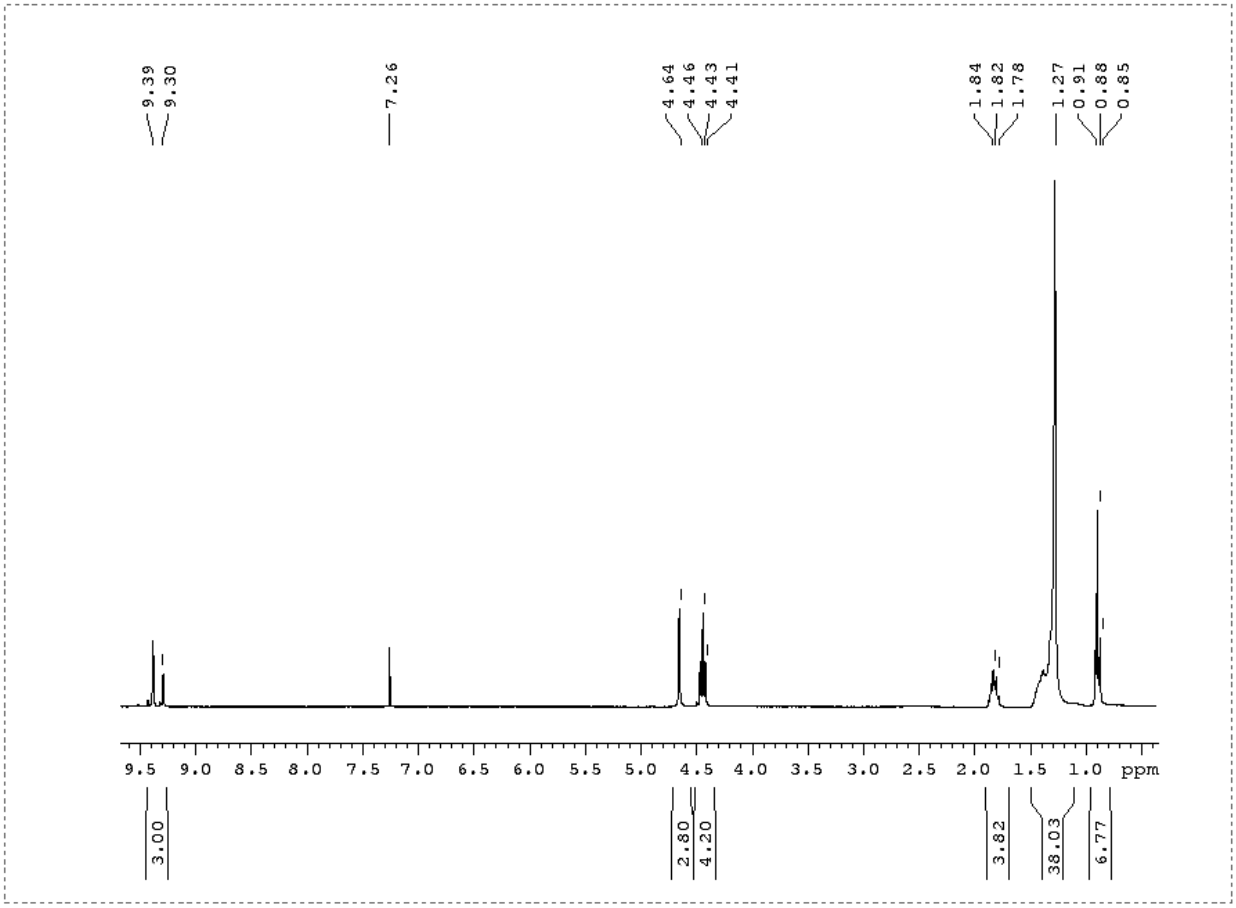

^{13}CNMR for compound ***2-15***

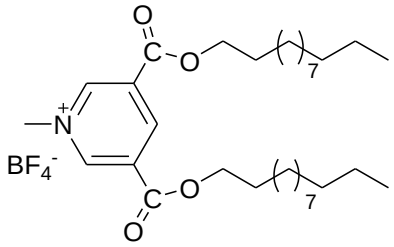

2-15

diC12:0

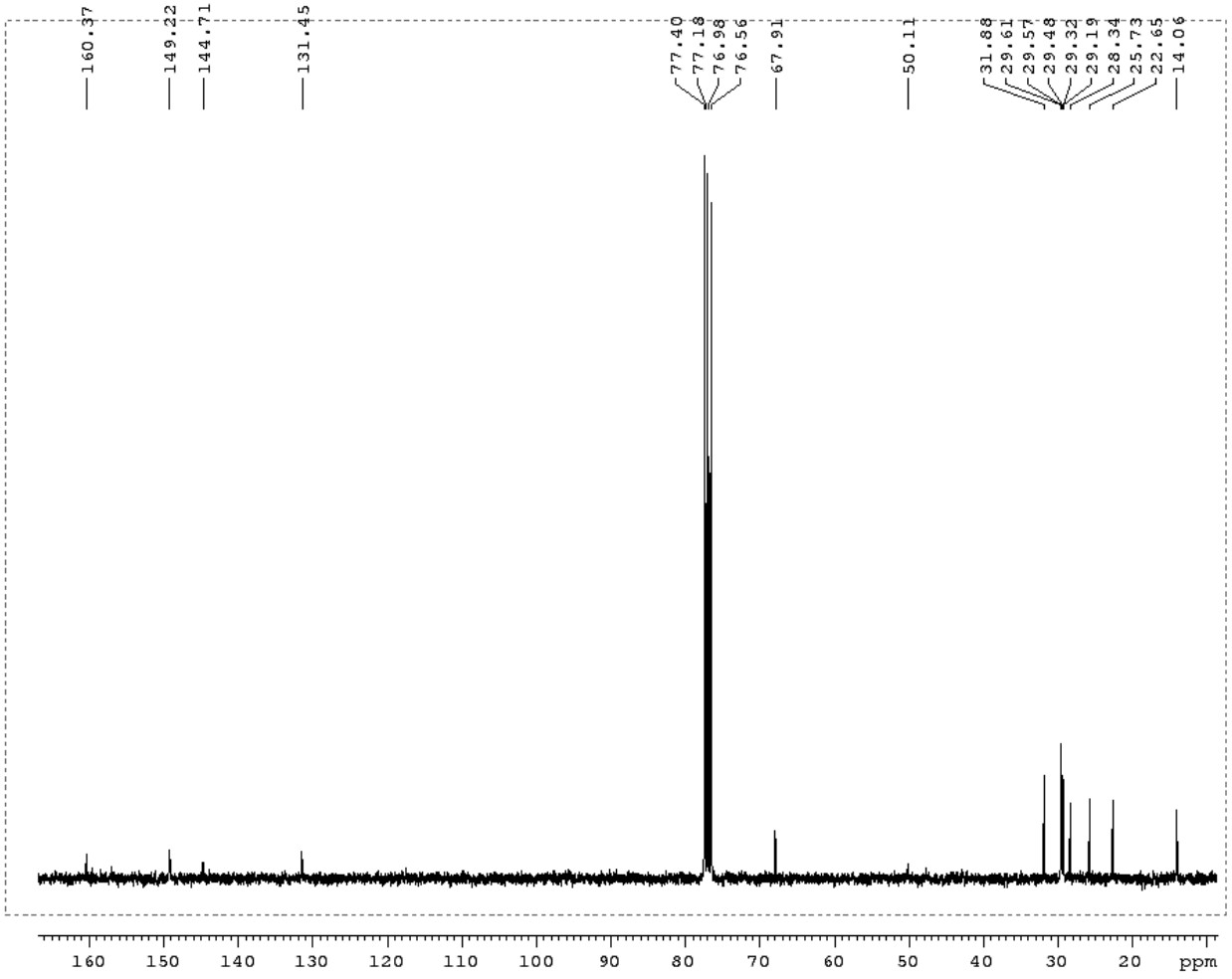

^{1}HNMR for compound ***2-16***

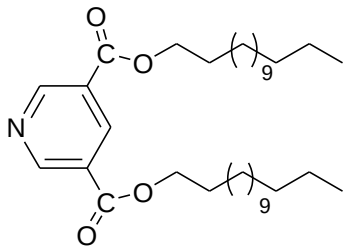

2-16

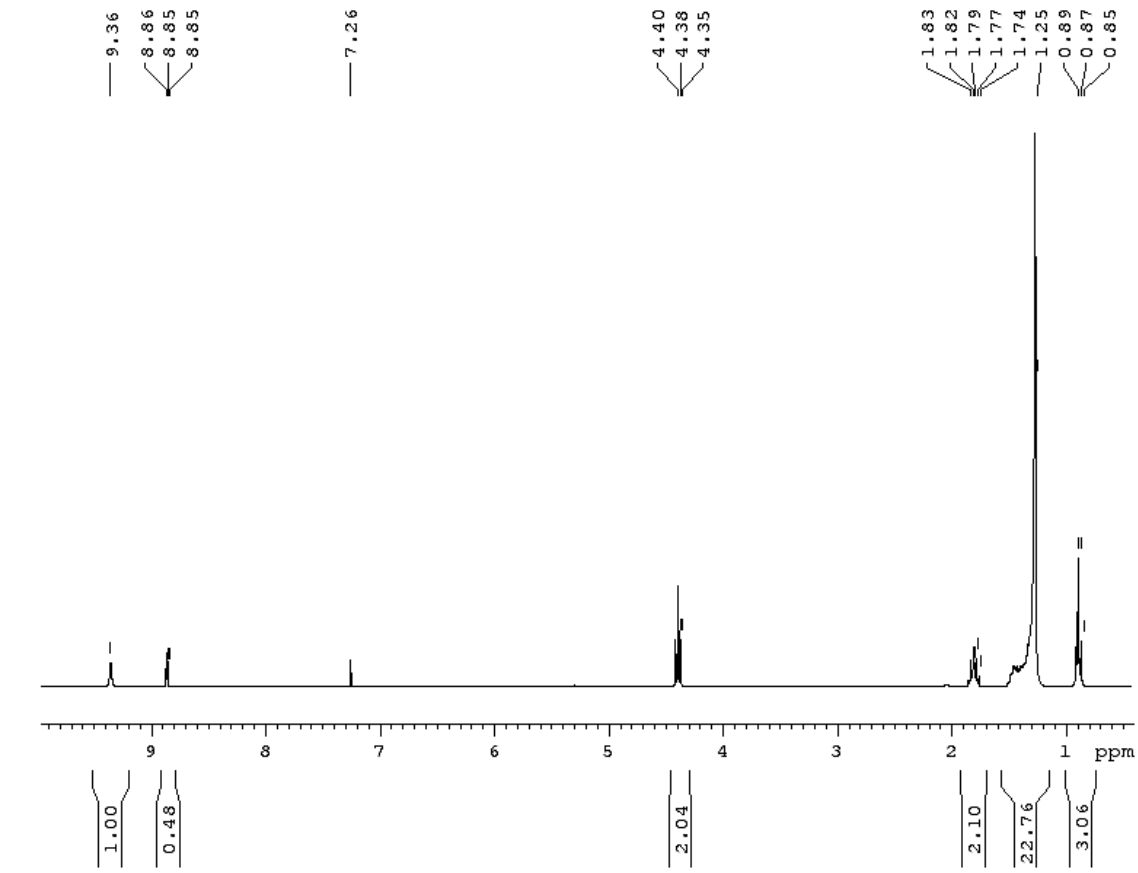

^{13}CNMR for compound ***2-16***

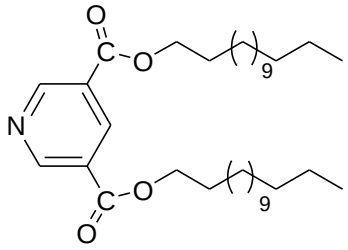

2-16

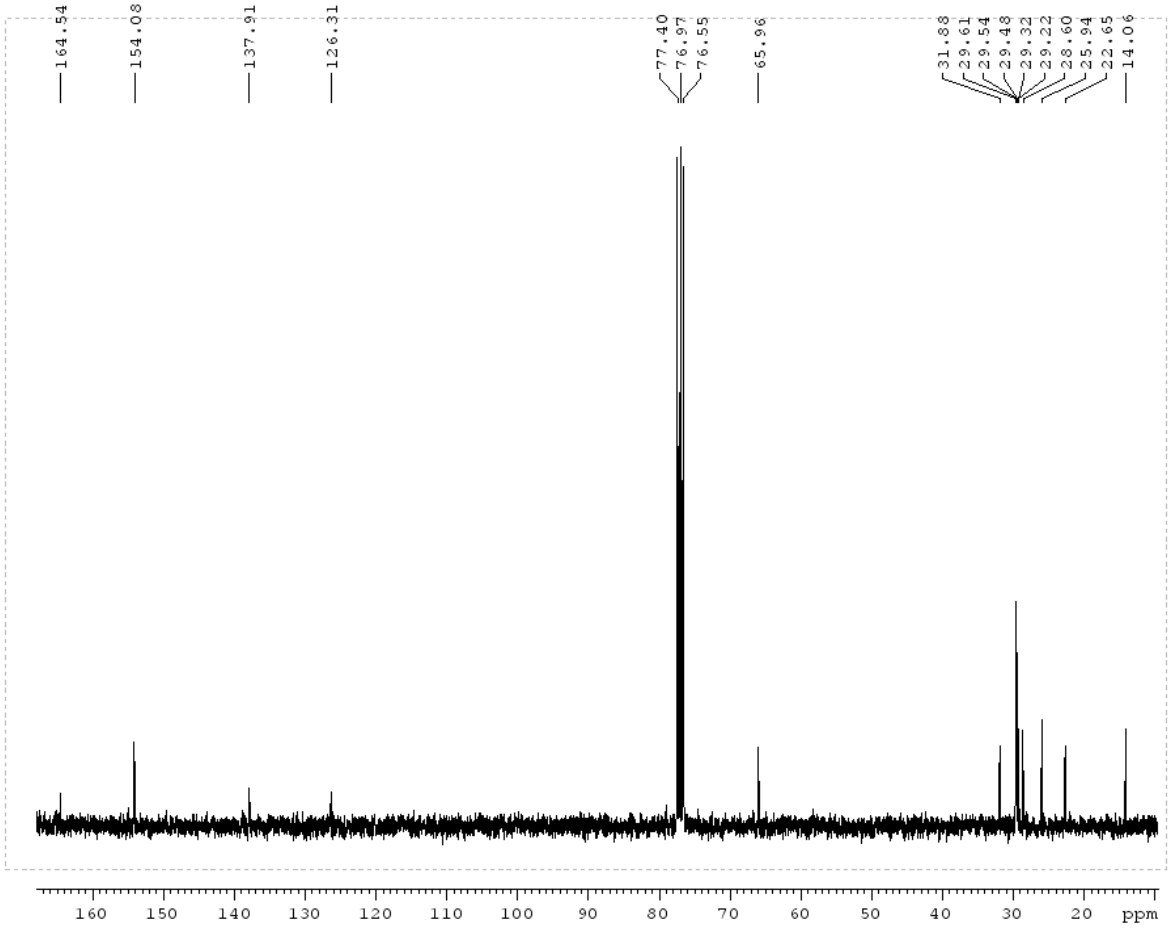

^{1}HNMR for compound ***2-17***

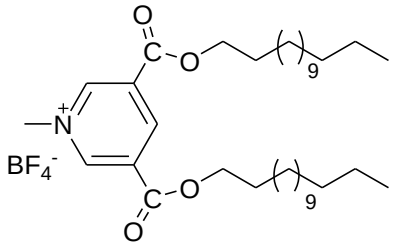

2-17

diC14:0

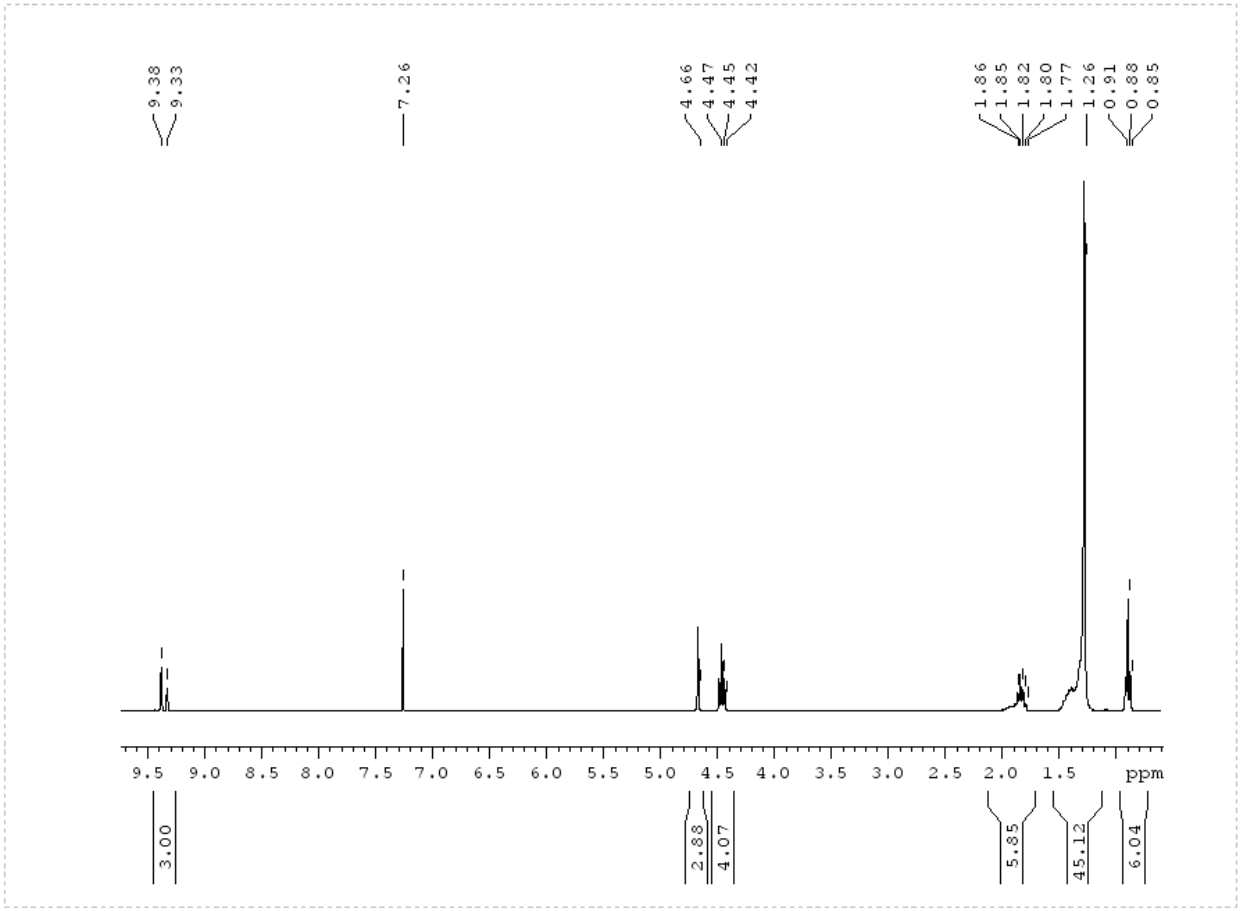

^{13}CNMR for compound ***2-17***

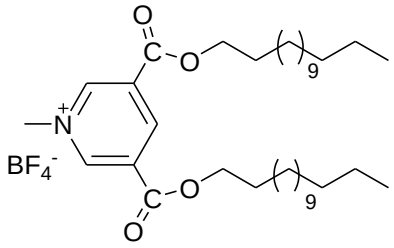

2-17

diC14:0

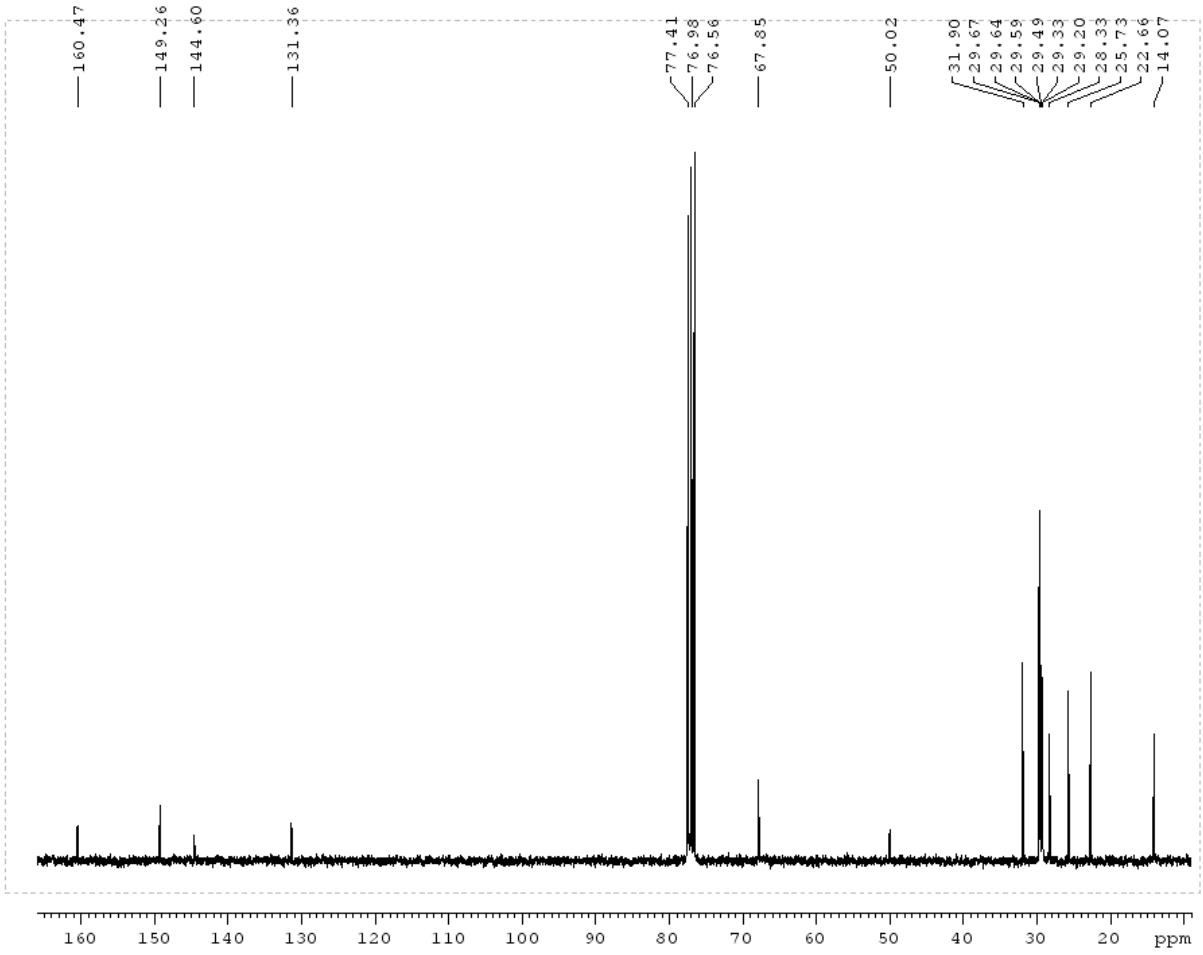

^{1}HNMR for compound ***2-18***

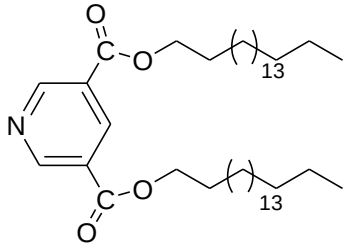

2-18

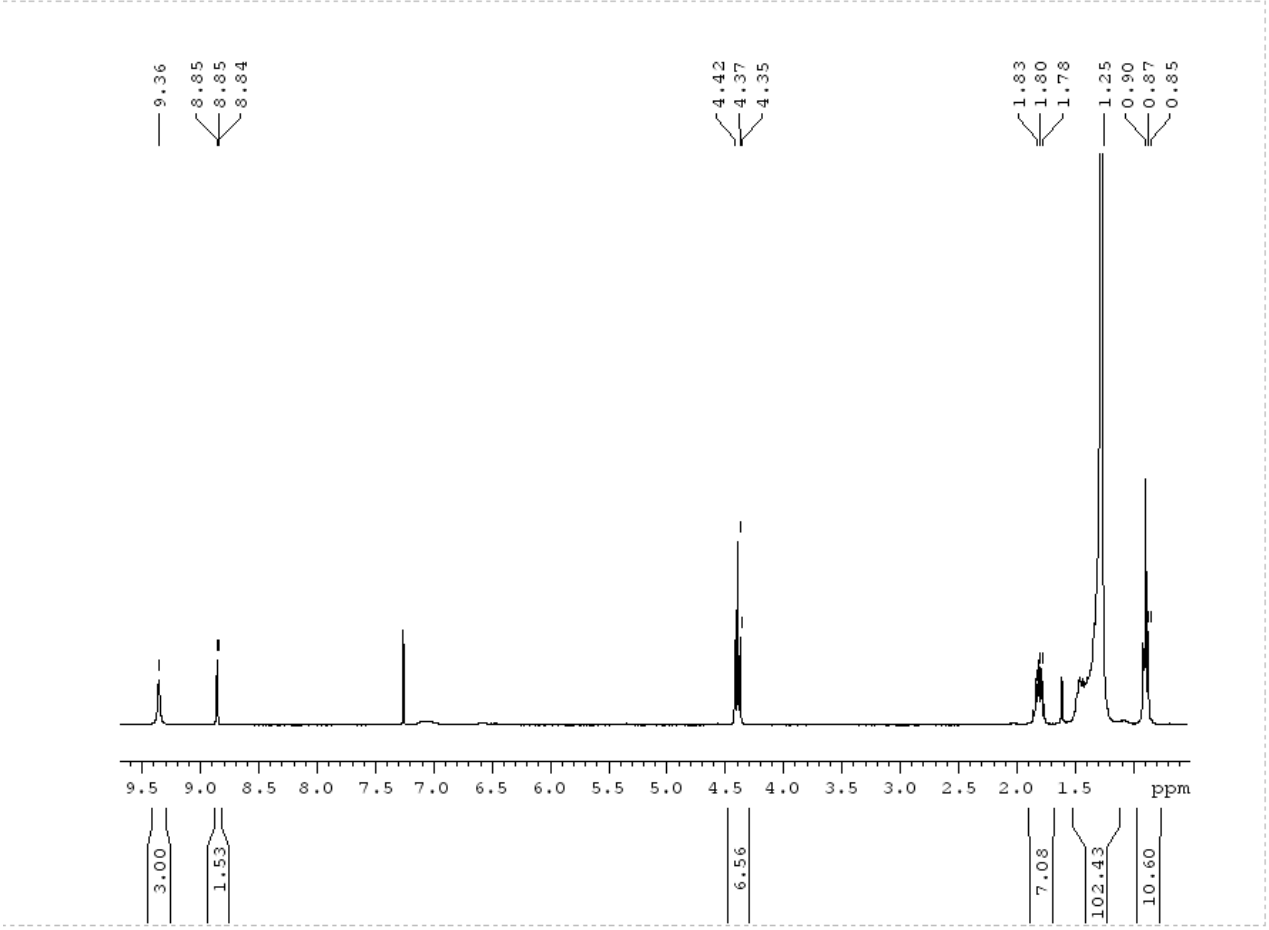

^{13}CNMR for compound ***2-18***

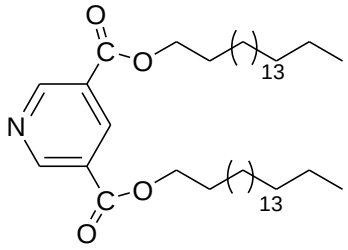

2-18

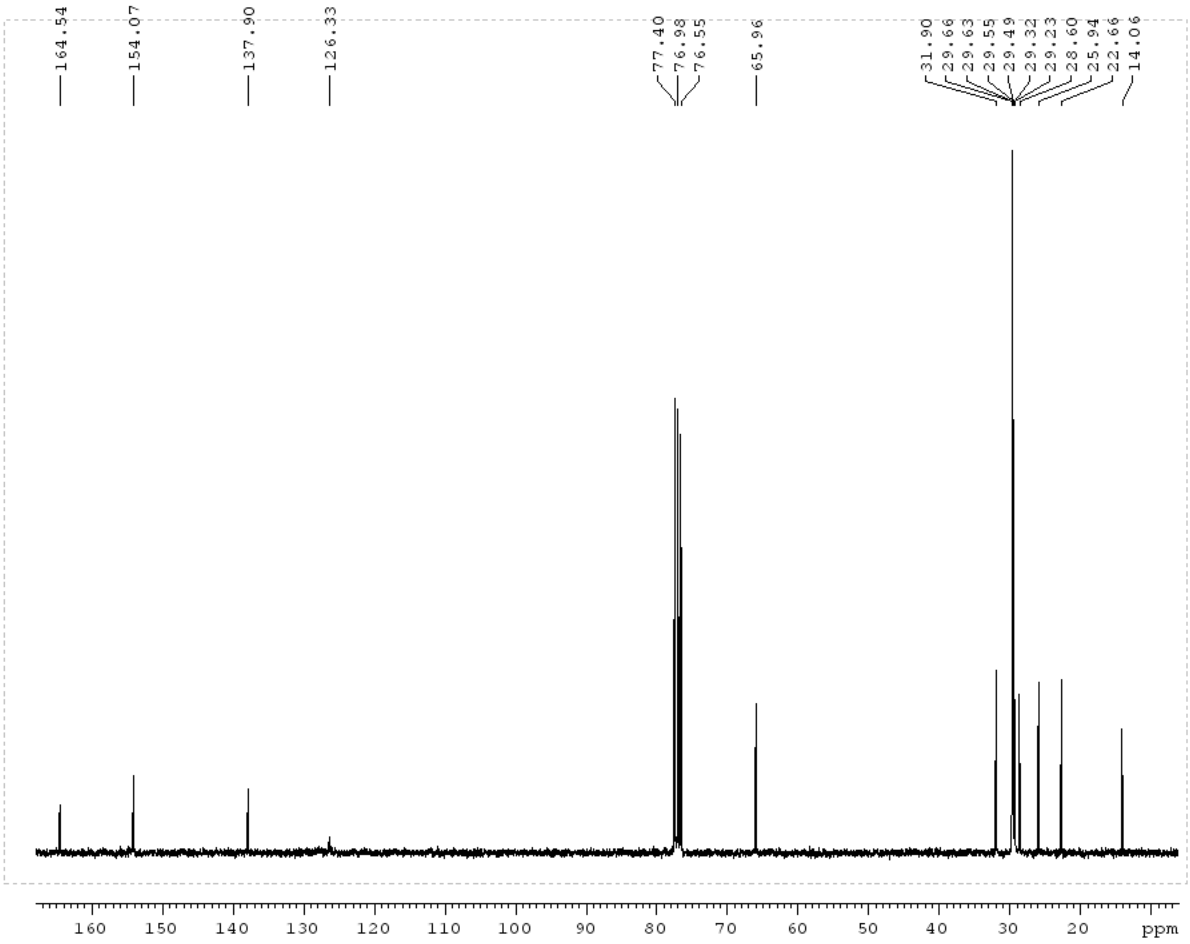

^{1}HNMR for compound ***2-19***

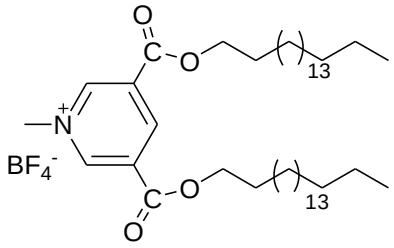

2-19

diC18:0

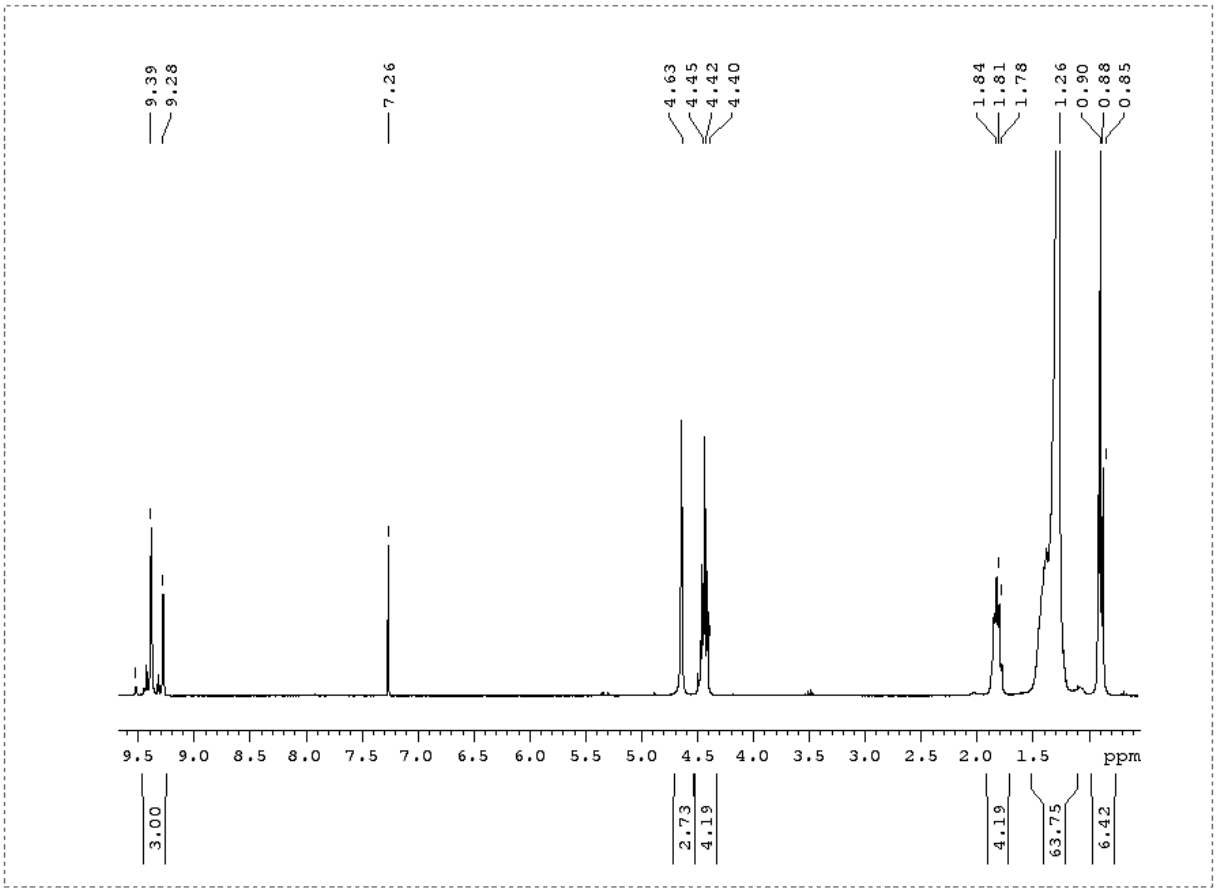

^{13}CNMR for compound ***2-19***

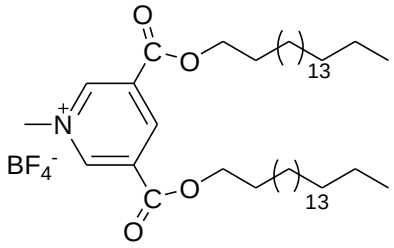

2-19

diC18:0

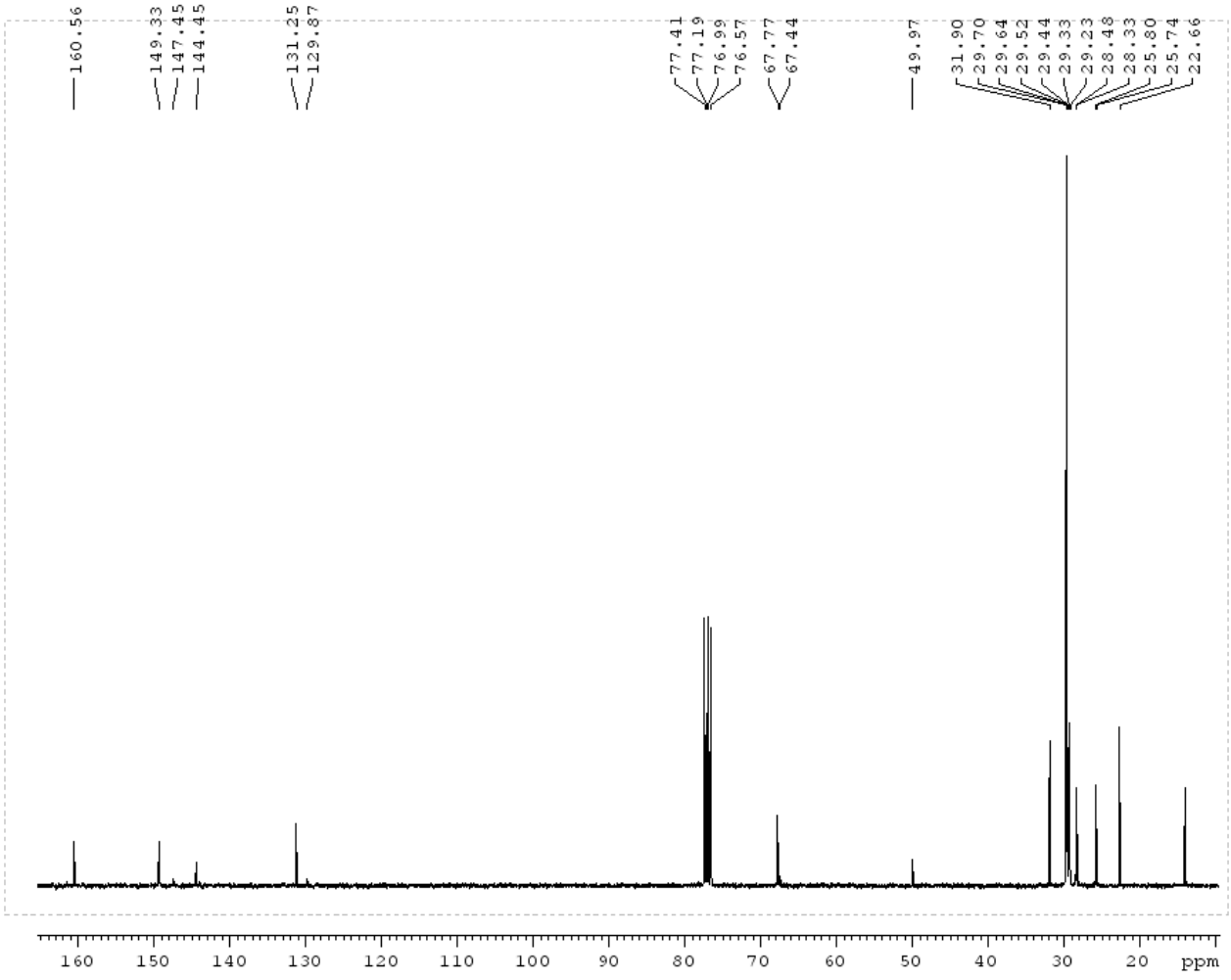

^{1}HNMR for compound ***2-20***

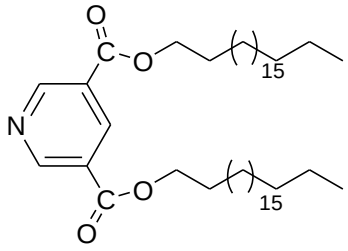

2-20

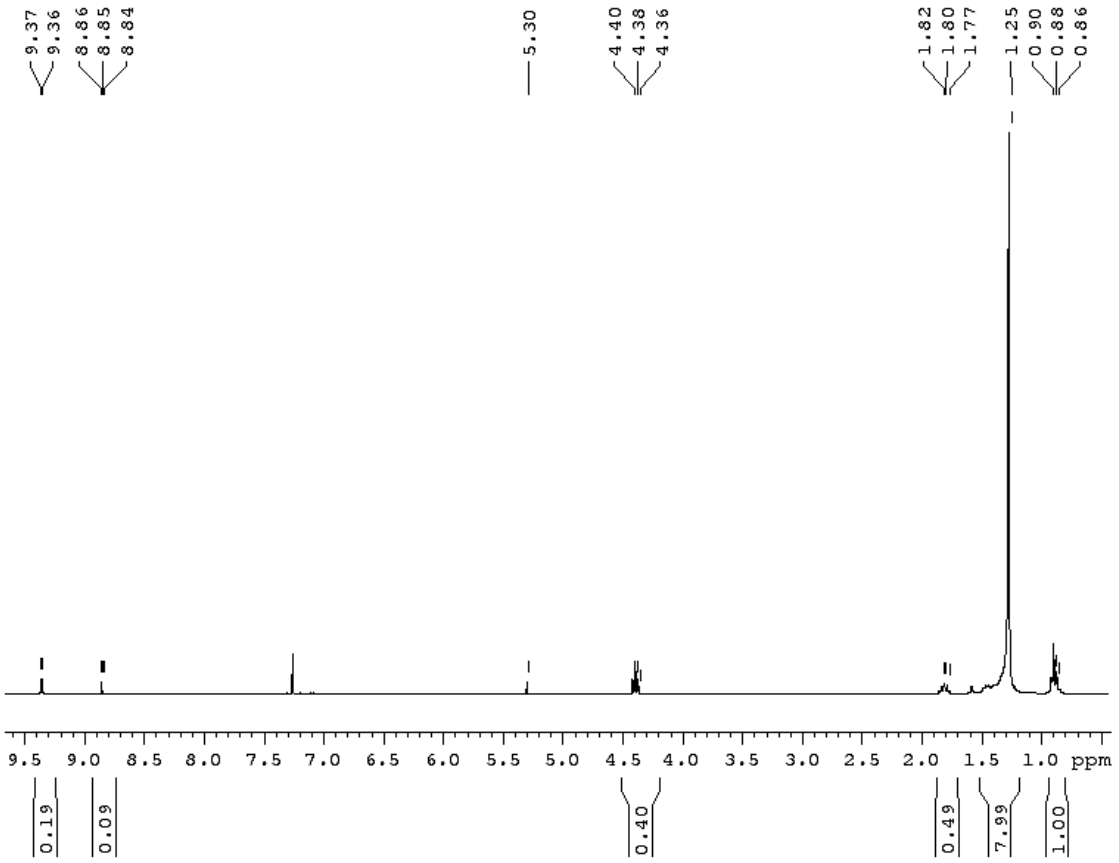

^{13}CNMR for compound ***2-20***

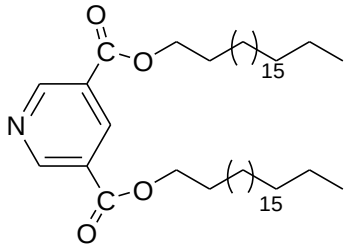

2-20

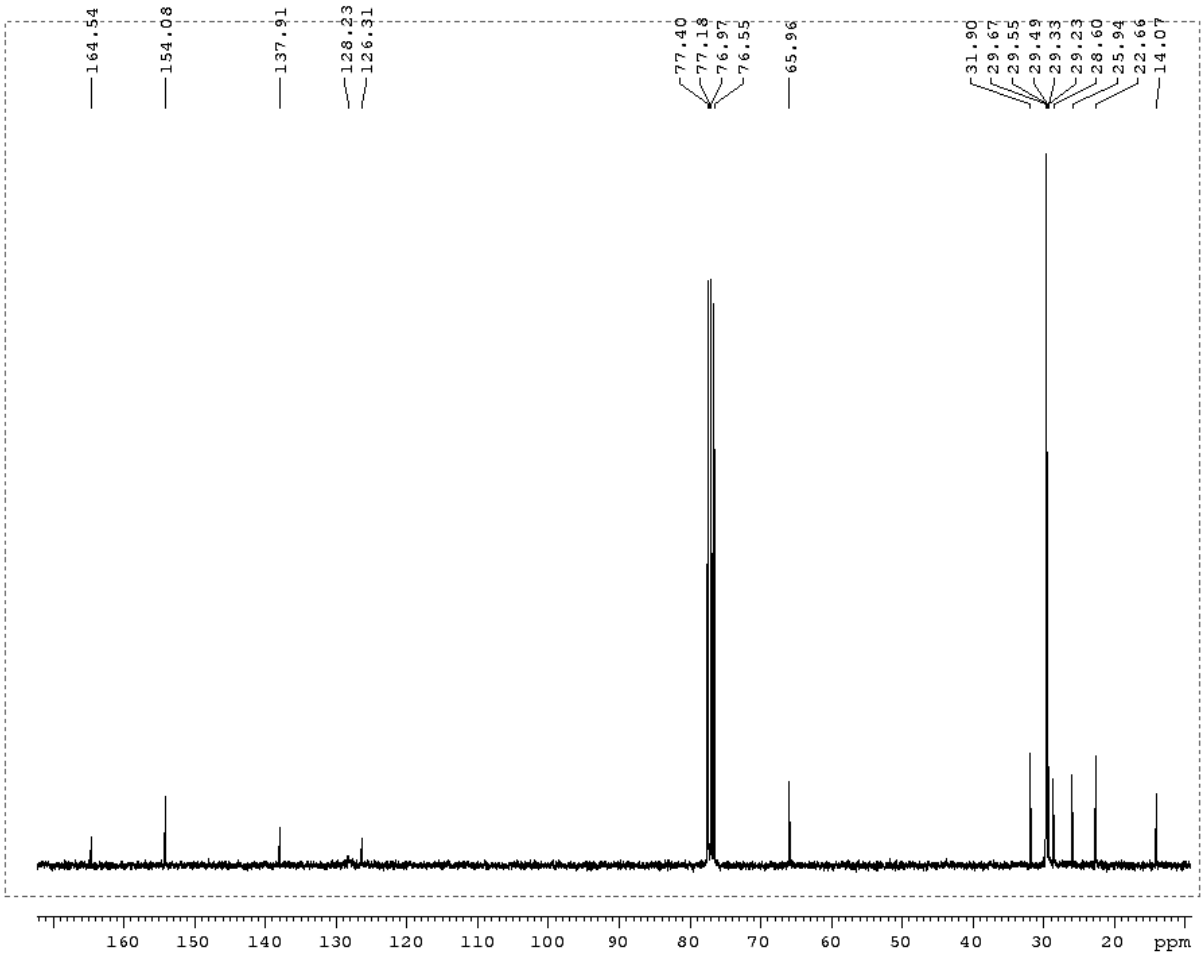

^{1}HNMR for compound ***2-21***

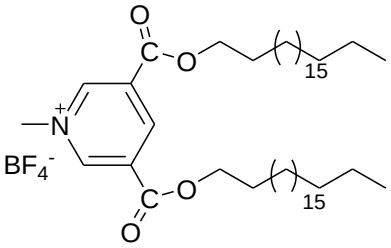

2-21

diC20:0

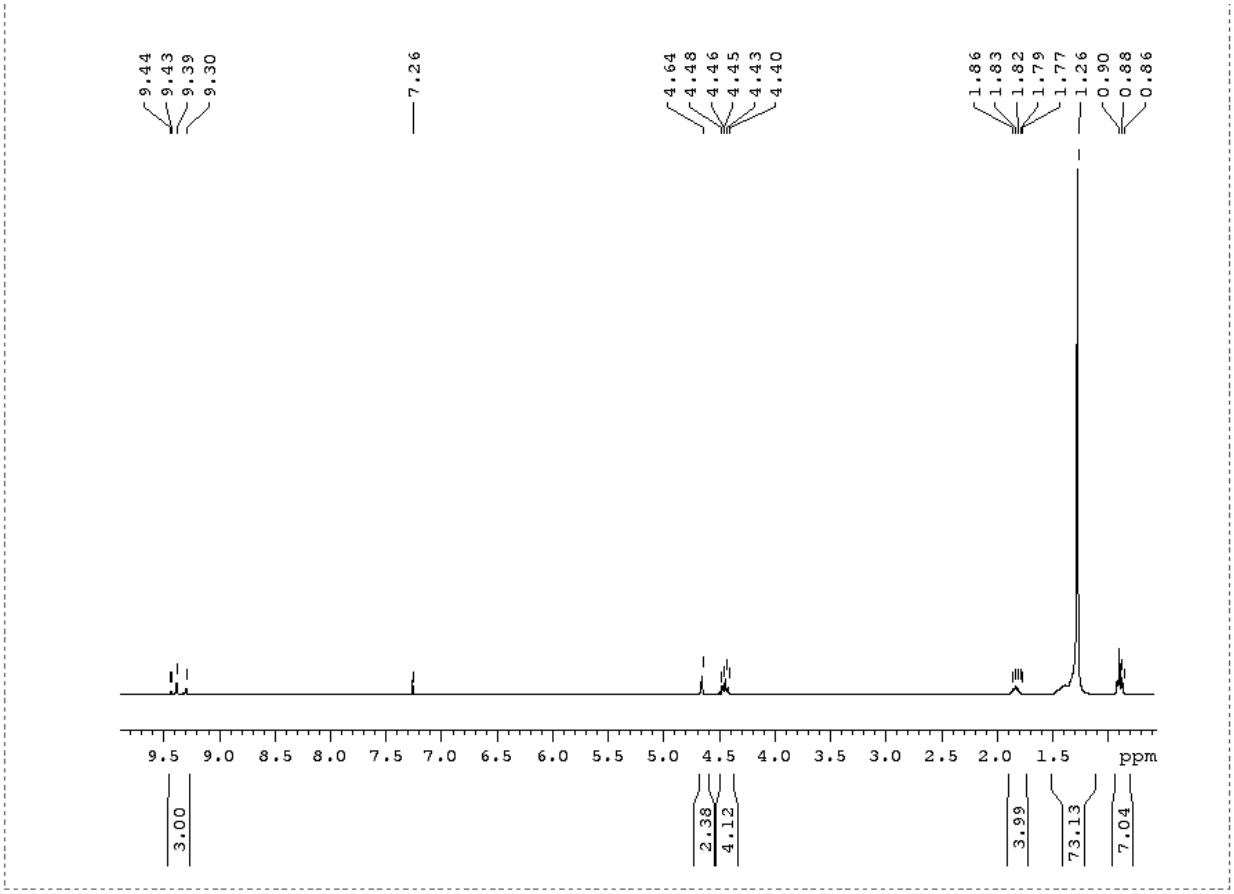

^{13}CNMR for compound ***2-21***

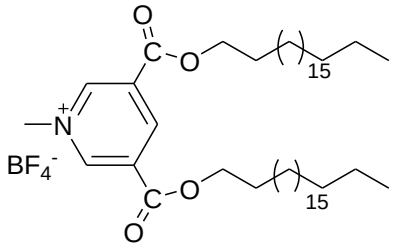

2-21

diC20:0

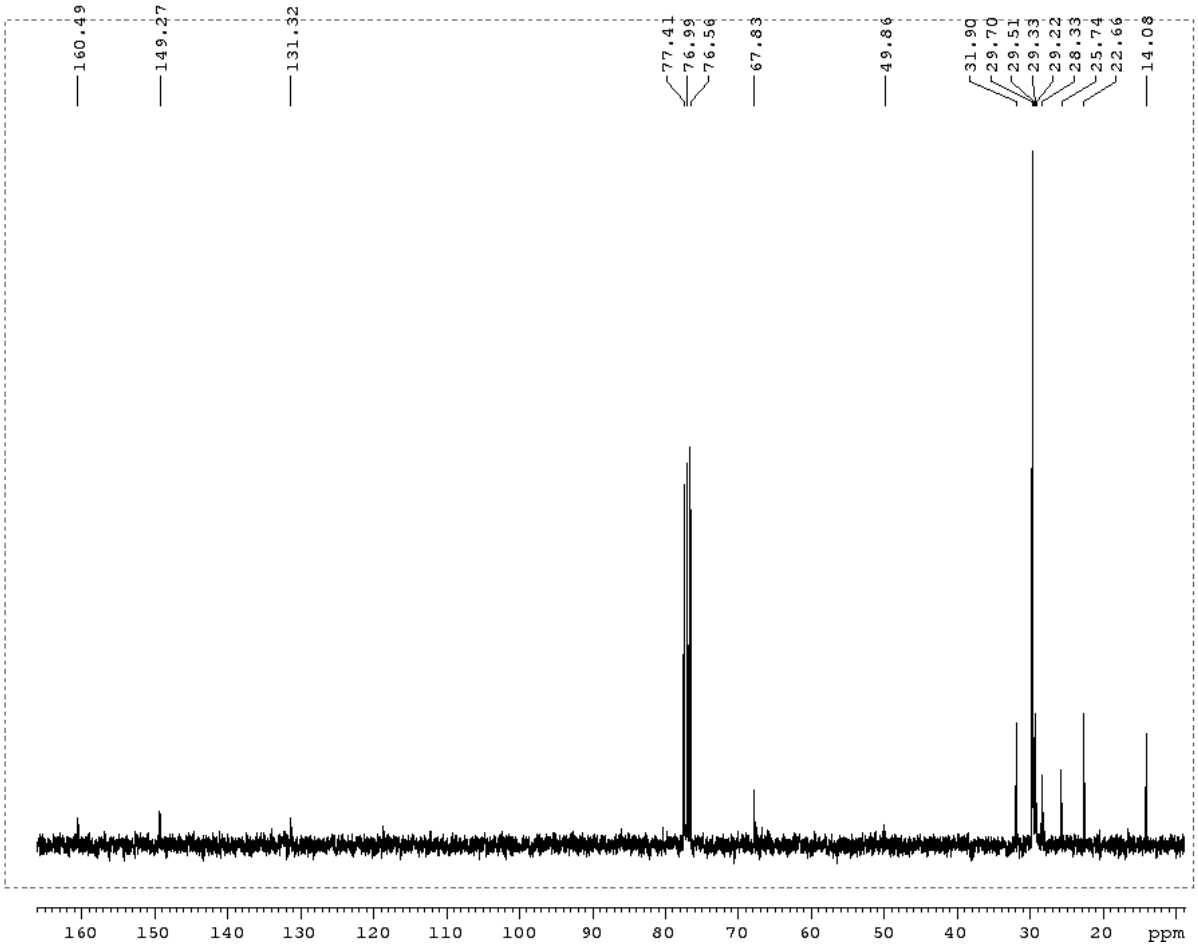

^{1}HNMR for compound ***2-22***

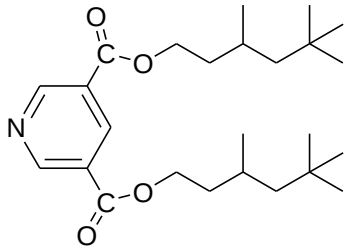

2-22

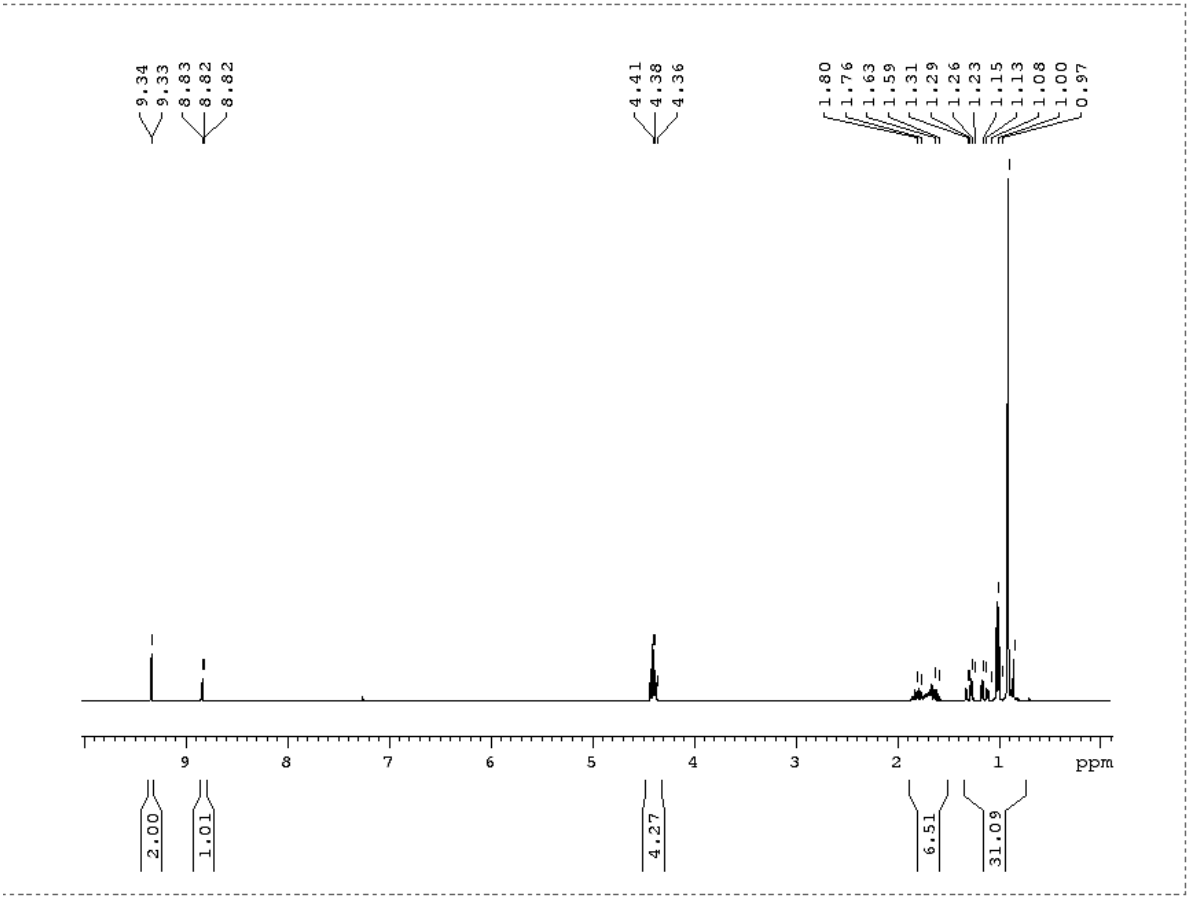

^{13}CNMR for compound ***2-22***

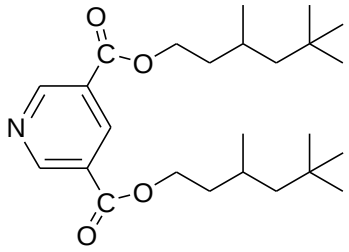

2-22

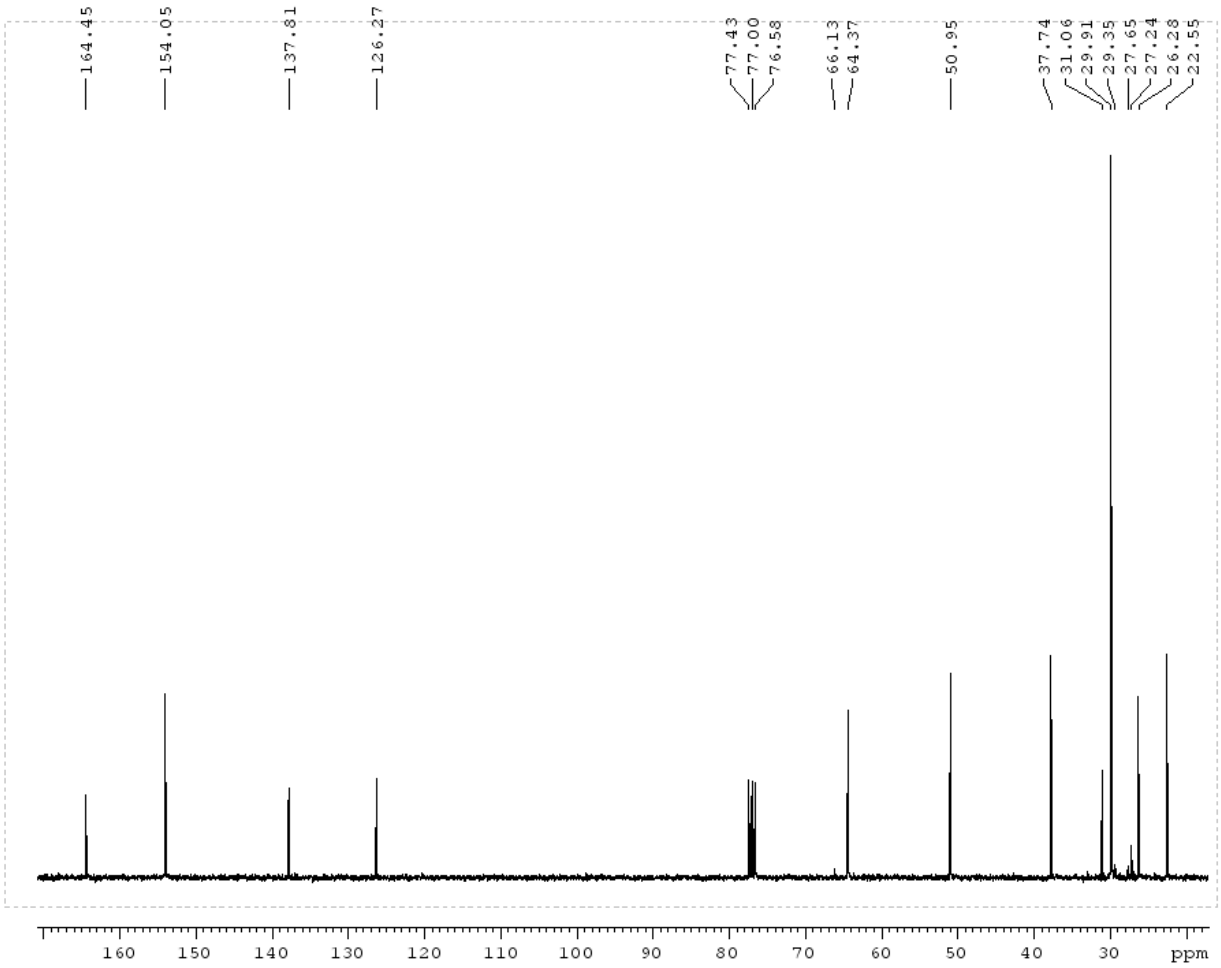

^{1}HNMR for compound ***2-23***

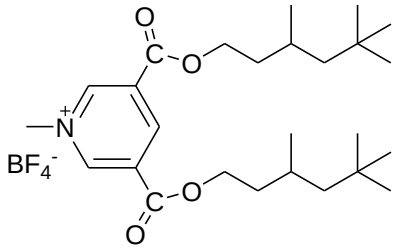

2-23

diisoC9:0

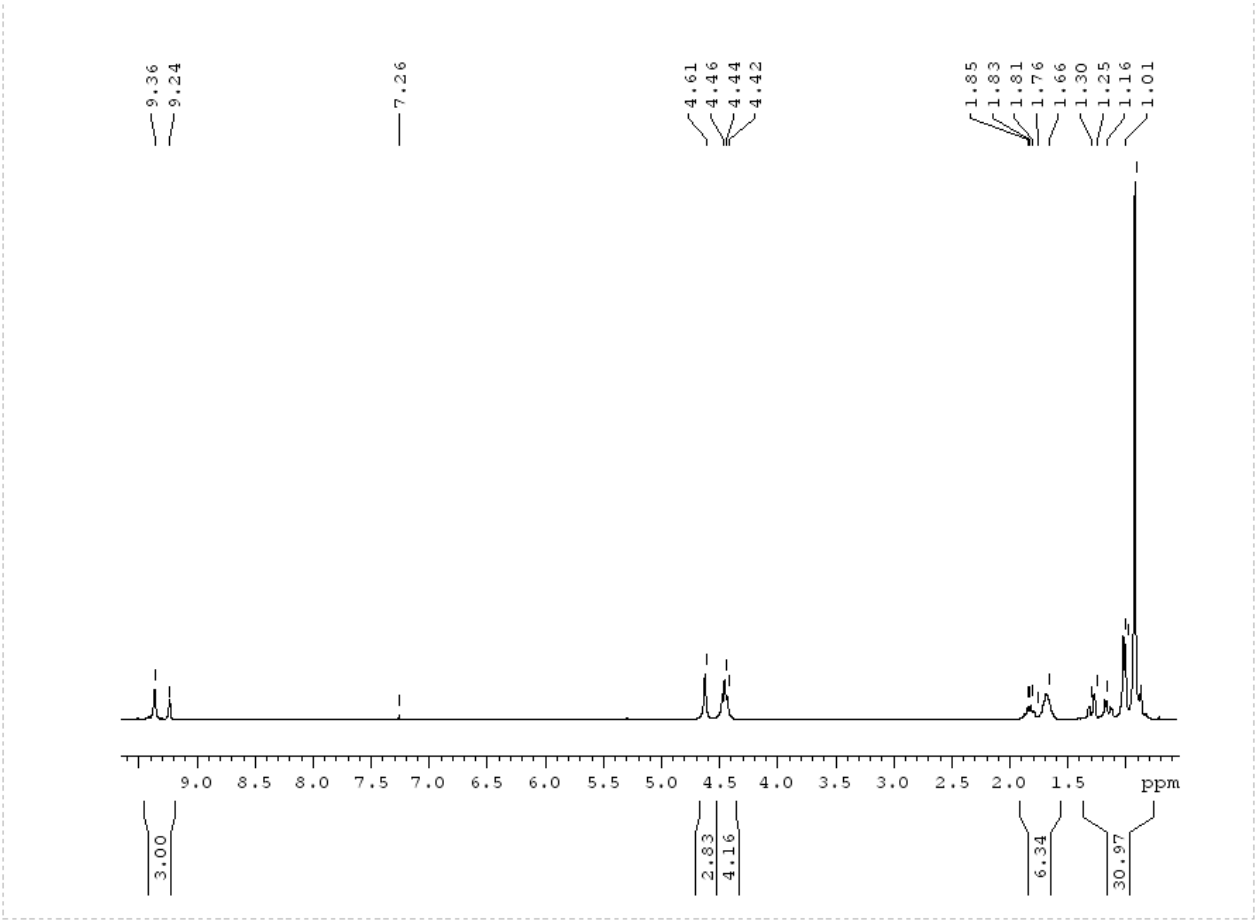

^{13}CNMR for compound ***2-23***

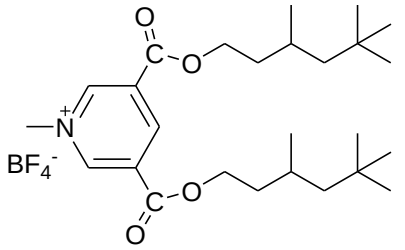

2-23

diisoC9:0

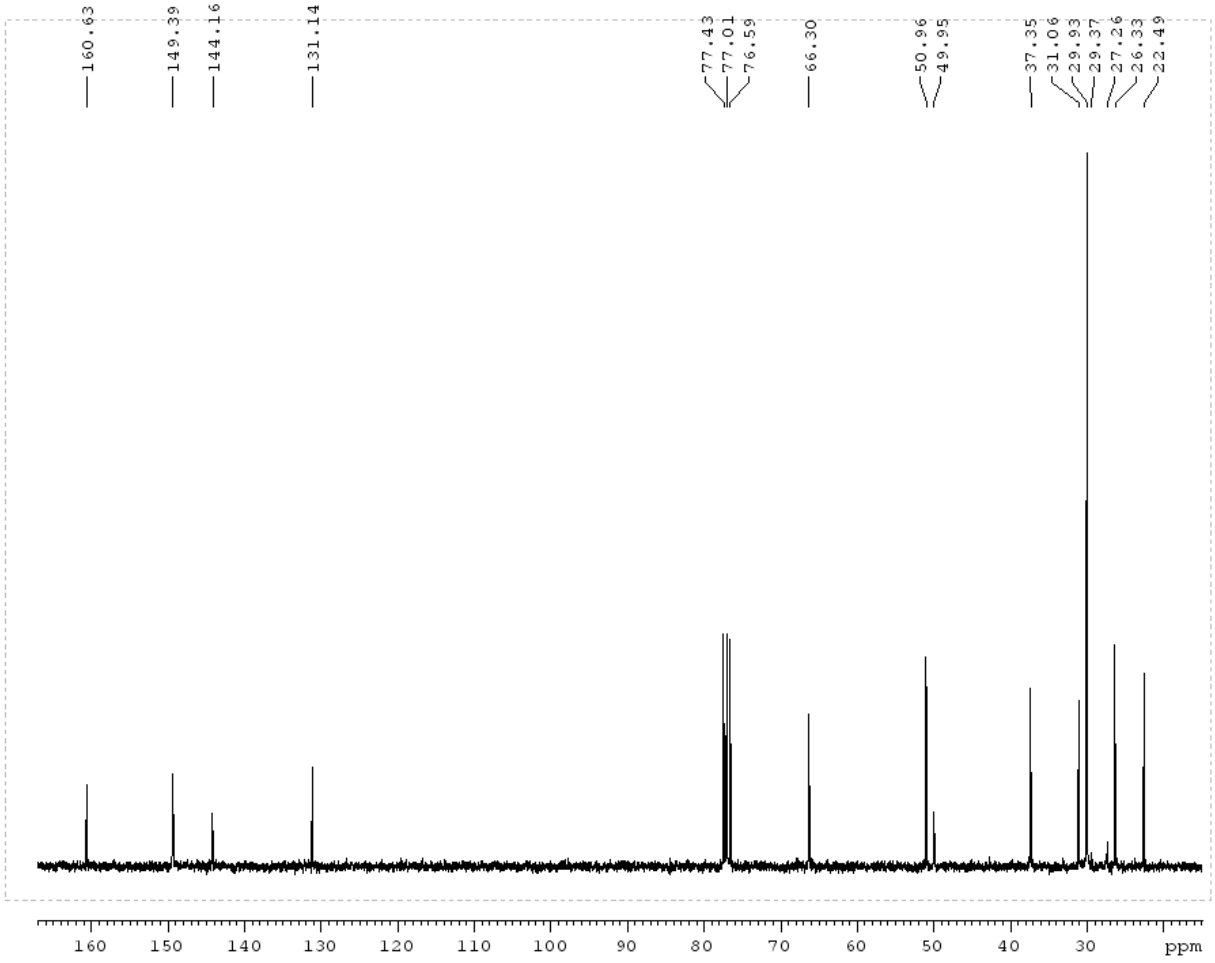

^{1}HNMR for compound ***2-24***

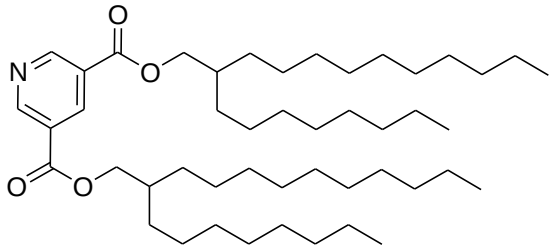

2-24

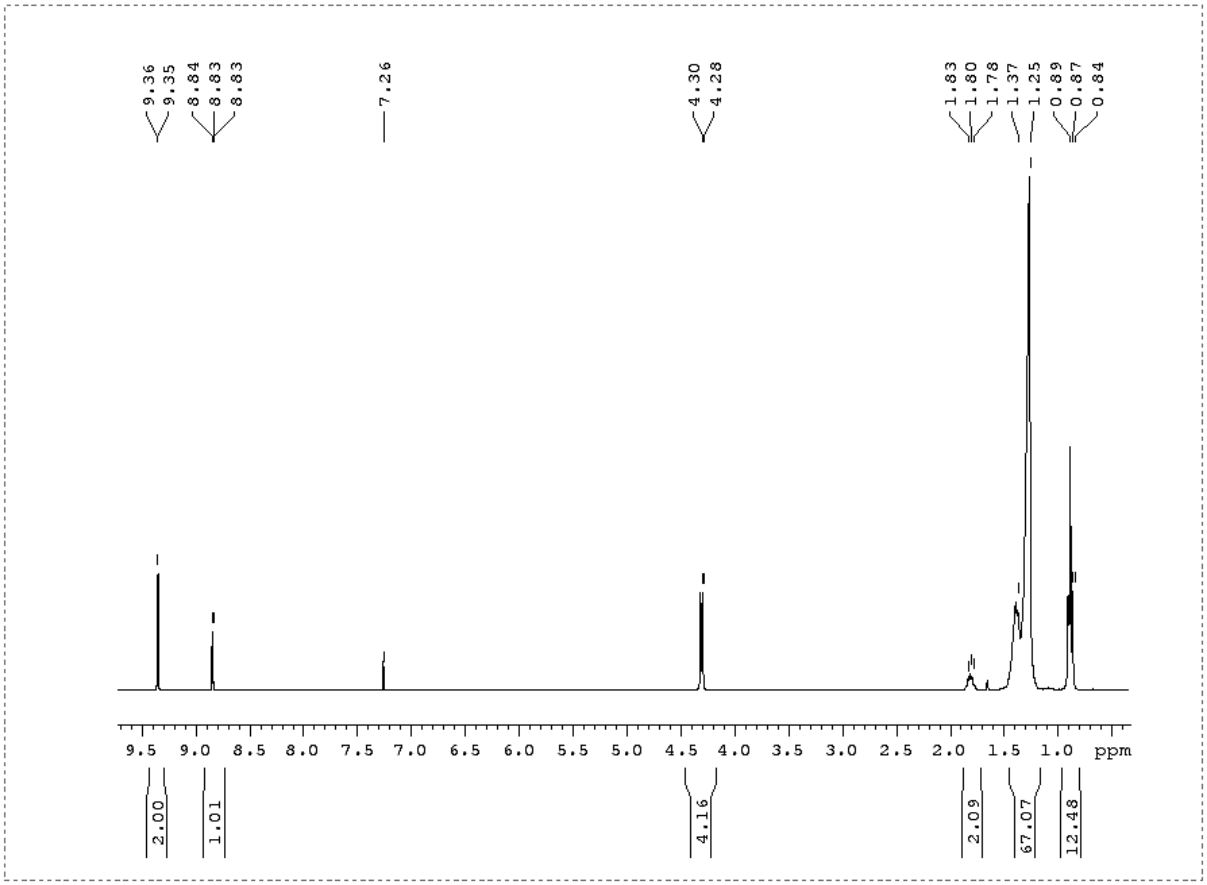

^{13}CNMR for compound ***2-24***

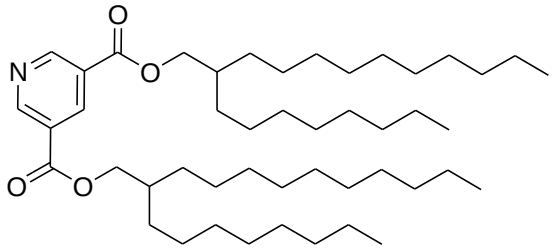

2-24

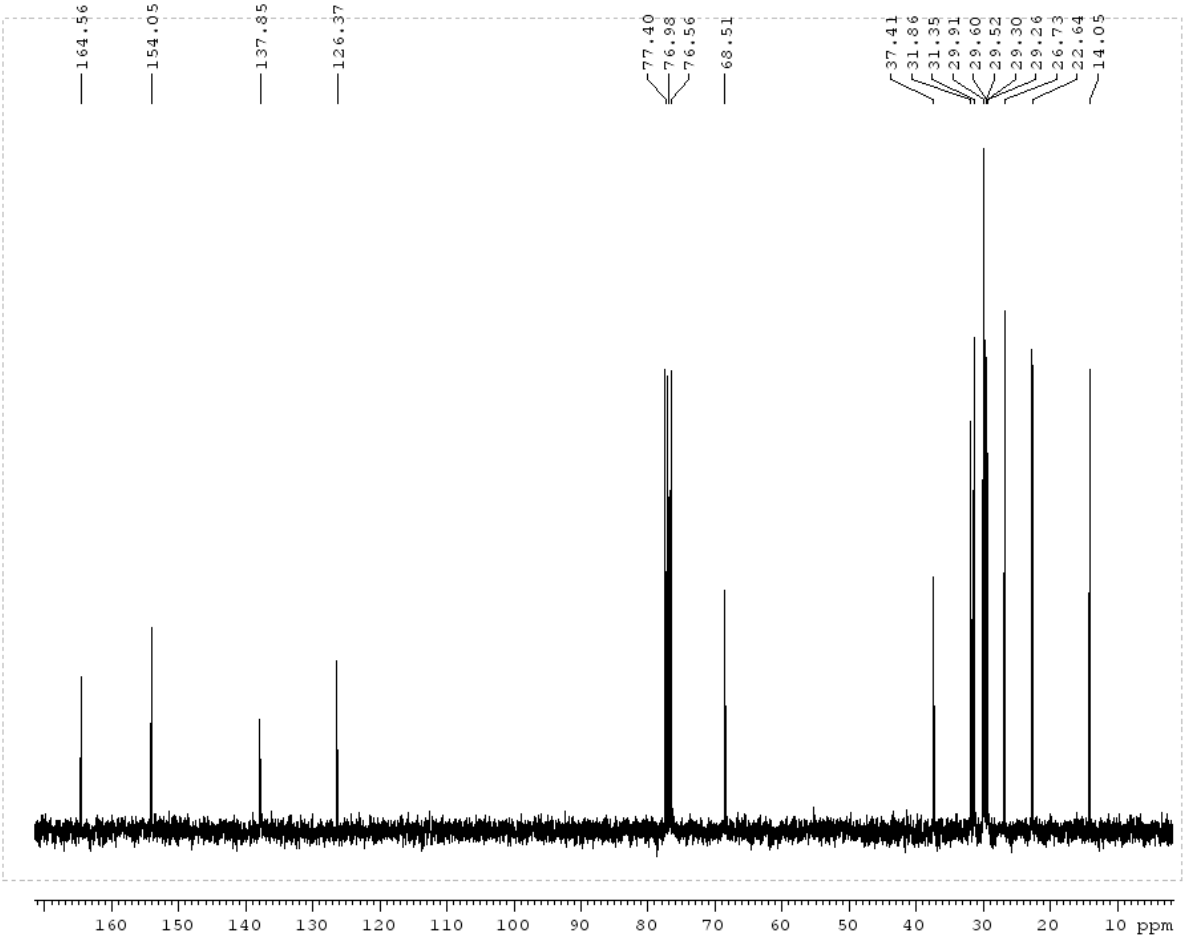

^{1}HNMR for compound ***2-25***

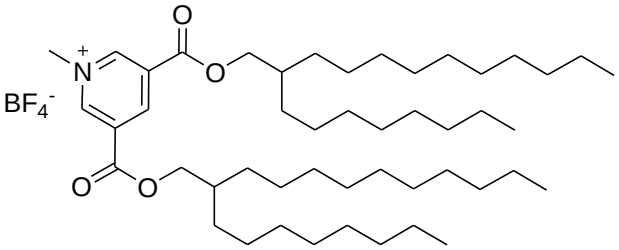

2-25

dibrC20:0

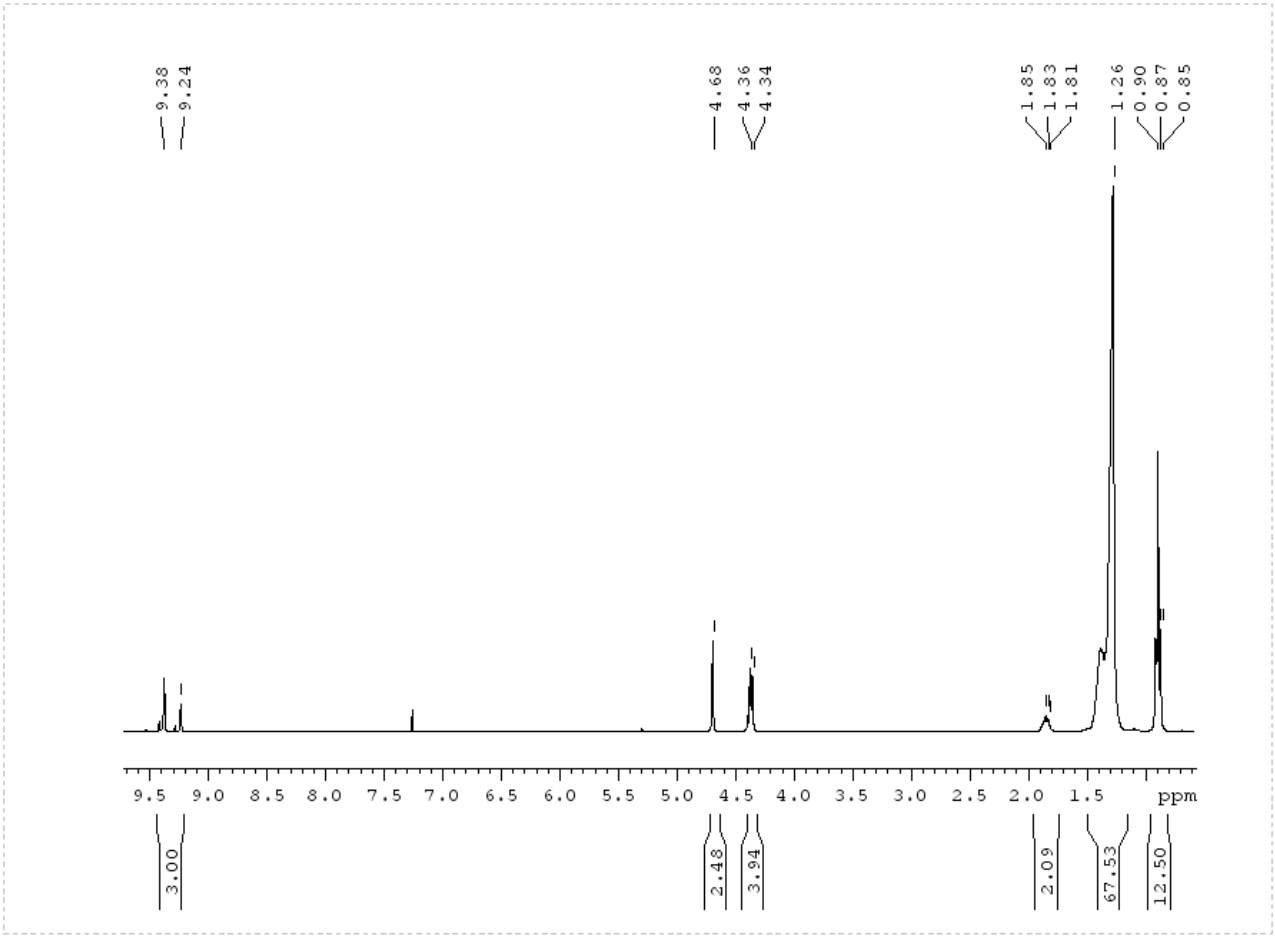

^{13}CNMR for compound ***2-25***

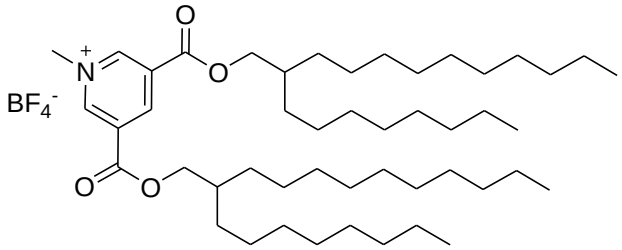

2-25

dibrC20:0

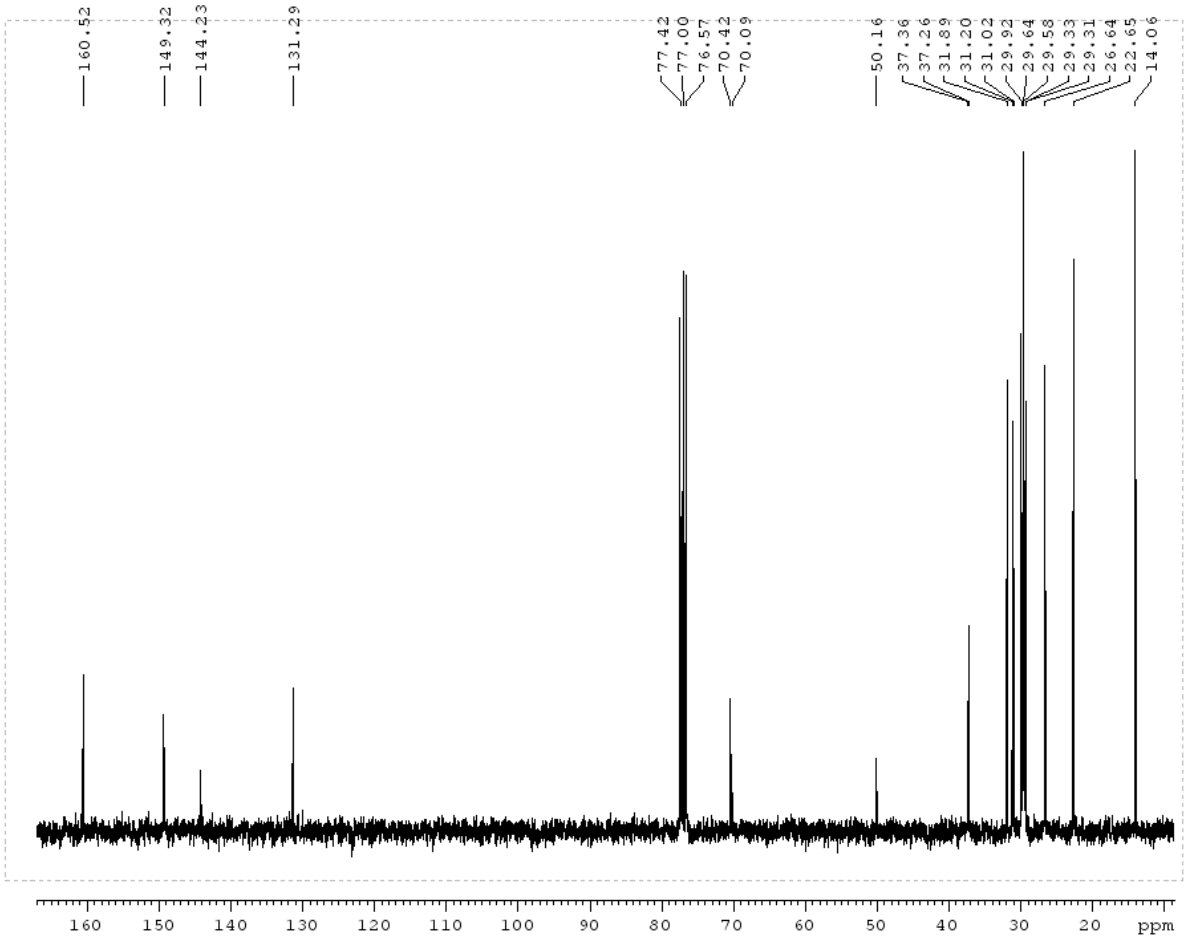

^{1}HNMR for compound ***2-26***

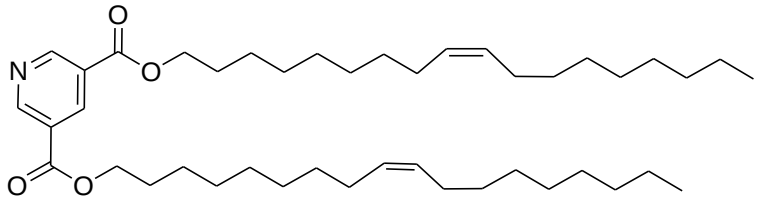

2-26

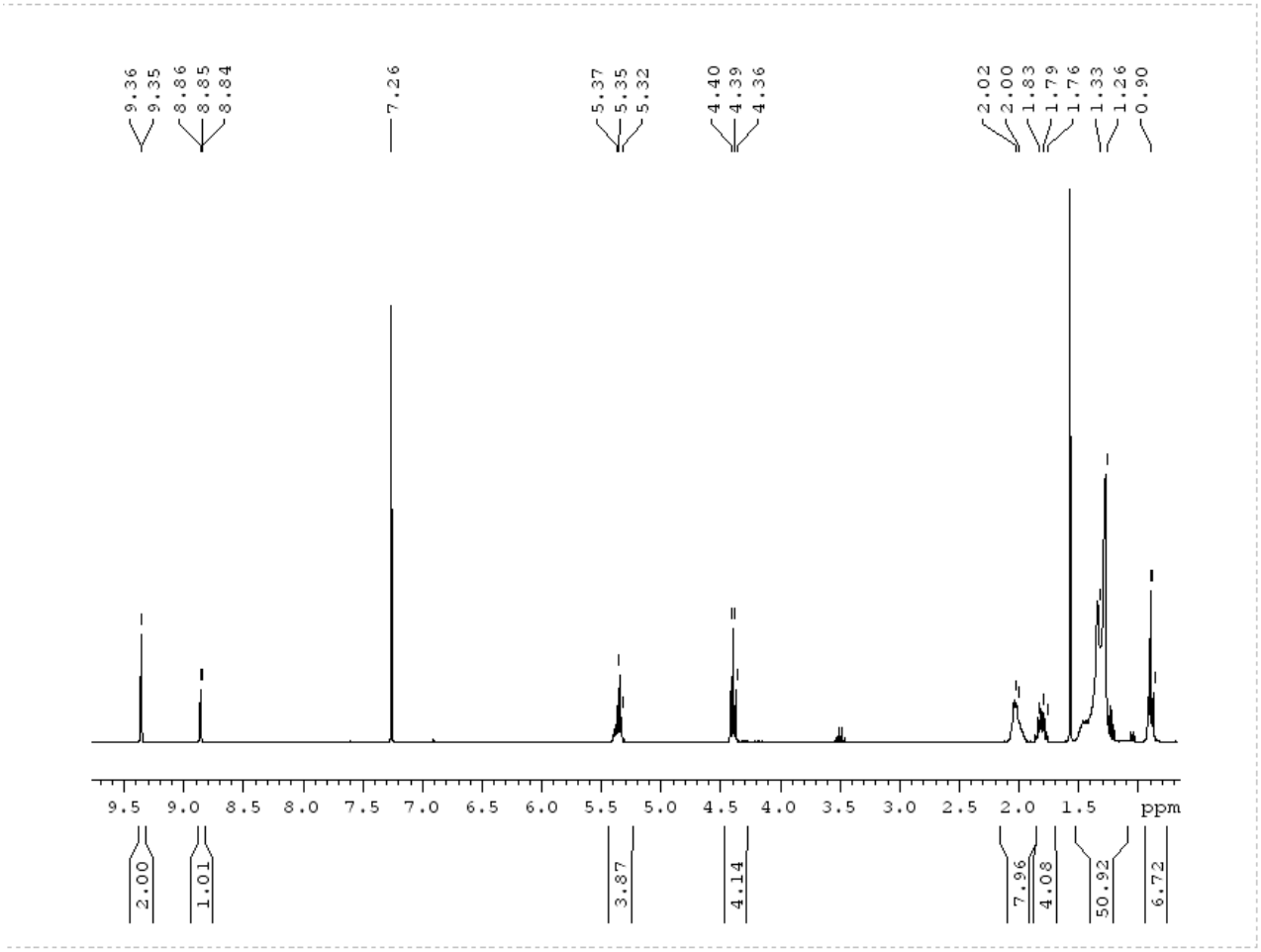

^{13}CNMR for compound ***2-26***

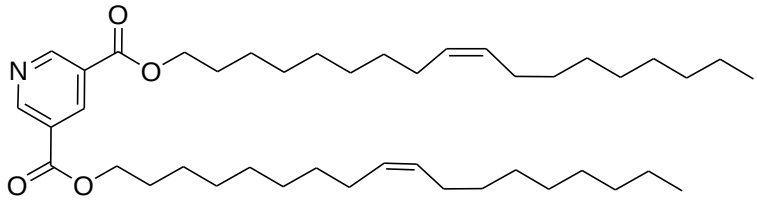

2-26

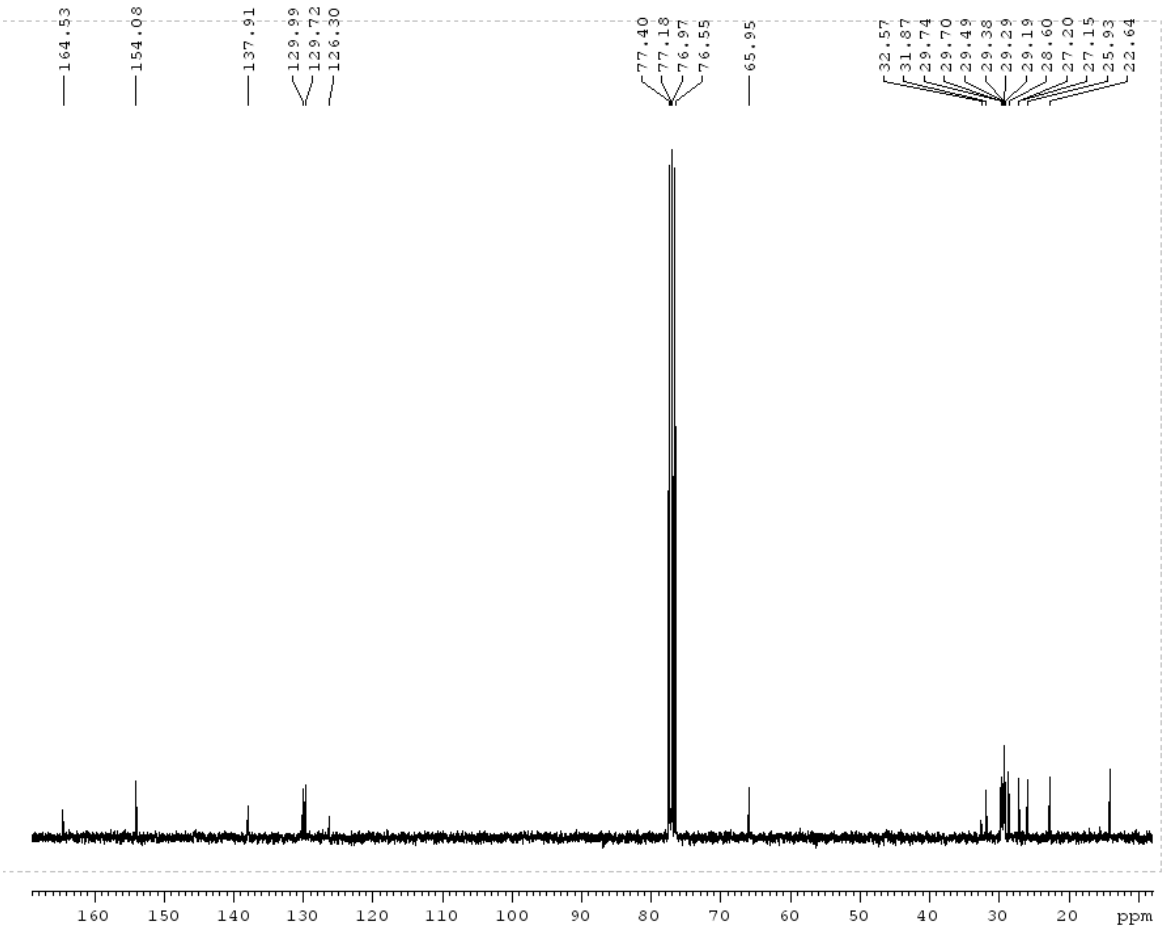

^{1}HNMR for compound ***2-27***

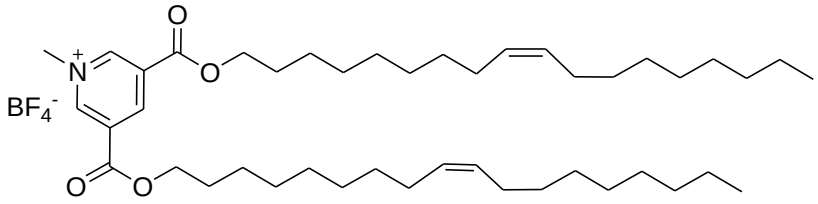

2-27

diC18:1

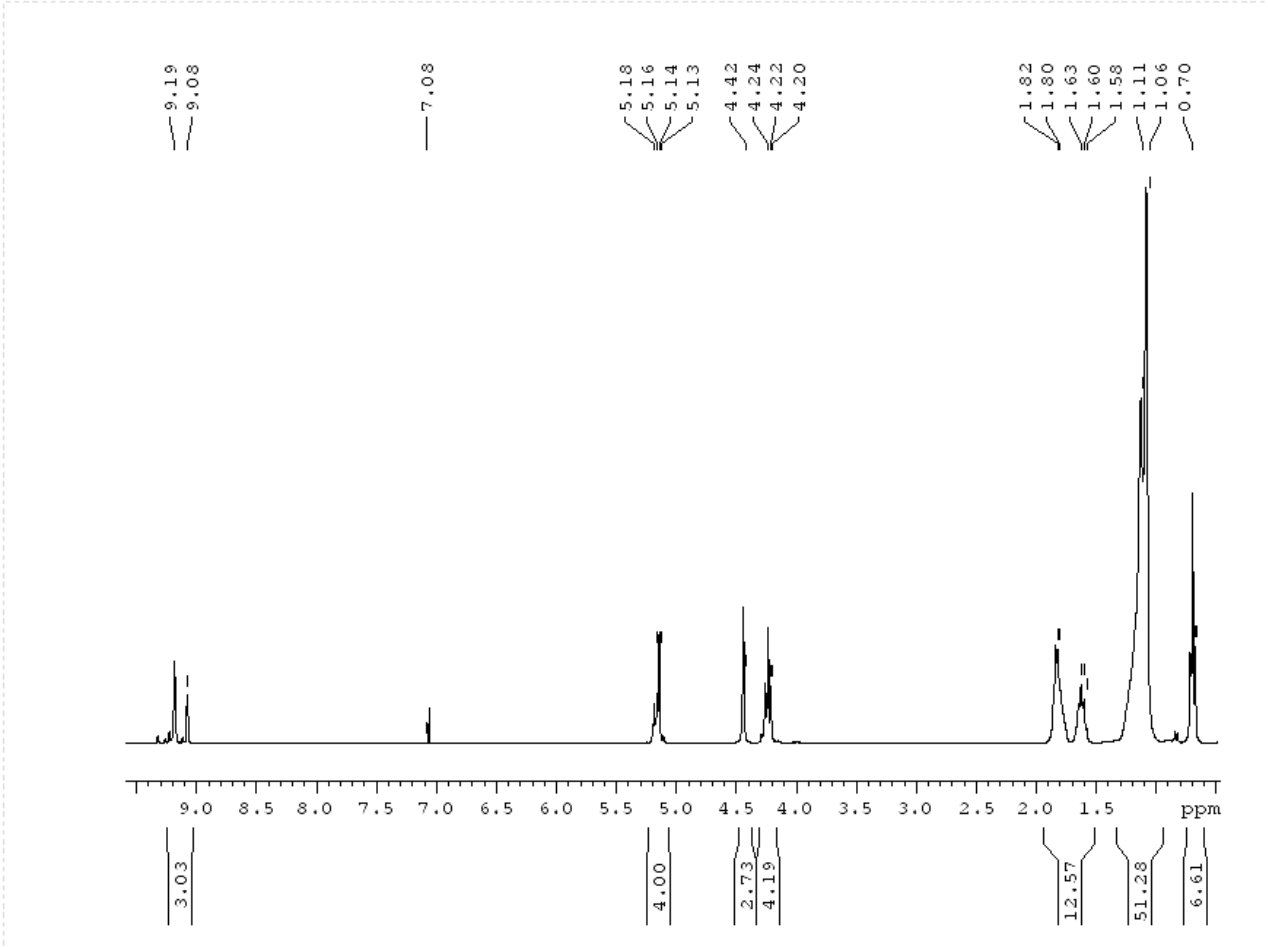

^{13}CNMR for compound ***2-27***

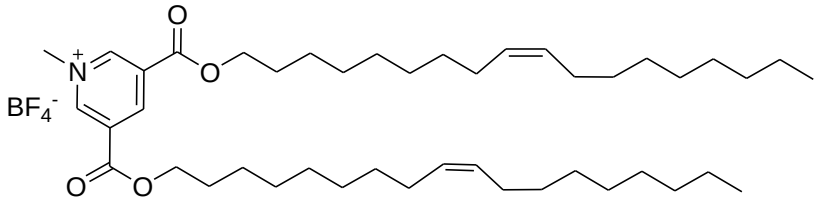

2-27

diC18:1

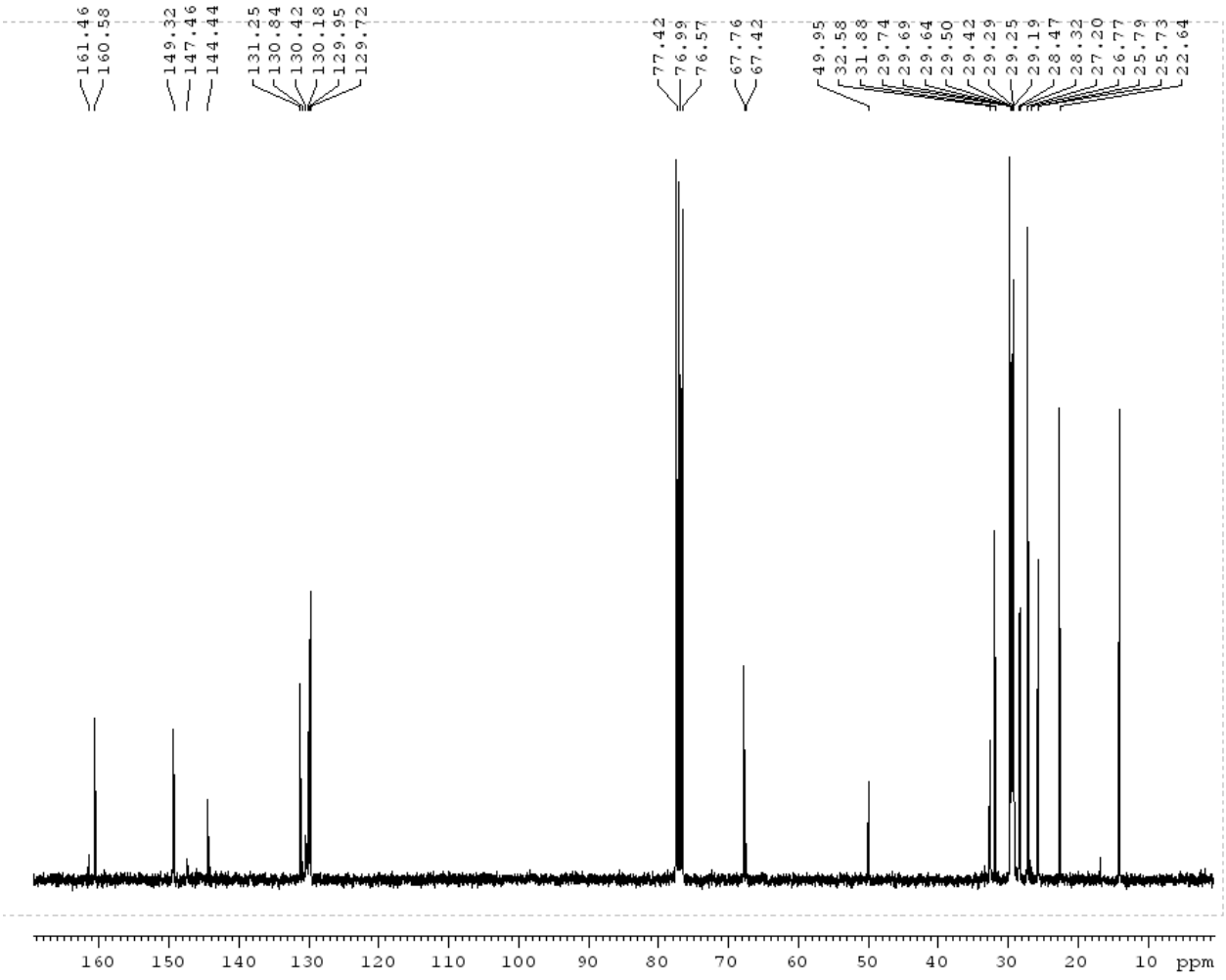

[1]HNMR for compound ***2-28***

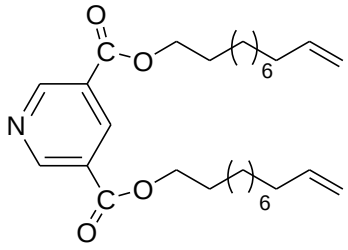

2-28

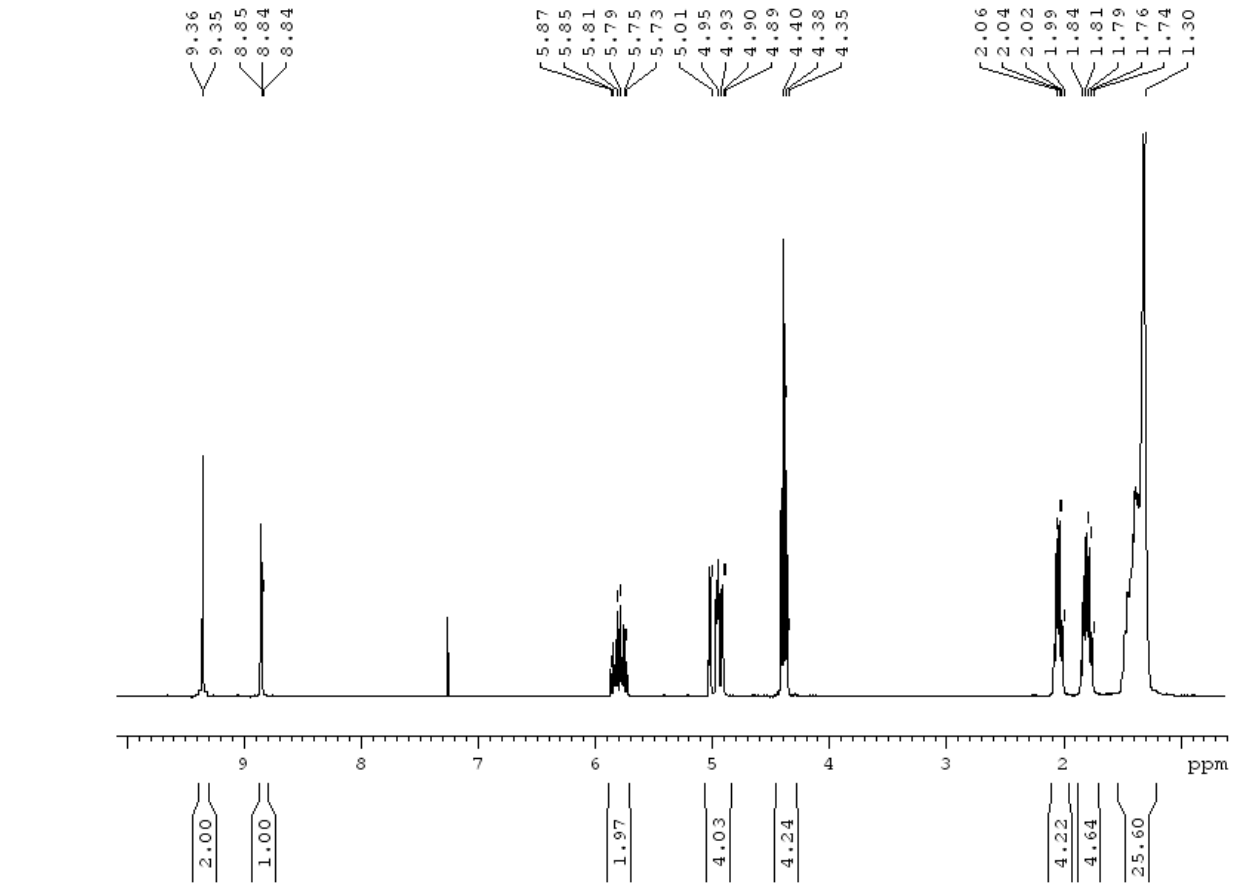

^{13}CNMR for compound ***2-28***

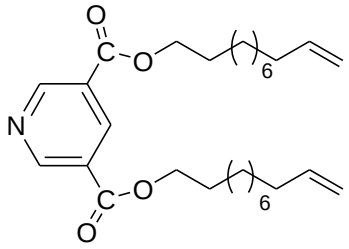

2-28

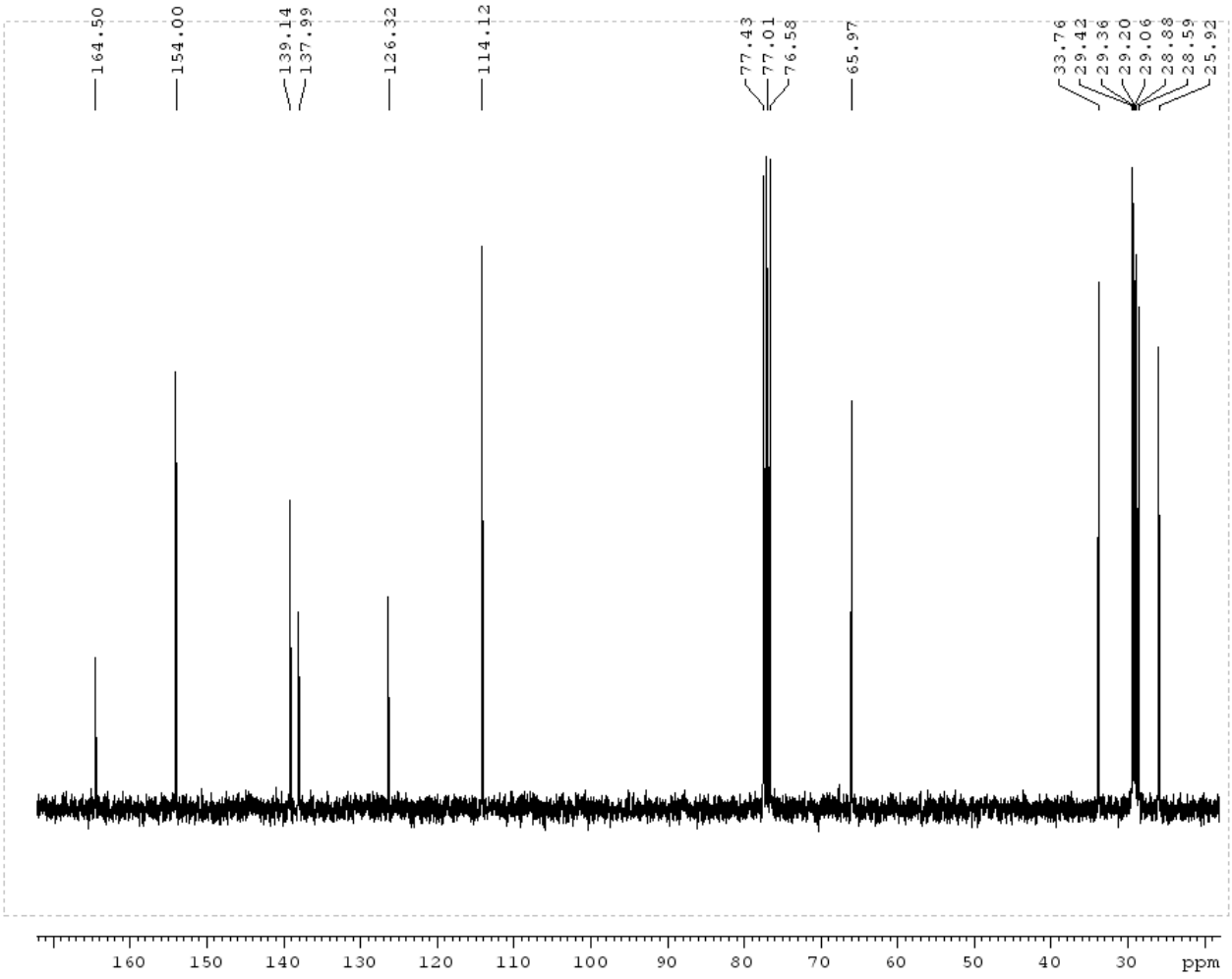

^{1}HNMR for compound ***2-29***

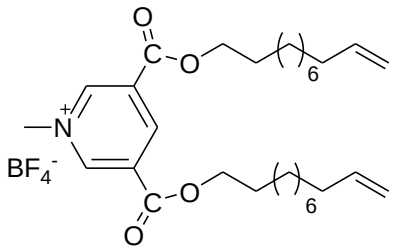

2-29
diC11:1

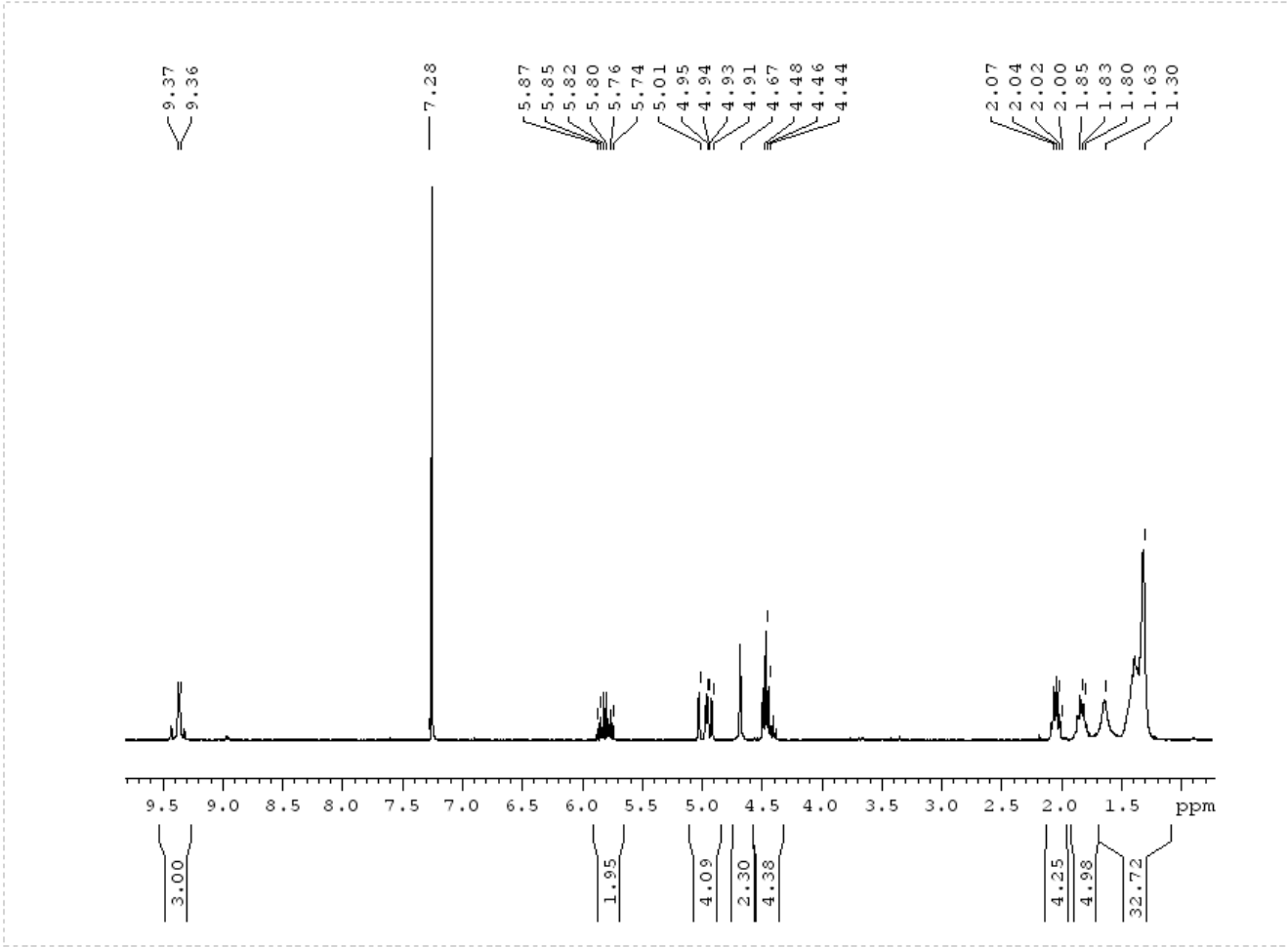

^{13}CNMR for compound ***2-29***

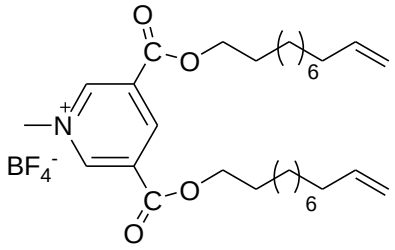

2-29

diC11:1

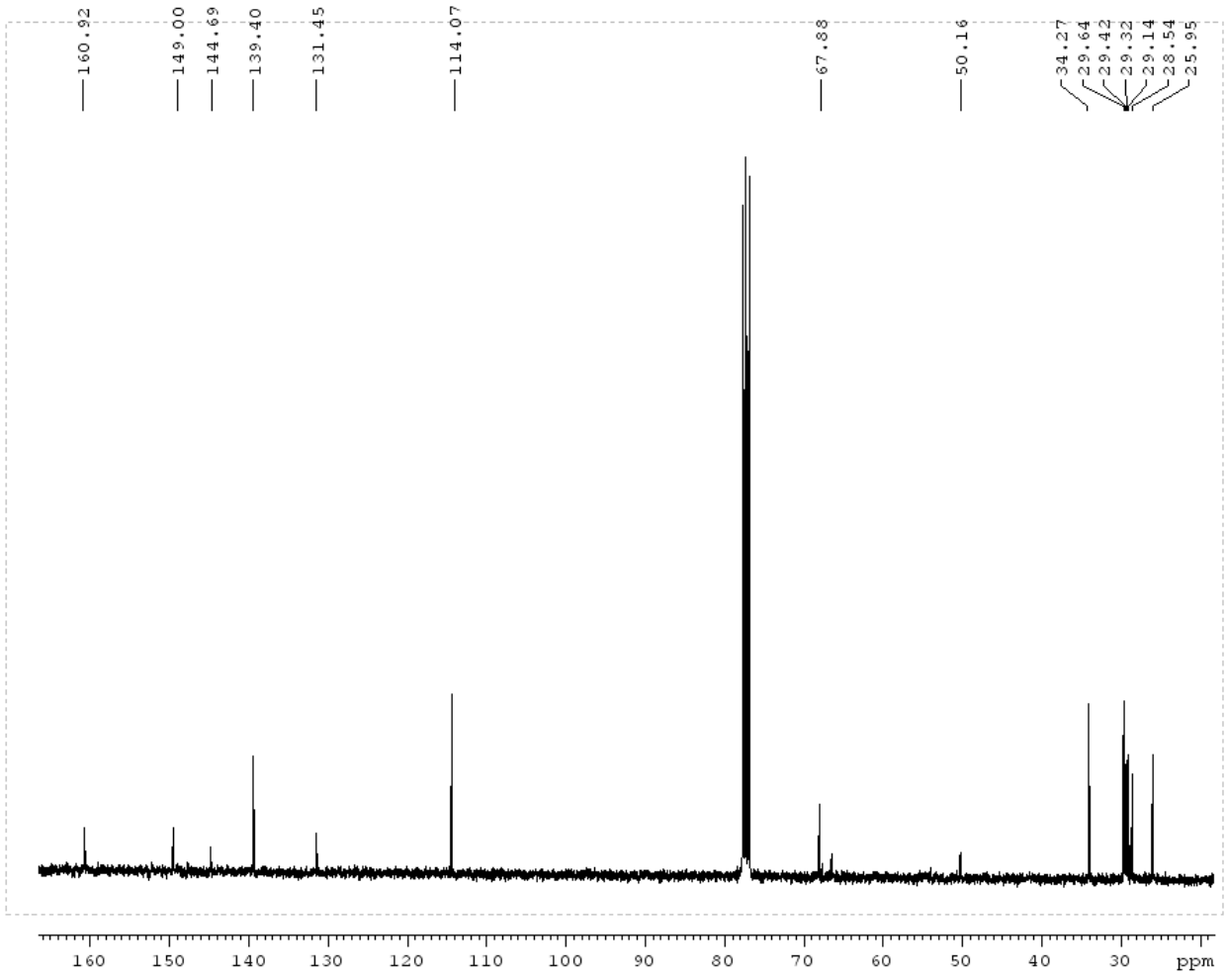

^{1}HNMR for compound ***3-1***

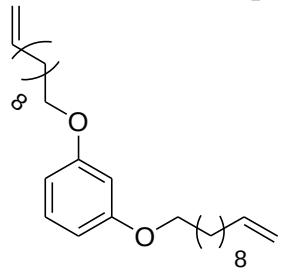

3-1

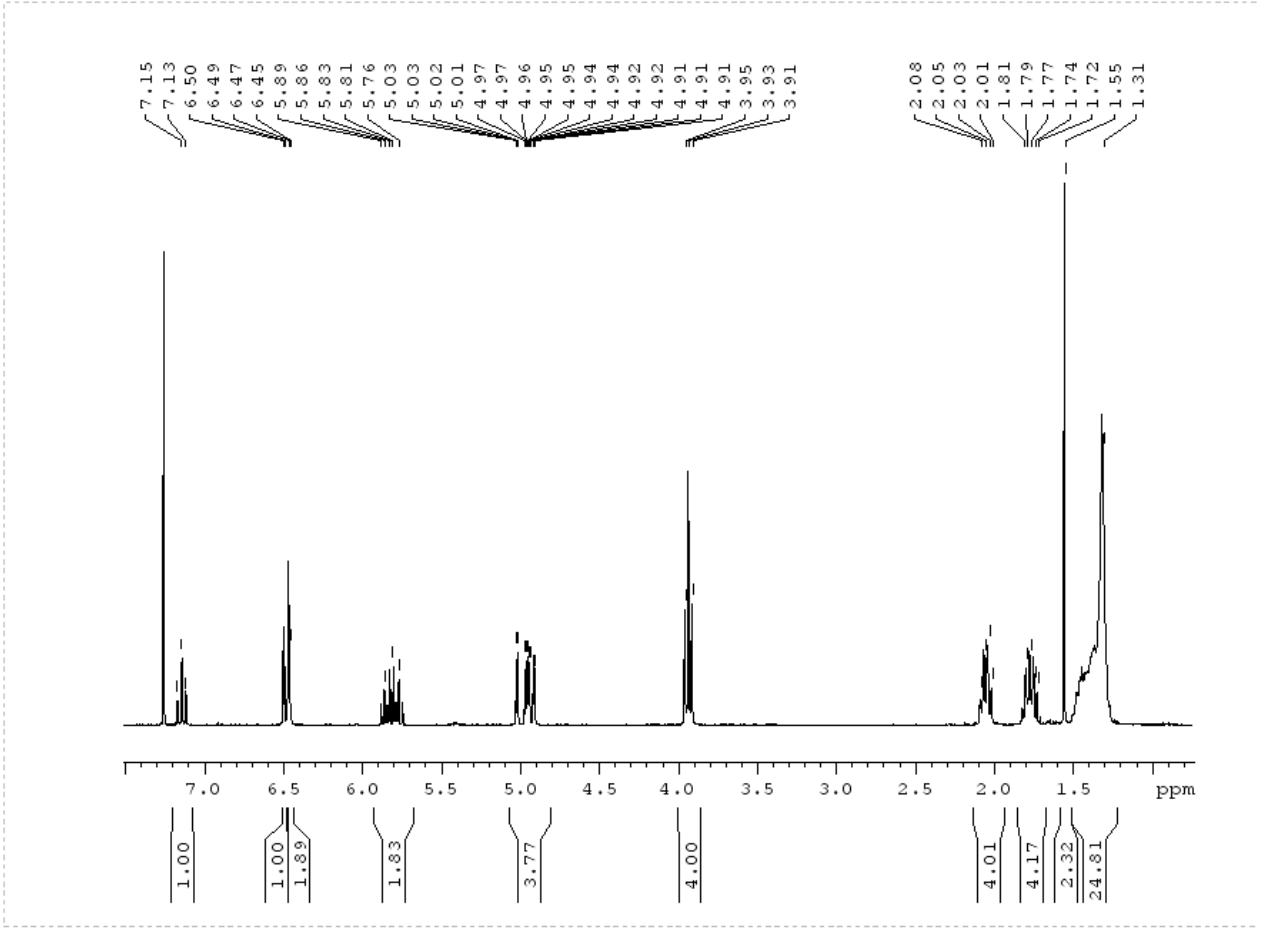

^{13}CNMR for compound ***3-1***

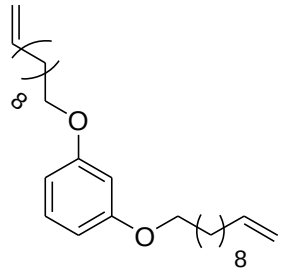

3-1

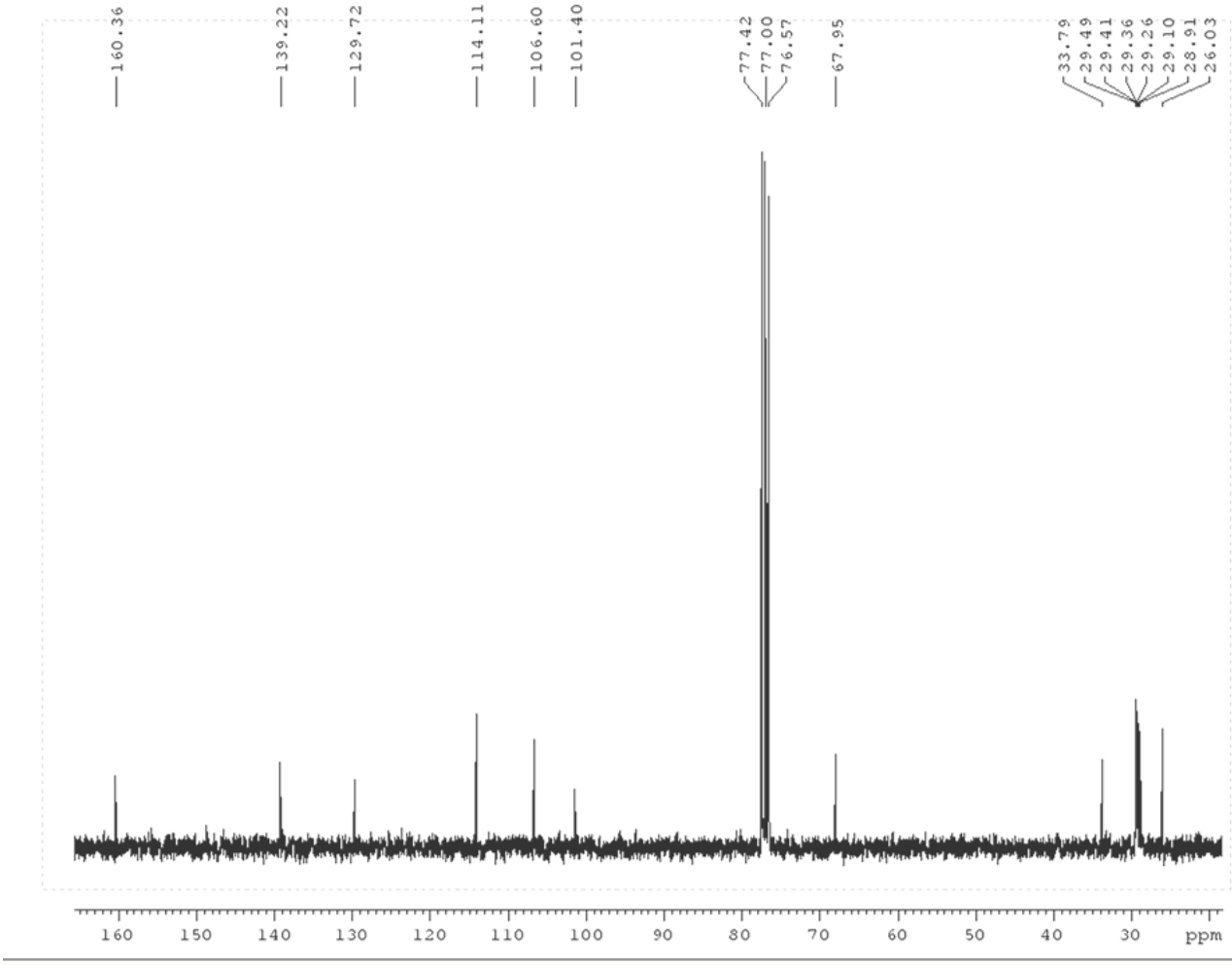

^{1}HNMR for compound ***3-2***

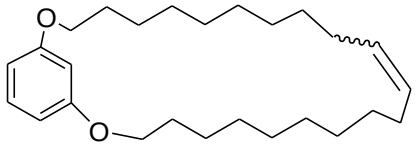

3-2

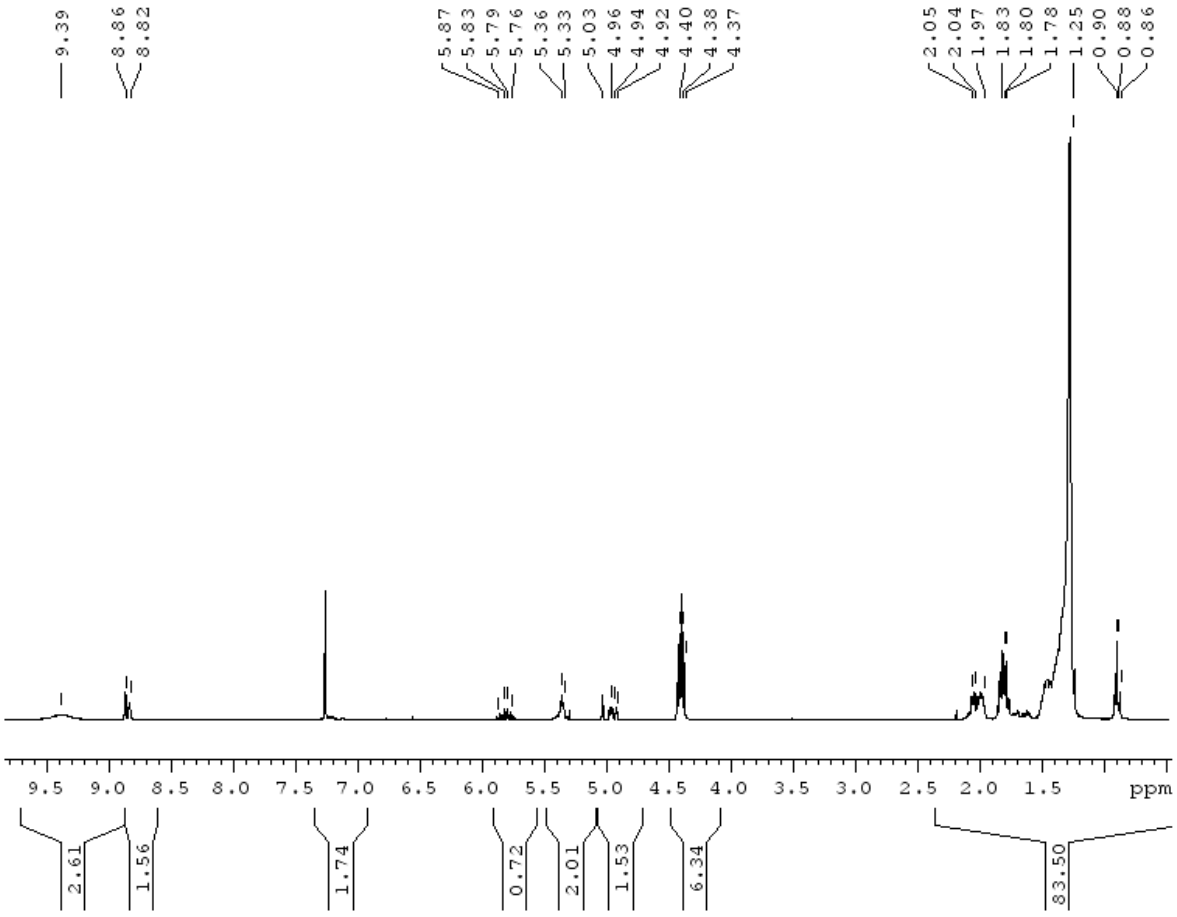

^{13}CNMR for compound ***3-2***

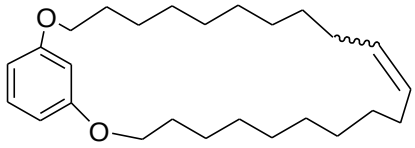

3-2

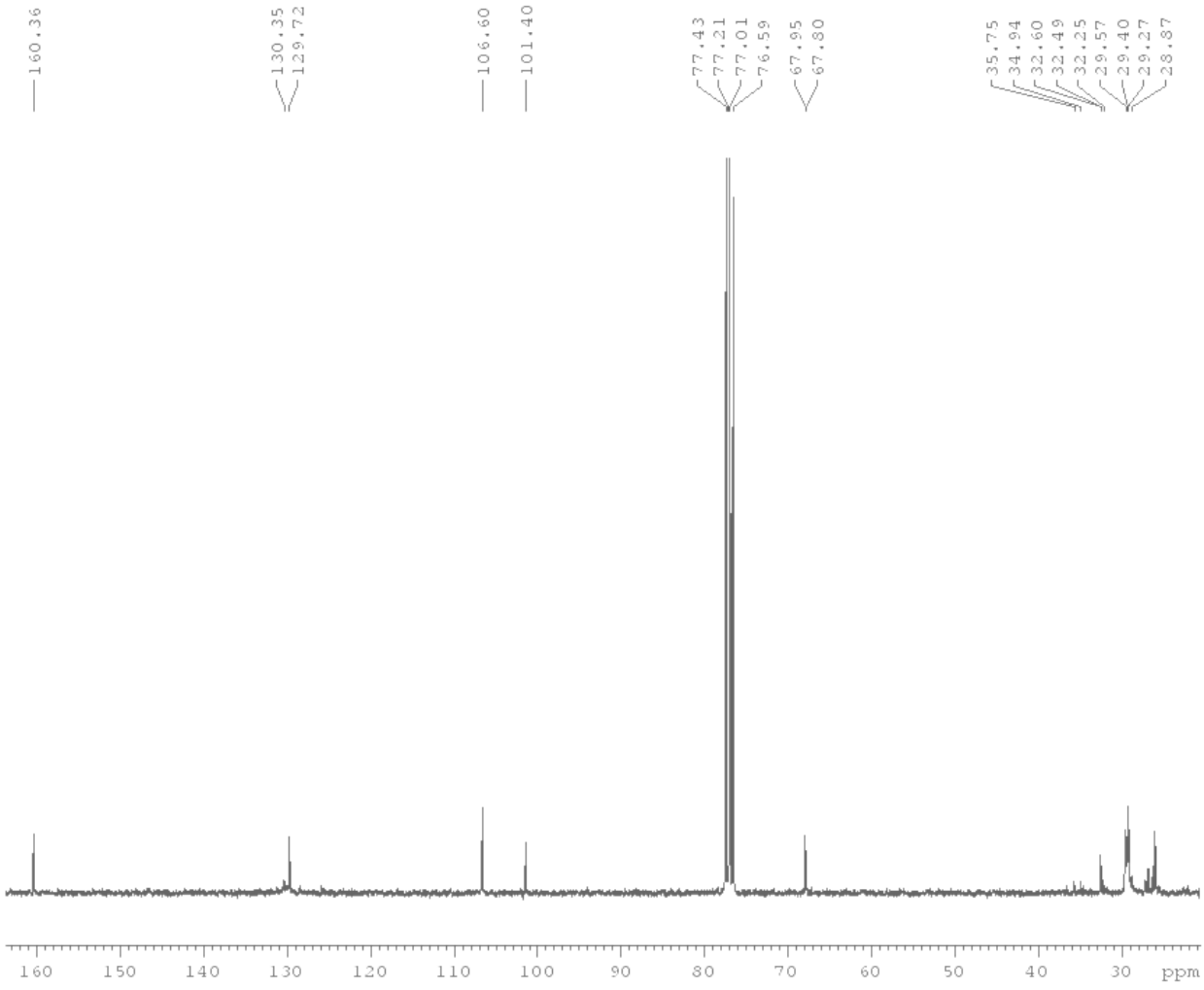

^{1}HNMR for compound ***3-3***

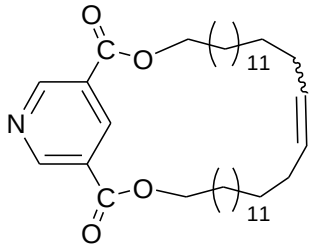

3-3

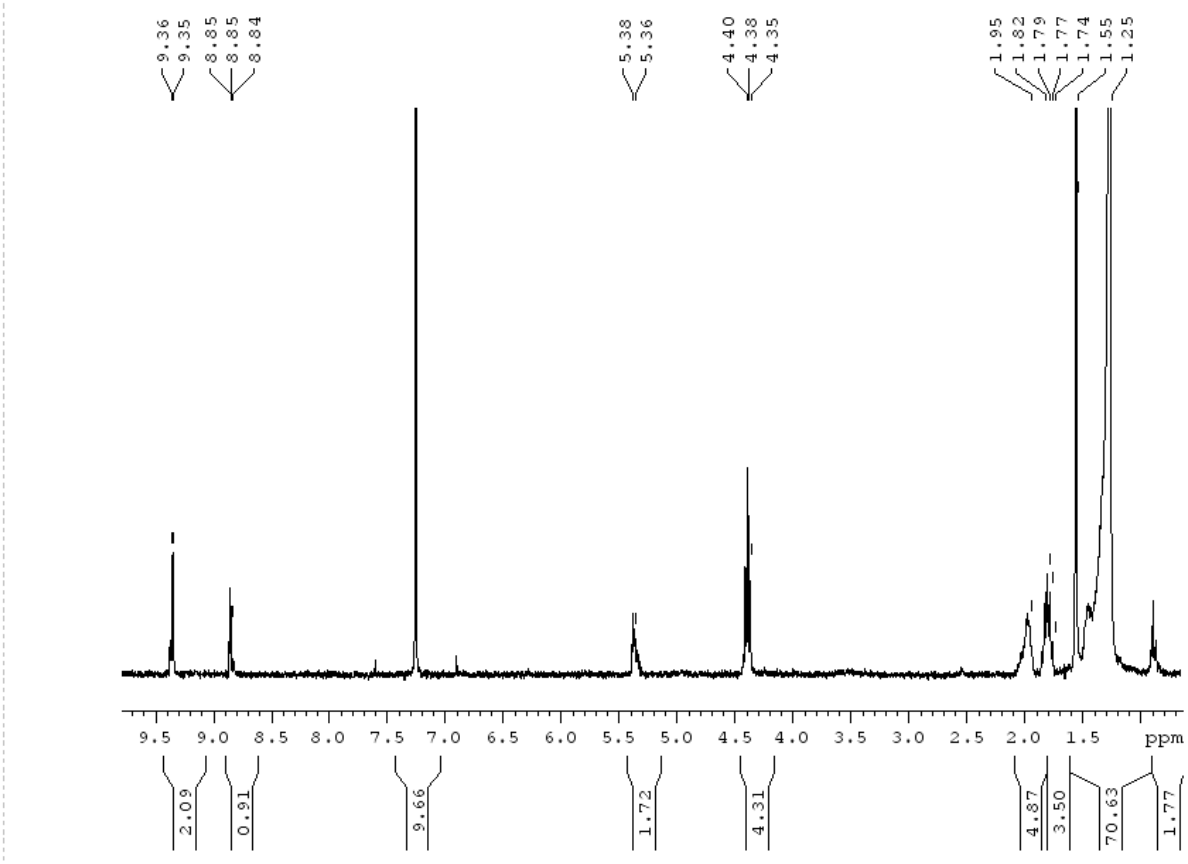

^{13}CNMR for compound ***3-3***

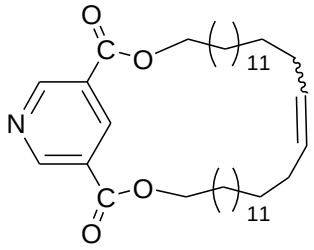

3-3

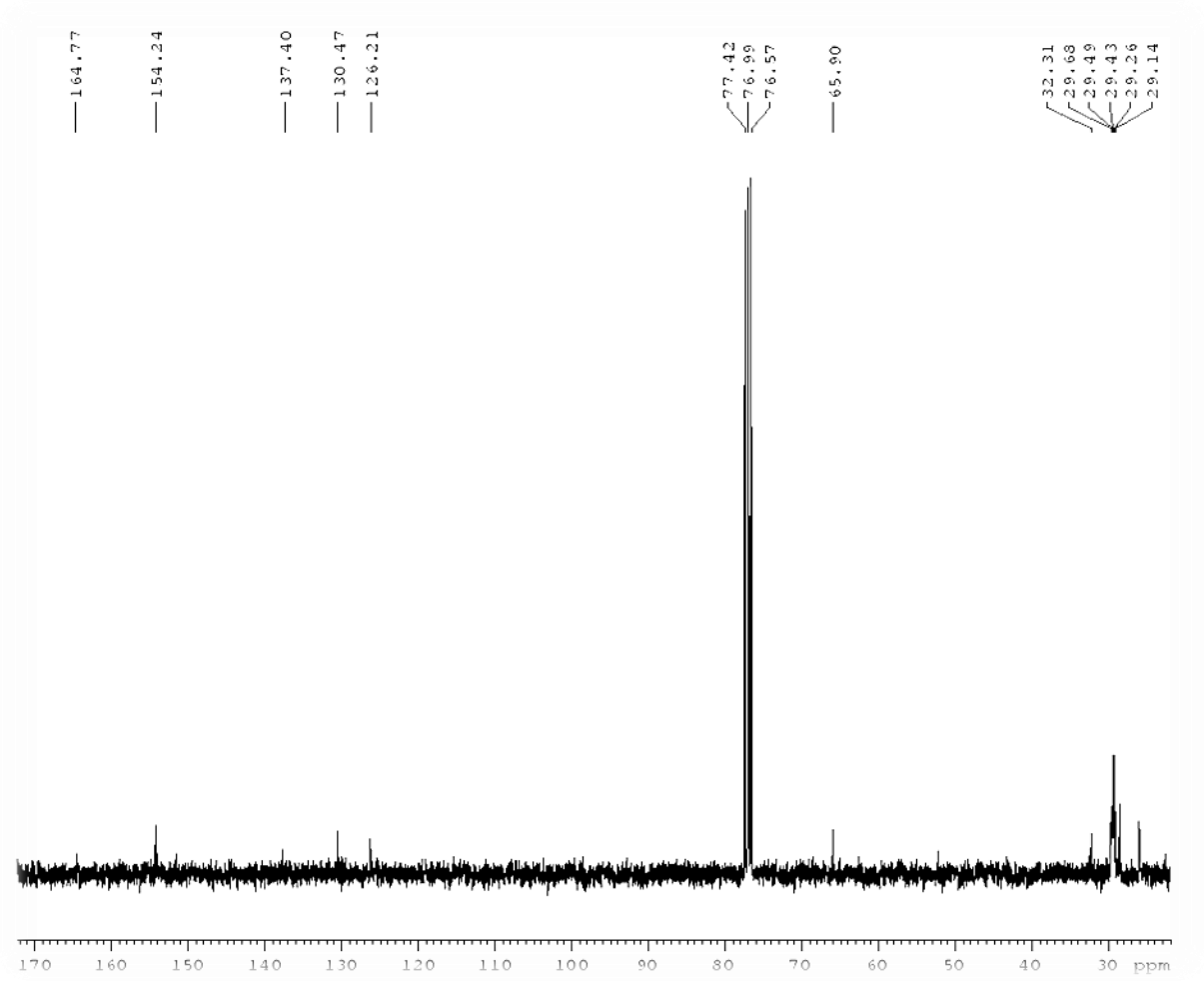

^{1}HNMR for compound ***3-4***

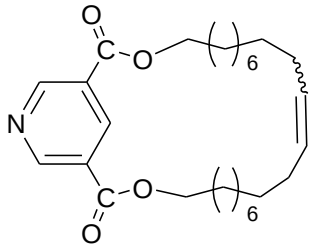

3-4

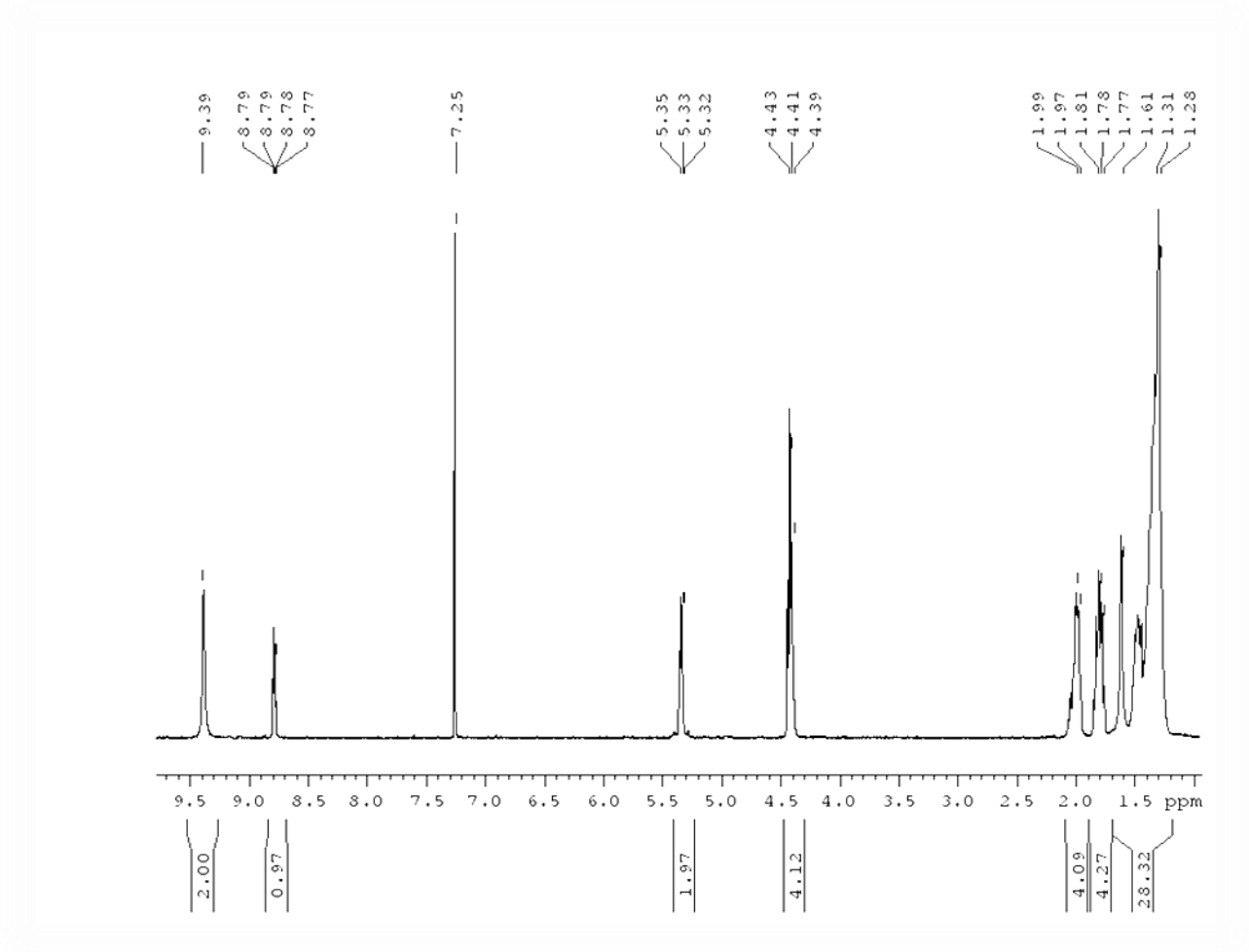

^{1}CNMR for compound ***3-4***

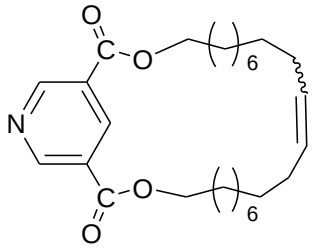

3-4

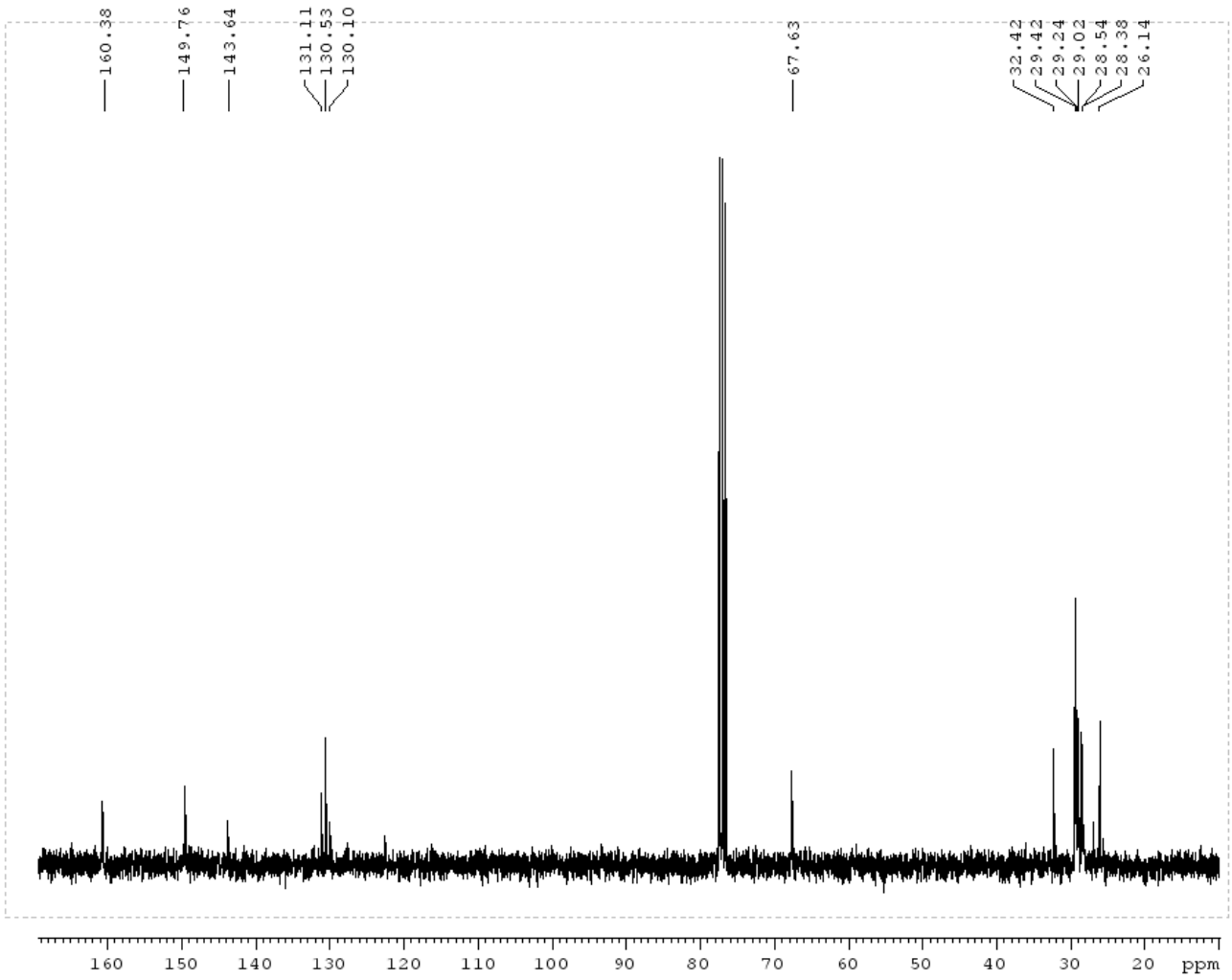

^{1}HNMR for compound ***3-5***

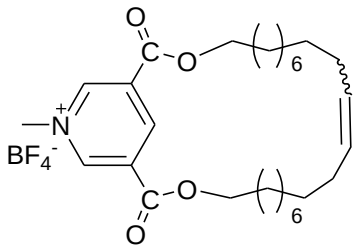

3-5
cycloC20

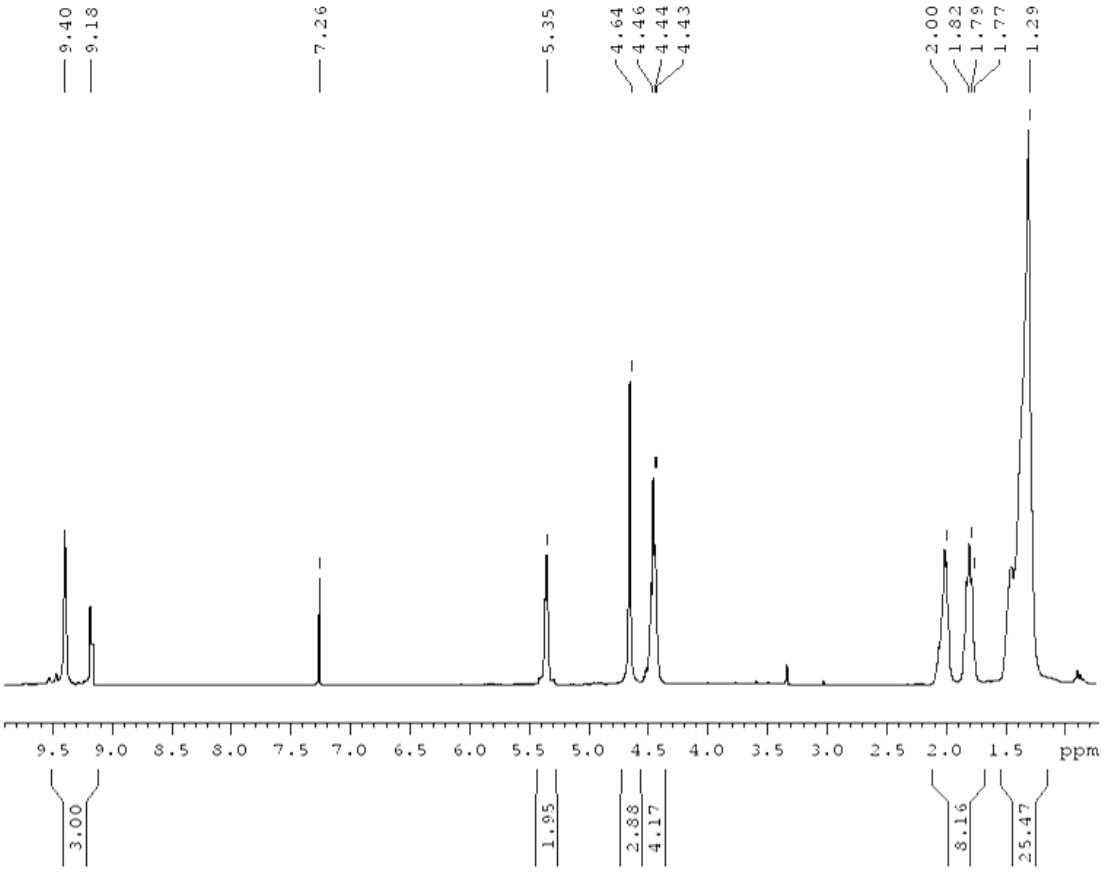

^{13}CNMR for compound ***3-5***

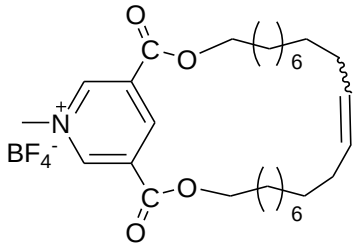

3-5
cycloC20

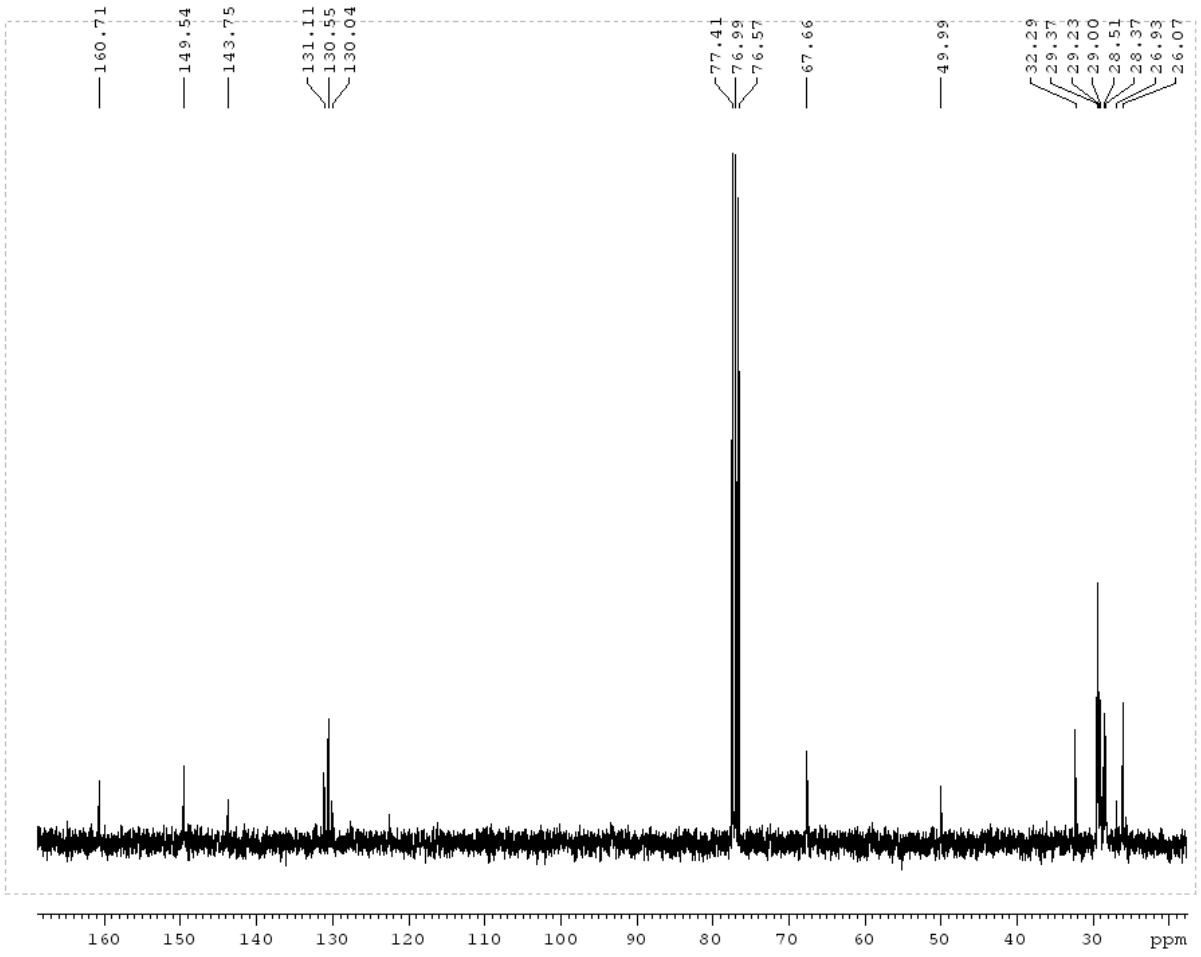

^{1}HNMR for compound ***4-1***

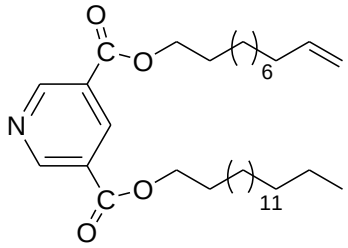

4-1

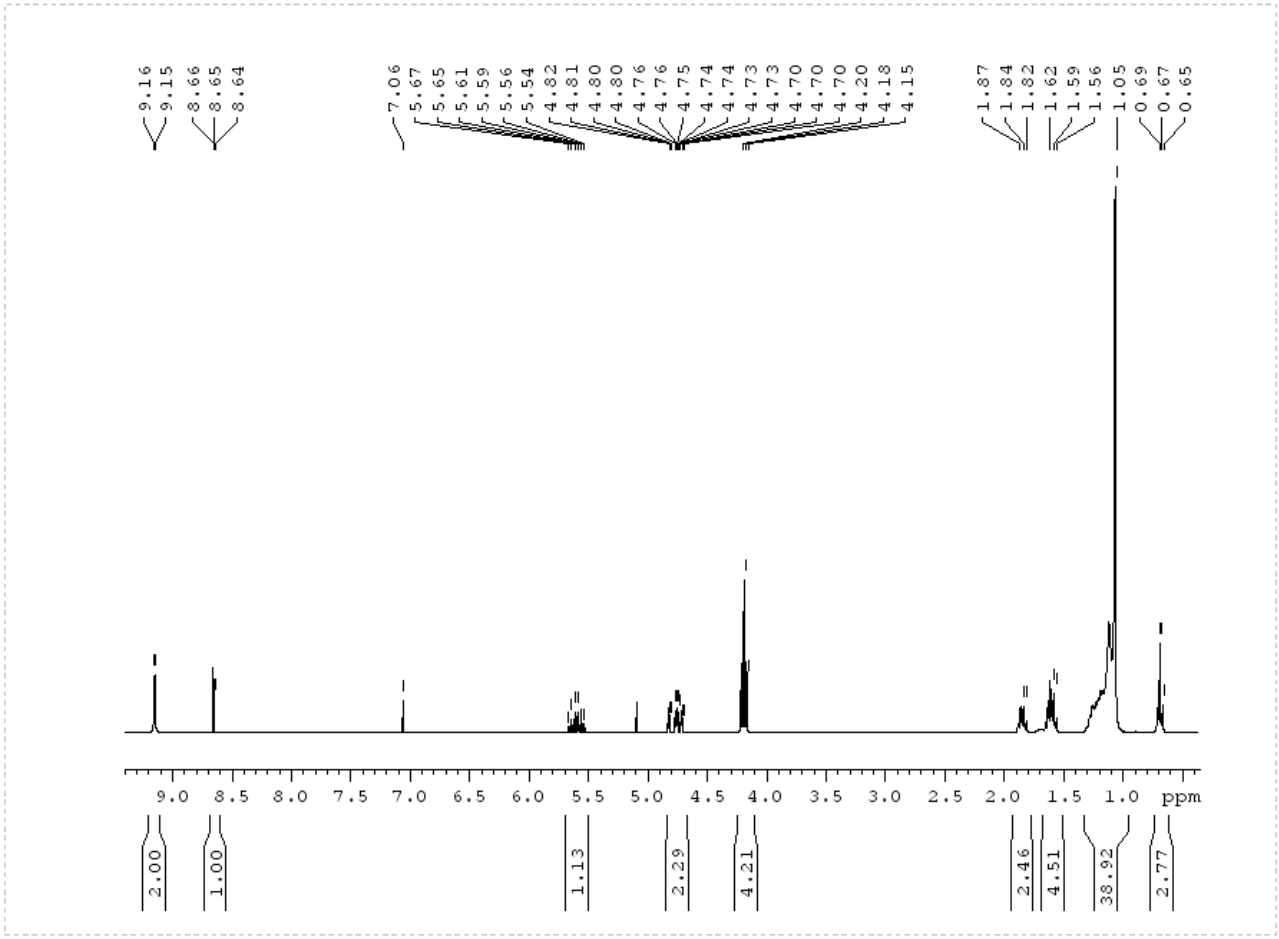

^{13}CNMR for compound ***4-1***

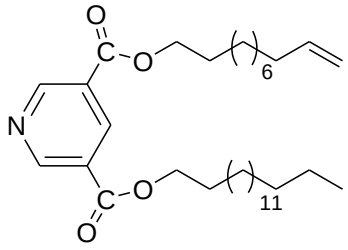

4-1

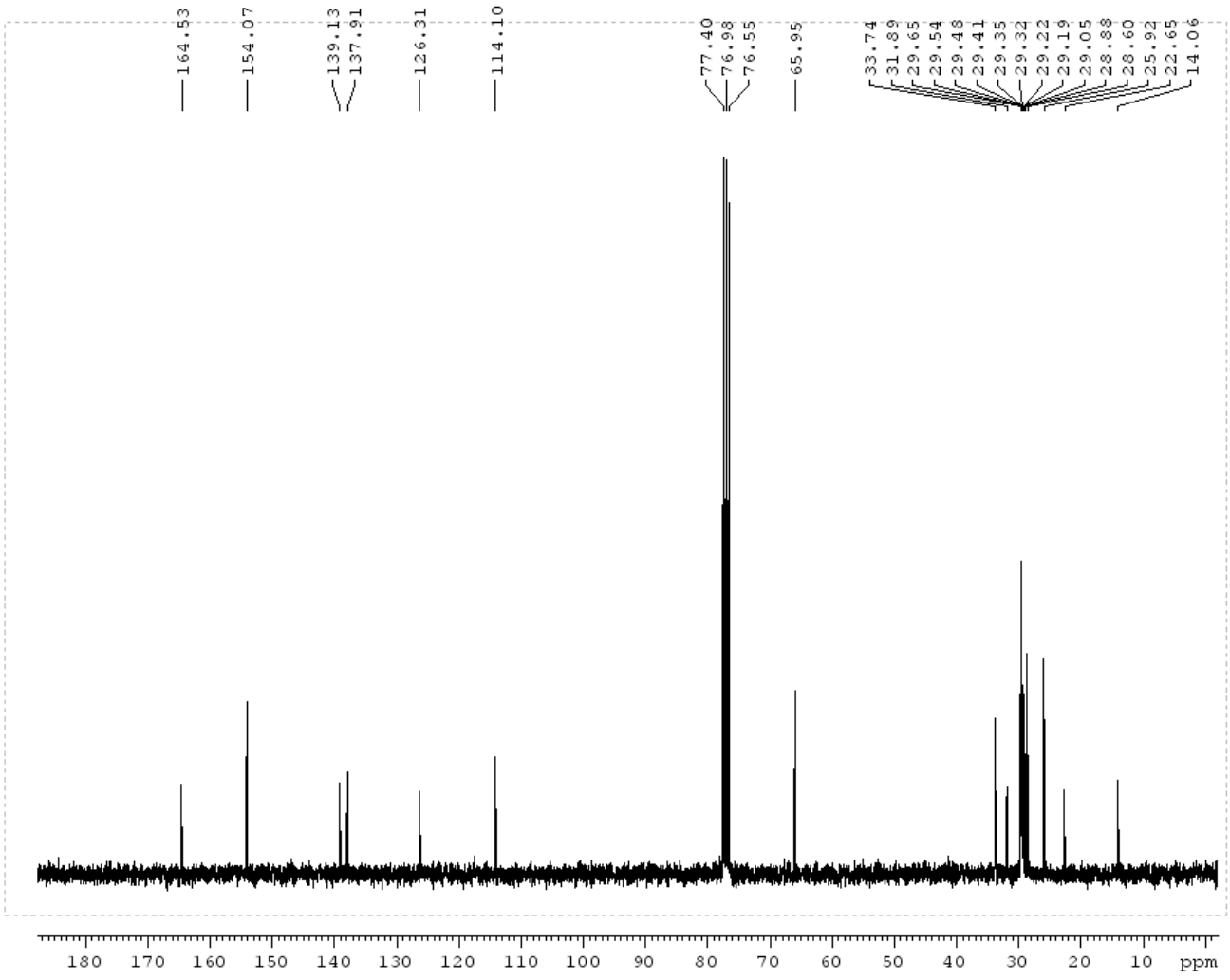

^{1}HNMR for compound ***4-2***

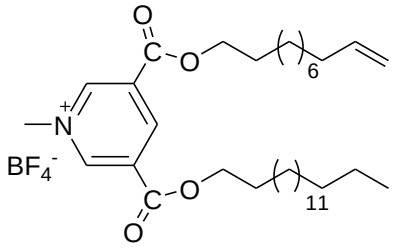

4-2

(C16:0)(C11:1)

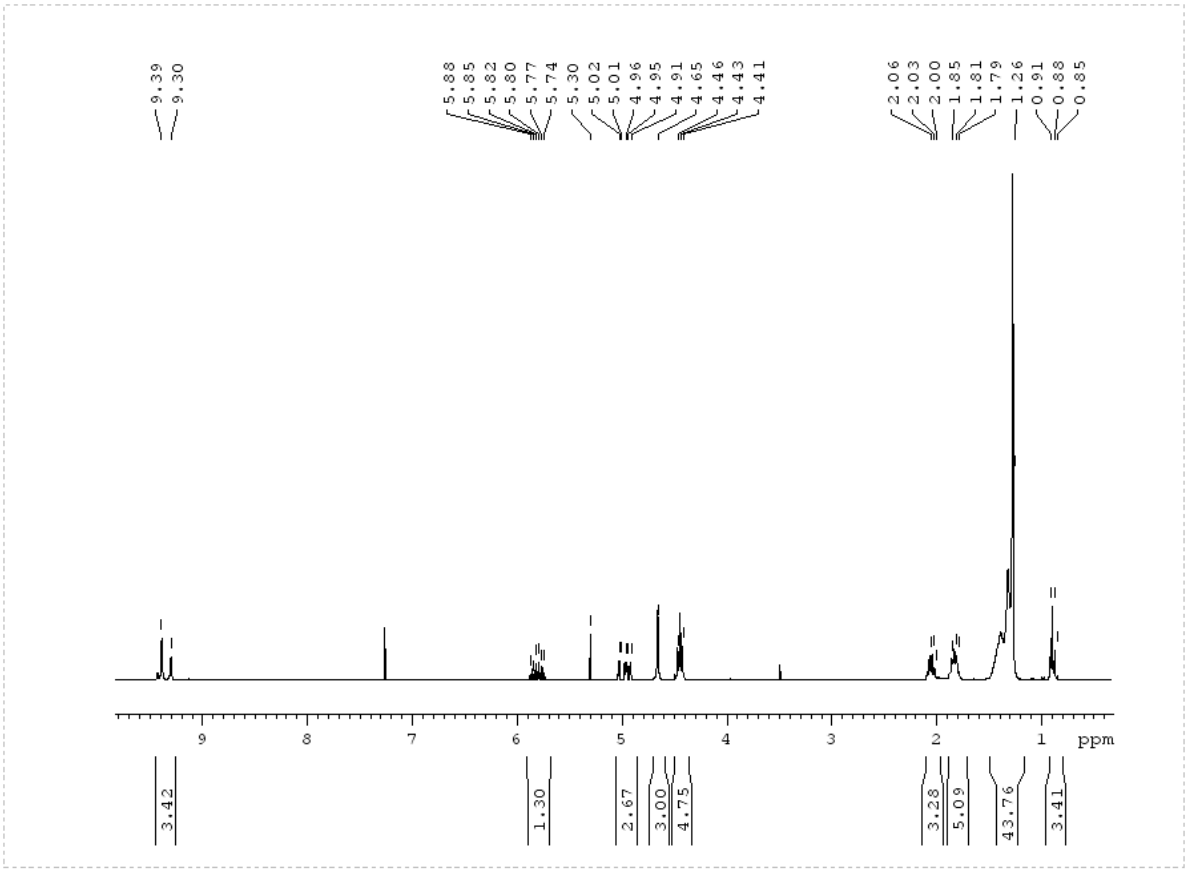

^{13}CNMR for compound ***4-2***

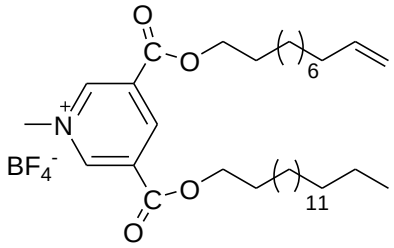

4-2

(C16:0)(C11:1)

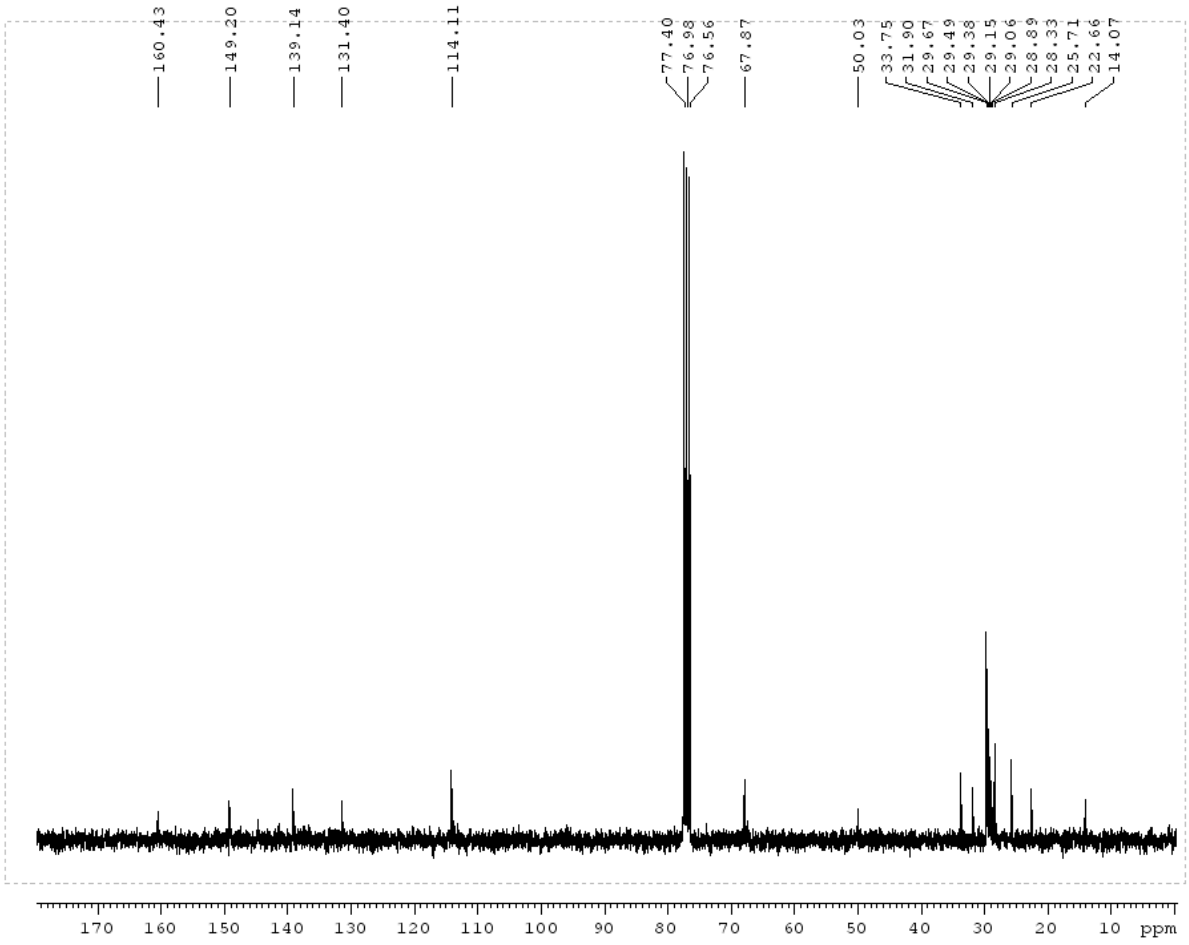

^{1}HNMR for compound ***4-3***

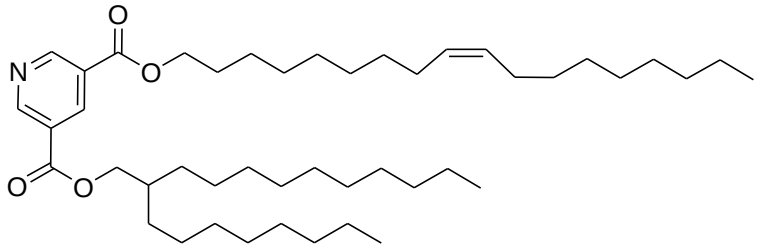

4-3

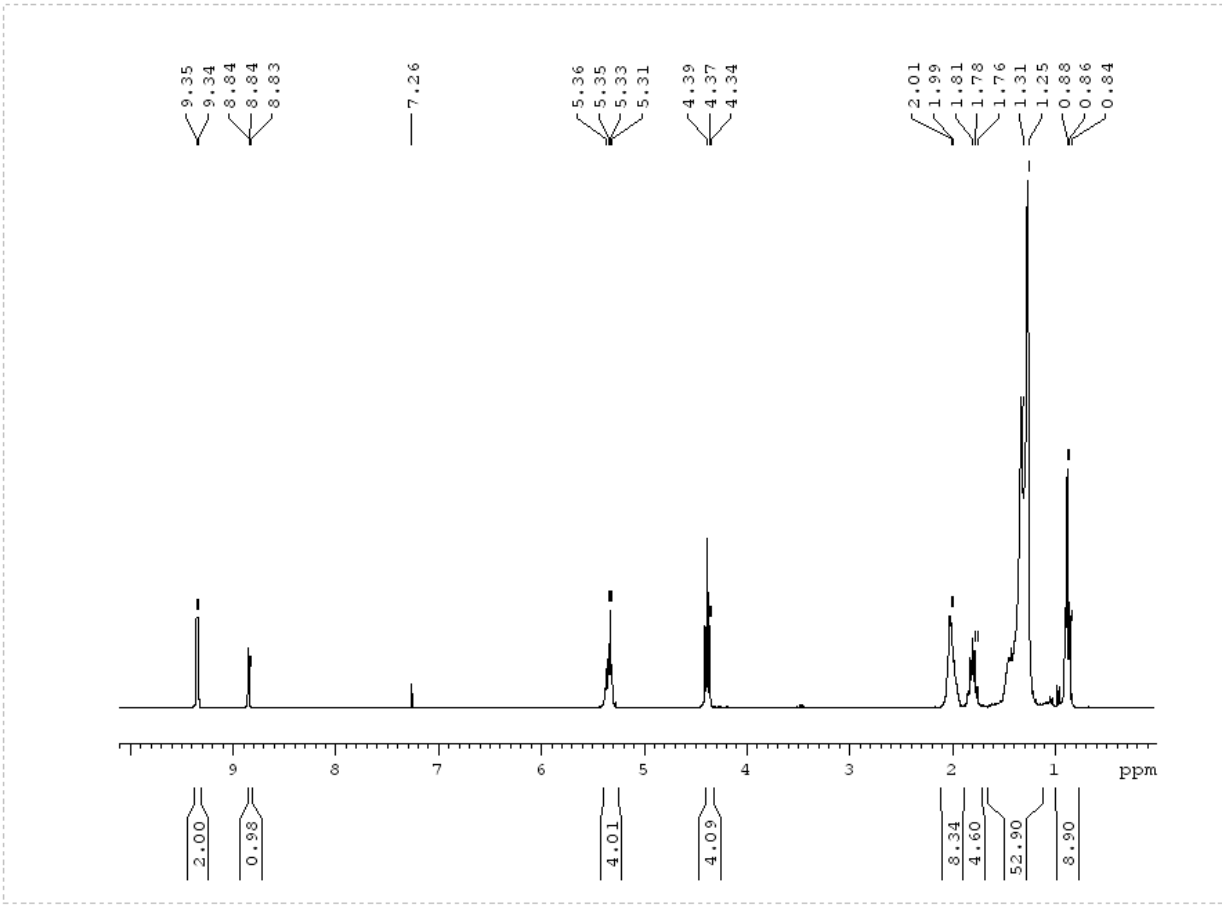

^{13}CNMR for compound ***4-3***

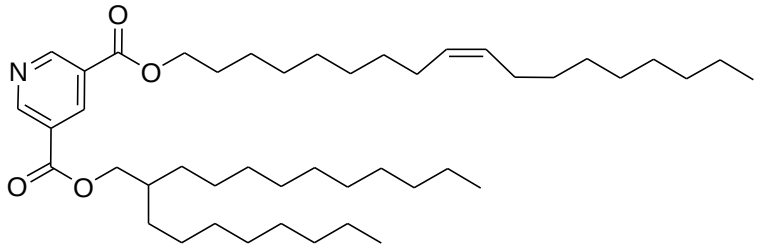

4-3

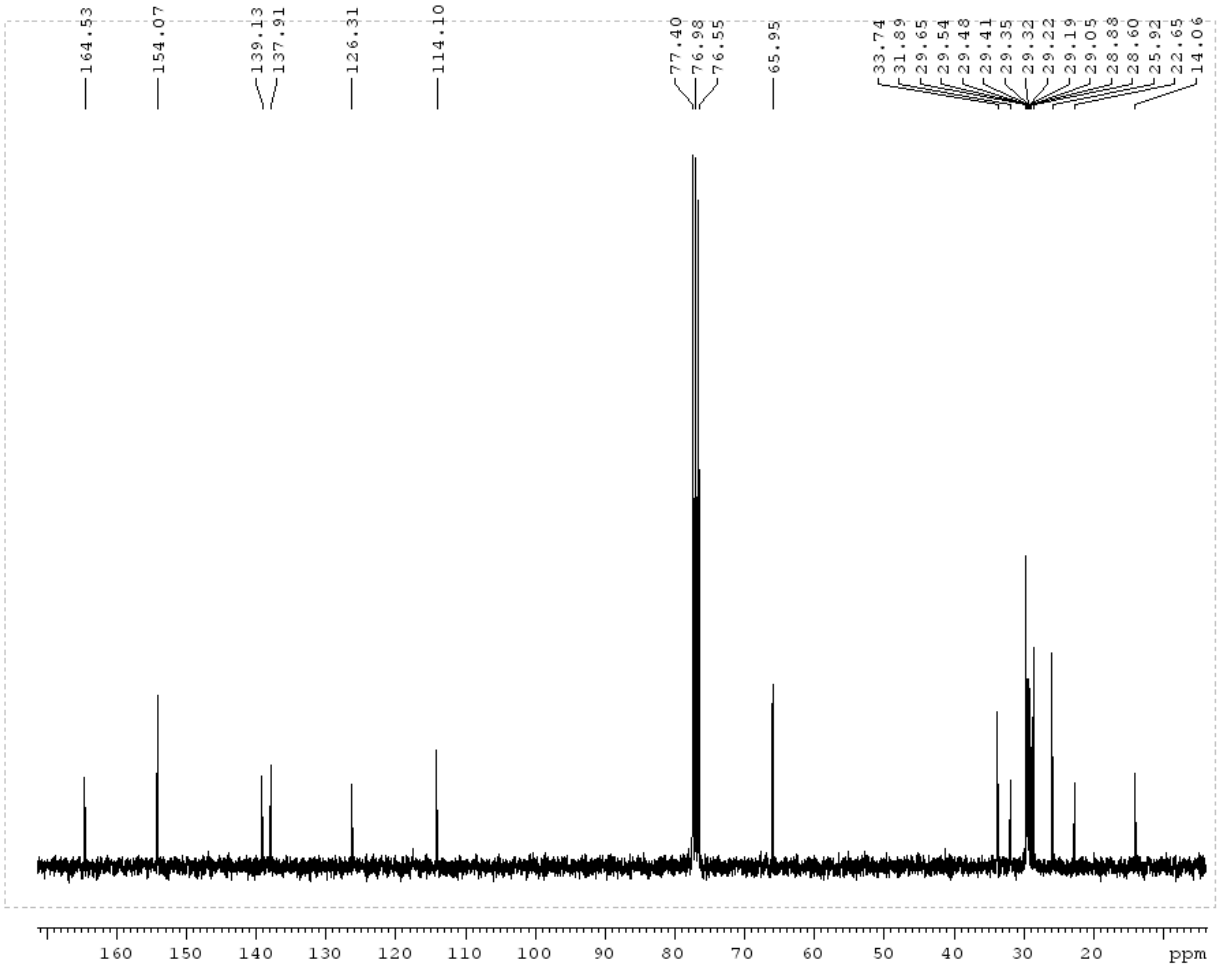

^{1}HNMR for compound ***4-4***

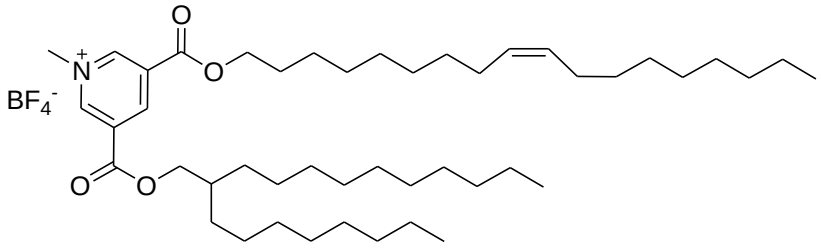

4-4

(C18:1)(brC20:0)

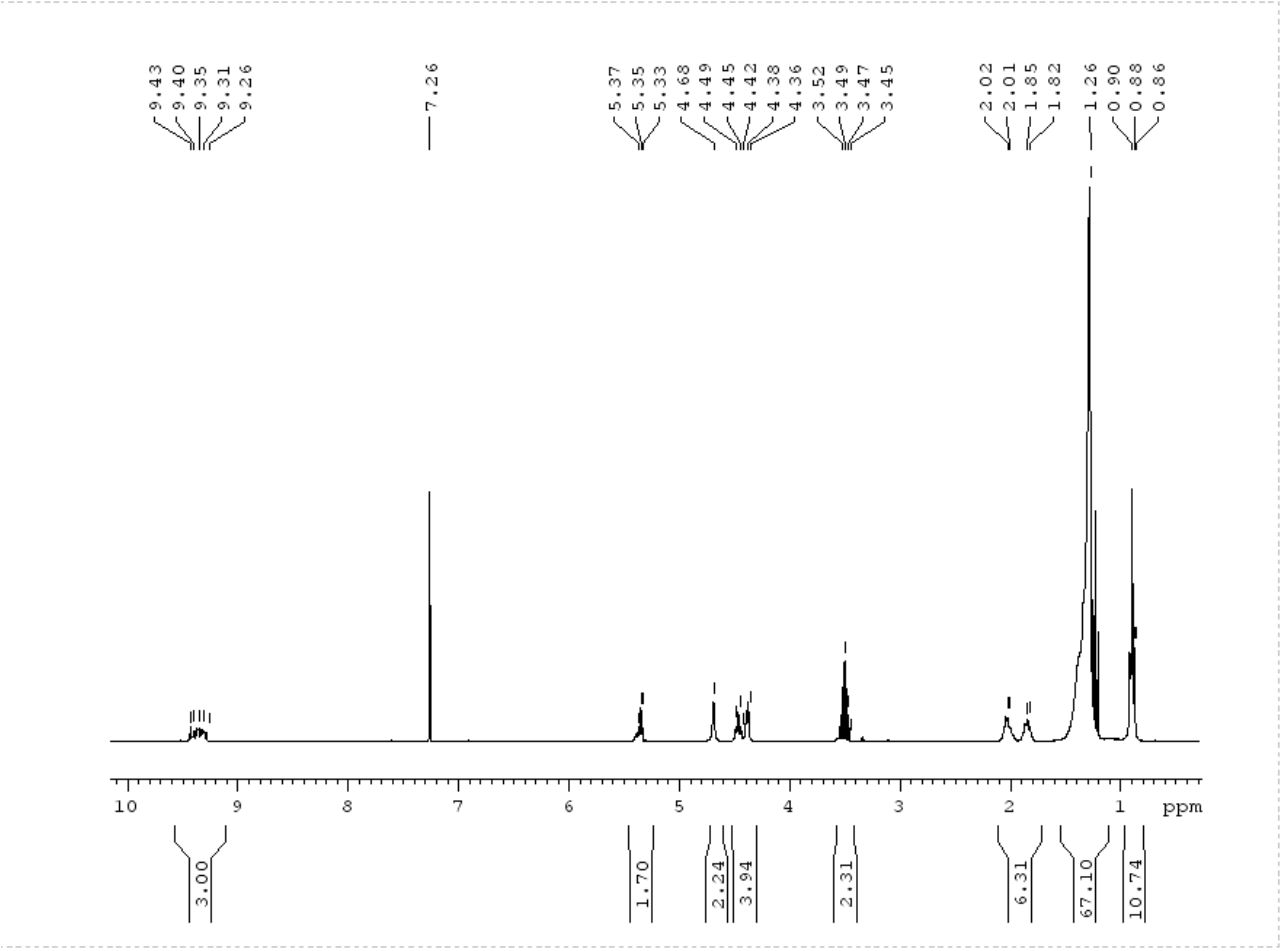

^{13}CNMR for compound ***4-4***

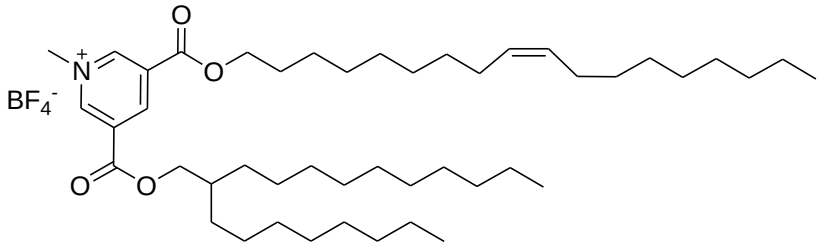

4-4

(C18:1)(brC20:0)

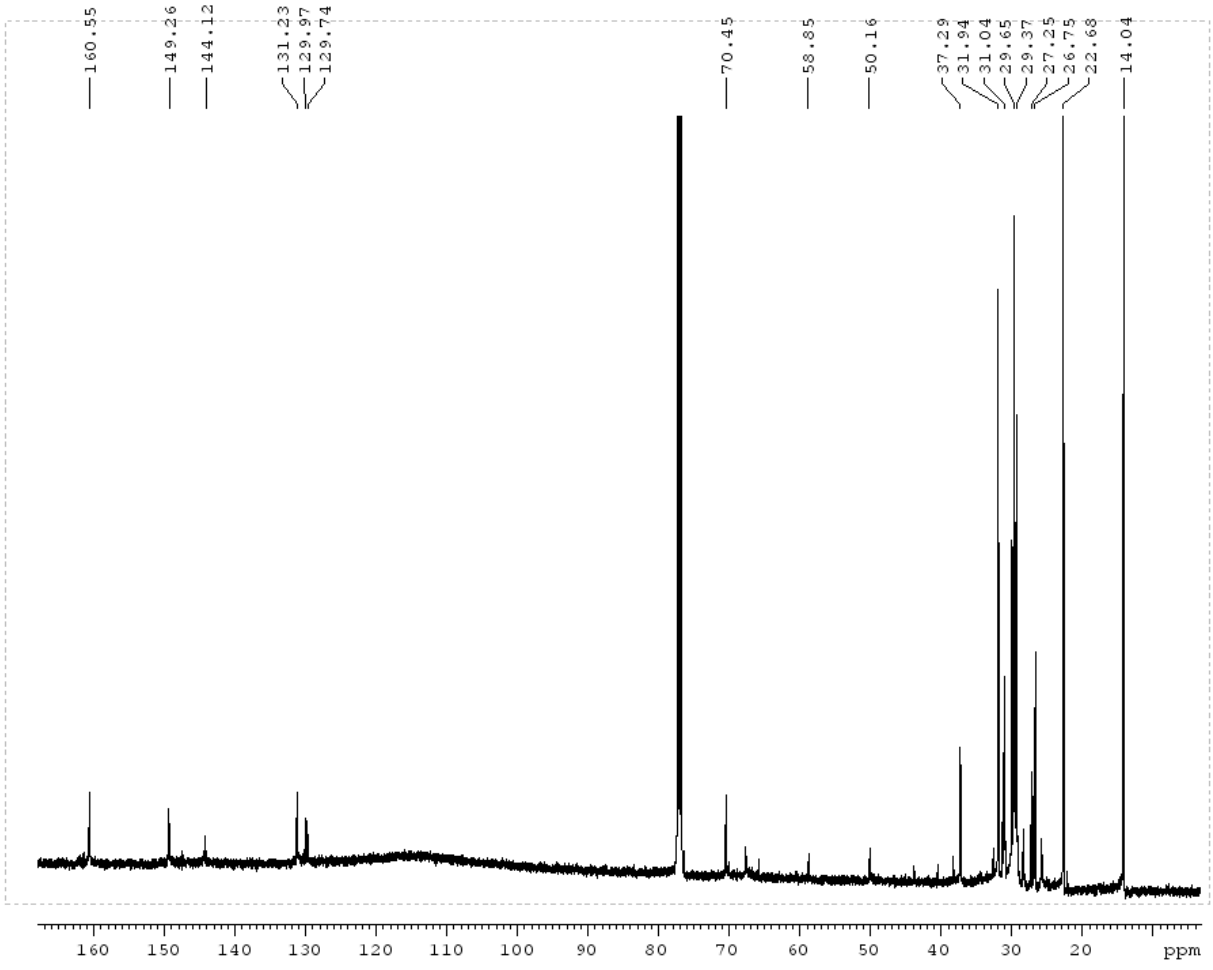

Appendix C: Supplementary information for transfection experiments (only for review)

Appendix C: Supplementary information for transfection experiments (only for review)

This appendix includes supplementary data received from our collaborators in Qatar at the Premedical Unit, Weill Cornell Medical College, from the group of Dr. Michael Pungente. Within the Pungente group Dr. Emile Jubeli, Nada Abdul Khalique, Liji Raju, Ahmed Almeer, Hebatalla Allam, Maryem Al Manaa and Zara Awais formulated the lipoplexes and determined particle sizes, then conducted the gel retardation and DNase I degradation assays, followed by transfection and cytotoxicity bioassays. The small angel X-ray scattering (SAXS) experiments were conducted at the European Synchrotron Radiation Facility in Grenoble, France. Samples were prepared on site by Dr. Michael Pungente, Dr. Emile Jubeli, Nada Abdul Khalique and Liji Raju. The experiments were conducted under the supervision of Prof. David Nicholson, Norwegian University of Science and Technology with he data being analyzed by Dr. Helge Larsen, University of Stavanger, Norway.

This Appendix presents supporting data form collaborators from which the various sections of the thesis were derived. The following table shows the correspondences to thesis materials.

Experiment number	Thesis section	Appendix section	Compounds
Exp 1	Chapter 4.1	Section C.1 Page 2-9	**diC16:0**, **diC16:1**
Exp 7	Chapter 5.2	Section C.2 Page 9-16	**diCn:0 12 < n< 20**
Exp 8	Chapter 5.3.1 & 5.3.2	Section C.3 & C.4 Page 17-28	**diC9:0**, **diisoC9:0** **diC20:0**, **dibrC20:0**
Exp 9	Chapter 5.3.3	Section C.5 Page 28-35	**Blends 50**, **66**, **85**
Exp 17	Chapter 5.4	Section C.6 Page 35-42	Ternary synthesized mixture, binary blend

C.1.1-Liposome/lipoplex formulation and particle sizing

A thin layer of lipid was prepared by removal of the ethanol under reduced pressure from the desired lipid mixture solution and then hydrated in buffer and sonicated to give

liposomes. These liposomes were sized using dynamic light scattering (DLS) that indicated diameters in the range d_H = 360–1000 nm, with polydispersity index (PDI) values ranging from 0.2 to 0.6 (Figure C.1).

The prepared liposomes with varied formulation were combined with negatively charged DNA to form lipoplexes driven by electrostatic interaction between the cationic lipids and DNA. Particle sizes of the lipoplexes were found between d_H = 380–3900 nm, with PDI values ranging from 0.2 to 0.9 (Figure C.1). These large lipoplex particle sizes with high PDI values are associated with the highest N/P molar charge ratios, and are believed to be a result of aggregation and fusion of the liposomes during lipoplex formation in the buffer.

Lipoplexes	N:P ratio	Z-Ave (d.nm)	PdI	Peak 1 Ave
Di16:0/EPC/DOPE	0.5	890.9	0.3	1042.7
	1.5	981.6	0.4	1242.7
	3	1375.7	0.4	1067.2
	5	1205.3	0.4	1331.3
	10	1160.3	0.4	1048.6
Di16:1/EPC/DOPE	0.5	1142.7	0.3	1454.0
	1.5	1334.7	0.3	1488.7
	3	1568.3	0.4	1601.7
	5	2380.7	0.6	1042.7
	10	1118.3	0.3	1192.0
EPC/DOPE	0.5	616.4	0.6	948.1
	1.5	1392.0	0.4	2066.7
	3	1323.0	0.4	1503.3
	5	1502.0	0.4	1417.7
	10	193.4	0.7	127.2
Di16:0/EPC/Chol	0.5	876.2	0.3	1391.6
	1.5	952.9	0.3	1216.0
	3	1335.3	0.4	1488.7
	5	1203.2	0.4	999.4
	10	1244.0	0.5	2344.3
Di16:1/EPC/Chol	0.5	497.8	0.3	557.2
	1.5	436.8	0.3	556.8
	3	1290.7	0.4	1003.0
	5	9493.3	0.5	115.9
	10	2102.0	0.7	897.8
EPC/Chol	0.5	531.1	0.2	582.2
	1.5	1517.7	0.6	2606.3
	3	3808.3	0.7	2343.6
	5	2293.3	0.8	2236.1
	10	650.2	0.3	939.6

2MM LIPOSOMES	Z-Ave (d.nm)	PdI	Peak 1 Ave
Di16:0/EPC/DOPE	671.5	0.5	1202.2
Di16:1/EPC/DOPE	288.4	0.4	325.7
EPC/DOPE	108.6	0.3	143.6
Di16:0/EPC/Chol	501.4	0.5	664.4
Di16:1/EPC/Chol	256.0	0.3	327.9
EPC/Chol	160.3	0.6	230.3

Figure C.1-Sizing information for liposomes and lipoplexes with cationic lipids diC16:0 and diC16:1 with EPC and DOPE and cholesterol as co-lipids

C.1.2-Gel retardation and DNase I degradation assays of lipoplex (liposome-DNA) formulations

The gel retardation assay is used to assess the binding of DNA to liposomes. The data is given in Figure C2. These results show that as the N/P molar charge ratio of the formulation increases, the binding of DNA to the lipoplex improves (Figure C.2-(A)). The lipoplex formulations of EPC/DOPE and EPC/cholesterol show complete retention at a N/P molar charge ratios 3 and higher, whereas the formulation of **diC16:0** and **diC16:1** with either DOPE or cholesterol exhibited complete retention at N/P molar charge ratio 5 and above.

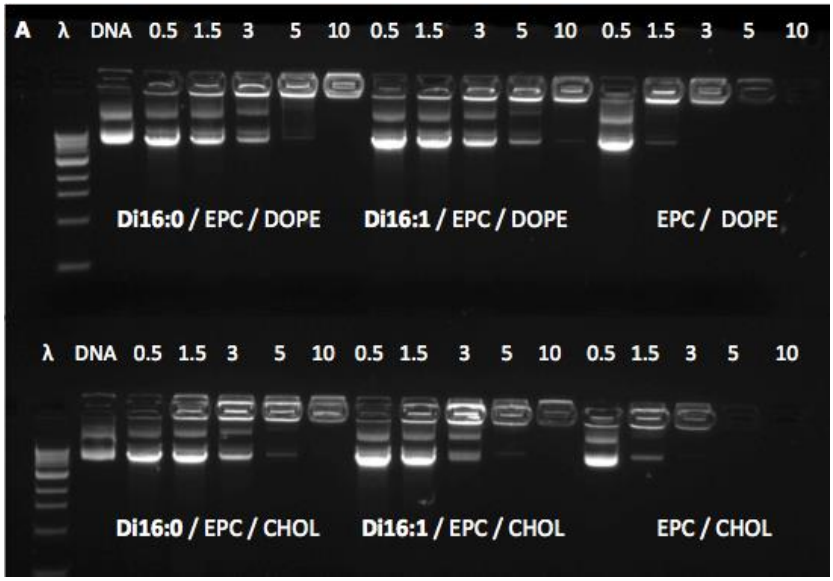

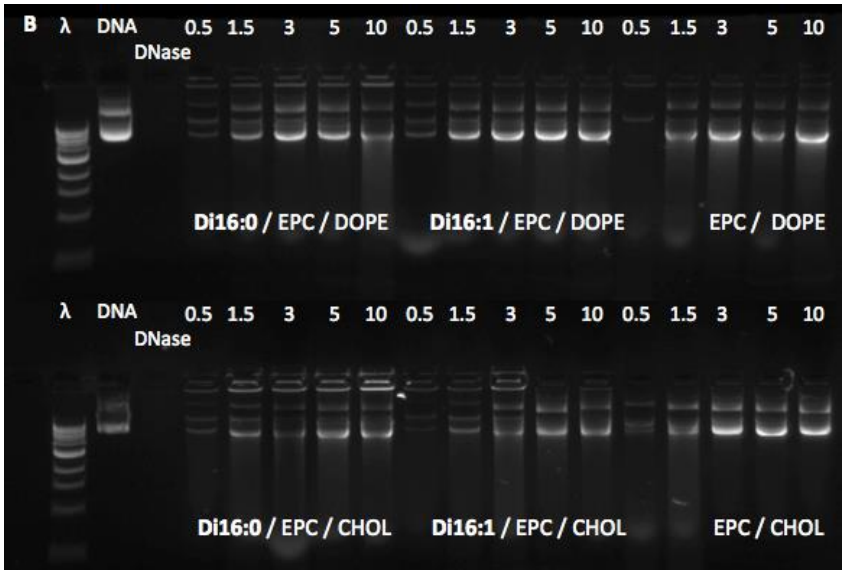

Figure C.2-(A) Gel retardation assay and (B) DNase I degradation assay of diC16:0 (DiC16:0) and diC16:1 (DiC16:1) co-formulated with commercial lipid EPC and neutral co-lipid DOPE or cholesterol at molar N/P molar charge ratios 0.5 to 10, and run through a 1% agarose gel impregnated with the pDNA gel stain, ethidium bromide. Lanes λ and D denote the 1 kb DNA ladder and pDNA, respectively.

A DNase I degradation assay was used to determine the accessibility of the lipid-associated DNA toward nucleases. All formulations at N/P molar charge ratios greater than 0.5 showed comparable DNA protection from nuclease degradation, though formulations with cholesterol showed less degradation compared to formulations with DOPE as the co-lipid (Figure C.2-(B)). These assays imply that below a critical value of CR the DNA can easily dissociate from the complex, but there is still some protection afforded to the DNA by the lipoplex.

C.1.3-Transfection efficiency and cytotoxicity

The transfection efficiency and cytotoxicity of the synthesized pyridinium lipids **diC16:0** and **diC16:1** with EPC as the co-cationic lipids in formulations with neutral co-

lipids DOPE and cholesterol has been studied and compared with Lipofectamine 2000™ as the positive control.

To determine the relative gene transfer efficiency, lipoplexes were formed using a plasmid that contained a gene encoding the enzyme, β-galactosidase (β-gal). CHO-K1 cells were chosen based on their common use as a target for transfection. All formulations were tested in three sets of triplicates each (total n = 9; mean ± SE) with the exception of Lipofectamine 2000™, which was tested in a single triplicate set (n = 3; mean ± SD). β-Galactosidase activity and sample protein concentration were determined 48 h after transfection (Figure C.3).

All pyridinium lipid formulations showed higher activity than the cells incubated with free soluble *p*DNA. The results show that formulations with cholesterol as the co-lipid gave better transfection compared to those with DOPE as co-lipid. The highest activity of **diC16:1**/EPC/Chol formulation at N/P molar charge ratio 3 was approximately 15-20% less efficient than Lipofectamine2000™.

Formulations of pyridinium lipids with EPC and EPC alone both (with DOPE) proved to be less toxic compared to those formulation with Cholesterol as the co-lipid. In general, all formulations showed less toxicity compared to Lipofectamine 2000™ (Figure C.3).

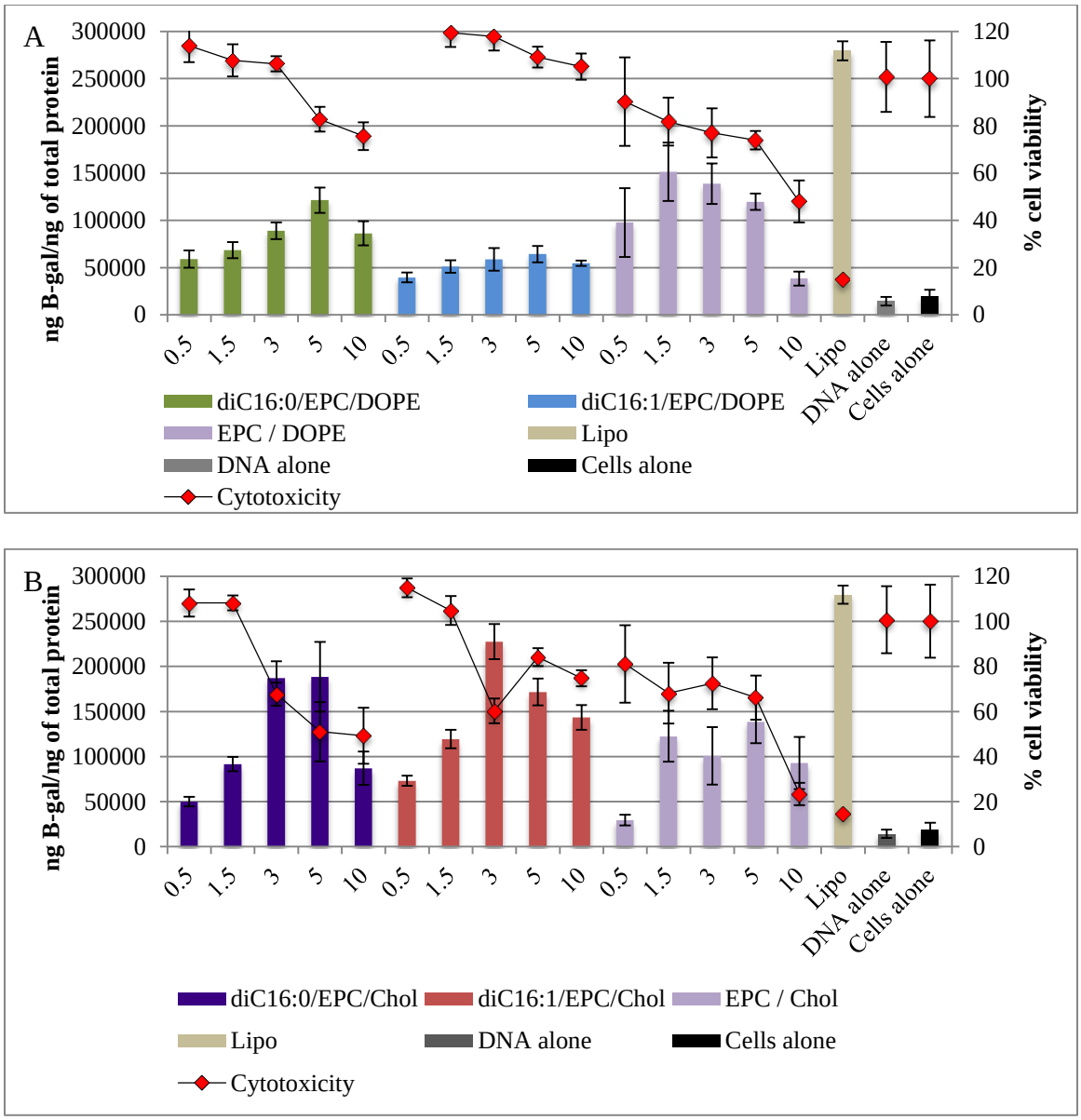

Figure C.3-Transfection efficiency and cytotoxicity (after 48 h) of synthetic lipid diC16:0 or diC16:1/co-lipid/DNA lipoplexes compared to EPC/co-lipid/DNA at molar N/P molar charge ratio of 0.5 to 10 (n = 9; mean ± SD) and Lipofectamine 2000™ (Lipo) (n = 3; mean ± SE) as positive controls, and plasmid DNA alone and CHO-K1 cells alone as negative controls (where A: co-lipid = DOPE; and B: co-lipid = cholesterol).

C.1.4-Fluorescence imaging

A green fluorescent protein (GFP) expressing plasmid was utilized to visually study and compare the efficacy of the various lipoplex formulations. Cells were incubated with

lipoplexes for 4 h then with complete RPMI media for further 44 h, and finally were imaged via inverted epifluorescence microscope (Figure C.4). The formulations with diC16:0 showed a small number of GFP expression cells, exhibiting moderate transfection efficiency. However, the number of GFP expression cells was higher in formulations with cholesterol in comparison to those with DOPE. Formulations with **diC16:1** with DOPE showed a similar efficiency, however when co-formulated with cholesterol, it resulted in much higher efficiency, shown by the greater GFP expression cells.

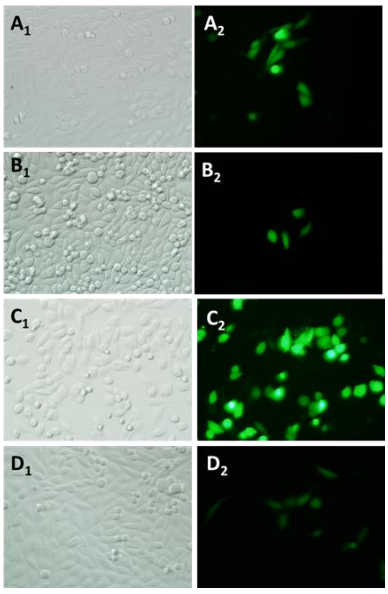

Figure C.4-Fluorescence images of GFP transfected cells. Transfection achieved with the pyridinium lipoplex formulations diC16:0/EPC/Chol (A), diC16:0/EPC/DOPE (B), diC16:1/EPC/Chol (C), diC16:1/EPC/DOPE (D) in the CHO-K1 cell line at N: P +/- molar N/P molar charge ratio 3:1. Cells were kept in contact with lipoplexes for 4 h prior to incubated for additional 44 h (48 h after initial transfection), and viewed by phase contrast (left panels) and green fluorescent channel (right panels).

C.1.5-SAXS studies on diC16:0 and diC16:1 lipoplexes

SAXS studies were carried out to determine the morphology of formed lipoplexes with **diC16:0** and **diC16:1** at N/P molar charge ratio 1.5. Results are shown in Figure C.5.

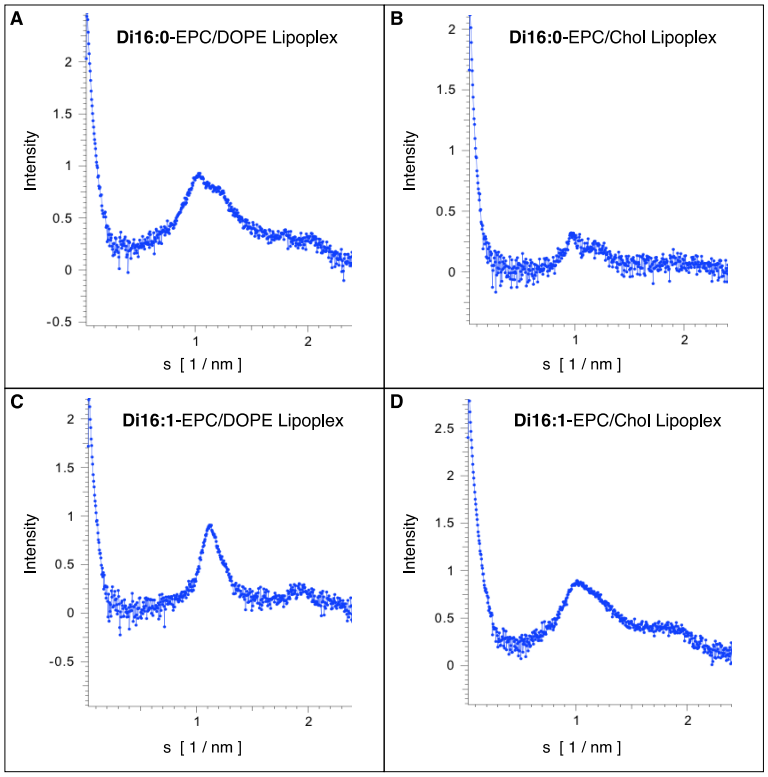

Figure C.5-Results of SAXS experiments on diC16:0 (Di16:0), (A and (B) and diC16:1 (Di16:1), (C) and (D) EPC/co-lipid/pDNA lipoplex formulations at (+/-) N/P molar charge ratio 1.5:1 (Abscissa: modulus of the scattering vector. Ordinate: intensity in arbitrary units.).

The summary of results is shown in Table C.1, showing the hexagonal packing for lipoplexes with the pyridinium lipids.

Table C.1-Summary of SAXS results for diC16:0 and diC16:1/EPC/co-lipid/pDNA and EPC/DOPE and EPC/Chol lipoplex formulations at (+/-) N/P molar charge ratio 1.5:1. δ refers to the actual packing in each case, with an estimated standard deviation of typically 1Å.

Lipid/DNA Lipoplex	Packing	Lattice Parameter	S_{mix}
diC16:0/EPC/DOPE	hexagonal	δ = 70Å	1.1
diC16:0/EPC/Chol	ND	δ = ND	1.2
diC16:1/EPC/DOPE	hexagonal	δ = 65Å	1.1
diC16:1/EPC/Chol	hexagonal	δ = 71Å	1.1
EPC/DOPE	lamellar	δ = 62Å	0.9
EPC/Chol	lamellar	δ = 62Å	1.0

C.2.1-Liposome/lipoplex formulation and particle sizing

Liposomes of synthesized pyridinium lipids (**diC12:0**, **diC14:0**, **diC16:0**, **diC18:0**, **diC18:1** and **diC20:0**) with EPC (commercial cationic lipid) were prepared with either of co-lipids, cholesterol and DOPE, in ratio of 3:2 ratio of cationic lipid to co-lipid.

A thin layer of lipid was prepared by removal of the ethanol under reduced pressure from the desired lipid mixture solution and then hydrated and sonicated to give liposomes. These liposomes were sized using dynamic light scattering (DLS) with diameters in the range d_H = 200–1800 nm, with polydispersity index (PDI) values ranging from 0.2 to 0.9 (Figure C.6).

The prepared liposomes with varied formulation were combined with negatively charged DNA to form lipoplexes driven by electrostatic interaction between the cationic lipids and DNA at fixed N/P molar charge ratio of cationic lipids to DNA of 3. Particle sizes were found between d_H = 340–3600 nm, with PDI values ranging from 0.2 to 0.6 (Figure C.7).

2 mM Liposomes		Z-Ave (d.nm)	PdI
EPC/DOPE		162.3	0.4
diC12:0/EPC/DOPE		1891.7	0.5
diC14:0/EPC/DOPE		908.6	0.5
diC16:0/EPC/DOPE		209.2	0.2
diC18:0/EPC/DOPE		357.1	0.3
diC18:1/EPC/DOPE		723.4	0.8
diC20:0/EPC/DOPE		392.3	0.3
diCbr20:0/EPC/DOPE		542.6	0.9
(18:1)(br20:0)/EPC/DOPE Blend50		481.0	0.5
(18:1)(br20:0)/EPC/DOPE Blend66		1923.7	0.7
(18:1)(br20:0)/EPC/DOPE Blend85		324.4	0.4
EPC/Chol		273.9	0.4
diC12:0/EPC/Chol		1367.0	0.5
diC14:0/EPC/Chol		330.1	0.9
diC16:0/EPC/Chol		842.1	0.5
diC18:0/EPC/Chol		372.4	0.3
diC18:1/EPC/Chol		338.4	0.4
diC20:0/EPC/Chol		668.2	0.5

Figure C.6-Liposome sizing of pyridinium lipids (diC12:0, diC14:0, diC16:0, diC18:0, diC18:1 and diC20:0) with EPC (commercial cationic lipid) were prepared with either of co-lipids, cholesterol and DOPE, in ratio of 3:2 ratio of cationic lipid to co-lipid.

Lipoplexes	N:P	Standard Formulations	
		Z-Ave (d.nm)	PdI
EPC/DOPE	3	5750.7	0.4
diC12:0/EPC/DOPE	3	2964.7	0.6
diC14:0/EPC/DOPE	3	2532.7	0.3
diC16:0/EPC/DOPE	3	3621.7	0.4
diC18:0/EPC/DOPE	3	649.1	0.3
diC18:1/EPC/DOPE	3	4992.3	0.4
diC20:0/EPC/DOPE	3	4219.3	0.4
diCbr20:0/EPC/DOPE	3	661.1	0.3
(18:1)(br20:0)/EPC/DOPE Blend50	3	864.4	0.5
(18:1)(br20:0)/EPC/DOPE Blend66	3	807.3	0.4
(18:1)(br20:0)/EPC/DOPE Blend85	3	470.5	0.3
EPC/Chol	3	4226.7	0.4
diC12:0/EPC/Chol	3	1096.7	0.4
diC14:0/EPC/Chol	3	1227.0	0.5
diC16:0/EPC/Chol	3	2451.3	0.5
diC18:0/EPC/Chol	3	1589.3	0.4
diC18:1/EPC/Chol	3	344.7	0.2
diC20:0/EPC/Chol	3	658.3	0.4

Figure C.7-Lipoplex sizing of pyridinium lipids (diC12:0, diC14:0, diC16:0, diC18:0, diC18:1 and diC20:0) with EPC (commercial cationic lipid) at N/P molar charge ratio of 3 were prepared with either of co-lipids, cholesterol and DOPE, in ratio of 3:2 ratio of cationic lipid to co-lipid.

C.2.2-Gel retardation and DNase I degradation assays of lipoplex (liposome-DNA) formulations

Gel retardation assay is used to assess the binding of DNA to liposomes. The results have shown that the change of chain length in lipids doesn't significantly affect the DNA retention (Figure C.8). The lipoplex formulations of EPC/DOPE and EPC/chol have shown a greater gel retention at N/P molar charge ratio 3, whereas the formulation of pyridinium lipids with either DOPE or cholesterol exhibited but reduced gel retention, relative to EPC.

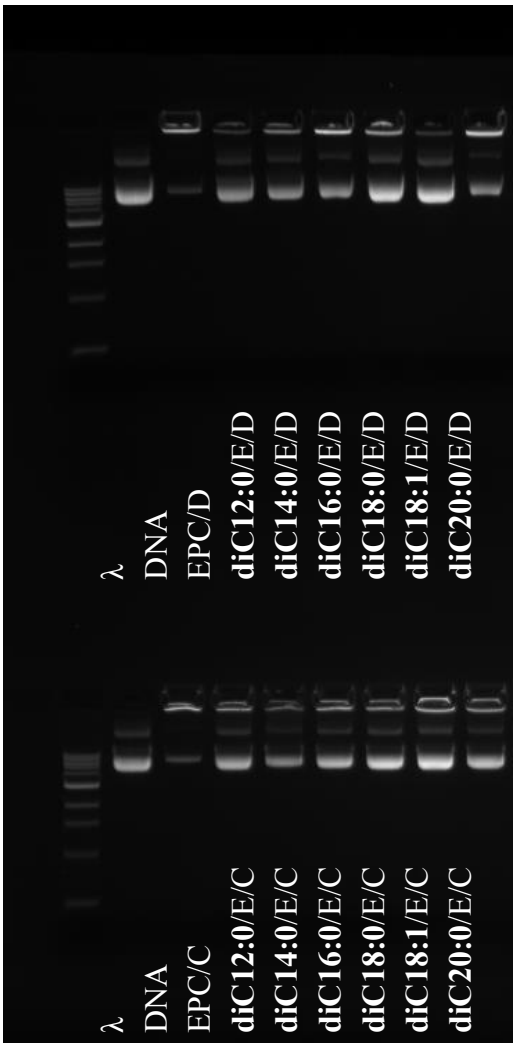

Figure C.8-Gel retardation assay of lipids diC12:0 to diC20:0 co-formulated with commercial lipid EPC (E) and neutral co-lipid DOPE (D) or cholesterol (C) at N/P molar charge ratios 3, and run through a 1% agarose gel impregnated with the pDNA gel stain, ethidium bromide. Lanes λ and DNA denote the 1 kb DNA ladder and pDNA, respectively.

A DNase I degradation assay was used to determine the accessibility of the lipid-associated DNA toward nucleases. All formulation at N/P molar charge ratio 3 showed the same DNA protection from nuclease degradation, though formulations with cholesterol showed less degradation compared to formulations with DOPE as the co-lipid (Figure C.9).

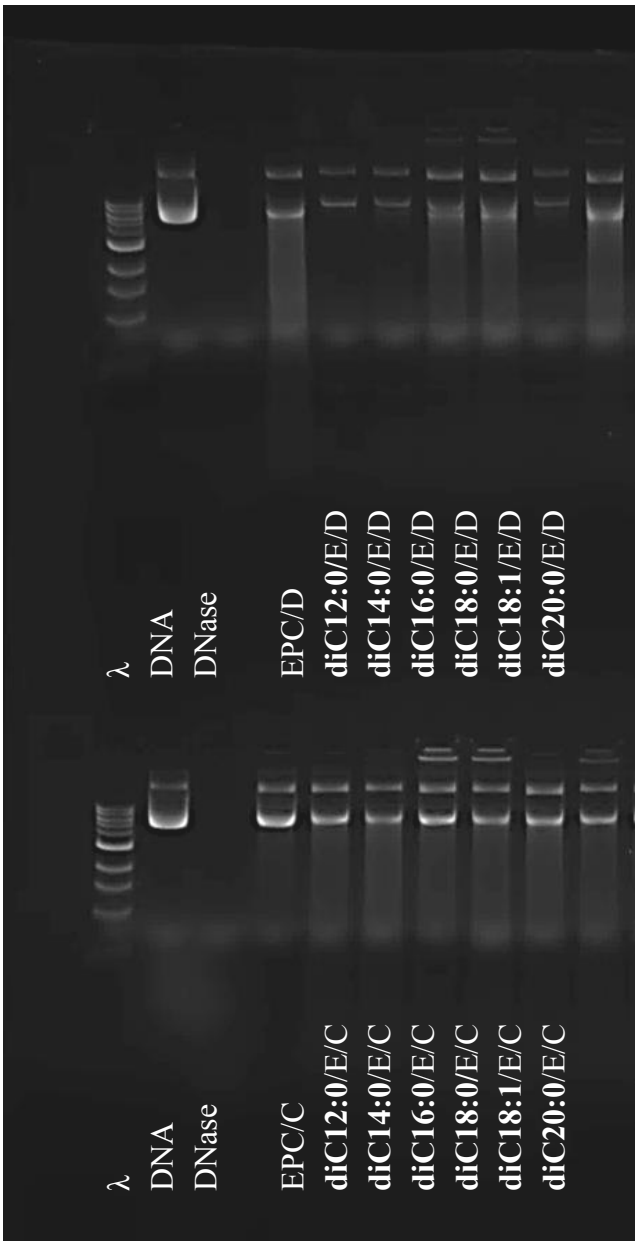

Figure C.9-DNase I degradation assay of lipids diC12:0 to diC20:0 co-formulated with commercial lipid EPC (E) and neutral co-lipid DOPE (D) or cholesterol (C) at N/P molar charge ratios 3, and run through a 1% agarose gel impregnated with the pDNA gel stain, ethidium bromide. Lanes λ and DNA denote the 1 kb DNA ladder and pDNA, respectively.

C.2.3-Transfection efficiency and cytotoxicity

The transfection efficiency and the toxicity of the synthesized pyridinium lipids **diC12:0** to **diC20:0** included Lipofectamine 2000^{TM} as the control.

To determine the relative gene transfer efficiency, lipoplexes were formed using a plasmid that contained a gene encoding the enzyme, β-galactosidase (β-gal). CHO-K1 cells were chosen based on their common use as a target for transfection. All formulations were tested in three sets of triplicates each (total n = 9; mean ± SE) with the exception of Lipofectamine 2000^{TM}, which was tested in a single triplicate set (n = 3; mean ± SD). β-Galactosidase activity and sample protein concentration were determined 48 h after transfection (Figure C.10).

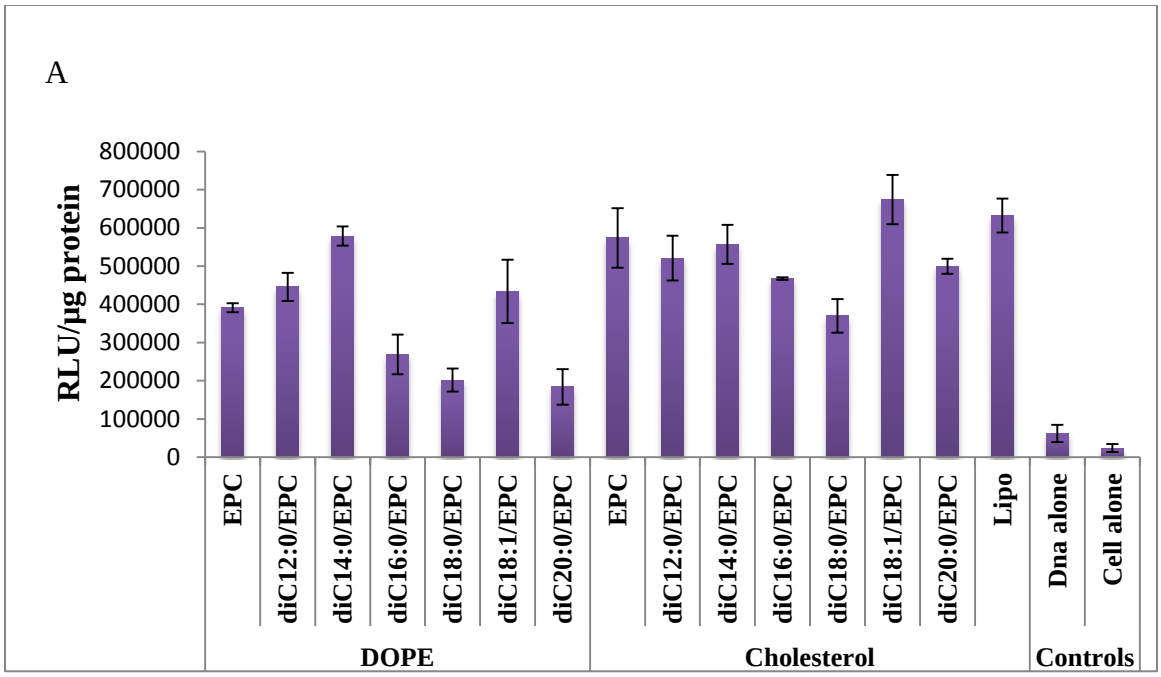

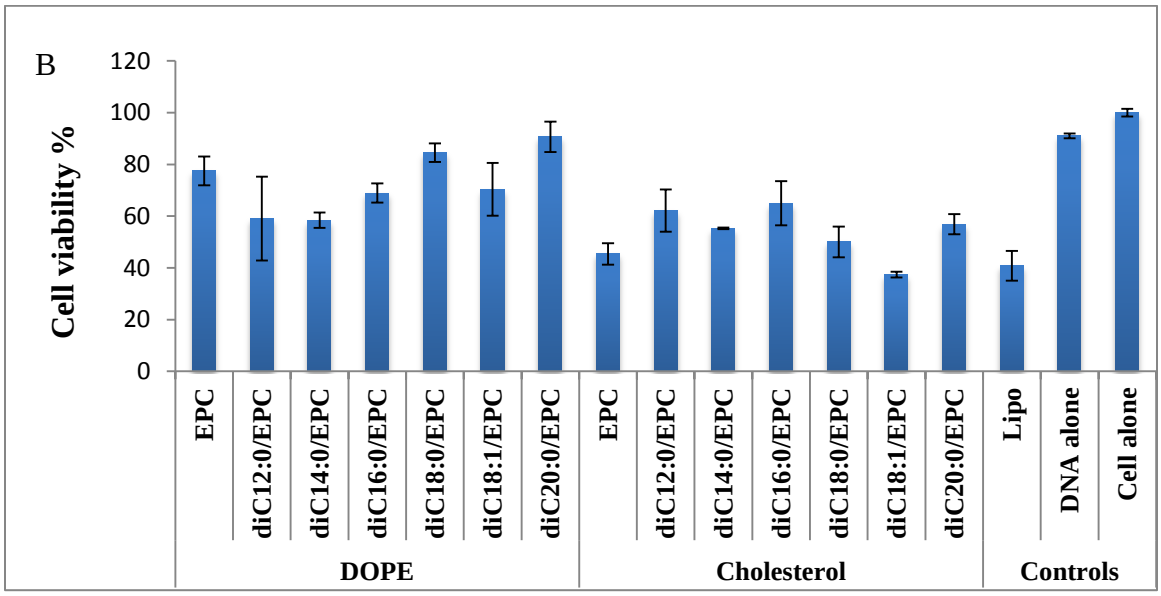

Figure C.10-Transfection efficiency as luminescence readings of β-galactosidase (A) and cytotoxicity (B) (after 48 h) of synthetic lipid diC12:0 to diC20:0/co-lipid/DNA lipoplexes compared to EPC/co-lipid/DNA at N/P molar charge ratio of 3 and Lipofectamine 2000™ (Lipo) (n = 9; mean ± SD) as positive controls, and plasmid DNA alone and CHO-K1 cells alone as negative controls.

C.2.4-SAXS studies on the prepared lipoplexes

SAXS studies were performed on the lipoplexes prepared with pyridinium lipids and co-lipids, DOPE and cholesterol at two N/P molar charge ratios 1.5 (Table C.2) and 3 (Table C.3).

Table C.2-Summary of SAXS results for pyridinium lipids/EPC/co-lipid/pDNA and EPC/DOPE and EPC/Chol lipoplex formulations at (+/-) N/P molar charge ratio 1.5:1. δ refers to the actual packing in each case, with an estimated standard deviation of typically 1Å.

Cationic lipids	Co-Lipid	CR	Packing	Lattice Parameter	S_{mix}
diC12:0/EPC	DOPE	1.5	**Hexagonal?**	δ = 63Å	1.1
diC14:0/EPC	DOPE	1.5	**Hexagonal?**	δ = 69Å	1.1
diC16:0/EPC	DOPE	1.5	**Hexagonal**	δ = 68Å	1.1
diC18:0/EPC	DOPE	1.5	**Hexagonal**	δ = 76-84Å	1.1
diC18:1/EPC	DOPE	1.5	**Hexagonal**	δ = 68Å	1.1
diC20:0/EPC	DOPE	1.5	**Nothing**	δ = NA	1.1
diC12:0/EPC	Cholesterol	1.5	**Hexagonal?**	δ = 80Å	1.1
diC14:0/EPC	Cholesterol	1.5	**Hexagonal**	δ = 84Å	1.1
diC16:0/EPC	Cholesterol	1.5	**Hexagonal?**	δ = 75-90Å	1.1
diC18:0/EPC	Cholesterol	1.5	**Indeterminate**	δ = ND	1.1
diC18:1/EPC	Cholesterol	1.5	**Hexagonal**	δ = 82Å	1.1
diC20:0/EPC	Cholesterol	1.5	**Indeterminate**	δ = ND	1.1

Table C.3-Summary of SAXS results for pyridinium lipids/EPC lipid/pDNA and EPC/DOPE and EPC/Chol lipoplex formulations at (+/-) N/P molar charge ratio 3:1. δ refers to the actual packing in each case, with an estimated standard deviation of typically 1Å.

Cationic lipids	Co-Lipid	CR	Packing	Lattice Parameter	S_{mix}
diC12:0/EPC	DOPE	3	**Hexagonal**	δ = 60-62Å	1.1
diC14:0/EPC	DOPE	3	**Hexagonal**	δ = 64Å	1.1
diC16:0/EPC	DOPE	3	**Indeterminate**	δ = ND	1.1
diC18:0/EPC	DOPE	3	**Hexagonal?**	δ = 73Å	1.1
diC18:1/EPC	DOPE	3	**Nothing**	δ = NA	1.1
diC20:0/EPC	DOPE	3	**Nothing**	δ = NA	1.1
diC12:0/EPC	Cholesterol	3	**Hexagonal?**	δ = 84Å	1.1
diC14:0/EPC	Cholesterol	3	**Indeterminate**	δ = ND	1.1

diC16:0/EPC	Cholesterol	3	**Hexagonal**	δ = 82Å	1.1
diC18:0/EPC	Cholesterol	3	**Lamellar**	δ = 70Å	1.1
diC18:1/EPC	Cholesterol	3	**Indeterminate**	δ = ND	1.1
diC20:0/EPC	Cholesterol	3	**Indeterminate**	δ = ND	1.1

C.3.1-Liposome/lipoplex formulation and particle sizing

Liposomes of synthesized pyridinium lipids with EPC were prepared with DOPE, in ratio of 3:2 ratio of cationic lipid to co-lipid.

A thin layer of lipid was prepared by removal of the ethanol under reduced pressure from the desired lipid mixture solution and then hydrated and sonicated to give liposomes. These liposomes were sized using dynamic light scattering (DLS) with diameters in the range d_H = 200–400 nm, with polydispersity index (PDI) values ranging from 0.2 to 0.5 (Figure C.11).

The prepared liposomes with varied formulation were combined with negatively charged DNA to form lipoplexes driven by electrostatic interaction between the cationic lipids and DNA at a range of N/P molar charge ratio of cationic lipids to DNA of 0.5, 1.5,3,5 and 10. Particle sizes were found between d_H= 800–5800 nm, with PDI values ranging from 0.2 to 0.8 (Figure C.12).

2 mM Liposomes		Z-Ave (d.nm)	PdI
EPC/DOPE		119.0	0.4
Di9:0/EPC/DOPE		196.6	0.2
Diiso9:0/EPC/DOPE		396.3	0.4
Di20:0/EPC/DOPE		369.0	0.4
Di br20:0/EPC/DOPE		473.0	0.5

Figure C.11-Liposome sizing of pyridinium lipids (diC9:0 and diisoC9:0, diC20:0 and dibrC20:0) with EPC (commercial cationic lipid) were prepared with either of co-lipids, cholesterol and DOPE, in ratio of 3:2 ratio of cationic lipid to co-lipid.

Lipoplexes	N:P	Standard Formulations	
		Z-Ave (d.nm)	PdI
EPC/DOPE	0.5	305.9	0.4
	1.5	4725.0	0.7
	3	3365.3	0.5
	5	253.3	0.2
	10	206.3	0.2
Di9:0/EPC/DOPE	0.5	1103.0	0.2
	1.5	1066.7	0.3
	3	834.2	0.3
	5	3782.3	0.3
	10	4756.7	0.6
Diiso9:0/EPC/DOPE	0.5	1394.7	0.3
	1.5	1677.0	0.3
	3	1526.0	0.4
	5	2468.7	0.3
	10	4150.3	0.6
Di20:0/EPC/DOPE	0.5	483.0	0.3
	1.5	541.0	0.3
	3	4388.7	0.5
	5	5339.7	0.4
	10	1989.3	0.4
Di br20:0/EPC/DOPE	0.5	542.7	0.2
	1.5	502.9	0.2
	3	505.2	0.2
	5	569.1	0.3
	10	4135.3	0.8

Figure C.12-Liposome sizing of pyridinium lipids (diC9:0 and diisoC9:0, diC20:0 and dibrC20:0) with EPC (commercial cationic lipid) at N/P molar charge ratio of 0.5 to 10 were prepared with either of co-lipids, cholesterol and DOPE, in ratio of 3:2 ratio of cationic lipid to co-lipid

C.3.2-Gel retardation and DNase I degradation assays of lipoplex (liposome-DNA) formulations

Gel retardation assay is used to assess the binding of DNA to liposomes. The results have shown that binding in general was poor (Figure C.13).

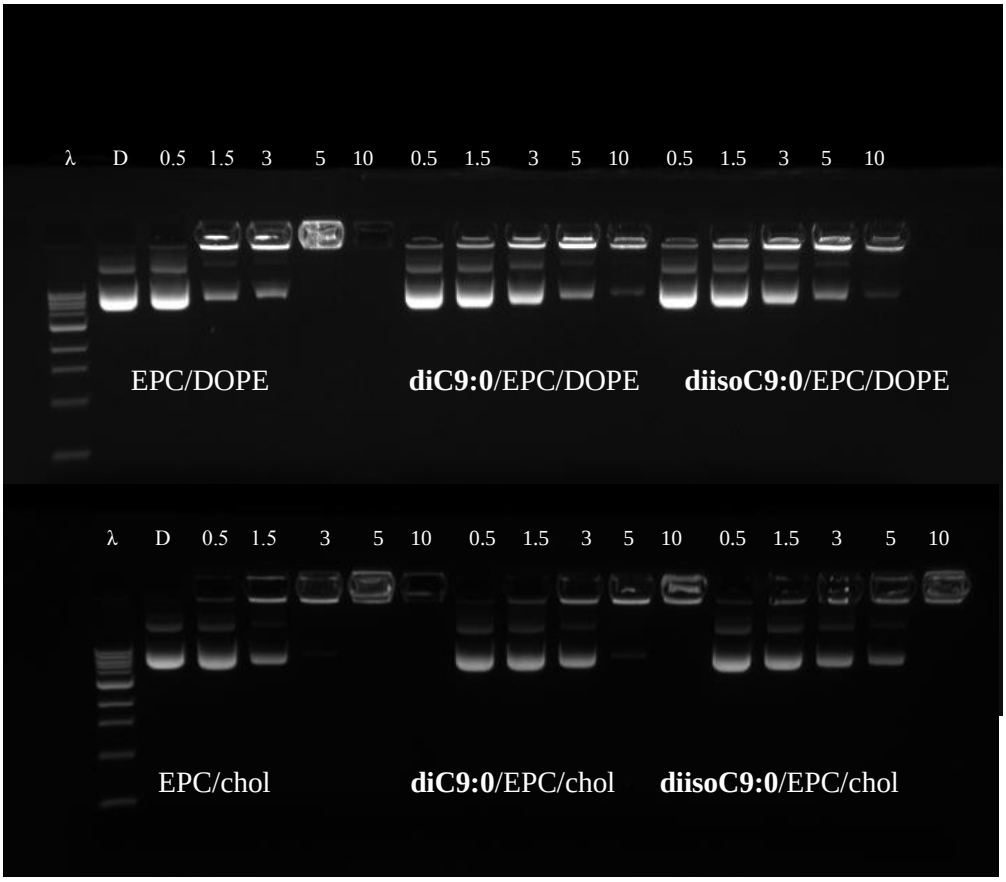

Figure C.13-Gel retardation assay of lipids diC9:0 and diCisoC9:0 co-formulated with commercial lipid EPC and neutral co-lipid DOPE or cholesterol at N/P molar charge ratios 0.5, 1.5, 3, 5 and 10 and run through a 1% agarose gel impregnated with the pDNA gel stain, ethidium bromide. Lanes λ and DNA denote the 1 kb DNA ladder and pDNA, respectively.

A DNase I degradation assay was used to determine the accessibility of the lipid-associated DNA toward nucleases. All formulations showed similar protection of DNA after CR = 1.5 (Figure C.14).

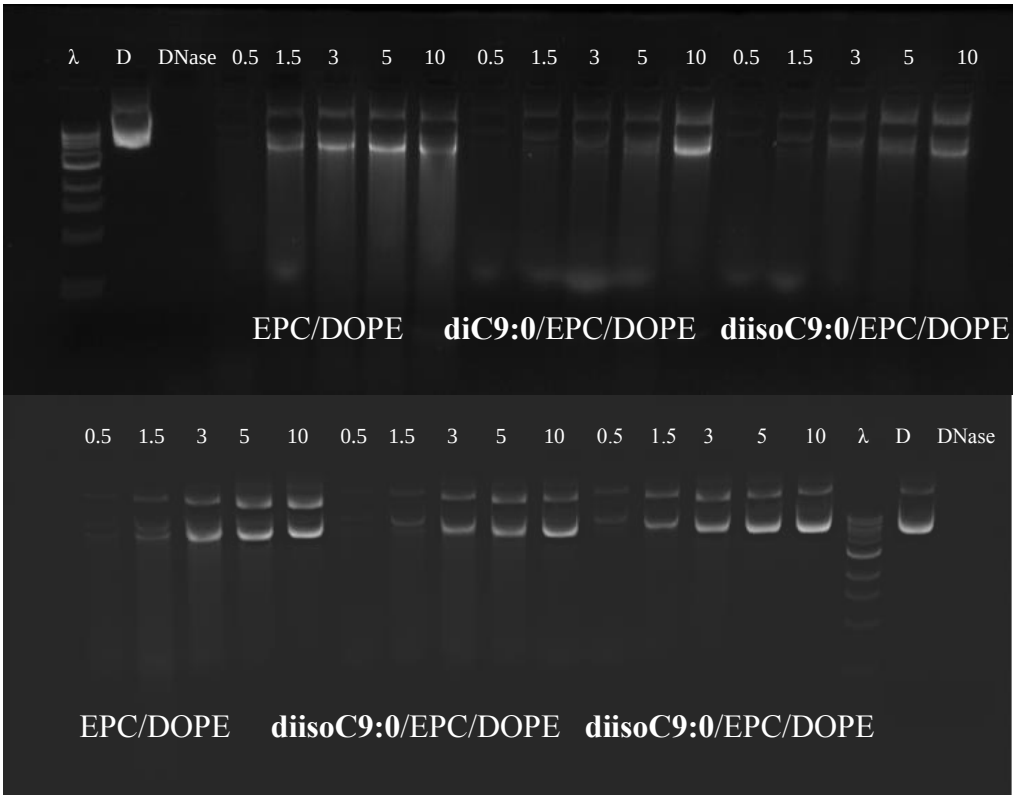

Figure C.14-DNase I degradation assay of lipids diC9:0 and diCisoC9:0 co-formulated with commercial lipid EPC and neutral co-lipid DOPE or cholesterol at N/P molar charge ratios 0.5, 1.5, 3, 5 and 10 and run through a 1% agarose gel impregnated with the pDNA gel stain, ethidium bromide. Lanes λ and DNA denote the 1 kb DNA ladder and pDNA, respectively.

C.3.3-Transfection efficiency and cytotoxicity

The transfection efficiency and toxicity of the synthesized pyridinium lipids, **diC9:0** and **diisoC9:0** with EPC as the co-cationic lipids in formulations with co-lipids DOPE and cholesterol has been studied and compared with Lipofectamine 2000^{TM} as the control (Figure C.15).

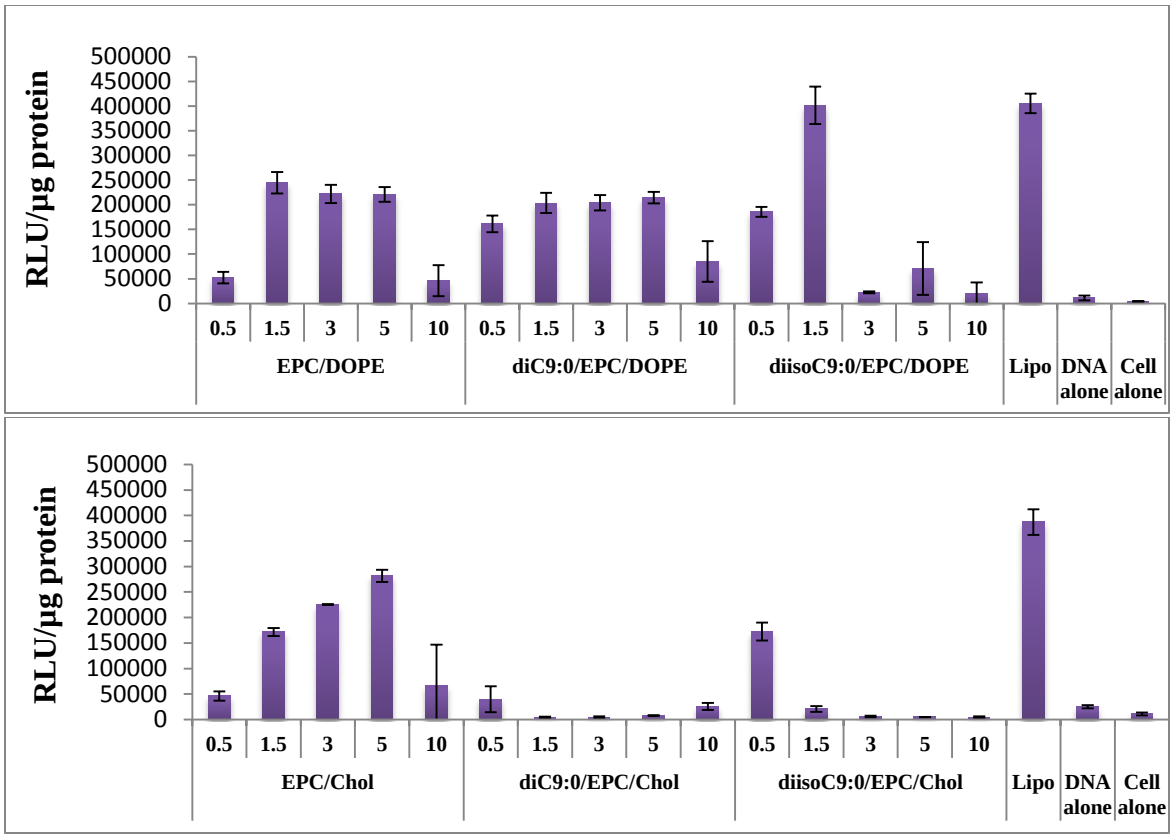

Figure C.15-Transfection efficiency as luminescence readings of β-galactosidase (after 48 h) of diC9:0 and diisoC9:0/co-lipid/DNA lipoplexes compared to EPC/co-lipid/DNA at N/P molar charge ratio of 0.5 to 10 and Lipofectamine 2000^{TM} (Lipo) (n = 9; mean ± SD) as positive controls, and plasmid DNA alone and CHO-K1 cells alone as negative controls

Those formulations containing pyridinium lipids with cholesterol as co-lipid showed poor transfection at all charge ratios (Figure 5.10). Formulations of **diC9:0**/EPC/DOPE were more efficient than **diisoC9:0**/EPC/cholesterol, and similar to the activity of EPC/DOPE formulations with the exception of **diisoC9:0**/EPC/DOPE at CR = 1.5 which had the highest activity in the dataset. The poor transfection observed with cholesterol as co-lipid is substantially less than that of EPC/cholesterol alone. This implies that theses pyridinium lipids when formulated with cholesterol give rise to some other morphologies or compositions which are particularly poor for transfection.

The toxicity of these short-chain pyridinium lipids is high as expected for the low value of clogP (Figure C.16). Formulations of either **diC9:0** and **diisoC9:0** with cholesterol had high toxicity. Formulations of **diC9:0** with DOPE have similar toxicity to EPC/DOPE, whereas the toxicity of **diisoC9:0** formulations in DOPE were high and increased as the N/P molar charge ratio increased, also in line with the previous correlation.

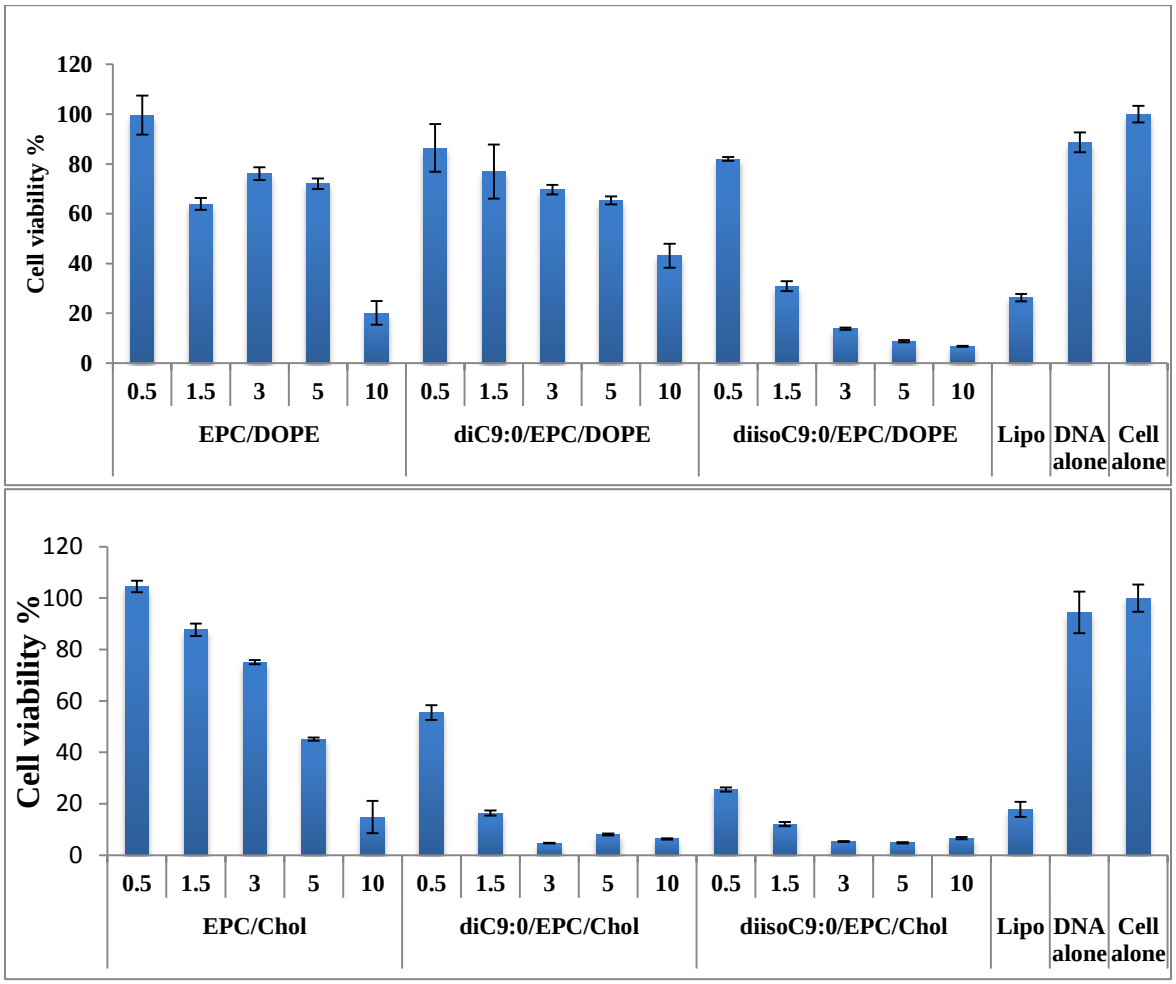

Figure C.16-Cytotoxicity (after 48 h) of diC9:0 and diisoC9:0/co-lipid/DNA lipoplexes compared to EPC/co-lipid/DNA at N/P molar charge ratio of 0.5 to 10 and Lipofectamine 2000^{TM} (Lipo) (n = 9; mean ± SD) as positive controls, and plasmid DNA alone and CHO-K1 cells alone as negative controls

C.3.4-SAXS studies on the prepared lipoplexes

SAXS studies were done on the lipoplexes prepared with pyridinium lipids and co-lipids, DOPE and cholesterol at two N/P molar charge ratio 1.5 and 3 (Table C.4).

Table C.4-Summary of SAXS results for pyridinium lipids/EPC/co-lipid/pDNA and EPC/DOPE and EPC/Chol lipoplex formulations at (+/-) N/P molar charge ratio 1.5:1 and 3:1. δ refers to the actual packing in each case, with an estimated standard deviation of typically 1Å.

Cationic lipids	Co-Lipid	CR	Packing	Lattice Parameter	S_{mix}
diC9:0/EPC	DOPE	1.5	Lamellar	δ = 63Å	1.1
diisoC9:0/EPC	DOPE	1.5	Hexagonal	δ = 68Å	1.2
diC9:0/EPC	DOPE	3	Lam/Hexagonal	δ = 64Å	1.1
diisoC9:0/EPC	DOPE	3	Hexagonal	δ = 68Å	1.2
diC9:0/EPC	Cholesterol	1.5	Lamellar	δ = 68Å	1.1
diisoC9:0/EPC	Cholesterol	1.5	Lamellar	δ = 66-85Å	1.2
diC9:0/EPC	Cholesterol	3	Lamellar	δ = 71Å	1.1
diisoC9:0/EPC	Cholesterol	3	Lamellar	δ = 70Å	1.2

C.4.1-Gel retardation and DNase I degradation assays of lipoplex (liposome-DNA) formulations

Gel retardation assay is used to assess the binding of DNA to liposomes. Generally the lipids showed a similar protection of the DNA by the lipoplexes at N/P molar charge ratio greater than 5 (Figure C.17).

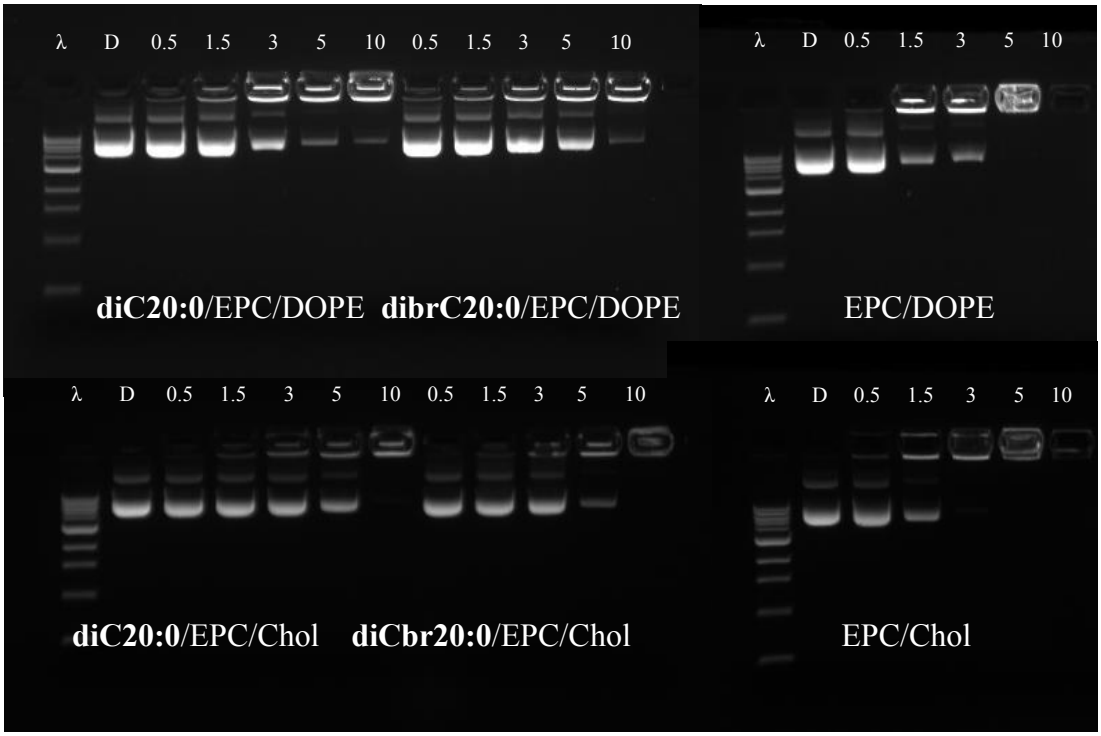

Figure C.17-Gel retardation assay of lipids diC20:0 and dibrC20:0 co-formulated with commercial lipid EPC and neutral co-lipid DOPE or cholesterol at N/P molar charge ratios 0.5, 1.5, 3, 5 and 10 and run through a 1% agarose gel impregnated with the pDNA gel stain, ethidium bromide. Lanes λ and DNA denote the 1 kb DNA ladder and pDNA, respectively.

A DNase I degradation assay was used to determine the accessibility of the lipid-associated DNA toward nucleases. All formulations showed similar protection of DNA after CR = 1.5. Formulations with DOPE showed better protection of DNA in general (Figure C18).

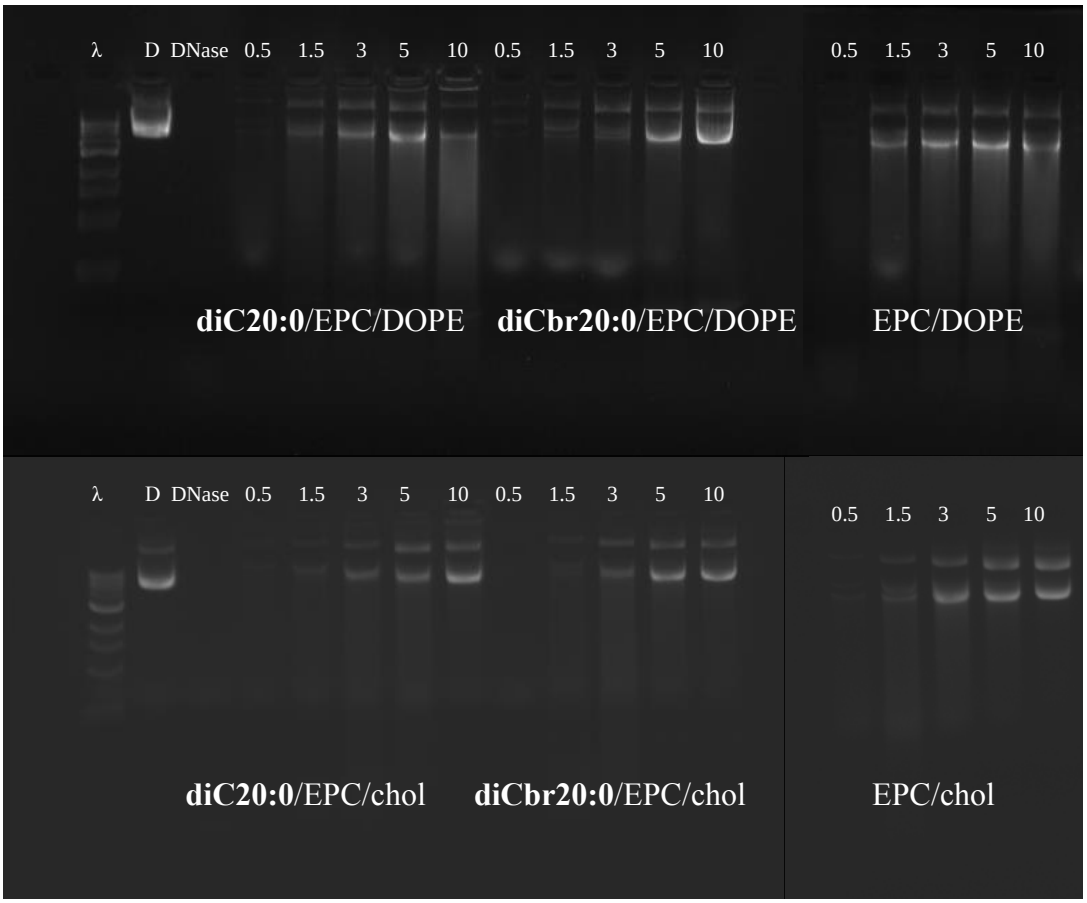

Figure C.18-DNase I degradation assay of lipids diC20:0 and dibrC20:0 co-formulated with commercial lipid EPC and neutral co-lipid DOPE or cholesterol at N/P molar charge ratios 0.5, 1.5, 3, 5 and 10 and run through a 1% agarose gel impregnated with the pDNA gel stain, ethidium bromide. Lanes λ and DNA denote the 1 kb DNA ladder and pDNA, respectively.

C.4.2-Transfection efficiency and cytotoxicity

The transfection efficiency and toxicity of the synthesized pyridinium lipids, **diC20:0** and **dibrC20:0** with EPC as the co-cationic lipids in formulations with co-lipids DOPE

and cholesterol has been studied and compared with Lipofectamine 2000™ as the control (Figure C.19).

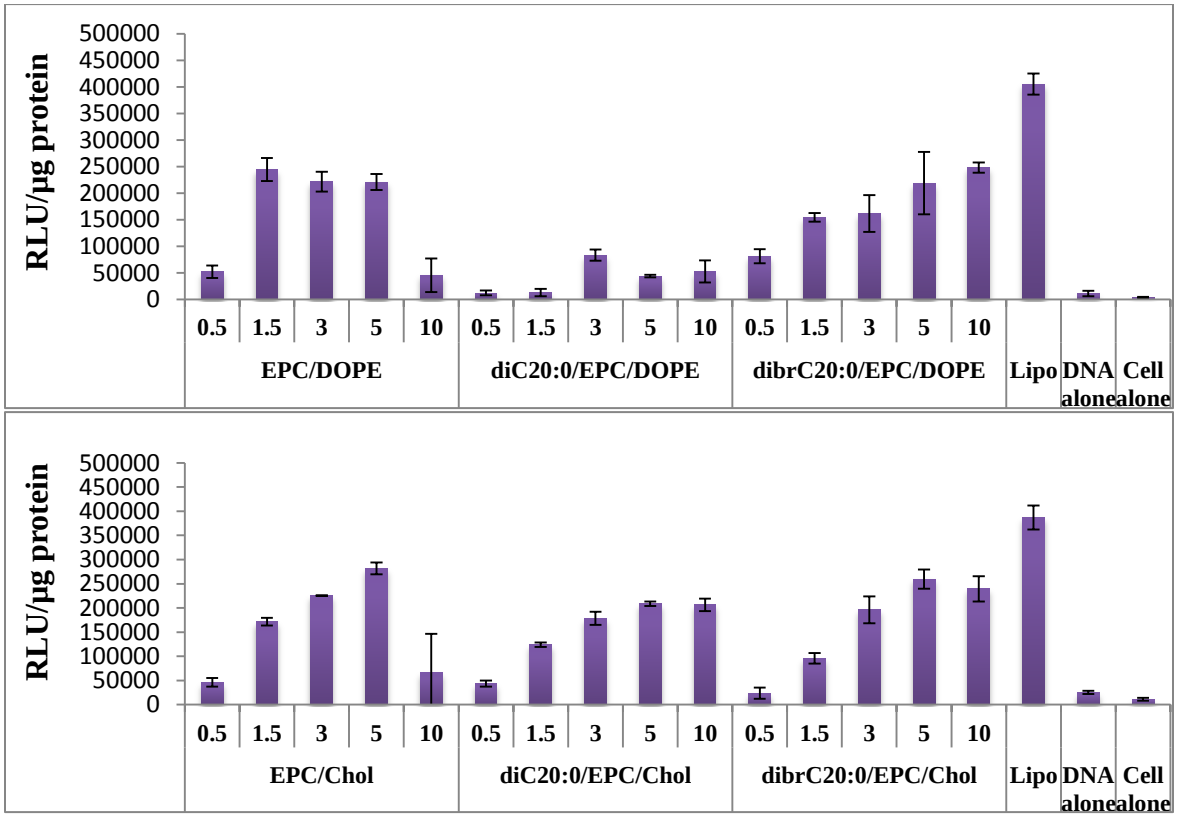

Figure C.19-Transfection efficiency as luminescence readings of β-galactosidase (after 48 h) of diC20:0 and dibrC20:0/co-lipid/DNA lipoplexes compared to EPC/co-lipid/DNA at molar N/P molar charge ratio of 0.5 to 10 and Lipofectamine 2000™ (Lipo) (n = 9; mean ± SD) as positive controls, and plasmid DNA alone and CHO-K1 cells alone as negative controls.

Formulations of both **diC20:0** and **dibrC20:0** with cholesterol or DOPE had similar toxicity to the binary EPC/co-lipid formulations (Figure C.20). In general these pyridinium compounds showed low toxicity at all N/P molar charge ratios. This is in line with the previous correlation with clogP and with S.

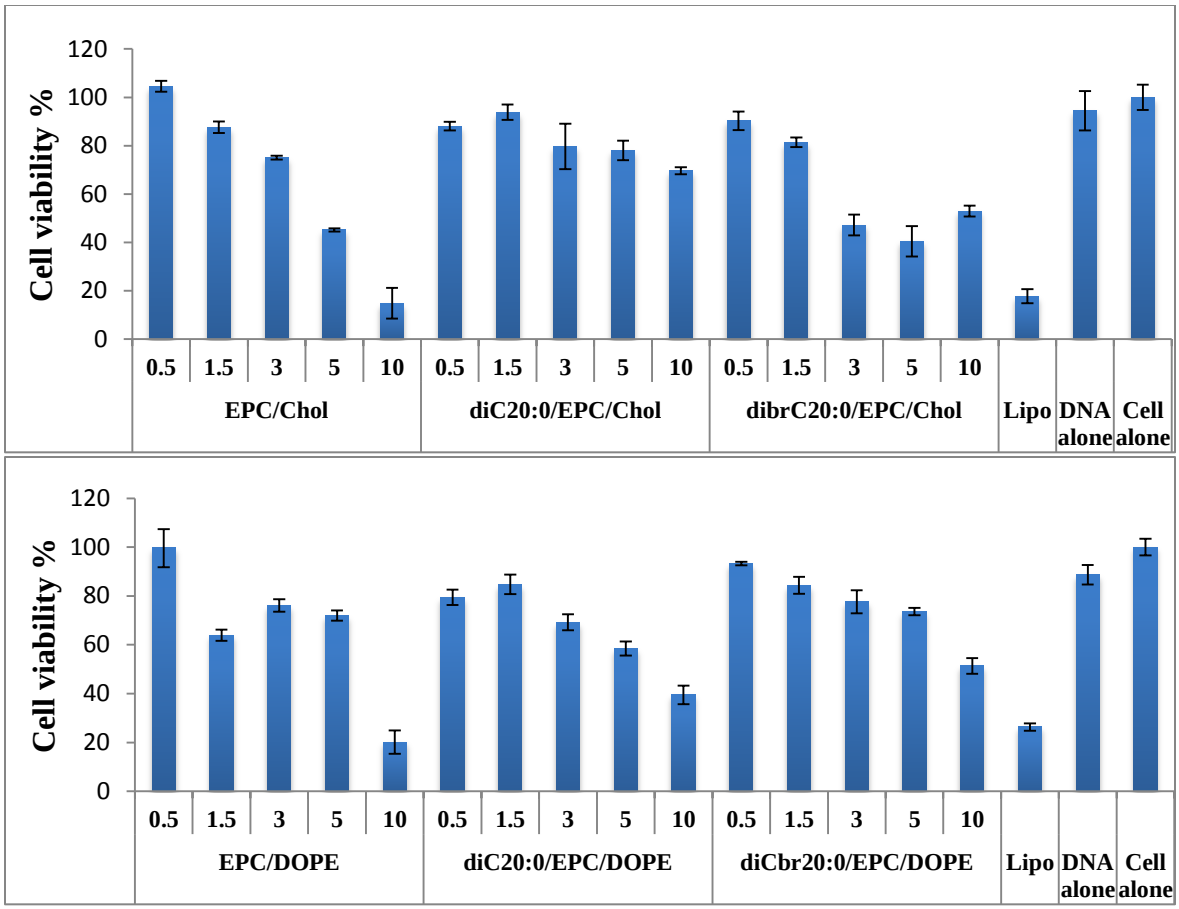

Figure C.20-Cytotoxicity (after 48 h) of diC20:0 and dibrC20:0/co-lipid/DNA lipoplexes compared to EPC/co-lipid/DNA at N/P molar charge ratio of 0.5 to 10 and Lipofectamine 2000^{TM} (Lipo) (n = 9; mean ± SD) as positive controls, and plasmid DNA alone and CHO-K1 cells alone as negative controls.

C.4.3-SAXS studies on the prepared lipoplexes

SAXS studies were attempted on the lipoplexes prepared with pyridinium lipids and co-lipids, DOPE and cholesterol at two N/P molar charge ratios 1.5 and 3.

Table C.5-Summary of SAXS results for pyridinium lipids/EPC/co-lipid/pDNA and EPC/DOPE and EPC/Chol lipoplex formulations at (+/-) N/P molar charge ratio 1.5:1 and 3:1. δ refers to the actual packing in each case, with an estimated standard deviation of typically 1Å.

Cationic lipids	Co-Lipid	CR	Packing	Lattice Parameter	S_{mix}
diC20:0/EPC	DOPE	1.5	nothing	δ = NA	1.1
dibrC20:0/EPC	DOPE	1.5	nothing	δ = NA	1.3
diC20:0/EPC	DOPE	3	nothing	δ = NA	1.1
dibrC20:0/EPC	DOPE	3	nothing	δ = NA	1.3
diC20:0/EPC	Cholesterol	1.5	Indeterminate	δ = ND	1.1
dibrC20:0/EPC	Cholesterol	1.5	nothing	δ = NA	1.4
diC20:0/EPC	Cholesterol	3	Indeterminate	δ = ND	1.1
dibrC20:0/EPC	Cholesterol	3	nothing	δ = NA	1.4

C.5.1-Liposome/lipoplex formulation and particle sizing

Liposomes of synthesized pyridinium lipids with EPC were prepared with DOPE, in ratio of 3:2 ratio of cationic lipid to co-lipid for synthesized ternary lipids (**New TF**) of **diC18:1** (***2-27***), **dibrC20:0** (***2-25***) ***and*** **(C18:1)(brC20:0)** (***4-4***) and binary blend of pure lipids (**blend**) **diC18:1** (***2-27***) and **dibrC20:0** (***2-25***).

A thin layer of lipid was prepared by removal of the ethanol under reduced pressure from the desired lipid mixture solution and then hydrated and sonicated to give liposomes. These liposomes were sized using dynamic light scattering (DLS) with diameters in the range d_H = 160–1900 nm, with polydispersity index (PDI) values ranging from 0.3 to 0.7 (Figure C.21).

2 mM Liposomes	Z-Ave (d.nm)	PdI
EPC/DOPE	162.3	0.4
(18:1)(br20:0)blend50/EPC/DOPE	481.0	0.5
(18:1)(br20:0)blend66/EPC/DOPE	1923.7	0.7
(18:1)(br20:0)blend85/EPC/DOPE	324.4	0.4
EPC/Chol	273.9	0.4
(18:1)(br20:0)blend50/EPC/Chol	274.2	0.3
(18:1)(br20:0)blend66/EPC/Chol	181.6	0.3
(18:1)(br20:0)blend85/EPC/Chol	414.2	0.5

Figure C.21-Liposome sizing of pyridinium lipids, blend 50, blend 66 and blend 85 with EPC (commercial cationic lipid) were prepared with either of co-lipids, cholesterol and DOPE, in ratio of 3:2 ratio of cationic lipid to co-lipid.

The prepared liposomes with varied formulation were combined with negatively charged DNA to form lipoplexes driven by electrostatic interaction between the cationic lipids and DNA at a range of N/P molar charge ratio of cationic lipids to DNA of 1.5,5 and 10. Particle sizes were found between d_H = 200–10000 nm, with PDI values ranging from 0.2 to 0.8 (Figure C.22).

Lipoplexes	N:P	Standard Formulations	
		Z-Ave (d.nm)	PdI
EPC/DOPE	1.5	2803.7	0.5
	5	312.5	0.2
	10	223.5	0.2
(18:1)(br20:0)blend50/EPC/DOPE	1.5	515.9	0.3
	5	641.4	0.3
	10	7320.3	0.5
(18:1)(br20:0)blend66/EPC/DOPE	1.5	618.6	0.3
	5	607.9	0.3
	10	3056.0	0.7
(18:1)(br20:0)blend85/EPC/DOPE	1.5	395.4	0.3
	5	522.5	0.3
	10	4961.3	0.5
EPC/Chol	1.5	655.3	0.3
	5	1827.0	0.6
	10	460.3	0.3
(18:1)(br20:0)blend50/EPC/Chol	1.5	301.2	0.2
	5	10153.3	0.4
	10	385.8	0.2
(18:1)(br20:0)blend66/EPC/Chol	1.5	251.8	0.2
	5	13990.3	0.6
	10	280.6	0.1
(18:1)(br20:0)blend85/EPC/Chol	1.5	409.9	0.3
	5	2745.0	0.6
	10	5680.7	0.8

Figure C.22-Lipoplex sizing of pyridinium lipids, blend 50, blend 66 and blend 85 with EPC (commercial cationic lipid) at N/P molar charge ratios of 1.5, 5 and 10 were prepared with either of co-lipids, cholesterol and DOPE, in ratio of 3:2 ratio of cationic lipid to co-lipid.

C.5.2-Gel retardation and DNase I degradation assays of lipoplex (liposome-DNA) formulations

Gel retardation assay is used to assess the binding of DNA to liposomes. The binding was similar for blends with different compositions (Figure C.23).

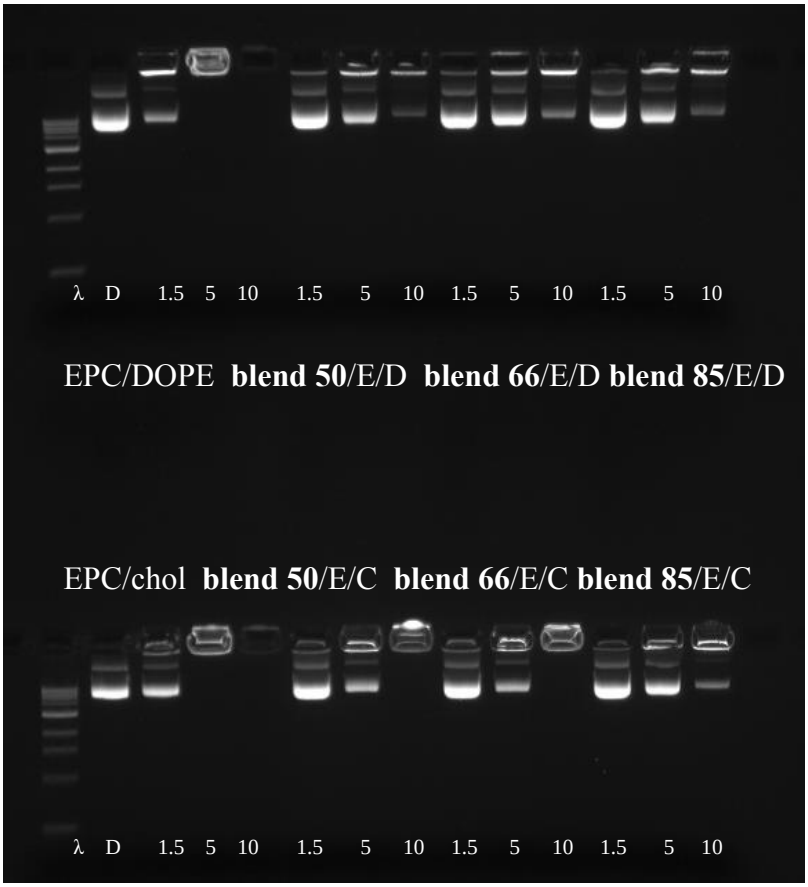

Figure C.23-Gel retardation assay of lipids for blend 50, blend 66 and blend 85 co-formulated with commercial lipid EPC (E) and neutral co-lipid DOPE (D) or cholesterol (C) at N/P molar charge ratios 1.5, ,5 and 10 and run through a 1% agarose gel impregnated with the pDNA gel stain, ethidium bromide. Lanes λ and DNA denote the 1 kb DNA ladder and pDNA, respectively.

A DNase I degradation assay was used to determine the accessibility of the lipid-associated DNA toward nucleases. All formulations showed similar protection of DNA after CR = 1.5 (Figure C.24).

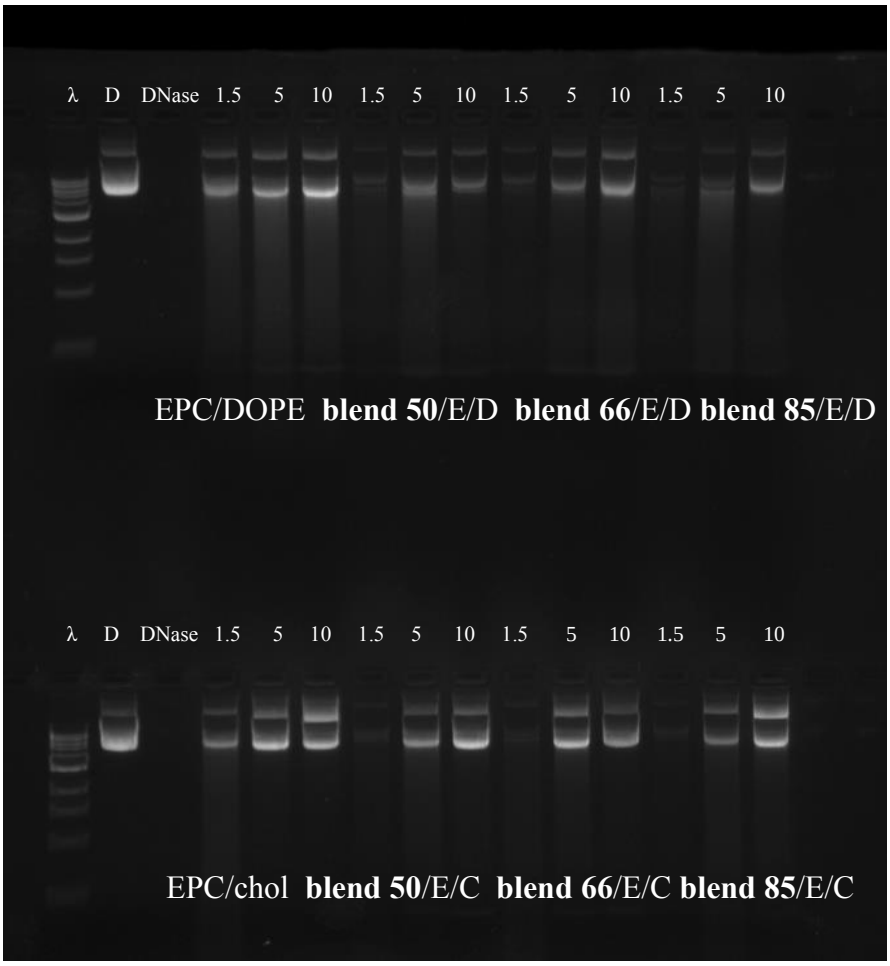

Figure C.24-DNase I degradation assay of blend 50, blend 66 and blend 85 co-formulated with commercial lipid EPC (E) and neutral co-lipid DOPE (D) or cholesterol (C)at N/P molar charge ratios 1.5, 5 and 10 and run through a 1% agarose gel impregnated with the pDNA gel stain, ethidium bromide. Lanes λ and DNA denote the 1 kb DNA ladder and pDNA, respectively.

C.5.3-Transfection efficiency and cytotoxicity

The transfection efficiency and toxicity of the synthesized pyridinium lipids, **blend 50, blend 66** and **blend 85** with EPC as the co-cationic lipids in formulations with co-lipids DOPE and cholesterol has been studied and compared with Lipofectamine 2000^{TM} as the control (Figure C.25).

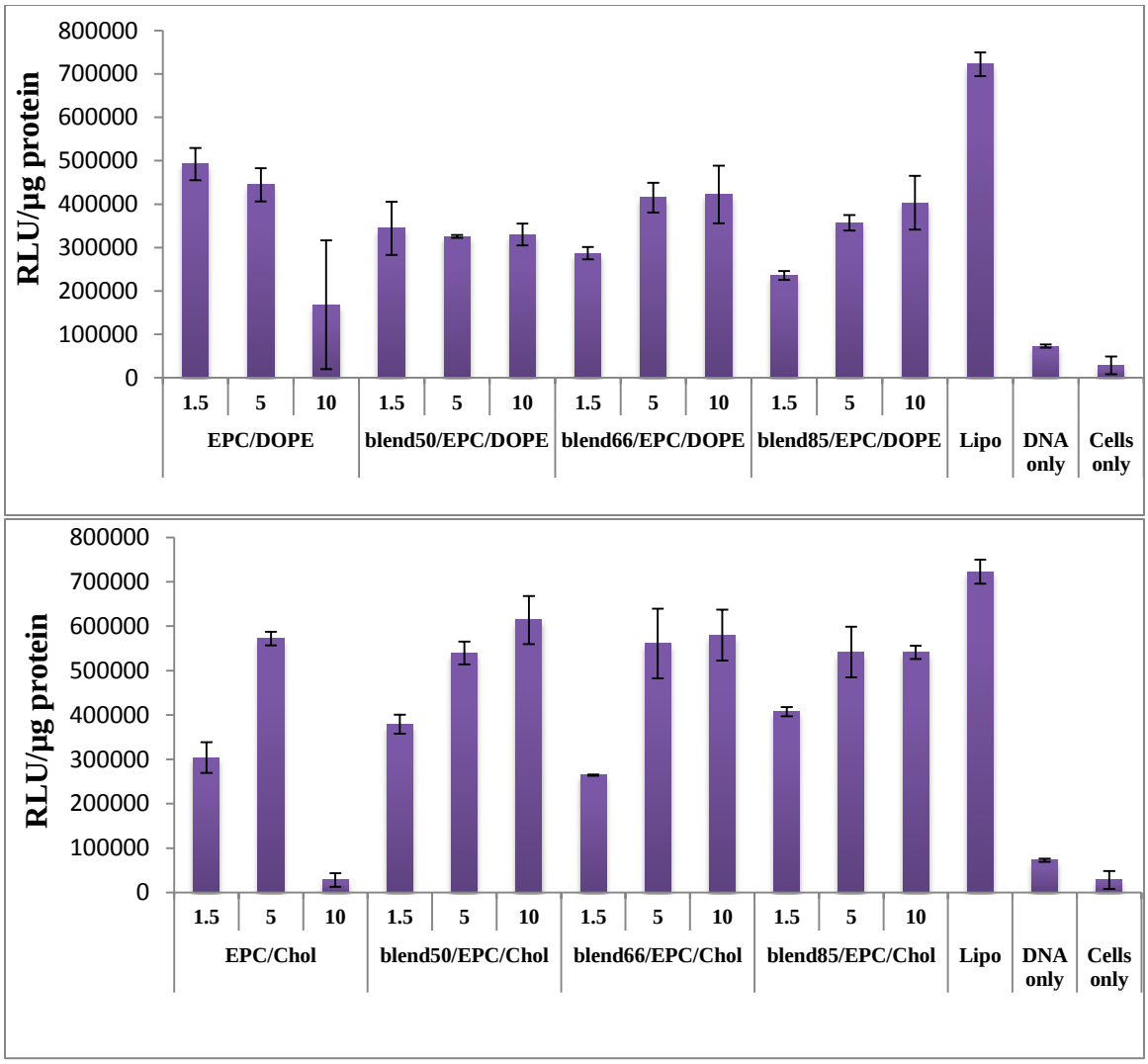

Figure C.25-Transfection efficiency as luminescence readings of β-galactosidase (after 48 h) of blend 50, blend 66 and blend 85/co-lipid/DNA lipoplexes compared to EPC/co-lipid/DNA at N/P molar charge ratios of 1.5, 5 and 10 and Lipofectamine 2000™ (Lipo) (n = 9; mean ± SD) as positive controls, and plasmid DNA alone and CHO-K1 cells alone as negative controls.

The transfection results of the blends in Figure C.25 showed that the transfection efficiency in blends is better with cholesterol rather than DOPE. The toxicity of these lipids are shown in Figure C.26, showing the folrmulation with DOPE are less toxic than cholesterol, and some compositions are less toxic compared to others.

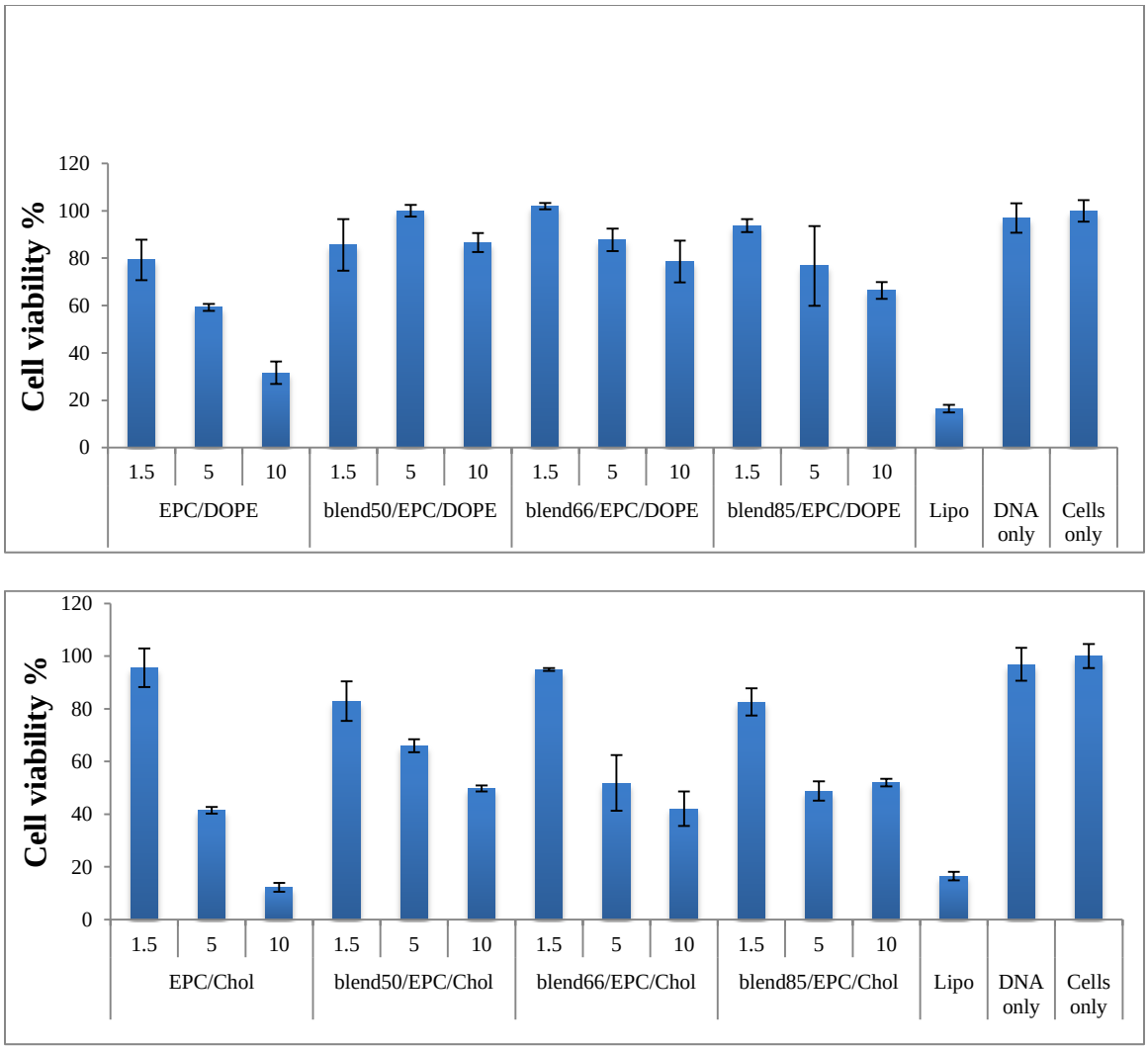

Figure C.26-Cytotoxicity (after 48 h) of blend 50, blend 66 and blend 85/co-lipid/DNA lipoplexes compared to EPC/co-lipid/DNA at N/P molar charge ratios of 1.5, 5 and 10 and Lipofectamine 2000™ (Lipo) (n = 9; mean ± SD) as positive controls, and plasmid DNA alone and CHO-K1 cells alone as negative controls.

C.5.4-SAXS studies on the prepared lipoplexes

SAXS studies were done on the lipoplexes prepared with **blend 50, blend 66** and **blend 85** and co-lipids, DOPE and cholesterol at two N/P molar charge ratio 1.5 and 3 (Table C.6).

Table C.6-Summary of SAXS results for blend 50, blend 66 and blend 85/EPC/co-lipid/pDNA and EPC/DOPE and EPC/Chol lipoplex formulations at (+/-) N/P molar charge ratio 1.5:1 and 3:1. δ refers to the actual packing in each case, with an estimated standard deviation of typically 1Å.

Cationic lipids	Co-Lipid	CR	Packing	Lattice Parameter	S_{mix}
blend 50/EPC	DOPE	1.5	**Indeterminate**	δ = NA	1.2
blend 66/EPC	DOPE	1.5	**Indeterminate**	δ = NA	1.2
blend 85/EPC	DOPE	1.5	**Indeterminate**	δ = NA	1.3
blend 50/EPC	DOPE	3	**Indeterminate**	δ = NA	1.2
blend 66/EPC	DOPE	3	**Indeterminate**	δ = NA	1.2
blend 85/EPC	DOPE	3	**Lamellar**	δ = 74**Å**	1.3
blend 50/EPC	Cholesterol	1.5	**Lamellar?**	δ = 76**Å**	1.2
blend 66/EPC	Cholesterol	1.5	**Indeterminate**	δ = NA	1.3
blend 85/EPC	Cholesterol	1.5	**Indeterminate**	δ = NA	1.3
blend 50/EPC	Cholesterol	3	**Lamellar**	δ = 72**Å**	1.2
blend 66/EPC	Cholesterol	3	**Lamellar**	δ = 71**Å**	1.3
blend 85/EPC	Cholesterol	3	**Indeterminate**	δ = NA	1.3

C.6.1-Liposome/lipoplex formulation and particle sizing

Liposomes of synthesized pyridinium lipids with EPC were prepared with DOPE, in ratio of 3:2 ratio of cationic lipid to co-lipid for synthesized ternary lipids (**New TF**) of **diC18:1** (***2-27***), **dibrC20:0** (***2-25***) and **(C18:1)(brC20:0)** (***4-4***) and binary blend of pure lipids (**blend**) **diC18:1** (***2-27***) and **dibrC20:0** (***2-25***).

A thin layer of lipid was prepared by removal of the ethanol under reduced pressure from the desired lipid mixture solution and then hydrated and sonicated to give liposomes. These liposomes were sized using dynamic light scattering (DLS) with diameters in the range d_H = 200–700 nm, with polydispersity index (PDI) values ranging from 0.2 to 0.6 (Figure C.27).

FORMULATIONS	Z-ave	Pdi
EPC/DOPE	741.3	0.6
EPC/chol	272.3	0.4
EPC/DOPE/**blend**	445.4	0.3
EPC/chol/**blend**	379	0.5
EPC/DOPE/**New TF**	462.2	0.4
EPC/CHOL/**New TF**	319.3	0.4

Figure C.27-Liposome sizing of pyridinium lipids (for synthesized ternary lipids (New TF) and binary blend of pure lipids (blend) with EPC (commercial cationic lipid) were prepared with either of co-lipids, cholesterol and DOPE, in ratio of 3:2 ratio of cationic lipid to co-lipid

The prepared liposomes with varied formulation were combined with negatively charged DNA to form lipoplexes driven by electrostatic interaction between the cationic lipids and DNA at a range of N/P molar charge ratio of cationic lipids to DNA of 0.5, 1.5,3,5 and 10. Particle sizes were found between d_H = 200–2000 nm, with PDI values ranging from 0.2 to 0.8 (Figure C.28).

FORMULATIONS	CHARGE RATIO	Z-ave	Pdi
EPC/DOPE	0.5	593	0.2
	1.5	795.1	0.2
	3	5943	0.5
	5	6926	0.4
	10	1358	0.3
EPC/chol	0.5	268.4	0.2
	1.5	3409	0.6
	3	2867	0.6
	5	335	0.2
	10	225.8	0.2
EPC/DOPE/**blend**	0.5	689	0.3
	1.5	586.5	0.3
	3	827.9	0.3
	5	5750	0.5
	10	6887	0.4
EPC/chol/**blend**	0.5	277.1	0.4
	1.5	324.7	0.3
	3	7738	0.3
	5	3625	0.7
	10	294.7	0.2
EPC/DOPE/**New TF**	0.5	737.2	0.4
	1.5	530	0.3
	3	468.4	0.3
	5	798	0.3
	10	5409	0.4
EPC/chol/**New TF**	0.5	251	0.3
	1.5	301.6	0.2
	3	8004	0.3
	5	1745	0.4
	10	264.1	0.2

Figure C.28-Lipoplex sizing of pyridinium lipids (for synthesized ternary lipids (New TF) and binary blend of pure lipids (blend) with EPC (commercial cationic lipid) at N/P molar charge ratio of 0.5 to 10 were prepared with either of co-lipids, cholesterol and DOPE, in ratio of 3:2 ratio of cationic lipid to co-lipid.

C.6.2-Gel retardation and DNase I degradation assays of lipoplex (liposome-DNA) formulations

Gel retardation assay is used to assess the binding of DNA to liposomes. The binding was similar for blend and the mix (Figure C.29).

Figure C.29-Gel retardation assay of lipids for synthesized ternary lipids (New TF) and binary blend of pure lipids (blend) co-formulated with commercial lipid EPC and neutral co-lipid DOPE or cholesterol at N/P molar charge ratios 0.5, 1.5, 3, 5 and 10 and run through a 1% agarose gel impregnated with the pDNA gel stain, ethidium bromide. Lanes λ and DNA denote the 1 kb DNA ladder and pDNA, respectively.

A DNase I degradation assay was used to determine the accessibility of the lipid-associated DNA toward nucleases. All formulations showed similar protection of DNA after CR = 1.5 (Figure C.30).

Figure C.30-DNase I degradation assay of lipids synthesized ternary lipids (New TF) and binary blend of pure lipids (blend) co-formulated with commercial lipid EPCand neutral co-lipid DOPE or cholesterol at N/P molar charge ratios 0.5, 1.5, 3, 5 and 10 and run through a 1% agarose gel impregnated with the pDNA gel stain, ethidium bromide. Lanes λ and DNA denote the 1 kb DNA ladder and pDNA, respectively.

C.6.3-Transfection efficiency and cytotoxicity

The transfection efficiency of the synthesized pyridinium lipids, synthesized ternary lipids (**New TF**) and binary blend of pure lipids (**blend**) with EPC as the co-cationic lipids in formulations with co-lipids DOPE and cholesterol has been studied and compared with Lipofectamine 2000^{TM} as the control (Figure C.31).

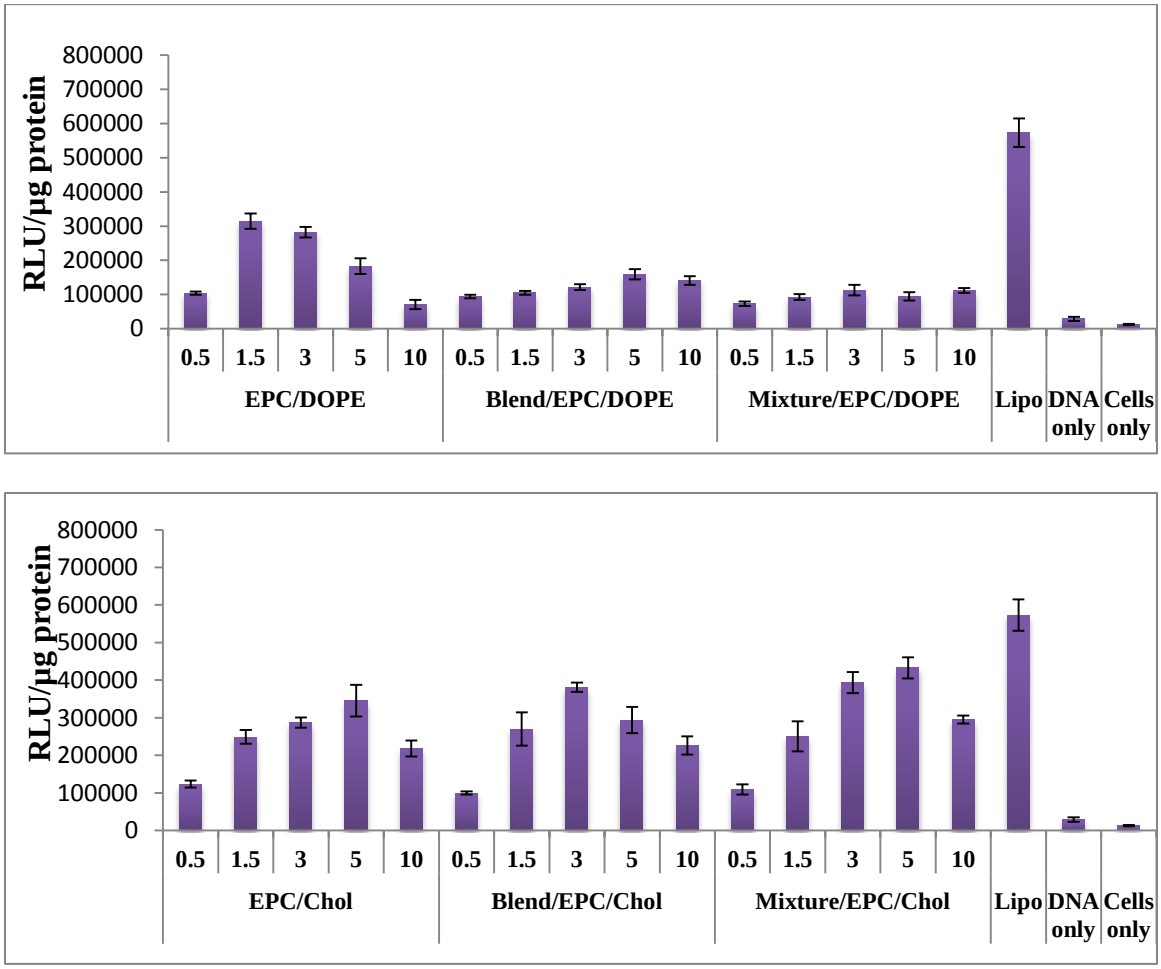

Figure C.31-Transfection efficiency as luminescence readings of β-galactosidase (after 48 h) of synthesized ternary lipids (mixture) and binary blend of pure lipids (blend)/co-lipid/DNA lipoplexes compared to EPC/co-lipid/DNA at N/P molar charge ratio of 0.5 to 10 and Lipofectamine 2000^{TM} (Lipo) (n = 9; mean ± SD) as positive controls, and plasmid DNA alone and CHO-K1 cells alone as negative controls.

The transfection efficiency of the ternary mixture and binary blend are similar, however the transfection with DOPE as co-lipid is quite poor and is much lower than

EPC/DOPE. The transfection with cholesterol as the co-lipid is slightly better with the mixture. The formulations with DOPE showed less toxicity (Figure C.32).

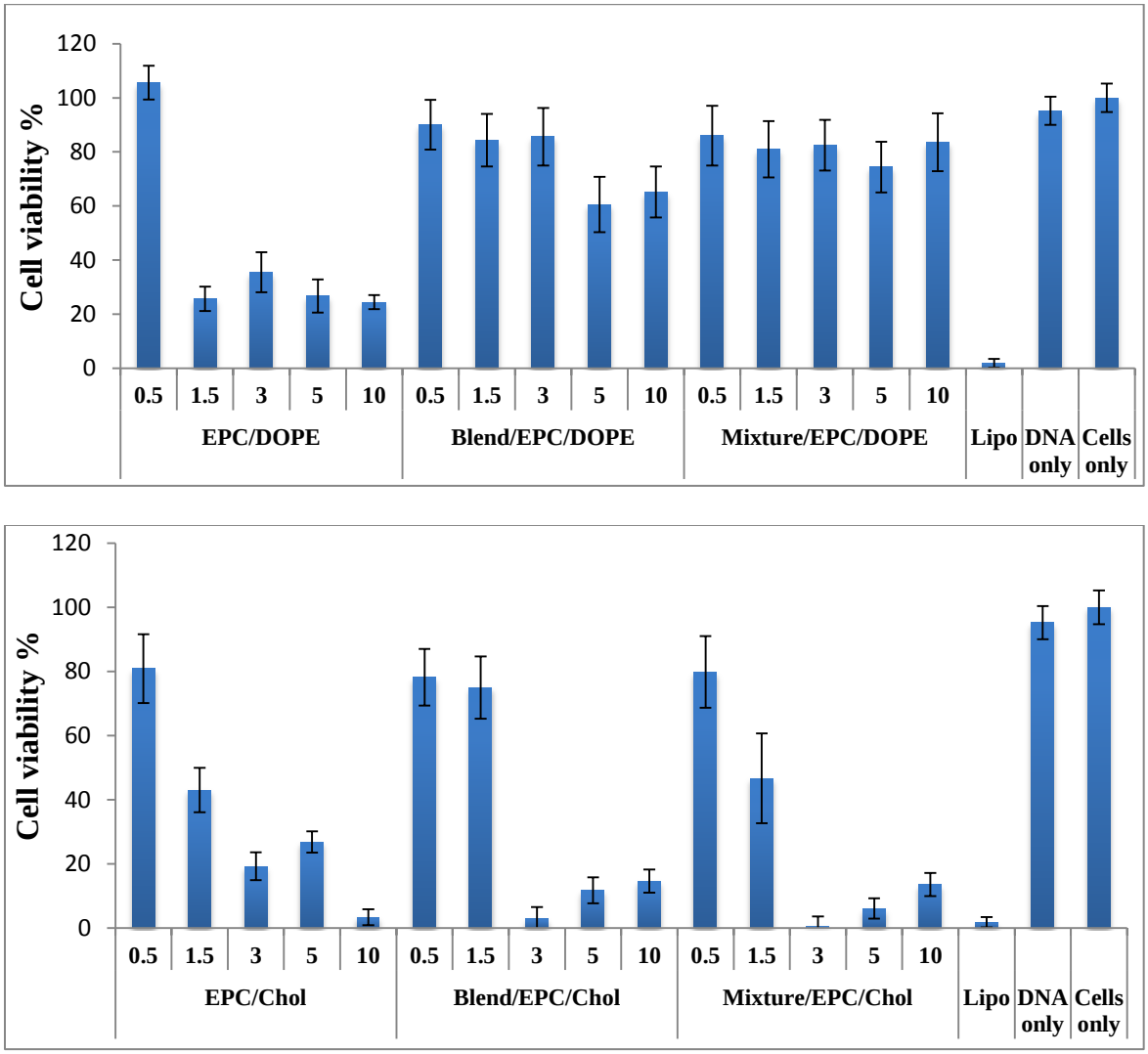

Figure C.32-Cytotoxicity (after 48 h) of synthesized ternary lipids (mixture) and binary blend of pure lipids (blend)/co-lipid/DNA lipoplexes compared to EPC/co-lipid/DNA at N/P molar charge ratio of 0.5 to 10 and Lipofectamine 2000™ (Lipo) (n = 9; mean ± SD) as positive controls, and plasmid DNA alone and CHO-K1 cells alone as negative controls.

C.6.4-SAXS studies on the prepared lipoplexes

SAXS studies were done on the lipoplexes prepared with pyridinium lipids and co-lipids, DOPE and cholesterol at two N/P molar charge ratio 1.5 and 3 (Table C.7).

Table C.7-Summary of SAXS results for pyridinium lipids/EPC/co-lipid/pDNA and EPC/DOPE and EPC/Chol lipoplex formulations at (+/-) N/P molar charge ratio 1.5:1 and 3:1. δ refers to the actual packing in each case, with an estimated standard deviation of typically 1Å.

Cationic lipids	Co-Lipid	CR	Packing	Lattice Parameter	S_{mix}
New TF/EPC	DOPE	1.5	nothing	δ = NA	1.2
blend/EPC	DOPE	1.5	indeterminate	δ = NA	1.2
New TF/EPC	DOPE	3	indeterminate	δ = NA	1.2
blend/EPC	DOPE	3	indeterminate	δ = NA	1.2
New TF/EPC	Cholesterol	1.5	indeterminate	δ = NA	1.4
blend/EPC	Cholesterol	1.5	Indeterminate (tendency to Lamellar)	δ = NA	1.4
New TF/EPC	Cholesterol	3	indeterminate	δ = NA	1.4
blend/EPC	Cholesterol	3	nothing	δ = NA	1.4